UC San Diego

UC San Diego Electronic Theses and Dissertations

Title

A Deep Dive into Sperm Whale Ecology Using Passive Acoustic Monitoring

Permalink

https://escholarship.org/uc/item/1wv6n833

Author

Posdaljian, Natalie

Publication Date

2023

Peer reviewed|Thesis/dissertation

UNIVERSITY OF CALIFORNIA SAN DIEGO

A Deep Dive into Sperm Whale Ecology Using Passive Acoustic Monitoring

A Dissertation submitted in partial satisfaction of the requirements

for the degree Doctor of Philosophy

in

Oceanography

by

Natalie Posdaljian

Committee in charge:
Professor Simone Baumann-Pickering, Chair
Professor Kaitlin Frasier
Professor John A. Hildebrand
Professor Sarah Mesnick
Professor Jonathan Shurin
Professor Lynne Talley

2023

The Dissertation of Natalie Posdaljian is approved, and it is acceptable in quality and form for publication on microfilm and electronically.

University of California San Diego

2023

Dedication

To my family and friends, and all my supporters along the way, especially my mom,
Maral Posdaljian, and husband, Eric Starks, who I am eternally grateful to.

Table of Contents

List of Figures

xii

List of Tables

Acknowledgements

I would like to express my heartfelt gratitude to all of those who have supported me throughout my doctoral journey including my dissertation committee members, collaborators, funders, family, friends, mentors, lab mates, and fellow SIO students, especially my BO cohort. Your unwavering encouragement, invaluable contributions, and enduring belief in my abilities have been instrumental in the successful completion of this dissertation.

First and foremost, I want to thank my family: my husband, mom, brother, uncles, aunts, cousins, my father and mother-in-law, my sister-in-law, and grandma. Your love, support, and understanding have been my anchor throughout this endeavor, and I am eternally grateful for your sacrifices and the countless ways you've supported me. I want to express my profound gratitude to my husband, Eric Starks, who has been my unwavering source of support, motivation, and love throughout every step of this doctoral journey. Your endless sacrifices, understanding, and selflessness have made it possible for me to dedicate myself fully to this dissertation. You have taken on extra responsibilities, provided a comforting presence during the most challenging times, and celebrated every milestone, no matter how small, with unwavering enthusiasm. Your faith in my potential has fueled my determination and inspired me to reach new heights. In every moment of self-doubt, and in every triumph, you have been my guiding light. With all my heart, I say thank you. This achievement is as much yours as it is mine. I also want to offer a heartfelt thank you to my mother, Maral Posdaljian, whose boundless love has been a driving force behind my doctoral journey. Even in the face of her own formidable challenges, she never wavered in her dedication to my academic aspirations. Her determination to ensure that I remained focused on my research, even during her most trying times, is a testament to her selflessness and her unwavering commitment to my success. I cherished the

moments when I overheard her proudly sharing with others the details of my research and what I was studying. Her enthusiasm and pride in my work were not only heartwarming but also a powerful motivation for me to excel. And to the rest of my family, I am deeply grateful for your incredible support during the last year and a half. Their selfless acts of kindness, such as coming to help care for my mother, dropping off food, and always finding ways to make me laugh and smile, have been my lifeline during the most challenging moments. Without their love and assistance, I would not have been able to navigate this journey with the same level of determination and resilience.

I am deeply grateful to my friends, the pillars of support and cherished companions who have played an indispensable role in my journey. Their commitment to my success, unwavering belief in my abilities, and constant reminders about the importance of maintaining a work-life balance have been invaluable throughout this endeavor. Melanie, Sabrien, Garren, Shant, Helen, Bex, Shane, Nicole, Whitney, Jerome, Mike, Sarah, David, Maggie, Judy, and so many others, you have truly been my lifeline, my source of motivation, and my cheerleaders on this path. I want to express my heartfelt appreciation to my Main Bs - Jessica, Lara, and Nairi. Their unwavering support has been a beacon of warmth in my life. They've not only listened to me but also offered a comforting shoulder to lean on, guiding me through life's challenges. I am immensely grateful for the countless Zoom productivity sessions, the reassuring check-in texts, the hearty laughs, the cherished memories, and the unforgettable adventures that have lit up even my darkest days. You ladies are the embodiment of true friendship, and I consider myself incredibly fortunate to have you right by my side. Your presence has been a source of strength and light, and for that, I extend my deepest gratitude. Thank you for being there for me in the most genuine and meaningful way.

Chapter 1, in full, is a reprint of the material as it appears in Global Change Biology 2022. Posdaljian, Natalie, Caroline Soderstjerna, Joshua M. Jones, Alba Solsona-Berga, John A. Hildebrand, Kristin Westdal, Alex Ootoowak, and Simone Baumann-Pickering. The dissertation author was the primary investigator and author of this paper.

Chapter 2, in full, is under review for publication of the material as it may appear in PLOS One, 2023, Posdaljian, Natalie, Alba Solsona-Berga, John A. Hildebrand, Caroline Soderstjerna, Sean M. Wiggins, Kieran Lenssen, and Simone Baumann-Pickering. The dissertation author was the primary researcher and author of this paper.

Chapter 3, in full is currently being prepared for submission for publication of the material. Posdaljian, N., Deans, A., Solsona-Berga, A., Hildebrand, J., Frasier, K.E., Murillo, S., Marques, T., DeAngelis, A., & Baumann-Pickering, S. "Demographic Specific Spatiotemporal Patterns and Density Trends for Sperm Whales in the Western North Atlantic". The dissertation author was the primary researcher and author of this material.

Chapter 4, in full is currently being prepared for submission for publication of the material. Posdaljian, N., Solsona-Berga, A., Oleson, E.M., Hildebrand, J. A., & Baumann-Pickering, S. "Demographic Dependent Habitat Associations and High Use Areas of Sperm Whales in the North Pacific". The dissertation author was the primary researcher and author of this material.

Vita

2014   Bachelor of Science in Environmental Systems – Ecology, Behavior, and Evolution, University of California San Diego

2019   Master of Science in Oceanography, University of California, San Diego

2023   Doctor of Philosophy in Oceanography, University of California San Diego

Publications

Posdaljian, Natalie, Caroline Soderstjerna, Joshua M. Jones, Alba Solsona-Berga, John A. Hildebrand, Kristin Westdal, Alex Ootoowak, and Simone Baumann-Pickering. "Changes in sea ice and range expansion of sperm whales in the eclipse sound region of Baffin Bay, Canada." Global change biology 28, no. 12 (2022): 3860-3870.

Solsona-Berga, Alba, **Natalie Posdaljian**, John A. Hildebrand, and Simone Baumann-Pickering. "Echolocation repetition rate as a proxy to monitor population structure and dynamics of sperm whales." Remote Sensing in Ecology and Conservation 8, no. 6 (2022): 827-840.

Posdaljian, Natalie, Alba Solsona-Berga, John A. Hildebrand, Caroline Soderstjerna, Sean M. Wiggins, Kieran Lenssen, and Simone Baumann-Pickering. "Sperm Whales Demographics in the Gulf of Alaska and Bering Sea/Aleutian Islands: An Overlooked Female Habitat." PLOS One (2023). *Under Review.*

Abstract of the Dissertation

A Deep Dive into Sperm Whale Ecology Using Passive Acoustic Monitoring

by

Natalie Posdaljian

Doctor of Philosophy in Oceanography

University of California San Diego, 2023

Professor Simone Baumann-Pickering, Chair

Although sperm whales are a cosmopolitan species, male and female sperm whales are sexually dimorphic, and the sexes have differences in behavior and habitat preference that result in differences in their distribution and seasonality. Understanding the complex spatiotemporal distribution patterns and demographic composition can be difficult with traditional, logistically challenging shipboard methods given the vast distances and depths these animals travel. Since sperm whales produce highly distinctive echolocation clicks while foraging and navigating, they're excellent candidates for passive acoustic monitoring (PAM), an alternative method to eavesdrop on these deep-diving animals. Here we show the utility of PAM as a robust tool for advancing our understanding of sperm whale ecology. This study incorporates acoustic data from over 40 recording sites across the northern hemisphere, yielding valuable insights into demographics, acoustic density estimation, and the identification of high-use areas and habitat

associations. In remote regions, PAM has enabled us to identify areas where sperm whales are adapting to changing environmental conditions by expanding their potential range in response to climate change, exemplified by observations in the eastern Canadian Arctic. Furthermore, our findings challenge conventional assumptions about male and female preferred habitats, as evidenced by the presence of females in high-latitude regions like the Gulf of Alaska and Bering Sea/Aleutian Islands. Our long-term PAM efforts have significantly expanded our knowledge of demographic specific presence, spatiotemporal distribution, acoustic density, and habitat associations of sperm whales. This underscores the importance of tailored conservation and management strategies that account for demographic variations for effective stewardship of this endangered species.

Introduction

One of the most intensive harvests under commercial whaling targeted sperm whales in the northern hemisphere (Yablokov & Zemsky 2000; Wade *et al.* 2007; Ivashchenko *et al.* 2014a). The long-term effects of this vigorous whaling and their recovery remain poorly understood. Although hunting became illegal in 1988, sperm whales are still endangered and face a number of anthropogenic threats, including vessel strikes, entanglement, plastic pollution, and climate change. (Carretta *et al.* 2018). To monitor recovering populations, managers need up-to-date animal density estimates, a better understanding of their demography, and large-scale seasonal movements. These metrics are difficult to quantify with traditional, logistically challenging shipboard methods given the vast distances and depths these animals travel. But since sperm whales produce highly distinctive echolocation clicks while foraging and navigating (Backus & Schevill 1966; Watkins 1980; Whitehead & Weilgart 1991), they are excellent candidates for passive acoustic monitoring (PAM). PAM provides an alternative to traditional, logistically challenging methods such as shipboard and aerial visual surveys. This dissertation aims to unravel the intricacies of sperm whale distribution, acoustic density estimation, and habitat association for different demographic groups in various regions in the northern hemisphere, ultimately contributing to a more comprehensive understanding of ecology.

Chapter 1 delves into the intriguing case of sperm whale distribution in the eastern Canadian Arctic's Baffin Bay, a region undergoing rapid sea ice loss and ocean warming. Historically, sperm whales were not known to frequent these icy waters, but recent sightings in 2014 and 2018 near Eclipse Sound have raised questions about their adaptability to changing conditions. By combining visual and acoustic data, this chapter investigates the spatiotemporal

distribution of sperm whales in the region, shedding light on their potential range expansion in response to climate change.

Chapter 2 takes us to the Eastern North Pacific, where traditional notions of sperm whale distribution are challenged. While it is commonly believed that females and their young prefer temperate and tropical latitudes, this chapter presents evidence of social groups in high-latitude regions like the Gulf of Alaska and Bering Sea/Aleutian Islands. Using passive acoustic data and sophisticated modeling techniques, this study uncovers the nuanced distribution and seasonal patterns of sperm whales, highlighting the need for a reevaluation of management protocols to address the complexities of their habitat use.

Chapter 3 further dissects the sexual dimorphism in sperm whales, emphasizing the importance of understanding demographic-specific spatiotemporal patterns for effective conservation and management. Focusing on the western North Atlantic, this chapter identifies three distinct classes of sperm whales and uncovers their distribution dynamics along a latitudinal gradient. The study goes beyond simple presence data and delves into the crucial aspect of density estimation. By utilizing two methods, one based on counting individual echolocation clicks and the other detecting animal groups in 5-minute time bins with at least one echolocation click, this research offers valuable insights into the acoustic density estimates for all three classes of sperm whales. These density estimates provide critical information about the relative abundance of each demographic group and their potential interactions with the ecosystem. Moreover, the findings not only reveal marked differences in seasonal presence but also suggest potential population recovery in certain regions, underscoring the necessity of tailored conservation strategies that account for the intricate dynamics of sperm whale populations in the western North Atlantic.

Chapter 4 explores the North Pacific once more, providing foundational insights into how sperm whale habitat preferences and associations vary across demographic groups. Leveraging passive acoustic data and statistical analysis, this chapter characterizes the spatial distribution of different groups, identifies significant demographic-dependent associations, and pinpoints seasonal high-use areas. These discoveries underscore the importance of considering demographic variations when assessing habitat associations, offering valuable insights for the conservation and management of North Pacific sperm whale populations.

This dissertation embarks on a multifaceted journey to unravel the mysteries of sperm whale distribution, habitat associations, and demographic dynamics in different regions of the northern hemisphere. By integrating findings from each chapter, we hope to highlight the importance of PAM in furthering our knowledge of sperm whale ecology and contributing to more informed conservation efforts and the sustainable management of this iconic species. Understanding the demographic composition is paramount in achieving these conservation and management goals, as it guides us in tailoring strategies to the unique needs of each group and ensuring the long-term well-being of sperm whales and the ecosystems they inhabit.

Chapter 1: Changes in Sea Ice and Range Expansion of Sperm Whales in the Eclipse Sound Region of Baffin Bay, Canada

Natalie Posdaljian[1], Caroline Soderstjerna[1], Joshua M. Jones[1], Alba Solsona-Berga[1], John A. Hildebrand[1], Kristin Westdal[2], Alex Ootoowak[2], Simone Baumann-Pickering[1]

[1] University of California San Diego, Scripps Institution of Oceanography, 9500 Gilman Drive, La Jolla, CA 92092-0205 USA

[2] Oceans North, 515-70 Arthur Street, Winnipeg, MB R3G 1B7, Canada

1.1 Abstract

Sperm whales (*Physeter macrocephalus*) are a cosmopolitan species but are only found in ice-free regions of the ocean. It is unknown how their distribution might change in regions undergoing rapid loss of sea ice and ocean warming like Baffin Bay in the eastern Canadian Arctic. In 2014 and 2018, sperm whales were sighted near Eclipse Sound, Baffin Bay: the first recorded uses of this region by sperm whales. In this study, we investigate the spatiotemporal distribution of sperm whales near Eclipse Sound using visual and acoustic data. We combine several published open-source, data sets to create a map of historical sperm whale presence in the region. We use passive acoustic data from two recording sites between 2015 and 2019 to investigate more recent presence in the region. We also analyze regional trends in sea ice concentration dating back to 1901 and relate acoustic presence of sperm whales to the mean sea ice concentration near the recording sites. We found no records of sperm whale sightings near Eclipse Sound outside of the 2014/2018 observations. Our acoustic data told a different story, with sperm whales recorded yearly from 2015-2019 with presence in the late summer and fall months. Sperm whale acoustic presence increased over the 5-year study duration and was closely related to the minimum sea ice concentration each year. Sperm whales, like other cetaceans, are ecosystem sentinels, or indicators of ecosystem change. Increasing number of days with sperm whale presence in the Eclipse Sound region could indicate range expansion of sperm whales as a result of changes in sea ice. Monitoring climate change-induced range expansion in this region is important to understand how increasing presence of a top-predator might impact the Arctic food web.

1.2 Introduction

Climate change is undoubtedly impacting Arctic marine environments (Hassol 2004; Kattsov *et al.* 2005; Ford *et al.* 2006). This region is undergoing loss of sea ice, ocean warming, changes in stratification from the introduction of freshwater, and ocean acidification (Comiso *et al.* 2008; Jackson *et al.* 2010; Carmack & McLaughlin 2011). Warming ocean temperatures and melting sea ice is leading to seasonal shifts of habitat use with some marine mammals showing increased presence and prolonged stays in areas that were historically covered in pack ice but are now open (Higdon & Ferguson 2011; Laidre *et al.* 2015; Insley *et al.* 2021). Rapid changes in sea ice could benefit marine mammals that are normally restricted to ice-free regions by exposing new habitats.

Sperm whales (*Physeter macrocephalus*) are a cosmopolitan toothed-whale species found in all of the world's oceans. Although sperm whales are ice avoiding, they have been documented in high latitude regions like the Davis Strait, Bering Sea, Norwegian Sea, and British Isles (Berzin 1972; Christensen *et al.* 1992; Evans 1997; Weir *et al.* 2001; Madsen *et al.* 2002; Davidson 2016) at the northernmost extent of their distribution. More recently, they have been recorded and observed within the Arctic Circle at approximately 75°N in eastern Baffin Bay, off northwest Greenland, extending their known range significantly north of previous reports (Frouin-Mouy *et al.* 2017). And although there have been no formal surveys to monitor sperm whale populations in western Baffin Bay (Cucknell *et al.* 2015; Davidson 2016) in 2014 the first sighting of a sperm whale was recorded by Inuit hunters in the Pond Inlet region (Cecco 2018), followed by a second rare sighting by scientists in 2018 (Lefort *et al.* 2022). Traditional ecological knowledge about marine mammals in the Canadian Arctic is extensive (Stevenson 1996; Ford *et al.* 2006; Worden *et al.* 2020) although little is known about sperm whales, even

by experienced hunters in Pond Inlet (Cecco 2018), most likely due to their infrequent presence in the region.

Baffin Bay has seen longer ice-free periods with sea ice retreating seven days earlier and sea ice advancing five days later per decade (Laidre *et al.* 2015). Walsh *et al.* (2017) reconstructed Arctic sea ice extent, including Baffin Bay, going back to 1850 and found no historical precedent for the minimum ice extent seen in the 21st century. And although patterns of sea ice loss differ between regions of the Arctic, the overall trend since 1990 shows a retreat of seasonal sea ice, with an acceleration during the last decades (Polyak *et al.* 2010). Loss of sea ice is so severe that climate simulations are predicting a seasonally ice-free Arctic Ocean as early as mid-century (Holland *et al.* 2006; Wang & Overland 2009; Masson-Delmotte *et al.* 2020).

Rapid changes to the region as a result of climate change coupled with newly documented sightings of sperm whales in the basin highlight the importance of closely studying their high latitude habitat use. Since sperm whales were heavily whaled beginning in the 1700s (Evans 1997), historical whaling records can also provide baseline information of whale distribution and presence. However, no records exist of sperm whales being caught in the Baffin Bay whaling grounds (Smith 2021). More recent studies of sperm whales using traditional visual surveys and satellite-tags in the western Baffin Bay and Davis Strait region have sightings between 63° N and 70° N, usually associated with the continental shelf and slope (Davidson 2016; Lefort *et al.* 2022), with no records as high north as the Pond Inlet (72.7° N) outside of the 2014/2018 observations (Cecco 2018; Lefort *et al.* 2022).

In this study, we use historical sighting and acoustic data to explore sperm whale presence in Baffin Bay. Published open-source data sets were synthesized to investigate the historical distribution of sperm whales in the region. Passive acoustic recordings from 2015-2019

in the Eclipse Sound were used to create a timeseries of recent animal presence in the region.

Decadal scale changes in sea ice concentration dating back to 1901 were analyzed using a linear

model and the acoustic data was related to mean sea ice concentration near the recording sites to

understand why the animals are expanding their northernmost boundaries. Results from this

study confirm and provide more detail on the increasing presence of sperm whales in the Eclipse

Sound, a historically rare habitat for these animals to exploit that may be linked to climate

change.

1.3 Methods

1.3.1 Historical Sperm Whale Distribution in Baffin Bay

Sighting data was compiled from eight published datasets and studies to gain a better

understanding of the historical distribution of sperm whales in Baffin Bay. Sampling effort for

the sighting data was only available for two of the eight data sets. First, for the Programme

Intégré de recherches sur les oiseaux pélagiques (PIROP) data set (CWS 2021), effort was

calculated by plotting the boundaries of where sperm whales were not sighted during their

surveys between 1970-2000 (Gjerdrum *et al.* 2012). Second, data points for sperm whale

sightings and survey effort area from Shell's marine mammal visual monitoring and mitigation

program from 2012-2014 were extracted and replicated from Frouin-Mouy *et al.* (2017) using

WebPlotDigitizer (Rohatgi 2017).

Although there was no sampling effort available for the remaining six data sets they were

included in the analysis as opportunistic sightings. Commercial whaling records for sperm

whales were accessed on the Ocean Biodiversity Information System (OBIS) from the History of

Marine Animal Populations (HMAP) Data Set 04: World Whaling (Smith 2021). Opportunistic

and incidental sightings of sperm whales were also retrieved from the Maritimes Region Whale

Sightings Database (WSDB) from Fisheries and Oceans Canada (Whalesightings Database 2021), the Incidental Sightings of Marine Mammals data set from the Institute of Marine Research (IMR) (Hartvedt 2020), and from environmental surveys done by the Northwest Atlantic Fisheries Organization (NAFO 2014). Opportunistic sightings from citizen scientists were included from the Happywhale database (Happywhale 2021). One additional opportunistic sighting of a sperm whale in Eclipse Sound and tag data from sperm whales in Baffin Bay reported in Lefort *et al.* (2022) were also used. The synthesized data are given in an associated data publication in Dryad Digital Repository (https://doi.org/10.5061/dryad.c2fqz619z; Posdaljian et al. 2022).

1.3.2 Acoustic Data Collection

We used passive acoustic recordings from two sites in the eastern Canadian Arctic near Eclipse Sound between July 2015 and September 2019 over the span of five deployments (Figure 1.1, Table 1.1). The temporal coverage among sites and between deployments varied as a result of field work timing to retrieve/deploy the instruments, the battery life and storage space of the instruments, and different duty cycle regimes discussed in further detail in the last Methods subsection. The two sites were approximately 23 km apart and have an approximate maximum detection range of 20 km for sperm whales based on previous studies (Tran *et al.* 2014). The Guys Bight (GB) instrument had one deployment at a depth of ~100 m in 2015. The depth of the instrument is not ideal for recording a deep-diving animal such as the sperm whale, but the recordings from 2015 were still included in the analysis as an opportunistic data set, in the sense that it was not necessarily acquired for this specific study. The instrument at Pond Inlet (PI) was at depths between 670 and 800 m over four deployment periods from 2016-2019 (Table 1.1). We used data from two types of autonomous, bottom-mounted recording devices to collect passive

acoustic recordings: Song Meter SM2M (SM2M; Wildlife Acoustics Inc, Concord, MA, USA) and High-frequency Acoustic Recording Package (HARP; (Wiggins & Hildebrand 2007). The SM2M was deployed at the GB site and recorded at a sampling rate of 192 kHz. The HARPs were deployed at the PI site and collected recordings at a sampling rate of 200 kHz. These two sampling rates were chosen to detect the high-frequency echolocation clicks of marine mammals, including but not limited to sperm whales.

1.3.3 Acoustic Data Analysis at the Guys Bight Recording Site

Sperm whales regularly produce high-frequency echolocation clicks (2 - 32 kHz) with a duration of 100 μs and are distinguishable from other high-frequency odontocetes (Weilgart & Whitehead 1988; Goold & Jones 1995; Møhl *et al.* 2000, 2003) (Figure 1.2). Trained analysts (NP and CS) manually screened the acoustic recordings from the GB site for sperm whale echolocation clicks using long-term spectral averages (LTSAs; averaged over 5 s and 100 Hz bins), which provide a compressed spectrogram view allowing large time series data sets to be analyzed (Wiggins & Hildebrand 2007) (Figure 1.2). Data were manually scanned in the custom software program *Triton* (Wiggins & Hildebrand 2007) developed in *MATLAB* (Inc. 2016). Analysts viewed 1-hour LTSA segments across a frequency range of 0 to 40 kHz to identify potential sperm whale encounters. Spectrograms of 10 s in length were used to confirm species identification (Fast Fourier transform length 2000 points, 75% overlap, bandwidth 40 kHz). A sperm whale encounter was defined as a series of clicks within a recording period of 5 minutes. The start and end times of these encounters were logged in *Triton* (Wiggins & Hildebrand 2007) and used for further analysis.

Since all LTSA detections were visually verified by trained analysts, we assumed there were no false positives. And given the distinguishable echolocation clicks of sperm whales and

the short duration of the data, we assumed negligible missed detections because of the feasibility of listening to and viewing all spectrograms of interest.

1.3.4 Acoustic Data Analysis at the Pond Inlet Recording Site

Clicks at the PI site were automatically detected using a multi-step approach (Roch *et al.* 2011; Soldevilla *et al.* 2011; Solsona-Berga *et al.* 2020). This approach was developed for acoustic data that was sampled at 200 kHz (PI recording site), which is why manual analysis was conducted for the GB site that was sampled at 196 kHz (Table 1.1).

Since sperm whale clicks are characterized by multiple pulses approximately 5 ms apart (Møhl *et al.* 2000), clicks closer than 30 ms apart were merged. Band passing all acoustic data (5-95 kHz) minimized the effects of low-frequency noise from vessels or weather. Calculating the spectra of detected signals required 4 ms of data and a 512-point Hann window centered on the click with 50% overlap. To account for the frequency dependent instrument response of each deployment, spectra were corrected for the hydrophone transfer function.

Sperm whale echolocation clicks are similar to the impulsive signals from ship propeller cavitation, so an automated detector was used to exclude periods of ship passages in the PI data to reduce the number of false positive detections. The detector, developed by Solsona-Berga et al. (2020) identified potential ship passages from LTSAs. Average power spectral densities (APSD) were computed in 2-hour data blocks over low (1-5 kHz), medium (5-10 kHz), and high (10-50 kHz) frequency bands. Using received sound levels, transient signals such as odontocetes, ship passages, and weather, were compared in the three frequency bands. Trained acousticians (NP and CS) manually verified identified ship passages in *Triton* (Wiggins & Hildebrand 2007; Solsona-Berga *et al.* 2020). Ship passage times were removed from further analysis and considered time periods with no recording effort.

Noise produced by the instruments and clicks produced by non-sperm whale odontocetes were also removed in the PI data to reduce the number of false positive detections. A basic classifier using spectral click shape and peak frequency was implemented, taking advantage of a sperm whale click's distinctive lower frequency spectral shape to remove clicks by delphinids and beaked whales which occur at higher frequencies (Solsona-Berga *et al.* 2020). The remaining acoustic encounters at site PI, containing presumed sperm whale echolocation clicks, were manually reviewed with *DetEdit* (Solsona-Berga *et al.* 2020). *DetEdit* provides users with interactive data visualizations that aid in efficiently annotating data, allowing deletion of false detections. Sperm whale clicks were binned into 5-minute intervals, and the number of 5-minute bins with sperm whale detections per day was considered for further analysis. Daily averages of 5-minute bins were calculated only for days with sperm whale presence since the time series was zero-inflated.

Only clicks exceeding a peak-to-peak received level (RL) of 125 dBpp re 1 µPa were included to provide a consistent detection threshold. This step of the detection process excluded clicks with low RLs. However, by binning clicks into 5-minute intervals, the chances of missing presence within a bin was low for sperm whales who click regularly. The acoustic metadata are given in an associated data publication in Dryad Digital Repository (https://doi.org/10.5061/dryad.c2fqz619z; Posdaljian et al. 2022).

1.3.5 Accounting for the Duty Cycle

Duty cycle regimes, or the process of turning an acoustic recorder on at specified intervals, are implemented to maximize the deployment duration by conserving battery power and storage space of the instrument (Wiggins & Hildebrand 2007; Au *et al.* 2013). Duty cycle regimes can widely vary based on the desired deployment duration, the sampling rate, and the

recording instrument. Two of the five deployments in this study had a duty cycle that was adjusted for.

The GB deployment had a duty cycle with a 5 minute recording duration in a 60 minute cycle (Table 1.1). Because there was only one deployment at this site, we had no continuous data to quantify the impact of the duty cycle. Instead, the number of 5-minute bins with sperm whale detections per day was linearly adjusted based on the recording effort in the duty cycle. The third deployment at the PI site also had a duty cycle with a 15 minute recording duration in a 20 minute cycle (Table 1.1). Since there was continuous data from three other deployments at this site, the duty cycle was evaluated on continuously sampled data from the first deployment (less presence of sperm whales) and the fourth deployment (more presence of sperm whales). Random samples of the 15/20 duty cycle were taken from the deployments, shifting the listening period by one minute to find the proportion of overall recording effort. Sperm whale clicks in the 2017 PI deployment were linearly adjusted by 0.0839, resulting from the mean of forced duty cycles on the 2016 and 2019 deployments (0.0939 and 0.0738 respectively).

1.3.6 Changes in Sea Ice Concentration

A monthly gridded sea ice concentration (SIC) product ranging from 1850 to 2017 was used to evaluate historical changes of sea ice within a 20 km radius around the PI recording site (Walsh *et al.* 2019). Only data from 1901 and beyond was included to avoid data sets that had non-observed data which were supplemented with estimates. The 20 km radius was selected as a maximum detection range for sperm whales clicks based on a previous study (Tran *et al.* 2014) and distance within which most interactions with the surface would likely occur. Six ¼ degree latitude by ¼ degree longitude grid cells were within 20 km of the recording site and included in the analysis. This sea ice product merges 18 different data sources and provides a single mid-

month day (MMD) average from each available source. The MMD average for the six grid cells near the recording site were averaged across the multiple sources (when available) to produce a single MMD average for the 20 km radius around the site. A linear regression was used to model the relationship between year and the median MMD SIC average by fitting a linear equation to the observed data in R Statistical Software (R Core Team 2022).

A finer resolution of mean daily SIC was used to compare with daily presence of sperm whales during our recording period from 2015-2019. Daily Advanced Microwave Scanning Radiometer 2 (AMSR2) sea ice maps were obtained from the University of Bremen (Spreen *et al.* 2008) and processed using Windows Image Manager (WIM) and Windows Automation Module (WAM) software (Kahru 2001) to produce an annual time series of mean daily SIC within a 20 km radius mask around the recording site. WAM software was used to compute the daily arithmetic mean, variance, and median of the SIC as a percent of the total mask area. The data excludes locations within 1 km from land to reduce edge effects and influence of snow on land.

1.4 Results

1.4.1 Historical Sperm Whale Distribution in Baffin Bay

Sperm whales have been historically observed throughout Baffin Bay. The highest concentration of sperm whales was seen in eastern Baffin Bay below 70ºN, although they have been documented in eastern Baffin Bay as far north as 75ºN (Figure 1.3). In northwestern Baffin Bay, a sperm whale was observed in September of 2018 in Eclipse Sound, 48 km west of the PI recording location (Lefort *et al.* 2022). All of the northernmost sightings of sperm whales were documented within the last decade, supporting our hypothesis that sperm whale presence in Eclipse Sound is a recent phenomenon.

1.4.2 Sperm Whale Presence

Daily sperm whale presence (total number of 5-min bins) was calculated from the Guys

Bight (GB) site in 2015 and from the Pond Inlet (PI) site during 2016-2019. Sperm whales were

acoustically detected during late summer and early fall months. At site GB, whales were present

for four days in September, with a median of 9 5-min bins per day (IQR = 6). At site PI in 2016,

sperm whales were present for three days in September, with a median of 24 5-min bins per day

(IQR = 18). At site PI in 2017 and 2018 animals were present for 12 days in September and 6

days in October respectively, with a median of 9 5-min bins per day (IQR = 17) in 2017 and 24

bins per day (IQR = 21) in 2018. At site PI in 2019, sperm whales were present for 17 days in

July and August, with a median of 47 bins per day (IQR = 64) (Table 1.2; Figure 1.4).

1.4.3 Changes in Sea Ice Concentration

The yearly median MMD of SIC had a linear relationship with year with a negative slope

and an equation of y = 170 – 0.039x. The variable year was significant and had a p-value of

1.41e-0.6 and an R-squared of 0.18 (Figure 1.5). The number of months with a MMD average

SIC of zero appears to increase over the decades. The 1910s and 1920s were the decades with the

least number of months with a MMD average SIC of zero (n = 3-4) and the 2000s had the

greatest number of months with a MMD average SIC of zero (n = 24) from decades with a

complete data set (Figure 1.5).

Mean daily SIC within a 20 km radius of the PI recording site ranged from nearly 0-

100% mean daily SIC from 2015-2019. When sperm whales were present, the mean daily SIC

was 2.1% (SD = 2.4), with the lowest mean daily SIC in 2016 (mean = 0.4%, SD = 0.1) and

2019 (mean = 0.8%, SD = 0.7 respectively) (Figure 1.4).

1.5 Discussion

Based on our acoustic data, there is clear evidence that sperm whales are frequenting the Eclipse Sound region of Baffin Bay in the late summer and fall months when SIC is at its lowest. Our findings are similar to Frouin-Mouy *et al.* (2017) who observed and recorded sperm whales in northeastern Baffin Bay for the first time at a latitude of 75º N in the summer and fall months between 2012 and 2014. There were no records of sperm whales in northwestern Baffin Bay (outside of the 2018 observation) from published information or open-source datasets. One sperm whale was reportedly sighted in 2014 in Eclipse Sound by residents of the community of Pond Inlet (Cecco, 2018), but documentation of this occurrence has not been published to date and therefore was not included in Figure 3. According to the unpublished MS thesis by Davidson (2016), sperm whales were observed as far north as 70ºN in western Baffin Bay during R/V Pâmiut annual surveys from 1999 to 2014. Survey lines from the R/V Pâmiut do indicate sampling effort as far north as 75ºN, including waters directly outside of the Eclipse Sound, where no observations of sperm whales were made (Davidson 2016).

The distribution of sperm whales from the open-source data sets are biased by sampling effort. Since most of the data collection was opportunistic and ship tracklines and visual effort are not available, observations cannot be adjusted for sampling. It is likely that effort was not consistent throughout the region and was concentrated in the southern half or eastern region of Baffin Bay. However, sightings and sampling effort from the R/V Pâmiut annual surveys do provide some evidence that sperm whales were not using habitats as far northwest as Eclipse Sound before 2014 (Davidson 2016). In addition, given that Inuit hunters, who are very familiar with this region and its marine mammals, were also surprised by the initial 2014 sighting provides further evidence that sperm whales are inhabiting new regions of Baffin Bay.

Over the span of the acoustic recording period from 2015-2019 the number of days with sperm whale presence appears to increase. In 2015 and 2016, they were only recorded for a few days but by 2019, sperm whales were in the area for at least 17 days. The instrument stopped recording on September 21st, 2019, so it is possible that we did not capture their entire stay in the area. Although there were only four days with presence in 2015, we cannot conclude there was a definite increase between 2015 and 2016, since differences in detectability of sperm whales between the two instruments (SM2M and HARP) and at the two sites is unknown. The shallow depth (100 m) of the opportunistic SM2M instrument at the GB site could also affect detectability of these deep diving animals. Sperm whales are more often found in deeper waters but sperm whale detections at our shallow site may be explained, at least partially, by the use of shallow habitats by male sperm whales in higher latitudes (Teloni *et al.* 2008).

Sperm whale presence during periods of lowest SIC, as described in this study, is similar to findings by Frouin-Mouy *et al.* (2017) who recorded sperm whales only before sea ice formation and after the sea ice had disappeared. The first known sightings of sperm whales in northern Baffin Bay occurred within the last decade (NE Baffin Bay – 2012; NW Baffin Bay – 2014). This coincides with the results of this study which reveal a decrease in the yearly median MMD SIC in Eclipse Sound and the increase of the number of months with a MMD average SIC of zero, particularly in the last decade. On a larger scale, Arctic sea ice extent has likely decreased for every month of the year since 1979 with the most reduction (~40%) seen in September months. Several climate projections even anticipate at least one practically sea ice free September before 2050 (Masson-Delmotte *et al.* 2020).

Loss of sea ice and longer open water seasons will likely benefit sperm whales who appear to be expanding their range further north than previously known. Similar northern

expansions have already been recorded in other marine mammals in the eastern Canadian Arctic such as killer, humpback, and minke whales (Higdon & Ferguson 2009, 2018). There is also evidence of northerly expansion of sperm whales in the Russian Arctic significantly beyond their range end (Popov & Eichhorn 2020) and in Svalbard waters (Storrie *et al.* 2018). These observations in higher latitudes may also be related to reduced ice cover, increased open water seasons, increasing ocean temperatures, and changes in their prey distributions. Like other marine mammals, sperm whale distribution is closely related to the distribution of their preferred prey of fish and cephalopods. Several species of cephalopod that sperm whales prefer, particularly the armhook squid (*Gonatus fabricci*), have already been recorded in high but patchy concentrations throughout Baffin Bay including in Eclipse Sound (Gardiner & Dick 2010; Davidson 2016). With lower SIC and longer open water seasons, sperm whales may be expanding their range to specific northern areas like the Eclipse Sound to take advantage of the particularly high cephalopod concentrations.

Increased presence of a top predator in the northern region could impact the Arctic food web and increase competition for other toothed whales and fisheries species who consume cephalopods. Narwhals and belugas are endemic to the Arctic region and have a cultural and socioeconomic importance for Inuit hunters (Lee & Wenzel 2006). In Eclipse Sound during the summer when sperm whales are also present, stomach contents of narwhals and belugas reveal that they mostly consume Arctic cod, Greenland halibut, and in more recent years, Capelin (Finley & Gibb 1982; Watt & Ferguson 2015). Narwhals are extremely common in Eclipse Sound, Nunavut (Jones *et al.* 2022), and although 92% of narwhals had armhook squid beaks in their stomachs, they were not representative of recent intake but more likely intake earlier in the summer (Finley & Gibb 1982). Belugas are considered rare in Eclipse Sound (Jones *et al.* 2022)

and although they consume armhook squid among other prey items in their wintering areas, they mostly prey on Arctic Cod in the Canadian Arctic during the summer (Heide-Jørgensen & Teilmann 1994; Gardiner & Dick 2010). This could imply that although sperm whales narwhals, and belugas can be found in the same region and both consume the same species of squid, their prey preference does not overlap spatially or temporally. The Greenland halibut fishery is extremely important to Baffin Bay and Davis Strait. Since both sperm whales and halibut prey on cephalopods, including armhook squid (Orr & Bowering 1997; Dawe *et al.* 1998), it will be important to monitor how increasing sperm whales in the region could impact the fishery (Gardiner & Dick 2010; Davidson 2016).

Long-term passive acoustic monitoring from this study increased our knowledge of sperm whale presence in a remote region that is difficult to study with traditional marine mammal monitoring techniques such as visual surveys. Acoustic data from this study, as well as Frouin-Mouy *et al.* (2017), reveal the highest latitudinal occurrence for sperm whales in the Baffin Bay. This study also provides evidence of increasing temporal occurrence of sperm whales in Eclipse Sound, Baffin Bay in the late summer and fall months when SIC is at its lowest. Our results highlight the effectiveness of passive acoustic monitoring in remote regions and the importance of a dedicated acoustic or visual survey for sperm whales in this region to improve understanding of their ecology at their range boundary and create a baseline knowledge of their spatiotemporal distribution in a rapidly changing ecosystem.

1.6 Acknowledgements

Chapter 1, in full, is a reprint of the material as it appears in Global Change Biology, Posdaljian, Natalie, Caroline Soderstjerna, Joshua M. Jones, Alba Solsona-Berga, John A. Hildebrand, Kristin Westdal, Alex Ootoowak, and Simone Baumann-Pickering. "Changes in sea ice and range expansion of sperm whales in the eclipse sound region of Baffin Bay, Canada." Global change biology 28, no. 12 (2022): 3860-3870. The dissertation author was primarily responsible for the investigation and writing of this material.

1.7 Figures and Tables
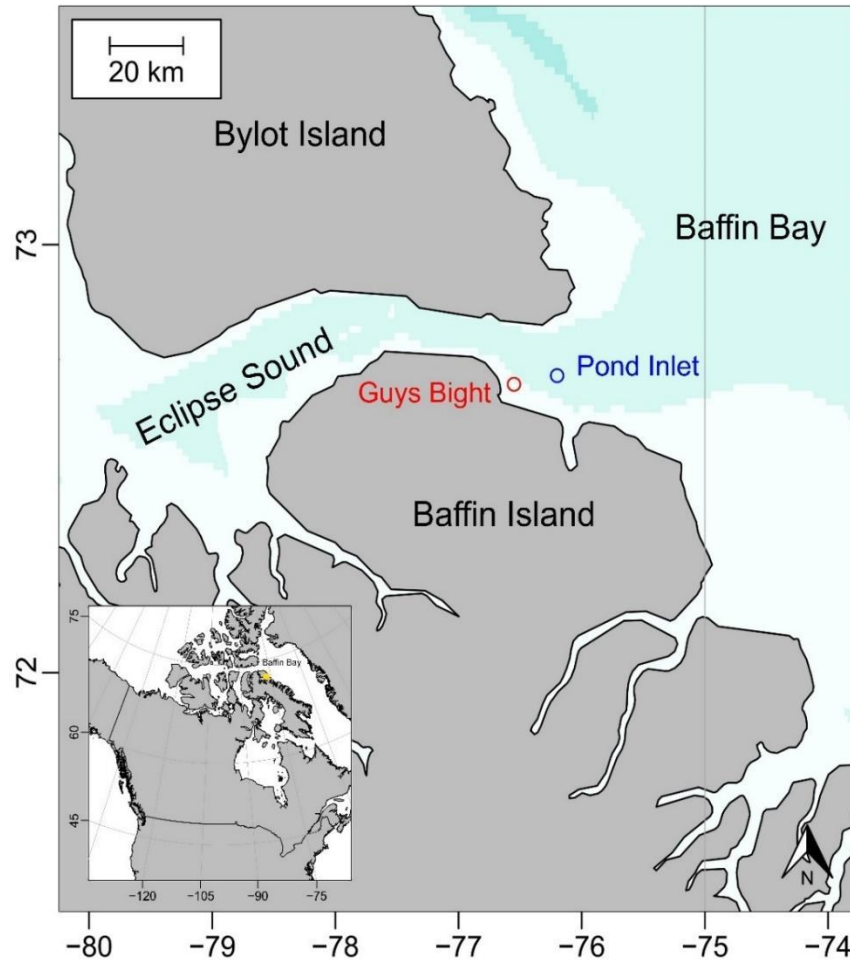
Figure 1.1. The Eclipse Sound region of Baffin Bay in the eastern Canadian Arctic with the Guys Bight recording site (red) and the Pond Inlet recording site (blue).

Table 1.1. Summary of passive acoustic monitoring effort in the eastern Canadian Arctic between 2015 and 2019. Dates are given as MM/DD/YYYY. Instrument type specifies either a Song Meter SM2M (SM2M) or a High-Frequency Acoustic Recording Package (HARP). If applicable, duty cycles are defined as the duration of the recording period (minutes on)/cycle period (minutes). Data collected by Oceans North (ON) and Scripps Institution of Oceanography (SIO).

Site	Location	Depth (m)	Recording dates	No. of recording days	Instrument type	Duty cycle	Sampling rate (kHz)	Data Owner
Guys Bight (GB)	72.65N, -75.56W	100	07/01/15 – 9/29/15	91	SM2M	5/60	192	ON
Pond Inlet (PI)	72.72N, -76.23W	800	5/28/16 – 10/05/16	130	HARP	--	200	SIO
		670	10/05/16 – 08/04/17	302		--		
		670	08/15/17 – 01/30/18	168		15/20		
		670	09/27/18 – 09/21/19	359		--		
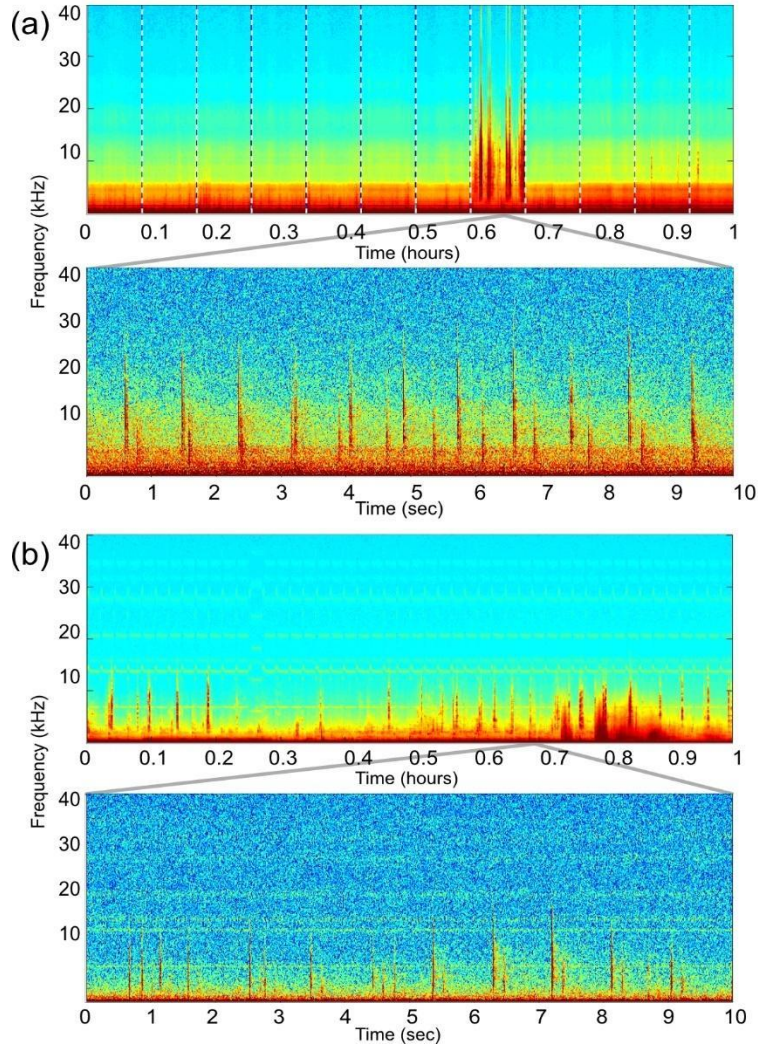
Figure 1.2. Sperm whale clicks from Guys Bight (a) recorded on September 23, 2015 and from Pond Inlet (b) recorded on August 8, 2019. The top panel from each site displays a long term spectral average (LTSA) and the bottom panel displays the spectrogram. The Guys Bight LTSA (a) has vertical lines delineating gaps in the data as a result of the duty cycle. So although the LTSA displays 1 hour of acoustic data, the overall length of the data shown encompasses 12 hours.
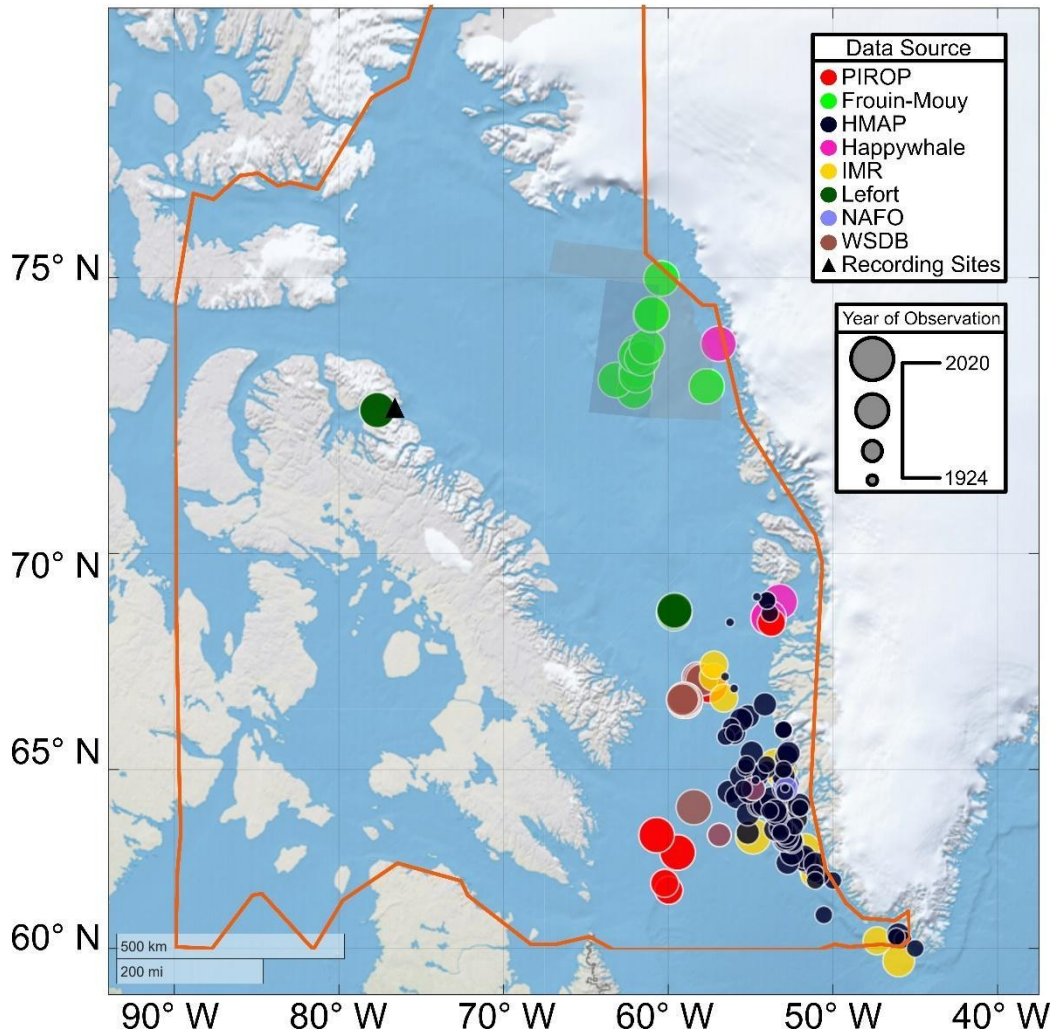
Figure 1.3. Sperm whale sightings in Baffin Bay from opportunistic survey sightings, historical whaling data, citizen science, and visual monitoring programs represented in different colors based on the source of the data. The orange boundary represents the spatial sampling effort for the PIROP surveys (Gjerdrum et al. 2012). The grey sampling area represents the boundaries of the visual monitoring program for Shell and other exploration licenses (Frouin-Mouy et al. 2017). The size of the bubbles represents the year the observation was made, with smaller bubbles indicating observations made earlier in time.
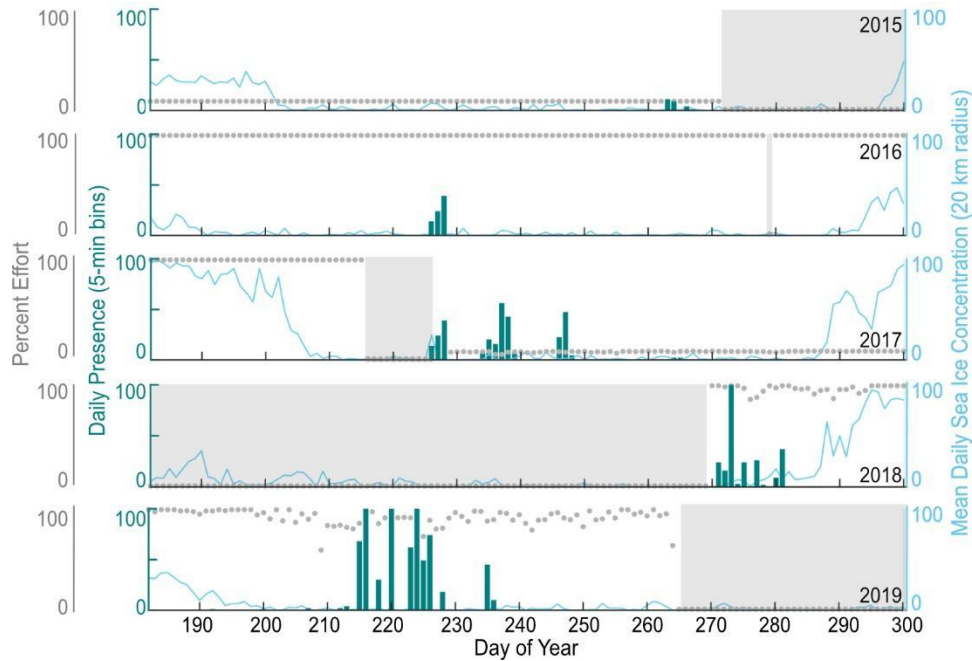
Figure 1.4. Daily presence of sperm whales (sum of 5-min bins) in teal from the Guys Bight recording site (2015) and the Pond Inlet recording site (2016-2019) between the 190th and 300th day of the year when there were sperm whale detections. Percentage of recording effort per day with grey dots. Time periods without recordings shaded grey. Mean daily sea ice concentration for a 20 km radius area centered on the Pond Inlet recording site in light blue.

Table 1.2. Summary of the number of days with sperm whale presence, the median number of 5-min bins per day, and the interquartile range for each deployment at each site.

Site	Deployment no.	No. of days with presence	Median no. of 5-min bins/day	Interquartile range (IQR)
Guys Bight (GB)	1	4	9	6
Pond Inlet (PI)	1	3	24	18
	2	12	9	17
	3	6	24	21
	4	7	27	64
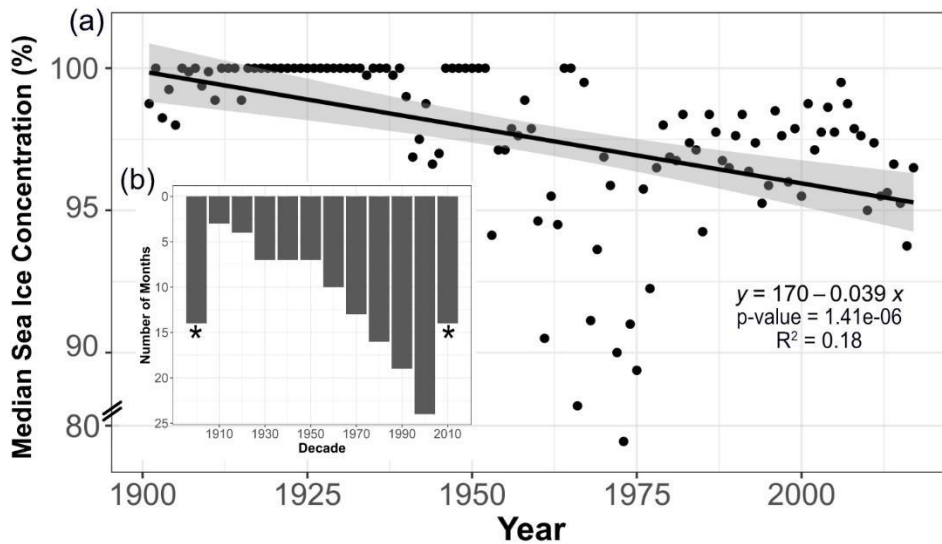
Figure 1.5. The yearly median mid-month day sea ice concentration from 1901 to 2017 with a regression line (black) and the standard error of the estimate (grey shading). The equation for the linear regression, the p-value for the variable year, and the R^2 are on the right side of the plot. The hash lines on the y-axis represent an omission in median sea ice concentration values to reduce the amount of empty space in the plot. (b) The inset plot shows a histogram of the number of months with a mid-month day average sea ice concentration of zero for each decade beginning from the 1900s to the 2010s. The black asterisks denote decades that are incomplete (1900s – missing 1 year, 2010s – missing 2 years).

Chapter 2: Sperm Whales Demographics in the Gulf of Alaska and Bering Sea/Aleutian Islands: An Overlooked Female Habitat

Natalie Posdaljian[1*], Alba Solsona-Berga[1], John A. Hildebrand[1], Caroline Soderstjerna[1], Sean M. Wiggins[1], Kieran Lenssen[1], Simone Baumann-Pickering[1]

[1] Scripps Institution of Oceanography, University of California San Diego, La Jolla, California, United States of America

2.1 Abstract

Sperm whales exhibit sexual dimorphism and sex-specific latitudinal segregation. Females and their young form social groups and are usually found in temperate and tropical latitudes, while males forage at higher latitudes. Historical whaling data and rare sightings of social groups in high latitude regions of the North Pacific, such as the Gulf of Alaska (GOA) and Bering Sea/Aleutian Islands (BSAI), suggest a more nuanced distribution than previously understood. Sperm whales are the most sighted and recorded cetacean in marine mammal surveys in these regions but capturing their demographic composition and habitat use has proven challenging. This study detects sperm whale presence using passive acoustic data from seven sites in the GOA and BSAI from 2010 to 2019. Differences in click characteristics between males and females (i.e., inter-click and inter-pulse interval) was used as a proxy for animal size/sex to derive time series of animal detections. Generalized additive models with generalized estimation equations demonstrate how spatiotemporal patterns differ between the sexes. Social groups were present at all recording sites with the largest relative proportion at two seamount sites in the GOA and an island site in the BSAI. We found that the seasonal patterns of presence varied for the sexes and between the sites. Male presence was highest in the summer and lowest in the winter, conversely, social group peak presence was in the winter for the BSAI and in the spring for the GOA region, with the lowest presence in the summer months. This study demonstrates that social groups are not restricted to lower latitudes and captures their present-day habitat use in the North Pacific. It highlights that sperm whale distribution is more complex than accounted for in management protocol and underscores the need for improved understanding of sperm whale demographic composition to better understand the impacts of

increasing anthropogenic threats, particularly climate change which could impact male and female sperm whales differently.

2.1 Introduction

Male and female sperm whales are sexually dimorphic and the sexes have differences in behavior and habitat preference that result in differences in their distribution and seasonality (Best 1979; Rice 1989; Gregr & Trites 2001). Females and their dependent young form social groups and are known to inhabit temperate and tropical latitudes (Best 1979; Whitehead 2003). As males mature, they leave their social group and travel to higher latitudes, where they form bachelor groups as juveniles and are mostly solitary as they mature sexually (Best 1979; Rice 1989; Whitehead 2003). The males are thought to make periodic migrations to lower latitude breeding grounds once they are sexually mature (Best 1979; Rice 1989; Whitehead 2003). Recognizing these demographic differences, sperm whales are managed within the North Pacific stock by the NOAA National Marine Fisheries Service as a single demographic group (Carretta *et al.* 2020) consisting of only adult males (Mesnick *et al.* 2011).

In the North Pacific, particularly in the Gulf of Alaska (GOA) and Bering Sea/Aleutian Islands (BSAI) regions, most sperm whale distribution data come from a combination of historical whaling data and visual surveys. Social groups were reported in whaling data in the North Pacific as far north as 50ºN in the summer (Tomlin 1967; Mizroch & Rice 2013) several records of sperm whales of both sexes overwintering in the western Aleutians (Berzin & Rovnin 1966; Nishiwaki 1966; Berzin 1971, 1972; Mizroch & Rice 2013; Fearnbach *et al.* 2014; Ivashchenko *et al.* 2014). Estimates for female sperm whale catches range from 6% of total catch above 50ºN (Mizroch & Rice 2013) to 80% in the western Aleutians, western Bering Sea, and the USSR defined Gulf of Alaska (Ivashchenko *et al.* 2014). More recent surveys report a

sighting of a group of females and immature sperm whales in the Central Aleutians (Fearnbach *et al.* 2014) and a group of eleven mixed-sex individuals, including one calf in the summer off the continental slope southwest of Kodiak Island (Rone *et al.* 2017). This historical and contemporary evidence demonstrates that social groups are not restricted to temperate and tropical latitudes and that their distribution is more complex than currently represented in management assessments.

Sperm whales are deep-diving cetaceans that spend more than 70% of their time in foraging dive cycles (Watwood *et al.* 2006). The high proportion of time spent at depth makes them difficult to study using typical visual line-transect surveys, but they are excellent candidates for Passive Acoustic Monitoring (PAM) due to their high-amplitude and easily identifiable echolocation signals (Watkins 1980). Three acoustic studies have documented the presence of sperm whales in the GOA (Mellinger *et al.* 2004; Diogou *et al.* 2019b; Rice *et al.* 2021). Additional recordings from more sites with longer time series would allow for characterization of the spatiotemporal patterns of these animals.

Differences between male and female body size is linked to differences in sperm whale click characteristics (Gordon 1991; Growcott *et al.* 2011; Solsona-Berga *et al.* 2022). Sperm whales produce broadband echolocation clicks in the 8 Hz to 20 kHz band, with a distinct spectral shape and a peak frequency at about 10 kHz (Møhl *et al.* 2000). Male sperm whale echolocation clicks have high source levels (236 dB re 1 μPa at 1 m; Møhl *et al.* 2000) resulting in their detection over long distances (9-90 km; (Madsen *et al.* 2002; Barlow & Taylor 2005; Mathias *et al.* 2013). Sperm whale echolocation clicks have a multipulse structure (Backus & Schevill 1966), and the time between these pulses is called the Inter-Pulse Interval (IPI). The IPI is a result of the time taken for the click to reflect multiple times between air sacs at opposite

ends of the spermaceti organ and to exit the rostrum in several subsequent pulses (Norris &

Harvey 1972; Møhl *et al.* 2000). Since the length of the spermaceti organ or the rostrum of the

animal is about one-third of the total body length (Nishiwaki *et al.* 1963), stereo photogrammetry

measurements of body length and the speed of sound in the spermaceti organ allow for the

derivation of two equations (based on two different populations) that relate IPI measurements to

body length (Gordon 1991; Growcott *et al.* 2011). Several studies have used manual and

automatic extraction methods to estimate the acoustic length from IPIs recorded by acoustic tags

and single sensor instruments (Caruso *et al.* 2015; Beslin *et al.* 2018). Average IPI values range

from 2-9 ms which translates to an acoustic body length estimate of 7.7 to 17.8 m. A key

application of these studies is to differentiate male and female animals based on their IPI and

inferred body size.

Due to source directionality, most recorded sperm whale clicks do not display a clear

multi-pulse structure and tend to have complex pulse trains (Møhl *et al.* 2003; Zimmer *et al.*

2005; Beslin *et al.* 2018). This limitation results in sparse information about demographic

composition since the number of IPI measurements that are possible from acoustic recordings is

limited. An alternative approach is to use the Inter-Click Interval (ICI), which is the time

between pulse trains, as a proxy for sperm whale body size and sex, particularly for large-scale

acoustic monitoring where clicking bouts can last for hours (Solsona-Berga *et al.* 2022). Adult

males and females also have different ICIs, with males clicking every ~1s and females clicking

every 0.5s (Goold & Jones 1995), which is like other odontocetes that display a relationship

between ICI and body size (Jensen *et al.* 2018).

In this study, we used acoustic recordings of sperm whale echolocation clicks and the

differences in their ICI to derive spatiotemporal patterns for male and female sperm whales at

five sites in the GOA and two sites in the BSAI spanning the years 2010 to 2019. These data were investigated on an hourly and daily level to understand temporal and spatial habitat use. Generalized additive models (GAMs) with generalized estimation equations (GEEs) were used to evaluate significant spatiotemporal patterns for males and females and compared to available literature, including historical whaling data. Additionally, we used Generalized Linear Models (GLMs) to explain the relationship between sperm whale presence and drivers of presence like small- and large-scale climate variability. This study provides a baseline for sperm whale demographic presence and builds on spatiotemporal patterns described in a region experiencing environmental change. The demographic complexities revealed in this study suggest the need to re-evaluate management of the North Pacific stock, which currently only accounts for adult male presence. Demographic specific responses to climate change should be accounted for to develop the most effective plans for conservation and protection of this species.

2.3 Methods

2.3.1 Data Collection

Passive acoustic recordings were collected at seven sites, two along the BSAI and five in the GOA, between June 2010 and September 2019 (Figure 2.1, Table 2.1). Each site had from one to ten deployments which resulted in ~12 years of cumulative recordings between all sites. Individual site temporal coverage varied due to project goals, recorder battery life, data storage space, and duty cycle regimes as detailed below. The sites were in moderate water depths of 780 m to 1200 m (Table 2.1). We used High-frequency Acoustic Recording Packages (HARPs; Wiggins and Hildebrand 2007) with a sampling rate of 200 kHz which can detect the high-frequency echolocation clicks of odontocetes, including but not limited to, sperm whales.

2.3.2 Detecting Sperm Whales

Sperm whale echolocation clicks were detected using the multi-step approach described in Solsona-Berga *et al.* 2020 (appendix). These clicks have multiple pulses (Backus & Schevill 1966), 2-9 ms apart, depending upon the size of the animal (Norris & Harvey 1972). As a result, the detector had a lockout for clicks separated by less than 30 ms to avoid multiple detections of a single click. Band passing the data (5-95 kHz) minimized the effects of low-frequency noise from vessels, weather, or instrument self-noise on detections, but allowed for detection of the echolocation clicks of toothed whales. The Power Spectral Density (PSD) of detected signals was calculated with the *Pwelch* method (MATLAB, 39) using 4 ms of the waveform and a 512-point Hann window with 50% overlap (Welch 1967). Instrument specific full-system transfer functions were applied to account for the hydrophone sensor response, signal conditioning electronics, and analog-to-digital conversion. To provide a consistent detection threshold, only clicks exceeding peak-to-peak (pp) sound pressure level (RL) of at least 125 dBpp re 1 µPa were analyzed. This threshold was chosen to eliminate noise signals and the echolocation clicks of other odontocetes, while retaining sperm whale clicks.

Sperm whale echolocation clicks can be confused with the impulsive signals from ship propeller cavitation. An automated classifier developed by Solsona-Berga *et al.* 2020 (appendix) was used to exclude periods of ship passages. The classifier identified potential ship passages from long-term spectral averages (LTSA), which are long duration spectrograms (Wiggins & Hildebrand 2007). Further averaging was calculated as Average Power Spectral Densities (APSD) per 2-hour blocks over low (1-5 kHz), medium (5-10 kHz), and high (10-50 kHz) frequency bands with 100 Hz bins and 50% overlap. Using received sound levels, transient ship passage signals were separated from odontocete echolocation clicks and weather events. A

trained analyst manually reviewed identified ship passages using the MATLAB-based custom software program *Triton* (Wiggins & Hildebrand 2007). Ship passage times were removed from further analysis and considered time periods with no effort.

Instrument self-noise and the echolocation clicks of other odontocetes were also removed to reduce the number of false positive detections. A classifier using spectral click shape was implemented, taking advantage of a sperm whale click's distinct low-frequency spectral shape to remove dissimilar clicks by delphinid and beaked whales, which typically have higher frequencies (Solsona-Berga *et al.* 2020). The remaining acoustic encounters containing putative sperm whale echolocation clicks were manually reviewed with *DetEdit*, a custom, MATLAB-based graphical user interface (GUI) software program used to view, evaluate, and edit automatic detections (Solsona-Berga *et al.* 2020).

2.3.4 Click Characteristics as a Proxy for Demographics

Histograms of ICI provide a visualization that can be used to indicate sperm whale size and sex (Solsona-Berga *et al.* 2022). A plot of concatenated histograms, referred to as ICIgrams, was annotated and categorized for each time period at each site. Examples of the ICIgram GUI can be found in Solsona-Berga *et al.* (2022). We used three ICI groups to correspond to three size classes (Figure 2.2, bottom panels), as per Solsona-Berga *et al.* (2022). Detections with a modal ICI of 0.6 s or less were presumed to be females and their young, hereinafter referred to as Social Groups. Detections with a modal ICI of 0.8 s and greater were presumed to be adult males, hereinafter referred to as Adult Males. The detections with a modal ICI between the Social Groups and Adult Males (< 0.6 s and > 0.8 s) could contain large females or juvenile males, hereinafter referred to as Mid-Size.

The ICIgram method was originally developed for sperm whales in the Gulf of Mexico (Solsona-Berga *et al.* 2022), where the population is known to have small body size and consist mostly of females, their calves, and immature animals (Jaquet 2006; Jochens *et al.* 2008). To compare how effectively the ICIgram method can be used to categorize the size/sex of sperm whales in the GOA/BSAI, length estimates using IPI from individual animals were matched with the size/sex classification using the ICIgram method.

IPIs were extracted using the Cachalot Automatic Body Length Estimator (CABLE) of Beslin *et al.* (2018). This tool estimates the body length of sperm whales by compiling and clustering their IPI distributions. To avoid including the same animal more than once, only unique IPI values were retained in the final analysis. The length of the whale was estimated using two equations derived from regression analysis of IPI measurements and photogrammetrically estimated body lengths. The Gordon (1991) equation was developed based on measurements from eleven sperm whales off Sri Lanka and was applied to animals less than 11 m in length (Caruso *et al.* 2015). The Growcott *et al.* (2011) equation was developed based on measurements from 33 large male sperm whales off Kaikoura, New Zealand and was applied to animals greater than 11 m in length (Caruso *et al.* 2015).

2.3.5 Click Detection Processing

Sperm whale click detections were binned into 5-minute intervals. The mean daily presence per week was calculated by summing the number of 5-minute bins with detections for each size class and for each site. Since not all sperm whale clicks were categorized into a size class, a time series of unclassified clicks was also included for each site. The ratio of hourly as well as daily presence for each size class was calculated and displayed with Venn diagrams to show the overlap of the classes at each site. Finally, these data were grouped into one-hour bins

for statistical modeling, as described in the next section. The one-hour bins were chosen as a compromise to maintain data granularity while ensuring at least 30 minutes of recording effort in each one-hour bin for the two duty-cycled deployments.

2.3.6 Statistical Modeling

Generalized Additive Models (GAMs; Hastie & Tibshirani 1987) combined with Generalized Estimating Equations (GEEs; Liang & Zeger 1986) were used as a model framework, outlined by Pirotta *et al.* 2011, in the software *R* (R Core Team 2022) to test the significance of temporal predictors on sperm whale presence. Patterns were explored for all sperm whales combined, hereinafter referred to as the Inclusive model, and for each of the three size classes, referenced as the Social Group, Mid-Size, and Adult Male models. Models were built for each of these groups for each site with more than 270 days of recording (BD, CB, PT, and QN), for each region (GOA and BSAI), and for an All-Site model. The response variable was binomial presence-absence of sperm whale clicks in one-hour bins (1 = presence and 0 = absence). The explanatory variable *Julian day* was included for all site-specific models while the variable *year* was only included at CB where more than five years of data were available. The region-specific models included *Julian day* and *site* (BD, KS, CB, PT, QN, AB, KOA) as explanatory variables. *Year* was only included in the regional GOA model where more than five years of data were available. Finally, for the All-Site model, *Julian day*, *region* (GOA and BSAI), and *year* were included. The variable *time lost* was originally included as the number of missing 5-minute recording bins in each hour to account for the differences in recording effort due to ship passage exclusions but ultimately removed from final models due to a lack of significance.

Sperm whale encounters lasted for many hours to days at all sites, indicating temporal autocorrelation whereby detections in a single one-hour bin increased the likelihood of detections in adjacent bins. To minimize the impacts of the temporal autocorrelation and to avoid data sub-sampling or using a coarse analysis resolution, the GAMs were combined with GEEs, a method previously used to address autocorrelation in marine mammal presence data (Panigada *et al.* 2008; Pirotta *et al.* 2011; Benjamins *et al.* 2017; Merkens *et al.* 2019). Under this approach, the data are grouped into blocks, within which residuals are allowed to be correlated, while independence is assumed between separate blocks. The *R* correlation function *acf* within the *stats* package (R Core Team 2022) was used to determine the time step for blocking. Blocks were defined by the value where the autocorrelation of the residuals of a Generalized Linear Model (GLM) dropped below 0.1. Block sizes varied between 226 - 1249 hours (9 – 52 days) for all 28 models. Although GEEs are considered robust against correlation structure misclassification (Liang & Zeger 1986) an autoregressive order 1 (AR-1) covariance structure was used to describe model error given the temporal autocorrelation in the data (Panigada *et al.* 2008; Pirotta *et al.* 2011; Bailey *et al.* 2013; Booth *et al.* 2013; Stimpert *et al.* 2015; Merkens *et al.* 2019).

The same GLM used to determine block size was also used to assess collinearity of covariates following (Zuur 2012). The *vif* (Variance Inflation Factor) function in the *R* package *car* (Fox 2019) identified potentially collinear covariates. None of the variables in the GLM model had a VIF value over 2.0 and all variables were retained for further modeling.

Models were built using the function *geeglm* in the *geepack* library (Halekoh *et al.* 2006) in *R*. Variables were treated differently (spline vs. factor) within each model based on the nature of the covariate. Given the long time series at each site and region, *Julian day* was included as a cyclic spline based on a variance-covariance matrix built using the *gam* function in the *mgcv*

37

package in *R* (Wood 2011) to fit a circular smooth in a GEE framework. Given the small number

of years for the time series, *year* was included as a factor to estimate year specific effects. *Site*

and *region* were input into models as factors given the categorical nature of both variables.

For models with more than one variable, model selection used the Quasilikelihood under

Independence model Criterion (QIC$_a$) value, an alternative to Akaike's Information Criterion for

GEE models (Pan 2001), available through the function *QIC* in the *geepack* library in R (v.1.1-6;

Halekoh *et al.* 2006). Manual backwards stepwise model selection was carried out where the

model with the lowest QIC$_a$ from the full model (all variables) and a series of models containing

all terms but one, was used in the following step (Pirotta *et al.* 2011; Benjamins *et al.* 2017). This

selection method continued until removing any of the remaining covariates caused the QIC$_a$ to

increase. The order of the variables in the final model was determined by which variable, when

removed, increased the QIC$_a$ the most. A Wald's Test was conducted on the final model using

the function *anova* in the *geepack* library to access the significance of each variable in the model.

Any non-significant covariates were removed from the models using backwards stepwise model

selection until all p-values of the remaining covariates were greater than 0.05. Partial-fit plots for

each variable in the final models were created using the approach of Pirotta *et al.* (2011). The x-

axis for *Julian Day* is represented by the months of the year and interpreted as sperm whale

occurrence among seasons (winter: December - February, spring: March - May, summer: June –

August, fall: September – November).

Goodness of fit for the models was evaluated using the *performance* package in *R*

(Lüdecke *et al.* 2021). The coefficient of discrimination, also known as Tjur's R2 (Tjur 2009),

was calculated for each model using the function *r2_tjur*. Binned residuals were also used to

assess the fit of the models. Binned residual plots were obtained using the function *binnedplot*

(Gelman & Hill 2007). A good fit was expected to have residuals within the 95% confidence intervals (Gelman & Hill 2007).

Generalized Linear Models (GLMs) examined the relationship between sperm whale presence and the El Niño Southern Oscillation's (ENSO) via the Oceanic Niño Index (ONI), the Pacific Decadal Oscillation (PDO) index, the North Pacific Gyre Oscillation (NPGO) index, and the Marine Heatwave Watch (MHW). The monthly PDO, ONI and NPGO values were extracted using the *rsoi* package in *R* (Albers 2020) and the MHW forecast was generated using Jacox *et al.* 2022. Hourly binary presence of sperm whales was averaged for each month and divided by the recording effort. To remove seasonality, the timeseries was deseasoned using the functions *stl* and *seasadj* in the *forecast* package in *R* (Rob J. Hyndman & Yeasmin Khandakar 2008; Hyndman *et al.* 2023). Previous studies in the GOA found an 8–12-month lag between ENSO events and sperm whale peak presence (Diogou *et al.* 2019b). And since PDO, ONI, and NPGO are connected to one another (Di Lorenzo *et al.* 2008), 8–12-month lags were tested for these indices as well.

2.4 Results

2.4.1 Comparison of IPI and ICI

Sperm whale body length estimates were calculated using both their IPI and ICI for 3,047 animals encountered across four sites. An effort was made to account for site, seasonal, and interannual variability. The animal lengths obtained from the IPI were divided into the size/sex classes obtained from the ICIgram and the results visualized using violin plots (Figure 2.3). These plots reveal clear distinctions between the ICI classes based on the body lengths measured by IPI. The Social Groups class is comprised of small animals with a median length of 10.2 m (n = 2,387) and a moderate interquartile range (IQR) of 1.9 m (the range of the middle 50% of the

distribution). The Adult Males class has large animals with median length of 15.7 m (n = 325) and a small IQR of 1.2 m. Whereas the Mid-Size class has median of 13.6 m (n = 335) and a broad range of body lengths with an IQR of 6.6 m. There were outliers within the Social Groups and Adult Males classes, where the length estimates from their IPIs indicated that the ICIgram method may have misclassified the size/sex of the animal. These usually occurred during encounters when more than one size/sex class were echolocating at the same time. Only 3% of animals classified as Social Group had body sizes larger than 12 m and were likely misclassified as Social Group. For Adult Males, 14% of classified animals had body sizes smaller than 10 m and were likely misclassified as Adult Male.

The distribution of ICI size classes varied between sites (Figure S2.1). Averaged across sites, the Social Groups had a mean ICI value of 680 ms, with a range from 600 to 700 ms across sites; the Mid-Size had a mean value of 800 ms, ranging from 750 to 800 ms across sites; and the Adult Males had a mean value of 980 ms ranging from 850 to 1050 ms across sites (Figure S2.1).

2.4.2 Spatial Overlap of Size Classes

All three size/sex classes were detected across all sites, with temporal overlap between classes when observed on both hourly and daily time scales (Figure 2.4). The highest proportion of overlap at all sites was between Mid-Size and Adult Males. Adult Male and Mid-Size animals were found in the same hourly bin 7% (range 2-16%) and daily bin 36% (range 17-63%) of encounters. Whereas for Social Groups and Mid-Size, they were found together in the same hourly bin only 2% (range 0-5%) and daily bin 8% (range 2-17%) of encounters. Similarly, Adult Males and Social Groups were found together in the same hourly bin 2% (range 0-4%) and daily bin 7% (range 2-20%) of encounters. As expected, encounters with all three size/sex

classes were rare with hourly bin overlap of 1% (range 0-2%) and daily bin overlap of 5% (range 0-15%).

At all sites, the proportion of Mid-Size and Adult Male presence was greater than Social Group on the hourly and daily scale (Figure 2.4). Sites CB, AB, and KOA, along the continental slope and deepwater of the GOA, had the smallest proportion of Social Group presence, while the seamount sites PT and QN had the highest. The proportion of Mid-Size and Adult Males were similar at all sites except for PT where the proportion of Mid-Size presence was the largest (Figure 2.4).

2.4.3 Presence by Site

Sperm whales of all size/sex classes were detected at every site and presence was reported as the mean daily presence (min and hr) per week, herein after referred as daily presence. AB, KS, and KOA had the highest normalized daily sperm whale presence and the lowest normalized recording effort (Figure 2.5-6). All three sites only captured 19, 12, and 22 weeks respectively, during the spring and summer when sperm whale presence was usually the highest. CB had the next highest normalized daily sperm whale presence and the highest normalized recording effort (> 5 years), followed by PT, BD, and QN (Figure 2.5, Figure 2.7).

Sperm whales were present almost every week during the nearly two years of recording at the Buldir Island (BD) site (Figure 2.5). Social Groups were almost exclusively present during the winter months between 2010 and 2012 with a maximum daily presence of 527 min (8.8 h) (Figure 2.5). Mid-Size were the most consistent size class present with a maximum daily presence of 331 min (5.5 hr) (Figure 2.5). Adult Males had a maximum daily presence of 586 min (9.7 hr) with the peak in presence seen in January of 2011 (Figure 2.5). Sperm whales were present every week at the Kiska Island (KS) recording site during the 13-week deployment (Fig

41

5). Mid-Size and Adult Male presence were higher and more consistent with a maximum daily presence 161 and 113 min (2.7 and 1.9 hr), respectively (Figure 2.5). Social Groups were present for 4 weeks and had a maximum daily presence of 71 min (1.2 hr) (Figure 2.5).

In the GOA, the continental slope (CB) site had the highest level of sperm whale presence compared to the other recording sites (Figure 2.8). Presence at CB was dominated by Mid-Size and Adult Males with maximum daily presence of 846 and 882 min (14.1 and 14.7 hr), respectively. Social Groups were present episodically throughout the eight-year recording period with a maximum daily presence of 104 min (1.7 hr). The two seamount sites, Quinn (QN) and Pratt (PT), had a more consistent presence of all size classes throughout the recording period (Figure 2.7). The maximum daily presence of Social Groups, Mid-Size, and Adult Males at QN were 196, 194, and 372 min (3.3, 3.2, and 6.2 hr), respectively (Figure 2.7). The maximum daily presence of Social Groups, Mid-Size, and Adult Males at PT were 325, 564, and 218 min (5.4, 9.4, and 3.6 hr), respectively.

Sperm whales were present every week of the recording period for the Abyssal Deep (AB) and Kodiak Island (KOA) sites in the GOA. Compared to the other size classes, there was less Social Group presence at AB and KOA with a maximum daily presence of 105 and 132 min (1.8 and 2.2 hr), respectively (Figure 2.6). There was more presence of Mid-Size and Adult Males at KOA with a maximum daily presence of 499 and 225 min (8.3 and 3.8 hr), respectively (Figure 2.6). AB had a maximum daily presence of Mid-Size and Males of 203 and 306 min (3.4 and 5.1 hr), respectively (Figure 2.6).

2.4.4 Modeling

Sperm whale presence was modeled for all sperm whale classes included together (Inclusive model), and for each of the three size classes independently. Data were used from

selected sites with good seasonal coverage (BD, CB, PT, and QN), from all the sites in each region (GOA and BSAI), and from all the sites combined (All-Site).

The average annual percentage of one-hour bins with presence for the Inclusive, Social Group, Mid-Size, and Adult Male models was 98% (8579), 4% (362), 44% (3902), and 32% (2779), respectively (Table S2.1). The highest performing models were the Adult Male models with 32 to 50% of Residuals within the 95% confidence intervals. The lowest performing models were the Social Group models with 7 to 25% within the 95% confidence intervals (Table S2.1). The models had low Tjur's $R2$ values and % of Residuals within the 95% confidence intervals suggesting that the temporal (Julian day and year) and spatial (site) variables included in the models are not good predictors of animal detections.

2.4.5 Seasonal Patterns

Significant seasonal patterns were found in the majority (26 out of the 28) of models (Table 2.2). The Inclusive models revealed a seasonal pattern of increased presence in the summer for all GOA sites and fall for the BSAI sites. The patterns revealed by the Inclusive models were like those of the Adult Males at all sites where presence was highest in the summer for GOA and fall for BSAI (Figure 2.9). The seasonal patterns for Mid-Size and Social Groups were more nuanced and varied from site to site. For the Mid-Size, peak presence was seen in the summer or fall across all sites and regions except QN where peak presence was observed in the spring (Figure 2.9, Figure S2.2-3). For Social Groups, peak presence was seen in the spring, except for QN and BD where the peak in presence was in the fall and winter, respectively (Figure 2.9, Figure S2.2-3). Peak presence of the Social Groups rarely overlapped with those of the Adult Males.

2.4.6 Interannual Variability

Interannual variability was only assessed for the CB site, GOA region, and the All-Site models where there was more than five years of data (Figure S2.3, Figure 2.10). At CB, the Inclusive and Adult Male models revealed a decrease in presence every year after 2011 with the lowest presence in 2014, 2015, and 2017, followed by an increase in 2018 and 2019 (Figure S2.3). For Social Groups, presence remained steady from year to year except in 2014 and 2019 where there was no Social Group presence whatsoever. Interannual variability was not significant for Mid-Size at CB. In the GOA, the Inclusive and Mid-Size models revealed a decrease in presence every year after 2011 with the lowest presence in 2013 and 2014, followed by an increase every subsequent year (Figure 2.10). Social Group presence remained steady from year to year with the highest presence in 2011 and a small dip in presence in 2014 and 2015. Interannual variability was not significant for Adult Males in the GOA region. For all seven sites, the Inclusive, Mid-Size, and Adult Male models revealed an increase in presence in 2011, followed by a decrease in presence and a minimum in 2013 with increasing presence in subsequent years. Social Group presence remained consistent from year to year with a dip in presence starting in 2014 and the lowest presence in 2018.

2.4.7 Environmental Variability

Sperm whale presence was correlated to the PDO, ONI, and NPGO indices in varying degrees depending on the model. The PDO index with an eight-month lag was significant for all models except for the Mid-Size at CB and Social Groups at GOA (Table S2.2). All significant models revealed a negative correlation between the PDO index and sperm whale presence (Figure 2.11, Figure S2.9-10). The decrease in sperm whale presence in 2013 aligns with the inflection point of the PDO from a cool to warm phase (Figure S2.6-8). The ONI was significant for less than half of the models with a nine-month lag being consistently significant for all

44

models (Table S2.2). All significant models revealed a negative correlation between the ONI and sperm whale presence (Figure 2.11, Figure S2.9-10). The decrease in sperm whale presence in 2013 aligns with the ENSO becoming neutral and is sustained as it transitions to El Nino (warm phase) (Figure S2.6-8). The NPGO index was significant for all models except for the Inclusive at CB, Social Groups at GOA, and all Mid-Size models (Table S2.2). Like the PDO index, an eight-month lag was significant for all models except for the Social Groups at CB. All significant models revealed a positive correlation between the NPGO index and sperm whale presence (Figure 2.11, Figure S2.9-10). The decrease in sperm whale presence in 2013 aligns with the inflection point of the NPGO from a positive to a negative phase (Figure S2.6-8). R^2 values for all the linear regressions revealed a weak correlation with values ranging between +/-0.27 and +/-0.55 (Table S2.2). The MHW forecast was not significant in any of the models (Table S2.2) although less sperm whale presence does appear to align with higher MHW probability (Figure S6-8).

2.5 Discussion

This study analyzed demographic composition of sperm whales at seven sites in the Gulf of Alaska and Bering Sea/Aleutian Islands over a wide range of years and seasons. Three size/sex classes were identified (Social Groups, Mid-Size and Adult Males) based on their echolocation ICI, supported by examining IPI for individual clicks. The median body length of animals in the Social Group class (10.2 m) is comparable to the average body lengths documented for sperm whale females and immature animals that ranges from 8 to 11 m (Omura 1950; Rice 1989; Dufault *et al.* 1999; Nowak 2003; Jaquet 2006; McClain *et al.* 2015). The median length of the Mid-Size class (13.6 m) is greater than the maximum length for females (12 m) (Dufault *et al.* 1999; Nowak 2003; McClain *et al.* 2015), suggesting that the Mid-Size group

consists of juvenile males. The median length of the Adult Male class (15.7 m) suggests that the males in this study are both physically mature [occurs at a mean length 15.5-15.9 m (Gaskin & MW 1973)] and sexually mature [occurs from 9.5 m (Nishiwaki *et al.* 1963)to 13.8 m (Gaskin 1970)]. The seasonal and interannual patterns of the Adult Male and Mid-Size groups show good alignment, further suggesting that the Mid-Size group may consist of juvenile males.

Adult Males were present year-round in the GOA and BSAI, although they were more common in the summer in GOA and fall in BSAI, and less common in the winter and spring. This seasonal occurrence is consistent with what was previously described from acoustic data in the GOA (Mellinger *et al.* 2004) and at Ocean Station PAPA in the southeast GOA (Diogou *et al.* 2019a). Whaling data from the northeastern Pacific also supports this seasonal pattern with an increased mean length of male sperm whales starting between May and June and sustained through September, attributed to the sexual maturity of the animals (Gregr & Trites 2001). Male sperm whales in the GOA are also notorious for longline depredation (Hamer *et al.* 2012) particularly from the sablefish fishery which has its season from mid-March to mid-November (Sigler *et al.* 2008), aligning with the peak in presence of Adult Males.

The summer peak in presence and winter low in presence is likely associated with long distance movements of males, between lower latitudes where breeding occurs in the winter/spring and higher latitudes, or feeding grounds, for improved foraging opportunities in the summer/fall (Best 1979). Although this seasonal trend appears to be migratory in nature, there is little evidence that sperm whales have a predictable pattern and/or route to established breeding areas. Rather, they are described as 'ocean nomads' based on Discovery Tags used by whalers, that revealed widespread movements between areas of concentration suggesting that their home ranges can span thousands of kilometers (Best 1979; Kasuya & Miyashita 1988; Whitehead

2003; Mizroch & Rice 2013). Discovery Tagged animals in southern California and northern Baja California were found in locations ranging from offshore California, Oregon, British Columbia, and the western Gulf of Alaska (Mizroch & Rice 2013). More recently, studies using satellite tags have corroborated the nomadic behavior of sperm whales. In a study that tagged 10 sperm whales in the GOA, seven stayed within the GOA, one traveled to British Columbia and back, while three traveled south to the Sea of Cortez, Baja, and offshore Mexico through the California Current without stopping and with no synchronized departure (Straley *et al.* 2014). Although the three southbound whales did all leave before winter when sperm whale presence was at its lowest, there is no evidence that the animals 'migrate' to a specific area outside of their home range. There is also photo-identification evidence from the North Atlantic that sperm whales travel from higher latitudes areas like the Azores, to tropical latitudes like the Gulf of Mexico and Bahamas (Mullin *et al.* 2022) but no concrete evidence that the animals have a pattern or routine to where and when they travel between presumed higher latitude foraging and lower latitude breeding grounds. Instead, it appears that sperm whales travel in response to the distribution of their often-patchy prey sources (Jaquet & Gendron 2002; Whitehead 2003) and are linked with temporary breeding sites with favorable prey conditions driven by the effects of oceanographic conditions. It has also been suggested that sexually mature males don't breed every year and may choose to remain in higher latitudes some years to feed (Whitehead & Arnbom 1987) further complicating their seasonal patterns in and out of their home ranges which can span ocean basins. This is also supported by our acoustic observation of year-round presence of Adult Males in the entire study region. Historical whaling and satellite tag studies provide evidence of highly variable timing and direction of sperm whale movement but incorporating increased observations over longer timescales is necessary to clarify their behavior as nomadic or

migratory. Genetic studies reveal that males in the North Pacific have widespread origin and are likely a mix of males from several independent populations in the Pacific (Mesnick *et al.* 2011) further supporting their nomadic nature. If in fact, sperm whales are truly nomadic animals, understanding how they spatiotemporally exploit available resources is important to establishing management and conservation strategies.

Mid-Size animals were also present year-round in the GOA and BSAI, with a slightly offset peak presence from the Adult Males in both regions. The Mid-Size class likely does not undergo long distance movements to breeding grounds since they are sexually immature animals. In the GOA, the peak presence of Mid-Size animals was in the fall or spring months. In the BSAI, peak presence of Mid-Size was in the summer, before the peak presence of Adult Males in the fall, suggesting avoidance of Adult Males by Mid-Size animals. There is evidence of aggression between mature sperm whales based on heavy scarring on their heads (Best 1979; Kato 1984; Whitehead 1993). Some juvenile males may avoid an area during peak presence of mature Adult Males to avoid direct competition, although these groups do overlap on an hourly scale in our data, suggesting temporal overlap of habitat use on some level.

Social Groups were present at all seven recording sites but were not present year-round and instead had distinct seasonal patterns that varied from site to site. Social Group presence in the winter months between 2010 and 2012 at site BD is consistent with the 2008 sighting of a group of females and immature animals in the Central Aleutians in winter (Fearnbach *et al.* 2014). That sighting was considered rare since only males had been observed in ten years of summer sighting surveys previously conducted in the BSAI region (Fearnbach *et al.* 2014). There is also historic whaling evidence that female sperm whales have overwintered in the western Aleutians (Berzin & Rovnin 1966; Nishiwaki 1966; Berzin 1971, 1972; Mizroch & Rice

2013; Fearnbach *et al.* 2014; Ivashchenko *et al.* 2014). The continued return of Social Groups to this region in the winter, when productivity is generally lower, could be a sign of site fidelity. Although sperm whales have been described as 'ocean nomads', there is evidence from females in the Eastern Caribbean (Gero *et al.* 2007; Vachon *et al.* 2022), North Atlantic (Engelhaupt *et al.* 2009), western Mediterranean (Carpinelli *et al.* 2014) and males in the GOA (Straley *et al.* 2014) that site fidelity is a factor in their habitat choice. The presence of Social Groups in certain regions of the BSAI in the winter could be evidence of geographic specializations (Vachon *et al.* 2022).

In the GOA, Social Group peak presence was in the spring. Seasonal prediction models in the waters of coastal British Columbia (BC) found female sperm whales virtually absent after May (Gregr & Trites 2001). The absence of females in the BC model predictions suggests that Social Groups could be traveling further north to the GOA in the spring months. The spring peak was also seen in historical whaling data from the northeastern Pacific where female sperm whales were more often caught from March-May and less often caught from June-September (Gregr & Trites 2001). Our current understanding of female sperm whale distribution post-whaling does not include the GOA.

Contemporary presence of Social Groups in the GOA and BSAI could represent a return to pre-whaling distributions of sperm whales. Females were illegally caught in high numbers in the North Pacific, removing a significant portion of the reproductively mature population (Ivashchenko *et al.* 2014). The impacts of whaling on their population, especially given their social ecology, may have been disproportionately large (Whitehead *et al.* 1997; Mizroch & Rice 2013). Social Group presence could also represent a change in the distribution of their preferred prey, given how closely sperm whale distribution is linked to squid (Jaquet & Whitehead 1996;

Jaquet & Gendron 2002). The BD recording site was located on the nutrient-rich northern side of the Aleutian Islands in the Bering Sea which would be a prime location for squid and provide suitable habitat for sperm whales. Presence of Social Groups could also be related to changes in the water temperature. Nishiwaki (1966) hypothesized that Social Group presence in the BSAI was related to water temperatures above 13°C. And in the GOA, ocean heat content (HC) was the most important sperm whale predictor, with a decrease in HC leading to a decrease in animal presence (Diogou *et al.* 2019b). However, from 2010 to 2012 when our instruments were recording in the BSAI, this region experienced a multi-year sequential continuation of colder than normal ocean temperatures (Zador 2011), likely below the 13°C threshold for Social Groups hypothesized by Nishiwaki (1996).

Year-round presence of sperm whales in the GOA and BSAI, especially through the winter, indicates high winter productivity and sustained prey availability (Boyd 1995; Whitney & Freeland 1999; Diogou *et al.* 2019b). CB had the highest relative presence of sperm whales, particularly of Mid-Size and Adult Males. This site is located along the continental slope which is popular with males in other regions (Gregr & Trites 2001) and this site had a sustained presence of sperm whales, even during years with low overall presence in the GOA (Rone *et al.* 2017) likely a result of richer biomass productivity. PT and QN, although relatively offshore, correspond to seamounts which are also important sperm whale habitat in the GOA (Rone *et al.* 2017) and several other regions due to their complex seafloor characteristics and water circulation (Gregr & Trites 2001; Morato *et al.* 2008; Wong & Whitehead 2014; Dede *et al.* 2022). There is evidence from whaling data that females were generally found farther from shore in the northeastern Pacific (Gregr *et al.* 2000) potentially explaining the higher proportion of Social Group presence at sites PT and QN. Social Groups also appeared linked to oceanographic

features and were present as far north as the western North Pacific Gyre in the western Aleutian Islands, and the Alaska Gyre and Alaska Current in the Gulf of Alaska (Kasuya & Miyashita 1988; Mizroch & Rice 2013). In the BSAI, site KS appeared to have the highest relative presence of Mid-Size and Adult Male sperm whales, however, this site has less recording effort than BD and a summer recording effort bias. Regional preference between GOA and BSAI was not significant for any of the size classes, indicating that the two regions are both equally capable of providing suitable foraging conditions.

There were temporal (hourly) and spatial (daily) overlaps between all groups at almost all sites. Temporal and spatial overlap of Adult Males and Social Groups occurred at all sites except AB and could imply that mating is possible in GOA or BSAI. Currently we understand that males travel to tropical latitudes to breed, but there is evidence from whaling data that sperm whales were mating in temperate latitudes off the coast of British Columbia where large bulls were mostly found associated with female schools in April and May (Pike 1965; Gregr *et al.* 2000). There is also evidence that the modal breeding month for sperm whales in the North Pacific was April (Ohsumi 1965) explaining the peak in presence of Social Groups in GOA in spring. Gregr and Trites (2001) hypothesized that by traveling north into temperate latitudes, Social Groups could improve their encounter rates with more mature males that are ready for breeding. There was more spatial than temporal overlap of Adult Males and Mid-Size, due to the offset peaks in presence of the two groups. Less temporal overlap could indicate habitat partitioning or avoidance of sexually mature Males by juvenile males.

Interannual variability of sperm whale presence is due to several ecological, behavioral, and environmental factors related to prey availability in the region, namely squid, fish, and skates (Okutani & Nemoto 1964; Santos *et al.* 1999; Fristrup & Harbison 2002; Das *et al.* 2003;

51

Wild *et al.* 2020). The dips and peaks of sperm whale presence interannually in our study are supported by visual surveys and reported squid catches. The peak in presence in 2011 for all size classes in this study, were also observed in southeast GOA (Diogou *et al.* 2019b) and could be correlated to the high squid catches reported that year (Ormseth 2017). Density and abundance values from visual surveys in the GOA also support the dip in presence seen in our study in 2013 by Adult Males and Mid-Size, with increasing density and abundance in 2015 (Rone *et al.* 2017). These dips and peaks in presence are likely a result of changes in prey distribution and abundance which can be difficult to study. Instead, researchers often rely on understanding how small- and large-scale drivers of ocean productivity optimize feeding and spawning conditions of their prey which ultimately impacts aggregation (Gregr *et al.* 2013; Palacios *et al.* 2013). However, the relationship between prey and their environment in the GOA and BSAI, particularly large-scale climate patterns like the PDO, ENSO, and NPGO, is complex and not well understood. Squid are a highly mobile and adaptable group of marine animals that can be found in a wide range of oceanic conditions driven by prey availability and abundance (zooplankton and forage fish), predator populations (salmon, toothed whales, sablefish, and grenadiers), and changes in habitat quality (Ormseth 2017). In the GOA and BSAI, there are 15 species of squid whose abiotic habitat preferences are unknown but are likely related to pelagic conditions and currents throughout the North Pacific over various spatial and temporal scales (Ormseth 2017). A large climate shift in the mid-1970s from a cold to warm regime (Mantua *et al.* 1997) resulted in a southward shift and intensification of the Aleutian Low pressure system and warmer ocean temperatures (Anderson & Piatt 1999). This led to increased zooplankton biomass and demersal, pelagic fish and cephalopod recruitment and abundance (Brodeur & Ware 1992; Anderson & Piatt 1999; Hatch 2013) while forage fish populations declined (Anderson

1997) impacting piscivorous sea birds and some marine mammal populations (Piatt & Anderson 1996; Merrick *et al.* 1997; Hatch 2013). While overall the regime shift appeared to increase cephalopod populations potentially as a result of warmer ocean temperatures that accelerate growth rates (Rodhouse & Hatfield 1990; Forsythe 2004) and increased zooplankton biomass, it also resulted in decreased forage fish populations (squid prey) and increased salmon populations (squid predator) (Mantua *et al.* 1997) and the species-specific impacts of the shift are not well understood. There is also evidence that warmer ocean temperatures and a shoaling of the Oxygen Minimum Zone in the California Current System are resulting in a northward and offshore expansion of some squid species (Crawford & Mckinnell 2013; Stewart *et al.* 2014; Peterson *et al.* 2016) creating an environmental refuge in the GOA and BSAI. So, although squid populations might appear to be increasing in warmer ocean temperatures, this increase could be a result of northward range expansion and the impacts on the endemic species are not understood.

In the southeast GOA, peaks in sperm whale acoustic presence seasonally and interannually were related to higher temperatures, a shallow mixed layer, a weaker Alaska Gyre, and enhanced eddy formation (Diogou *et al.* 2019b). These conditions are also associated with El Niño, (ENSO warm phase), (Jackson *et al.* 2006; Crawford, W.; McKinnell, S.; and Freeland 2012) which has been shown to be positively correlated with peaks in sperm whale presence up to one year later in the southeast GOA (Diogou *et al.* 2019b). El Niño conditions during our recording effort persisted in the GOA from 2014 to 2016 and 2018 to 2019 with very strong conditions from 2015 to 2016 (NOAA Climate Prediction Center 2023). Moderate to strong La Niña (ENSO cool phase) conditions were seen from 2010 to 2012 and a weak La Niña from 2016 to 2018 (NOAA Climate Prediction Center 2023). In this study, opposite to what was seen in the southeast GOA, higher monthly sperm whale presence was associated with La Niña

conditions, or a negative ONI. La Niña conditions in the northeastern Pacific are characterized

by decreased ocean temperatures, weaker than normal eddies, deeper mixed layer, increased

winter nutrient levels, and a return of summer upwelling (Whitney & Welch 2002). It is

important to note that although secondary effects of ENSO can be felt in the North pacific, it

primarily affects lower latitude climates (Mantua & Hare 2002).

Larger scale environmental variability such as the PDO could also influence the presence

of sperm whales. Like ENSO, the PDO has a positive, or warm phase, and a negative, or cool

phase. In fact, these two climate patterns interact with one another and when PDO is highly

positive, El Niño will likely be stronger and when the PDO is highly negative, La Niña will

likely be stronger (Gershunov & Barnett 1998). A positive PDO brings environmental conditions

that have been connected to increased sperm whale presence in the southeast GOA such as

higher temperatures and ocean heat content, a shallow mixed layer, and a weaker Alaska Gyre

(Mantua *et al.* 1997; Cummins & Lagerloef 2002; Crawford, W.; McKinnell, S.; and Freeland

2012). Our study found a significant negative correlation between PDO and sperm whale

presence of all classes. The GLM models with and without lags displayed a significant negative

correlation, implying that the effects of the PDO on sperm whale presence span larger time

scales. At the start of our recording effort in 2011, the PDO was in a cool phase until it flipped to

a warm phase in 2014 (Mantua 2023). This PDO inflection point is also reflected in the sperm

whale presence where several low presence years following the shift are associated with a very

positive PDO phase. Although the PDO remains in a warm phase for the remainder of our

recording effort, the PDO index does decrease dramatically after 2017, and is associated with a

steady increase of sperm whale presence through 2019. It is important to note that while our

nine-year time series likely does include an important phase switch of the PDO in 2014, the PDO

cycle occurs at approximately 20-to-30-year time intervals (Mantua *et al.* 1997) and it is unlikely that our data are sufficient to capture the full relationship between sperm whale presence and the PDO.

Related closely to ENSO and the PDO, the NPGO is a climate pattern that is significantly correlated to fluctuations in salinity, nutrients, and chlorophyll-a in the Gulf of Alaska (Di Lorenzo *et al.* 2008). Our study found a positive correlation between sperm whale presence and the NPGO index. Sperm whale presence was higher during the positive NPGO phases which are associated with lower SST, higher salinity, chlorophyll-a and nutrients (Di Lorenzo *et al.* 2008). There was no significant correlation between Mid-Size presence and the NPGO index or ONI, implying that juvenile male sperm whales are less linked to ENSO conditions and the NPGO compared to other classes. It is important to note that while the PDO accurately describes climate patterns north of 38ºN, the NPGO is most effective at capturing climate patterns south of 38ºN (Di Lorenzo *et al.* 2008) which may explain why there was more significance between PDO and sperm whale presence in this study.

Overall, higher sperm whale presence was related to large-scale environmental variability associated with cooler ocean temperatures, higher salinity, chlorophyll-a, and increased upwelling as seen during La Niña, cool PDO phase, and positive NPGO index. Increased nutrient-rich water and higher productivity from La Niña conditions could sustain higher squid populations, although no direct link has been made in the GOA or BSAI. Findings from this study that is focused on the central GOA and BSAI contradict what was seen at Ocean Station PAPA in the southeast GOA (Diogou *et al.* 2019b). Reasons for this include a difference in recording effort; recording at Ocean Station PAPA occurred for five years (Diogou *et al.* 2019b) while this study encompasses nine years of recording effort. It is also possible that the PDO and

NPGO are no longer effective tools for predicting changes in marine environments. A study by Litzow et al. 2020 found that since 1988/1989, the main drivers of the PDO and NPGO have become less active, making these large-scale climate patterns less effective at understanding and predicting marine productivity. There is also evidence that the relationship between the PDO and productivity are non-stationary and phase shifts in the PDO can result in distinct climate states that cannot be directly compared (Litzow *et al.* 2018).

During the period of 2014 to 2016, the northeastern Pacific experienced an unprecedented marine heatwave, often referred to as "The Blob" (Bond *et al.* 2015). The more than 2.5°C increase of the upper 100 m of the ocean (Yang *et al.* 2018) led to low chlorophyll concentrations that wreaked havoc on marine ecosystems from California to Alaska (Cavole *et al.* 2016). Low primary productivity likely resulted in poor foraging conditions revealed by the decrease of Mid-Size and Adult Males and complete absence of Social Groups in the GOA. However, there was no significant relationship between the MHW forecast and sperm whale presence for any of the models or classes. This could be a result of no recording effort in 2016 while the marine heatwave continued resulting in the inability of our data to capture the full effects of the marine heatwave in the GOA. Presence began to slowly increase in 2015 and continued to do so until the end of our recording effort. There appeared to be a large increase in presence of Adult Males and a decrease of Social Groups in 2018 for the All-Site model which is likely a result of recording effort bias since there was only acoustic data from one site that year (CB). Climate models for the North Pacific predict environmental changes that would support higher concentrations of prey and attract top predators like sperm whales in high latitudes (Hazen *et al.* 2013; Stewart *et al.* 2014; Diogou *et al.* 2019b). Although sperm whale presence in this study appears to increase at the end of the recording period in 2018 and 2019, recording effort

bias and the lack of consecutive years with increased presence prevents drawing conclusions about the GOA serving as a foraging refuge for the whales.

Since the spatiotemporal models in this study were only investigating seasonality, interannual trends, and differences in site and region, low model performance was not surprising. The spatiotemporal models would likely be improved with the inclusion of environmental data that is correlated with sperm whale presence such as ocean heat content, sea surface temperature, vertical stratification (Diogou *et al.* 2019b), chlorophyll-a (Wong & Whitehead 2014; Baumann-Pickering *et al.* 2016), mesoscale features like thermal fronts (Griffin 1999) and eddies (Wong & Whitehead 2014). This study was also limited by short and/or discontinuous time series at certain sites. Since sperm whales display seasonal patterns in this region, some of the models could be biased by recording effort. Continuation of acoustic monitoring at these sites will allow for more robust time series and potentially improve performance of spatiotemporal models. This is particularly important for the Aleutian Island and two seamount sites where Social Group presence was high, highlighting critical habitat for females and their young in this high latitude region.

2.6 Conclusion

This work highlights the importance of understanding sperm whale spatiotemporal distribution and regional demographics for informing appropriate management and conservation measures. Currently, management of the North Pacific stock of sperm whales does not account for Social Group habitat use and assumes that the region is dominated by juvenile and sexually mature males. This study reveals that Social Group presence in this region is likely overlooked and historical presence of females in whaling data and contemporary 'rare' occurrences should not be ignored when determining management practices for this stock. Male and female sperm

whales have differences in behavior and ecology that likely translate to demographic specific responses to increasing anthropogenic threats and climate change. Creating a baseline understanding of what Social Group presence looks like in the GOA and BSAI is crucial for monitoring future changes to the demographic composition of the North Pacific stock.

2.7 Acknowledgements

Chapter 2, in full, is under review for publication of the material as it may appear in PLOS One, 2023, Posdaljian, Natalie, Alba Solsona-Berga, John A. Hildebrand, Caroline Soderstjerna, Sean M. Wiggins, Kieran Lenssen, and Simone Baumann-Pickering. The dissertation author was the primary researcher and author of this paper.

2.8 Figures and Tables
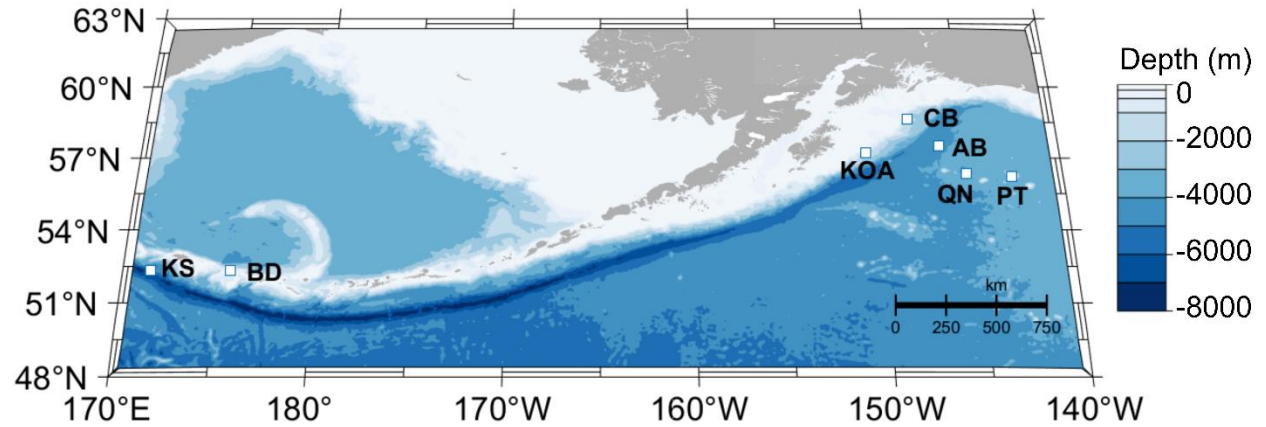
Figure 2.1. Recording locations (square markers with site abbreviations) in the GOA and BSAI regions. Bathymetry represented by blue color scale in meters.

Table 2.1. Summary of recording effort in the GOA and BSAI regions from 2010 to 2019. Each row represents an individual deployment. Recording effort includes region, site name (abbreviation), latitude, longitude, depth, recording dates, and total number of recording days for each deployment with the site total bolded in the final row. Deployments marked with an asterisk (*) have a duty cycle: the second continental slope (CB) deployment had a 10-minute recording duration every 12 minutes and the second Buldir Island (BD) deployment had a five-minute recording duration every ten minutes.

Region	Site	Latitude (N)	Longitude (W)	Depth (m)	Recording Dates (MM/DD/YY)	No. of Recording Days
Gulf of Alaska (GOA)	Continental Slope (CB)	58° 38.74'	148° 04.13'	1000	07/13/11 − 02/19/12	221
		58° 40.28'	148° 01.25'	900	05/03/12 − 02/21/13*	294
		58° 40.41'	148° 00.55'	877	06/06/13 − 09/05/13	91
		58° 40.31'	148° 01.31'	858	09/05/13 − 04/28/14	235
		58° 40.26'	148° 01.46'	914	04/29/14 − 09/09/14	133
		58° 40.25'	148° 01.46'	900	09/09/14 − 05/02/15	235
		58° 39.32'	148° 05.48'	929	05/01/15 − 09/06/15	128
		58° 40.26'	148° 01.45'	874	04/30/17 − 09/12/17	135
		58° 40.22'	148° 01.62'	900	09/14/17 − 06/16/18	275
		58° 40.18'	148° 01.57'	972	04/25/19 − 09/27/19	155
						1902
	Pratt Seamount (PT)	56° 14.61'	142° 45.44'	989	09/09/12 - 06/10/13	275
		56° 14.64'	142° 45.43'	987	06/11/13 - 08/20/13	70
		56° 14.58'	142° 45.41'	988	09/03/13 - 03/21/14	199
		56° 14.60'	142° 45.46'	987	04/30/14 - 09/10/14	134
						678
	Quinn Seamount (QN)	56° 20.36'	145° 11.24'	930	09/11/13 - 04/16/14	217
		56° 20.48'	145° 10.99'	900	09/10/14 - 05/2/15	234
		56° 20.44'	145° 11.11'	994	05/02/15 - 08/18/15	109
		56° 20.48'	145° 10.99'	964	04/30/17 - 09/14/17	138
						698
	Abyssal Deep (AB)	57° 30.82'	146° 30.05'	1200	04/28/17 - 09/14/17	**139**
	Kodiak Island (KOA)	57° 13.44'	150° 31.70'	1000	04/24/19-09/27/19	**157**
Bering Sea and Aleutian Islands (BSAI)	Buldir (BD)	52° 38.00'	175° 37.99'	783	08/27/10 - 05/26/11	272
		52° 04.56'	175° 38.39'	777	05/31/11 − 08/11/11*	438
						712
	Kiska (KS)	52° 19.01'	178° 31.24'	1092	06/03/10 − 08/26/10	**84**
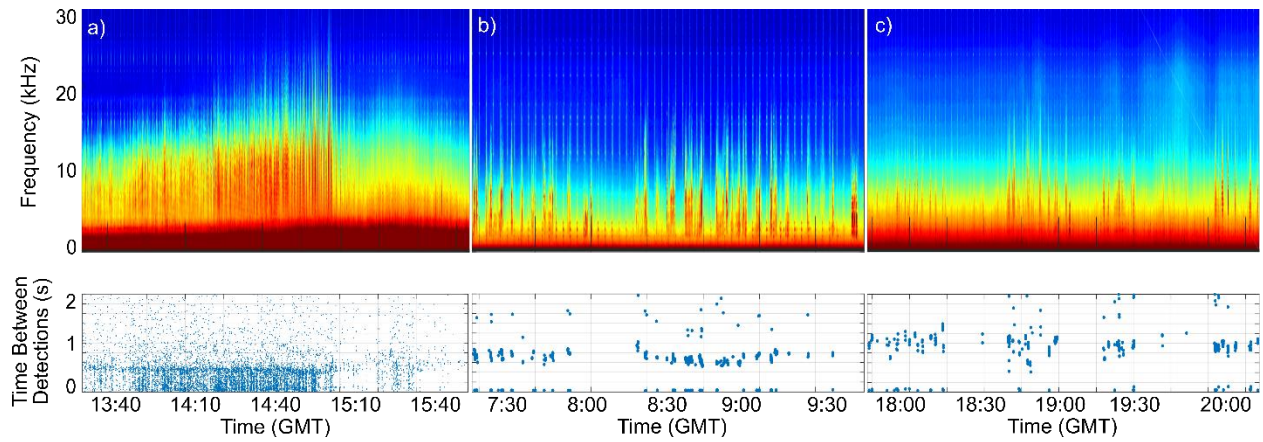
Figure 2.2. Sperm whale echolocation clicks in long-term spectral average (LTSA; top panel) with their time between detections (ICI; bottom panel). The panels represent three different modal ICIs: a) 0.5 s, b) 0.7 s, and c) 1.0 s. The size of the points on the first panel (a) were minimized for ease of visualization of the modal ICI.
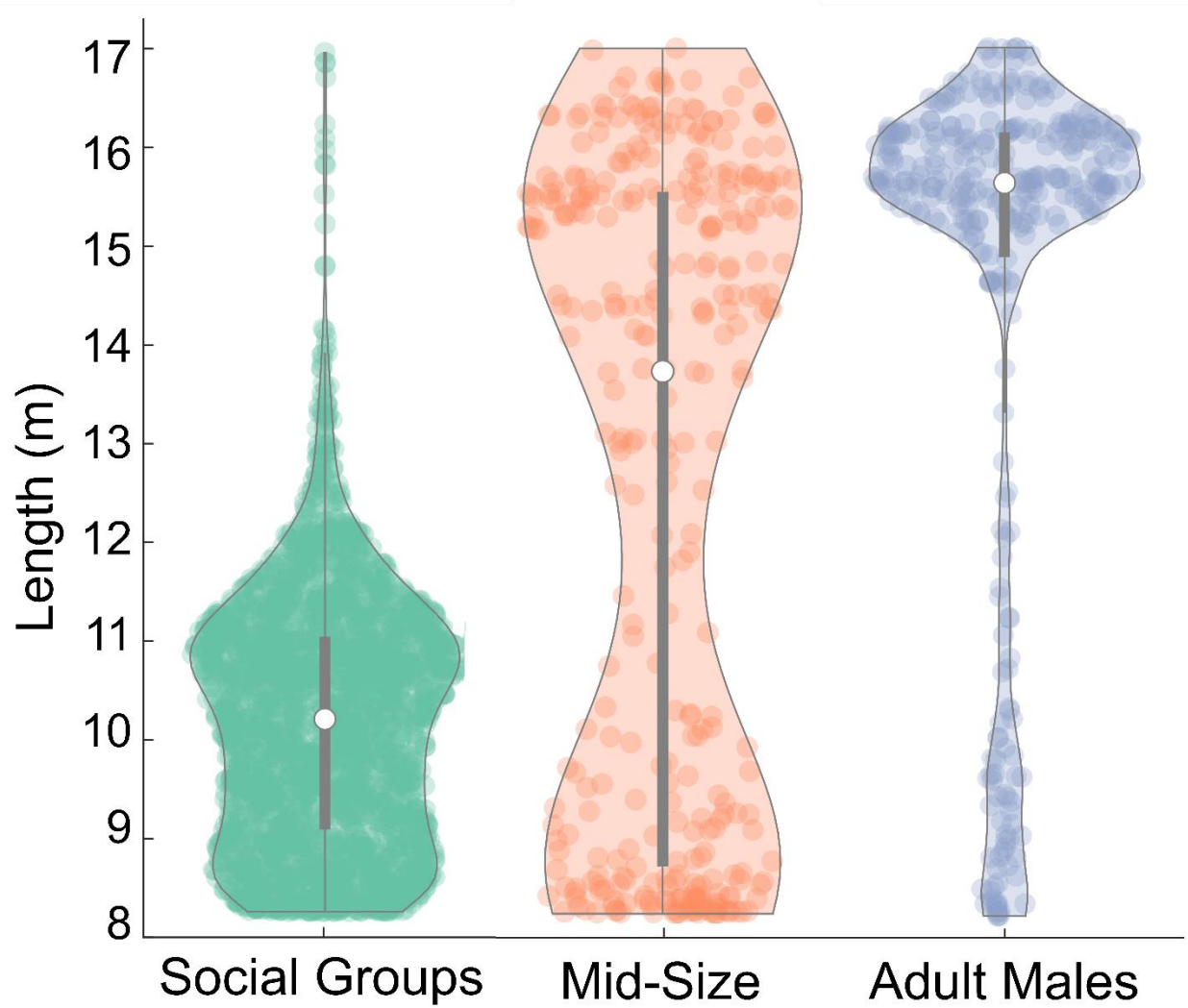
Figure 2.3. Estimated body length (m) from the IPI categorized into the three ICI size classes (Social Groups, Mid-Size, Adult Males). Median represented by the white dot and the interquartile range by the gray bar.
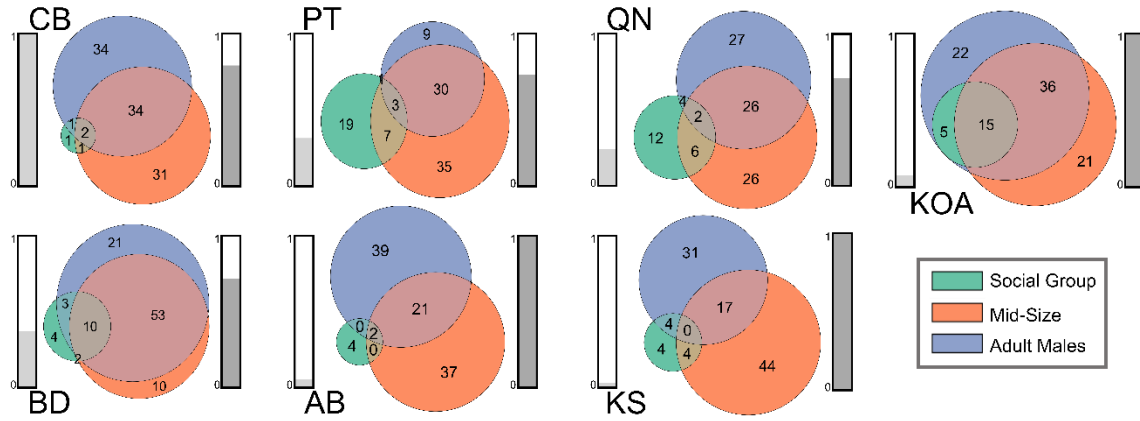
Figure 2.4. Ratio of hourly (left) and daily (right) presence of each size class at each recording site. Social Groups in green, Mid-Size in orange, and Males in blue. Overlap between groups represents simultaneous presence of those groups in the same hour or day. The bars on the left of each diagram (light grey) represent normalized recording effort at that site. The bars on the right (dark grey) represent normalized sperm whale presence at that site.
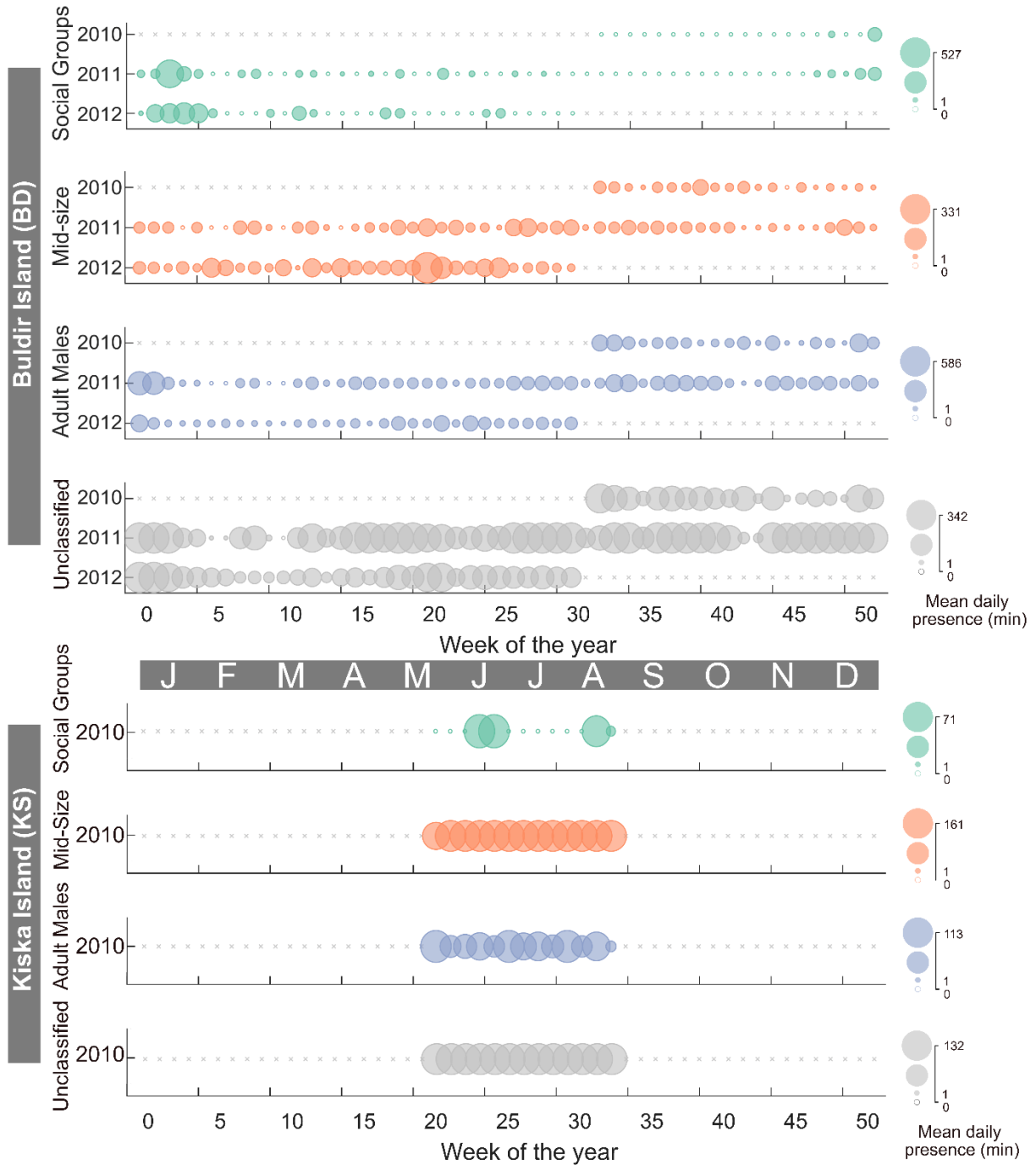
Figure 2.5. Sperm whale presence at the Buldir Island (BD) and Kiska Island (KS) sites. Each row represents a year. The color of the bubble represents the size class; Social Groups by green, Mid-Size by orange, Adult Males by blue, and unidentified clicks in grey. The size of the bubble is the mean daily presence in minutes represented with a scale on the right. Grey 'x' symbols represent no recording effort.
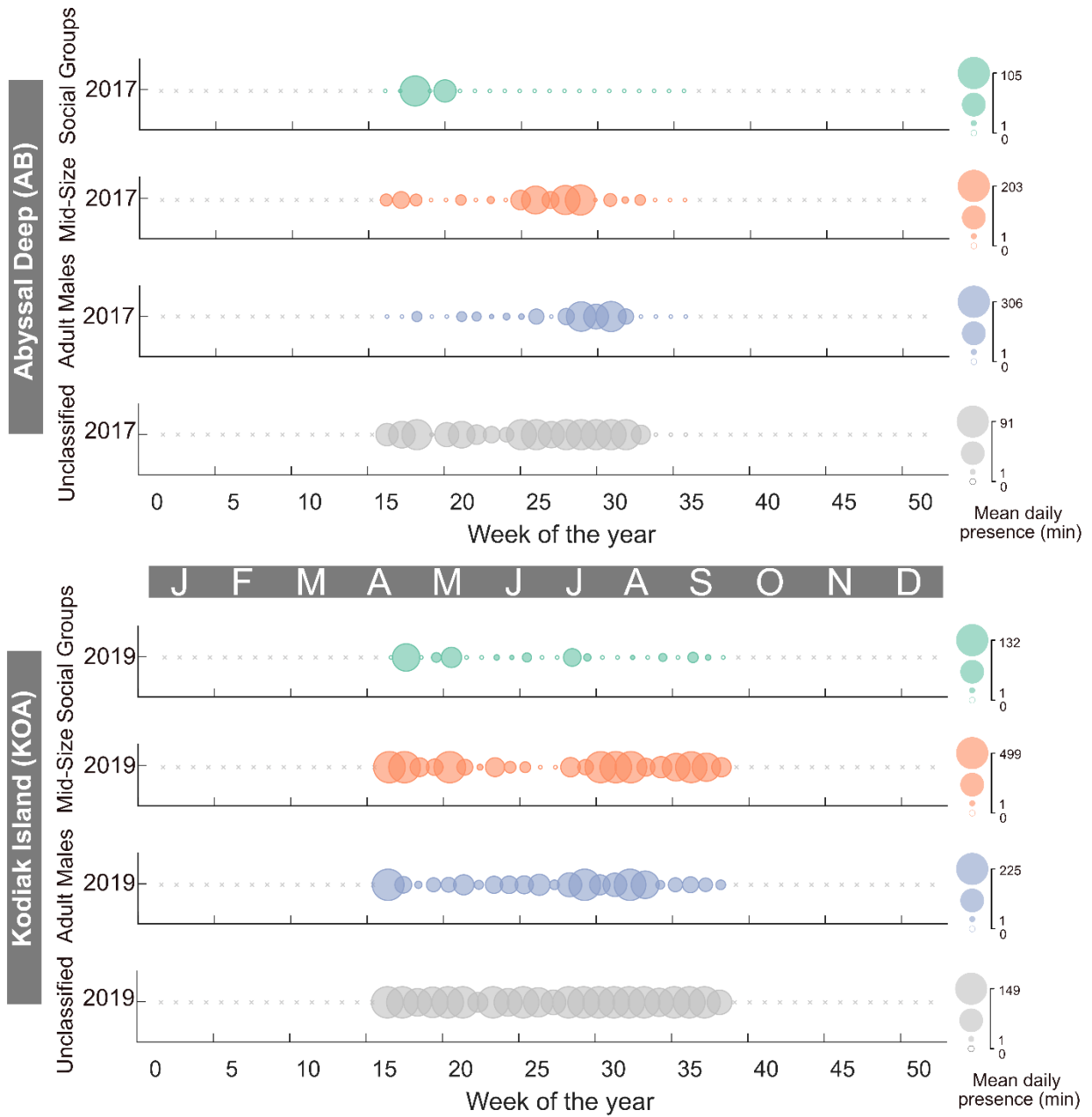
Figure 2.6. Sperm whale presence at the Abyssal Deep (AB) and Kodiak Island (KOA) sites. Colors and symbols as per Fig 5.
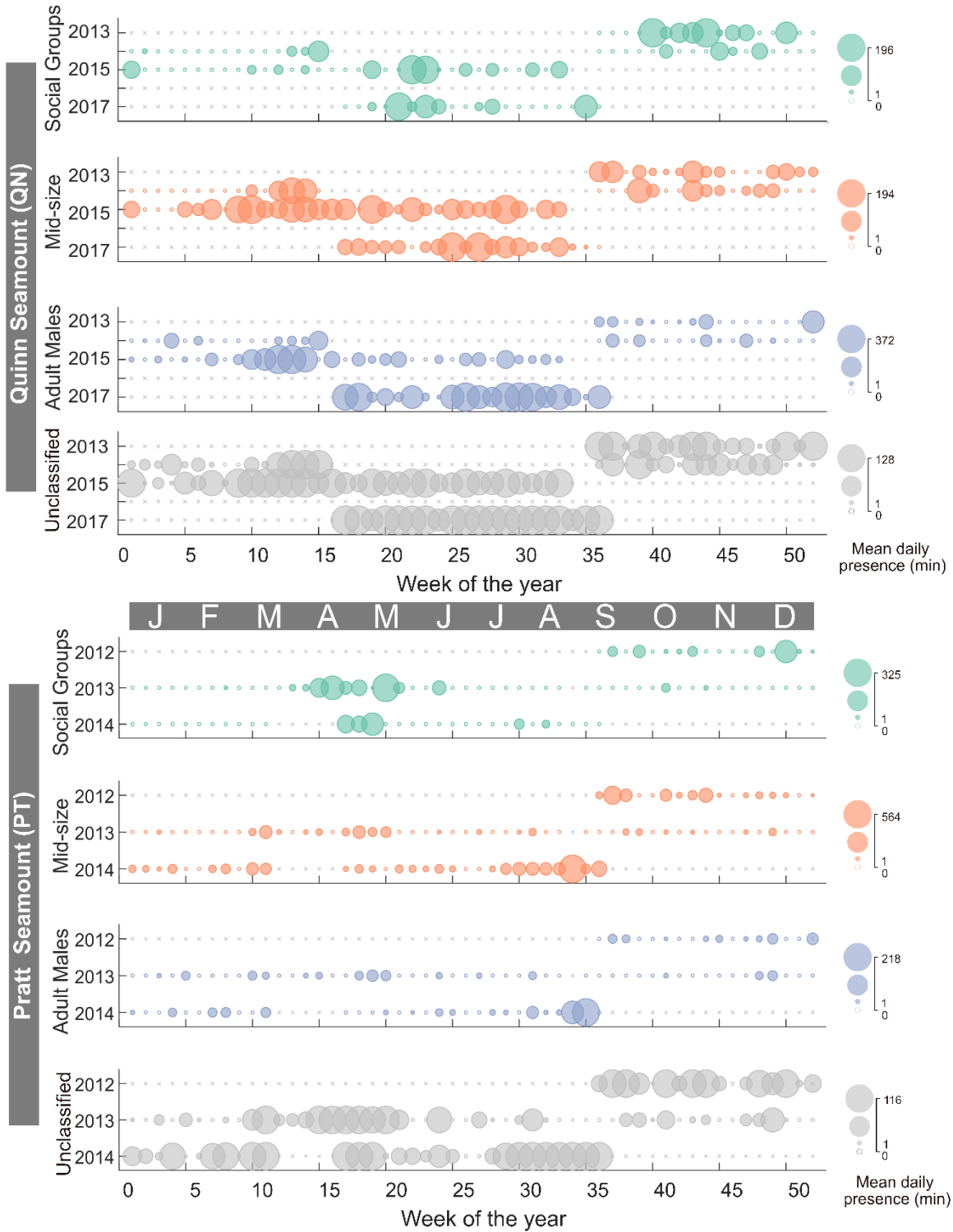
Figure 2.7. Sperm whale presence at the Quinn Seamount (QN) and Pratt Seamount (PT) sites. Colors and symbols as per Fig 5.
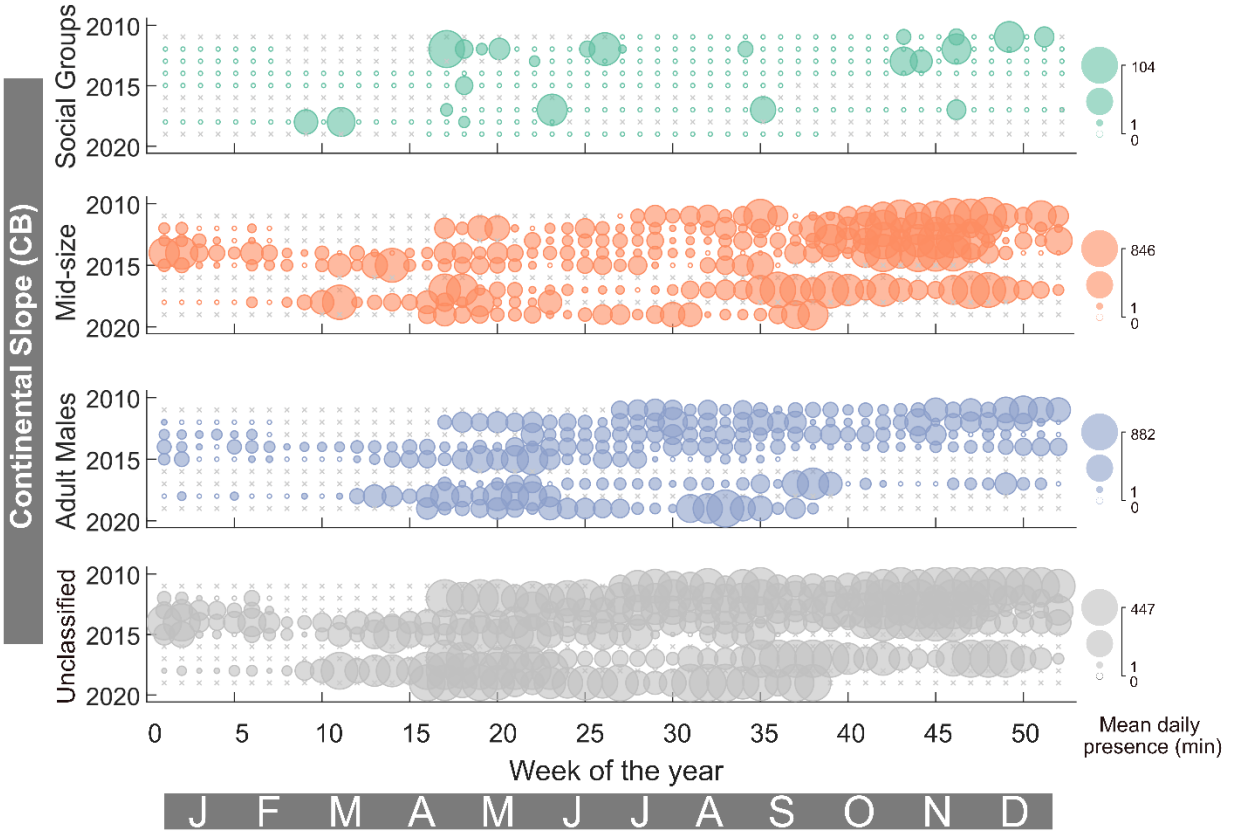
Figure 2.8. Sperm whale presence for the Continental slope (CB) site. Colors and symbols as per Fig 5.

Table 2.2. Model summaries for each site, regional, and All-Site models for the Inclusive, Social Groups, Mid-Size, and Adult Male classes. Model summaries include the p-value (P), degrees of freedom (Df), and the Chi-square statistic (X^2). The significance of the p-value is indicated by the following codes: '***' <0.001, '**' <0.01, and '*' <0.05. If a model had more than one variable, the listed order of the variables represents the order they were input into the model. Models that had different input orders have a subscript for the p-value indicating the order it was input into the model. Covariates that were not retained in the model or not significant are represented with 'NA'.

Model	Site/Region	Variable	Model Output	Inclusive	Social Groups	Mid-Size	Males
Site	BD	Julian Day	P	0.00020 ***	2.8e-09 ***	7.2e-05 ***	6e-06 ***
			Df	2	2	2	2
			X^2	16.6	39.4	19.1	24.1
	PT	Julian Day	P	0.026 *	0.00080 ***	0.016 *	NA
			Df	2	2	2	
			X^2	7.3	14.2	8.3	
	QN	Julian Day	P	7.8e-09 ***	0.0032 **	1.1e-09 ***	6e-08 ***
			Df	2	2	2	2
			X^2	37.3	11.5	41.3	33.3
	CB	Julian Day	P	NA	0.038² *	1.2e-05 ***	3.8e-06***
			Df		2	2	2
			X^2		6.6	22.6	24.9
		Year	P	3e-05***	<2e-16¹ ***	NA	0.00030 ***
			Df	7	7		7
			X^2	32.7	5437.6		27.66
Region	BSAI	Julian Day	P	0.0014 **	1.2e-06 ***	1.7e-07 ***	1.8e-05 ***
			Df	2	2	2	2
			X^2	13.2	27.3	31.2	21.9
		Site	P	4e-05 ***	0.0066 **		0.00020 ***
			Df	1	1	--	1
			X^2	16.9	7.4		14.4
	GOA	Year	P	<2e-16 ***	0.0031¹ **	7.2e-08 ***	NA
			Df	7	7	7	
			X^2	121.5	21.5	46.4	
		Julian Day	P	0.00083 ***	2.5e-05³ ***	4.7e-06 ***	0.012² ***
			Df	2	2	2	2
			X^2	14.2	21.4	24.5	8.8
		Site	P	NA	< 2.2e-16² ***	NA	< 2e-16¹ ***
			Df		4		4
			X^2		8513.6		91.23
All-Site		Year	P	<2e-16 ***	0.017 *	0.00019 ***	<2e-16 ***
			Df	8	8	8	8
			X^2	119.9	18.6	30.2	132.2
		Julian Day	P	7.04e-06 ***	7.2e-06 ***	5.1e-06 ***	8e-08 ***
			Df	2	2	2	2
			X^2	23.7	23.7	24.4	32.7
		Region	P	NA	NA	NA	NA
			Df				
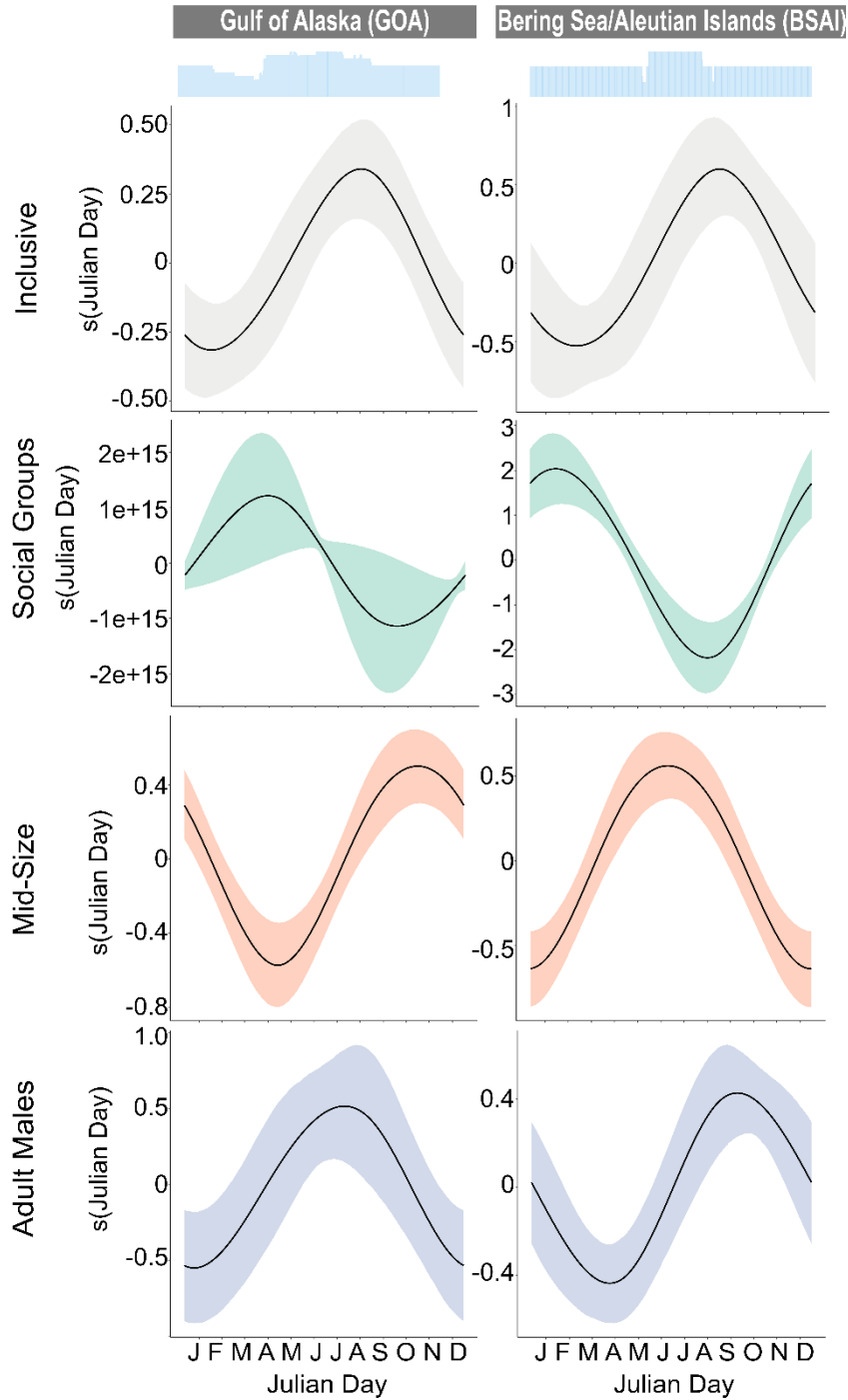
Figure 2.9. Seasonal plots for the sites in the Gulf of Alaska (left) and the Bering Sea/Aleutian Islands (right). Each row represents outputs from the different size class models for each site: a) Inclusive (grey), b) Social Groups (green), c) Mid-Size (orange), and d) Adult Males (blue). Julian day is represented as months. The blue histograms at the top denote effort. All plots include 95% confidence intervals represented by the grey shading surrounding the smooth.
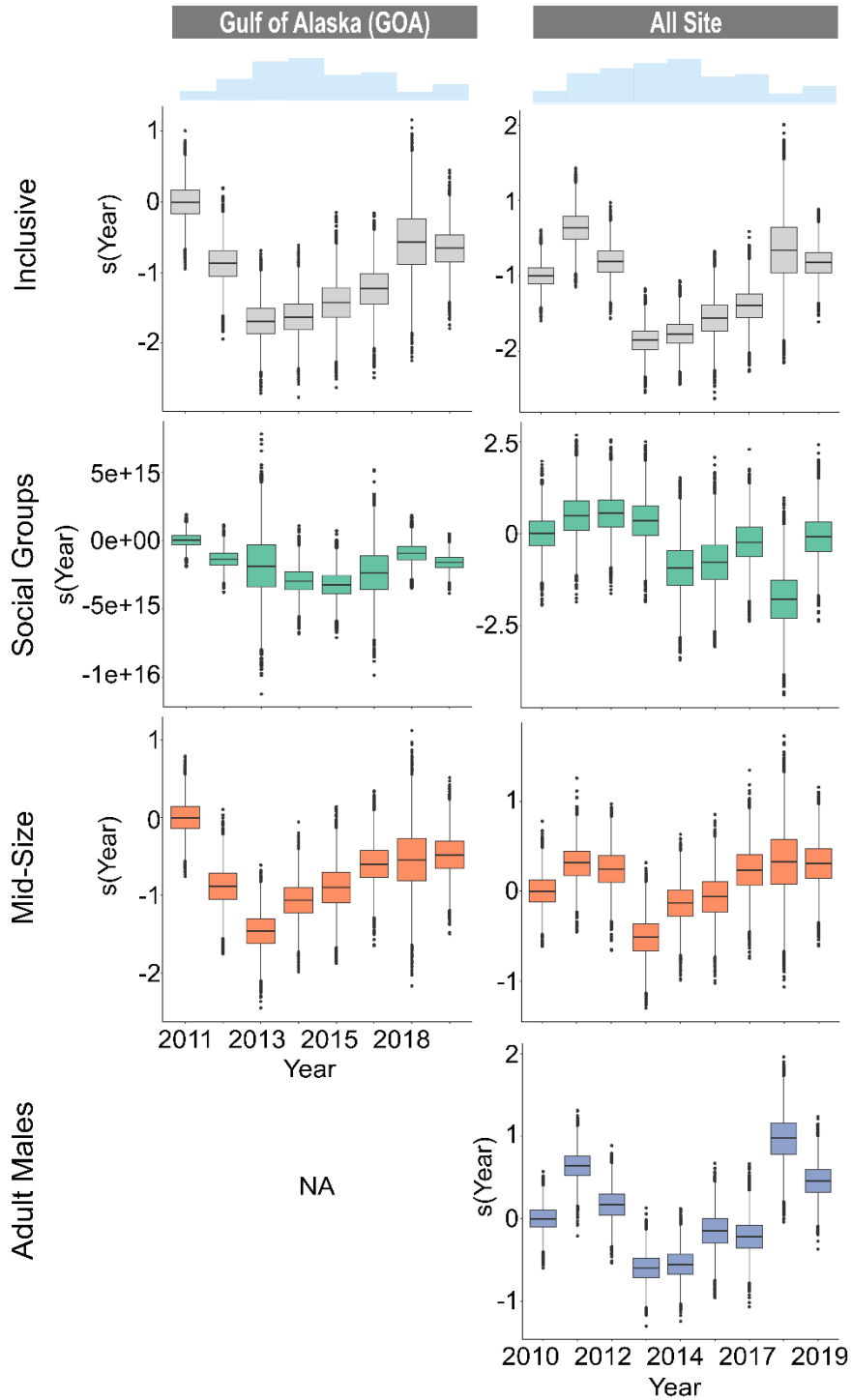
Figure 2.10. Presence by year for the Gulf of Alaska region (left) and All Sites (including Bering Sea/Aleutian Islands) (right). Each row represents outputs from the different size class models for each site: a) Inclusive (grey), b) Social Groups (green), c) Mid-Size (orange), and d) Adult Males (blue). Year is a categorical variable displayed as box plots with the first level centered on zero. Covariates that were not retained in the model or not significant are represented with 'NA'.
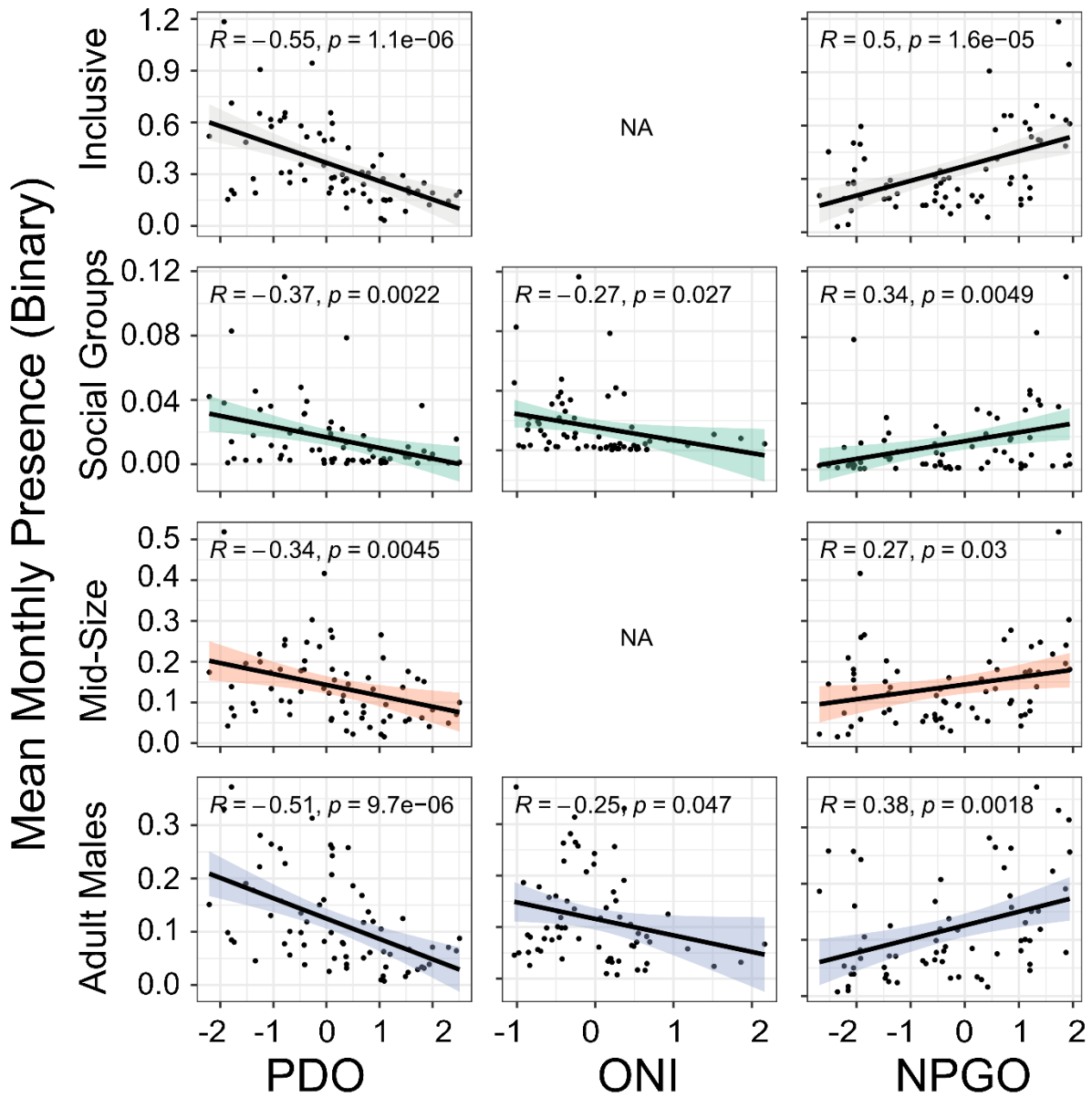
Figure 2.11. GLM plots displaying the relationship between mean monthly presence of sperm whales for All-Sites and the PDO, ONI, and NPGO index. All PDO and NPGO plots represent an eight-month lag, and all ONI plots represent a nine-month lag. Each row (and color) represents outputs from the different size class models for each variable: Inclusive, Social Groups, Mid-Size, and Adult Males. All plots include 95% confidence intervals represented by the grey shading surrounding the linear regression. The regression formula for each model is displayed in the top left-hand corner. Covariates that were not retained in the model or not significant are represented with 'NA'.

2.9 Supplementary Material
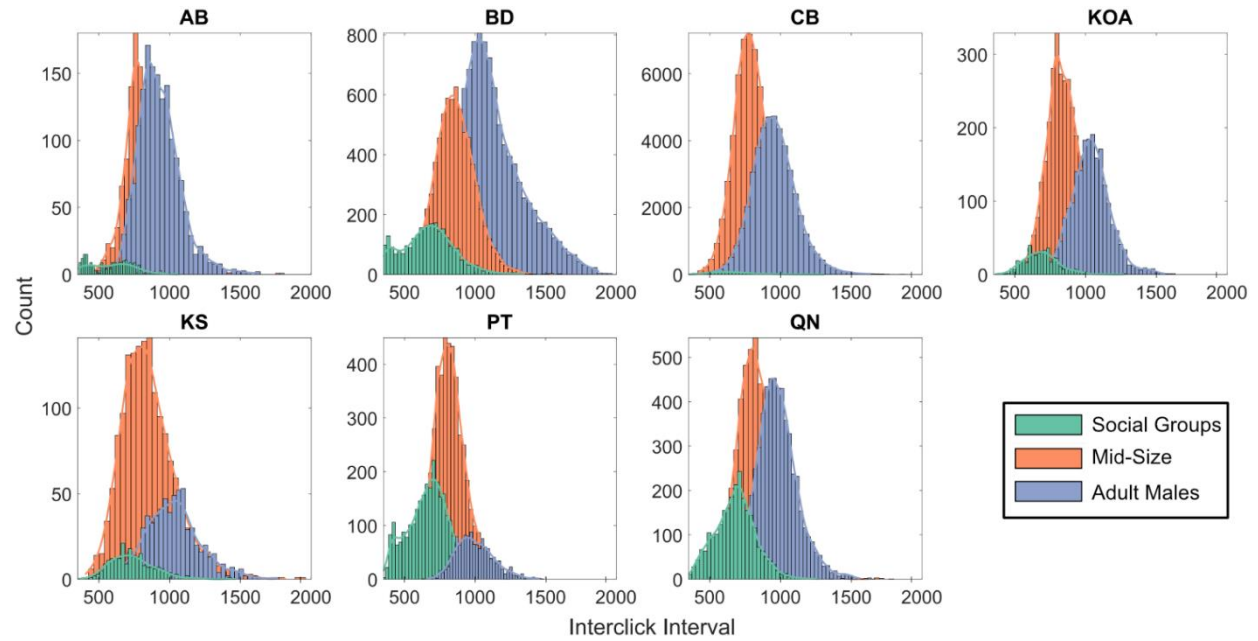
Figure S2.1. The distribution of interclick intervals at each site. Social Groups are in green, Mid-Size in orange, and Adult Males in blue. A kernel smoothing function is represented by the bold line outlining the distributions.

Table S2.1. Model evaluation summaries for all site-specific, regional, and All-Site models. The number of one-hour bins with presence are given by the # of Bins. The coefficient of discrimination is given by Tjur's R^2. The percent of residuals within the 95% confidence intervals of binned residual plots are given by the % of Residuals.

Model	Site/Region	Sex	# of Bins	Tjur's R^2	% of Residuals
Site	BD	Inclusive	8674	0.038	36%
		Social Groups	533	0.044	20%
		Mid-Size	2331	0.018	55%
		Adult Males	2547	0.012	50%
	PT	Inclusive	1862	0.010	43%
		Social Groups	361	0.020	11%
		Mid-Size	887	0.014	34%
		Adult Males	277	0.003	32%
	QN	Inclusive	3215	0.039	46%
		Social Groups	377	0.002	25%
		Mid-Size	954	0.014	38%
		Adult Males	874	0.023	48%
	CB	Inclusive	20567	0.039	50%
		Social Groups	178	0.007	7%
		Mid-Size	9389	0.045	30%
		Adult Males	7419	0.041	48%
Region	BSAI	Inclusive	9600	0.036	42%
		Social Groups	581	0.038	23%
		Mid-Size	2797	0.021	54%
		Adult Males	2700	0.015	49%
	GOA	Inclusive	27749	0.091	33%
		Social Groups	1028	0.007	25%
		Mid-Size	12092	0.038	38%
		Adult Males	9227	0.049	43%
All-Site		Inclusive	37349	0.077	35%
		Social Groups	1609	0.010	30%
		Mid-Size	14889	0.019	42%
		Adult Males	11927	0.034	48%
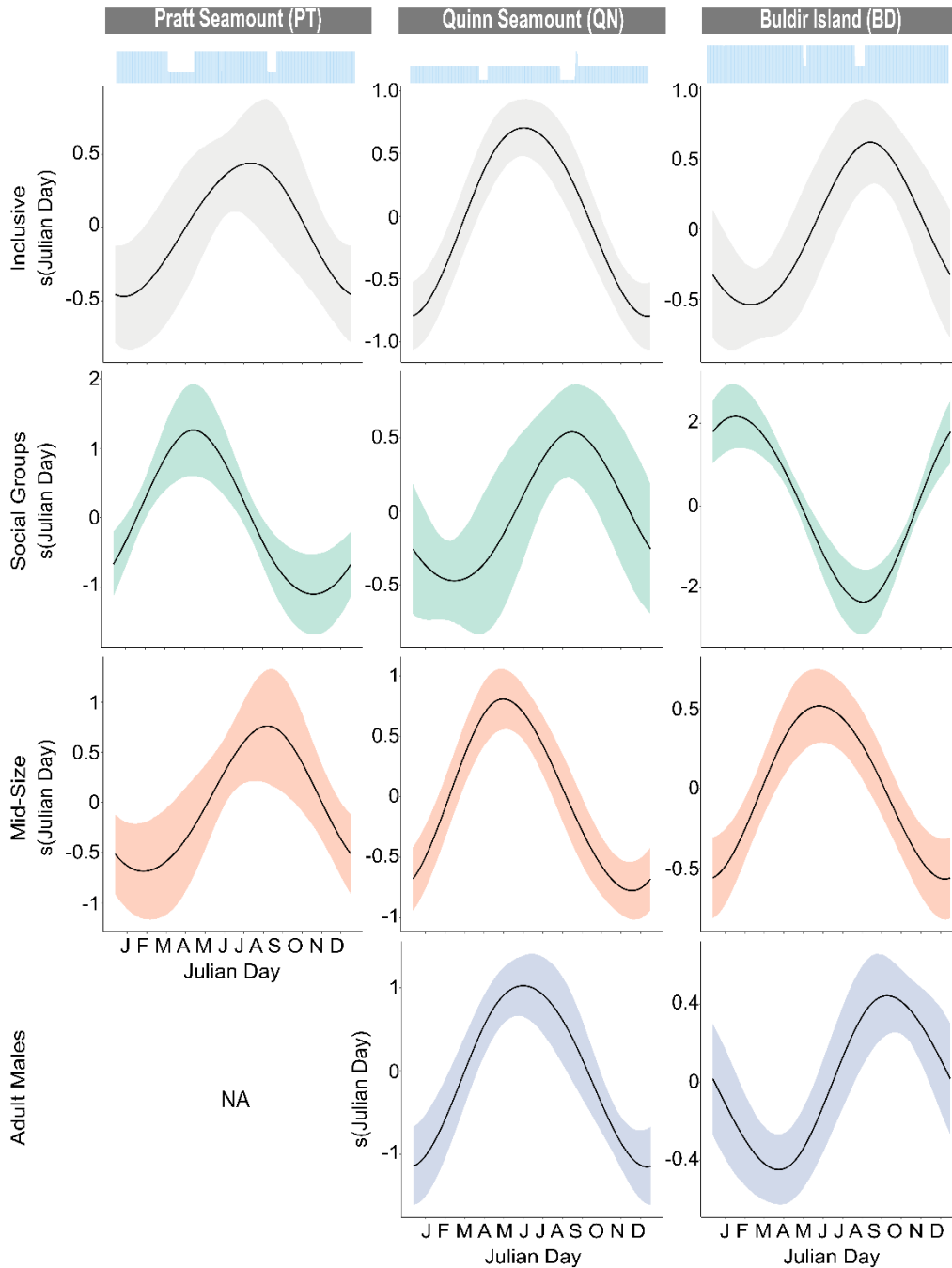
Figure S2.2. Seasonality plots for the two seamount sites in the GOA (PT and QN) and one of the island sites in the Bering Sea/Aleutian Islands (BD). Each row represents outputs from the different size class models for each site: a) Inclusive (grey), b) Social Groups (green), c) Mid-Size (orange), and d) Adult Males (blue). Julian day is represented as months. The blue histograms at the top denote effort. All plots include 95% confidence intervals represented by the grey shading surrounding the smooth. Covariates that were not retained in the model or not significant are represented with 'NA'.
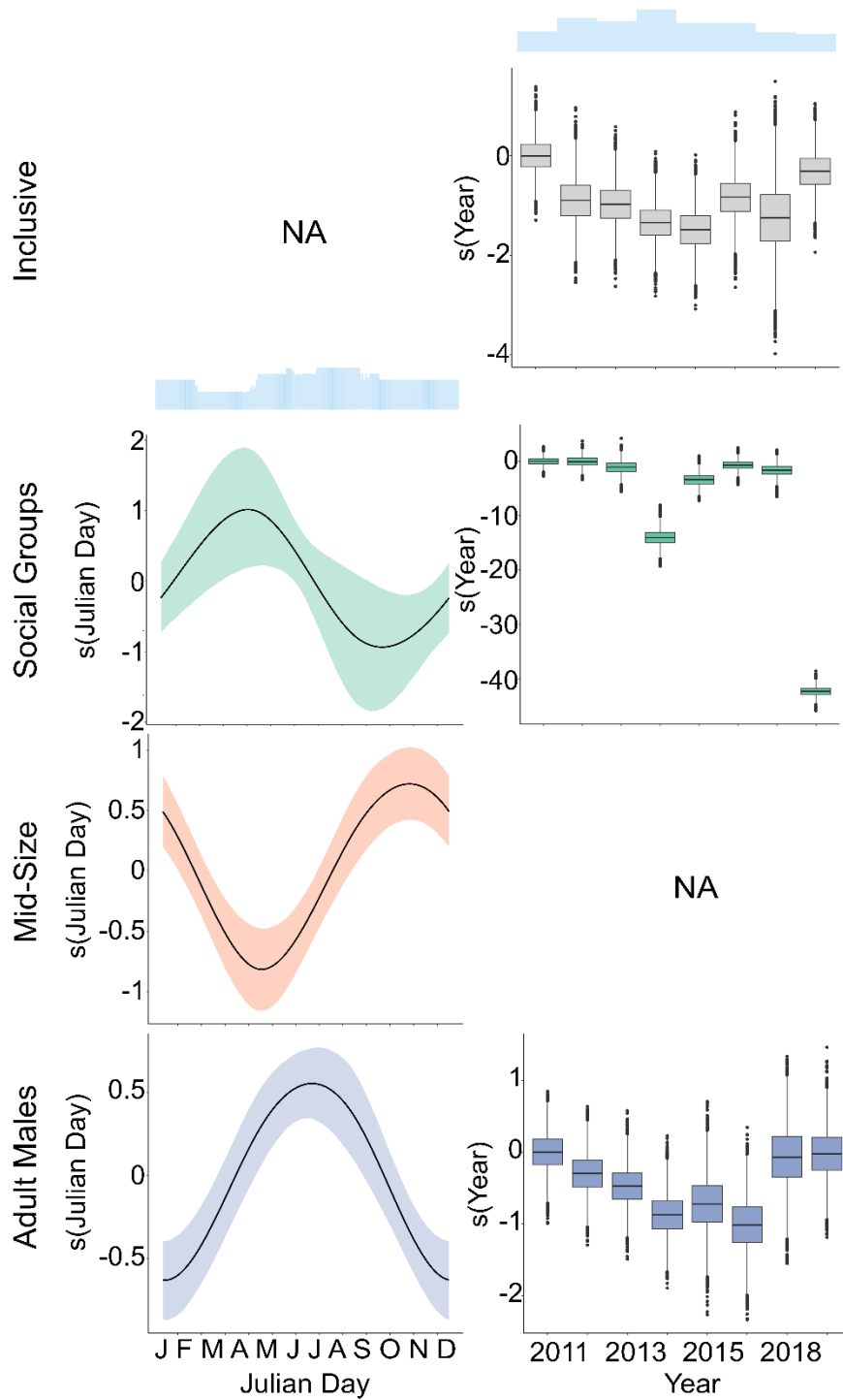
Figure S2.3. Seasonality plots (left) and presence by year (right) for site CB. Each row represents outputs from the different size class models for each site: a) Inclusive (grey), b) Social Groups (green), c) Mid-Size (orange), and d) Adult Males (blue). Year is a categorical variable displayed as box plots with the first level centered on zero. Covariates that were not retained in the model or not significant are represented with 'NA'.

75
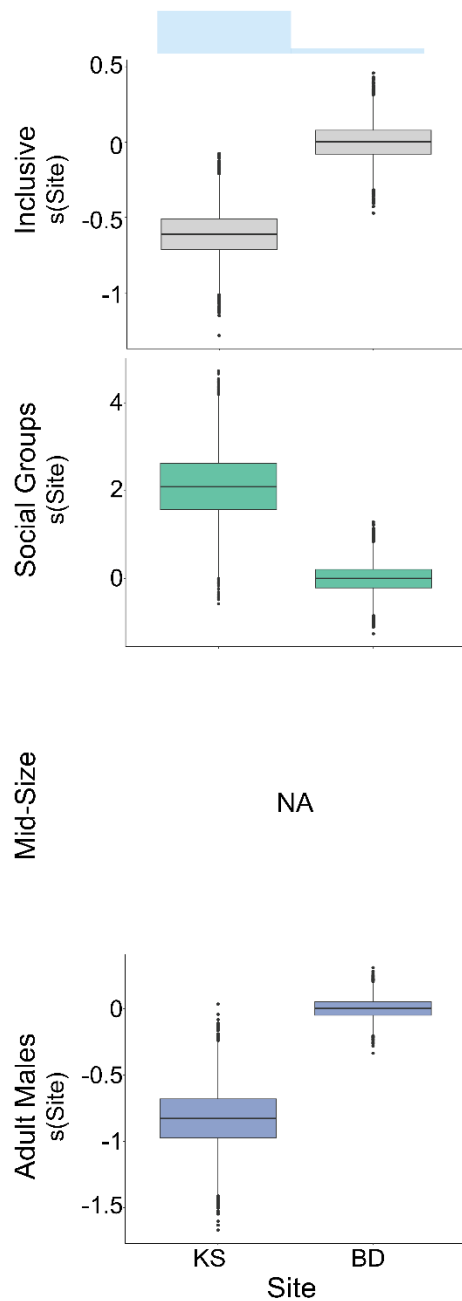
Figure S2.4. Presence by site for the Bering Sea/Aleutian Islands. Each row represents outputs from the different size class models for each site: a) Inclusive (grey), b) Social Groups (green), c) Mid-Size (orange), and d) Adult Males (blue). Site is a categorical variable displayed as box plots with the first level centered on zero. Covariates that were not retained in the model or not significant are represented with 'NA'.
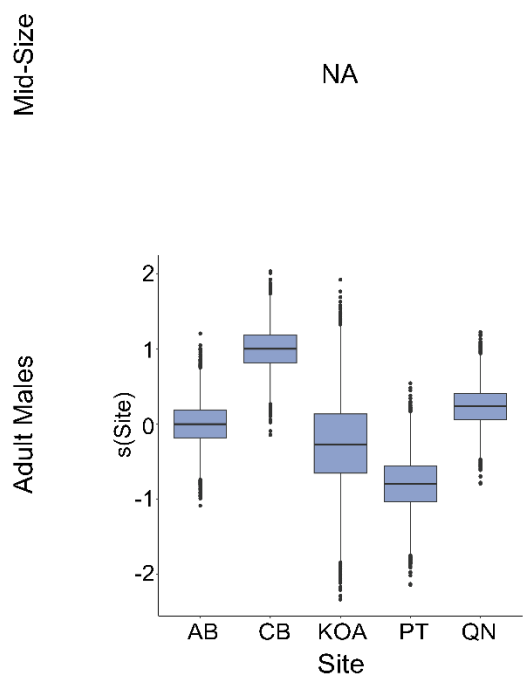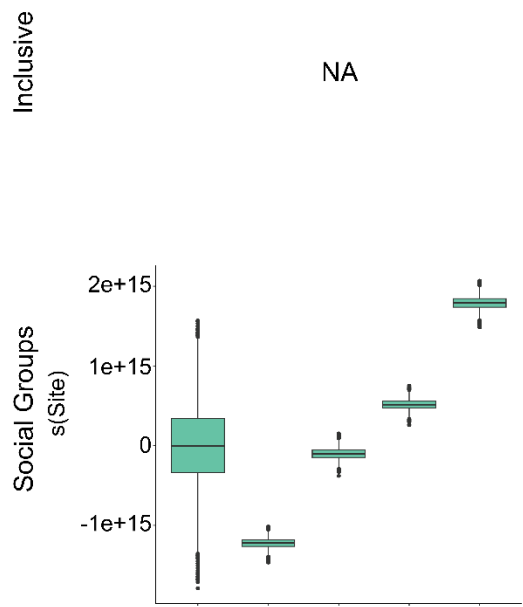
Figure S2.5. Presence by site for the Gulf of Alaska. Each row represents outputs from the different size class models for each site: a) Inclusive (grey), b) Social Groups (green), c) Mid-Size (orange), and d) Adult Males (blue). Site is a categorical variable displayed as box plots with the first level centered on zero. Covariates that were not retained in the model or not significant are represented with 'NA'.
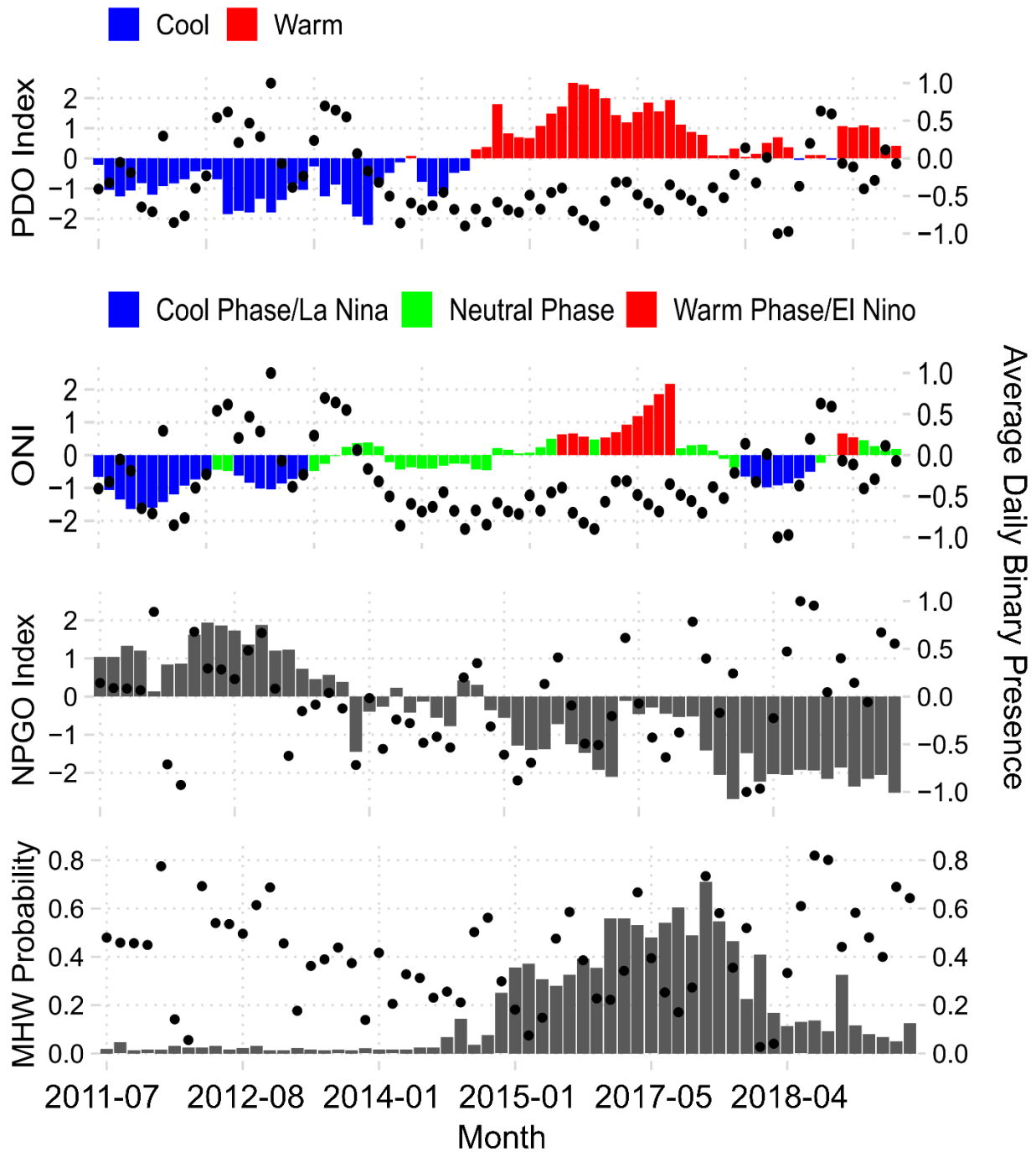
Figure S2.6. Timeseries of climate variability index/probability (PDO, ONI, NPGO, and MHW; left y-axis) and sperm whale presence (black points; right y-axis) for CB. Sperm whale presence for the PDO, ONI, and NPGO were normalized between -1 and 1 to align with the respective climate variability index axis.
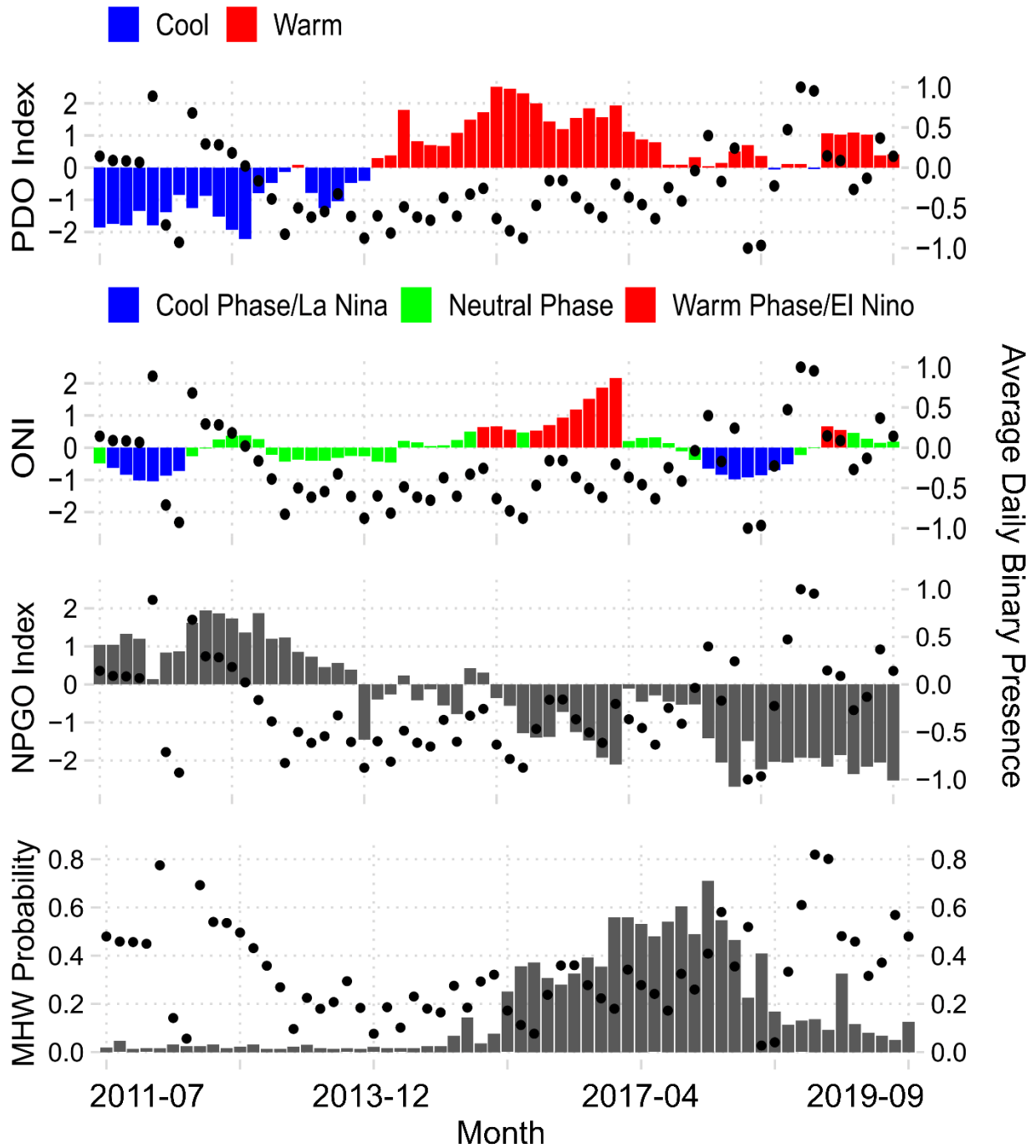
Figure S2.7. Timeseries of climate variability index/probability (PDO, ONI, NPGO, and MHW; left y-axis) and sperm whale presence (black points; right y-axis) for GOA. Sperm whale presence for the PDO, ONI, and NPGO were normalized between -1 and 1 to align with the respective climate variability index axis.
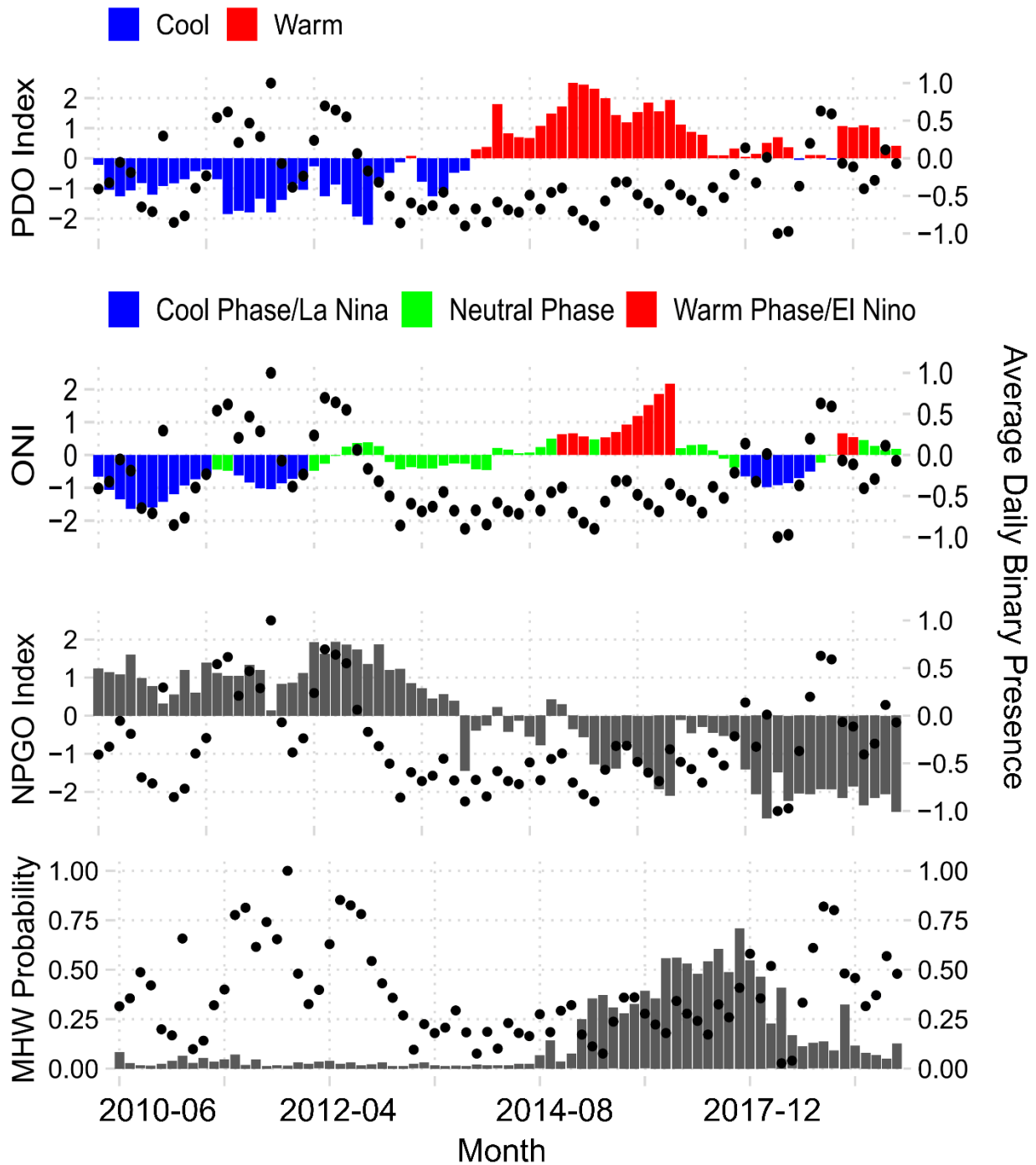
Figure S2.8. Timeseries of climate variability index/probability (PDO, ONI, NPGO, and MHW; left y-axis) and sperm whale presence (black points; right y-axis) for All-Sites. Sperm whale presence for the PDO, ONI, and NPGO were normalized between -1 and 1 to align with the respective climate variability index axis.
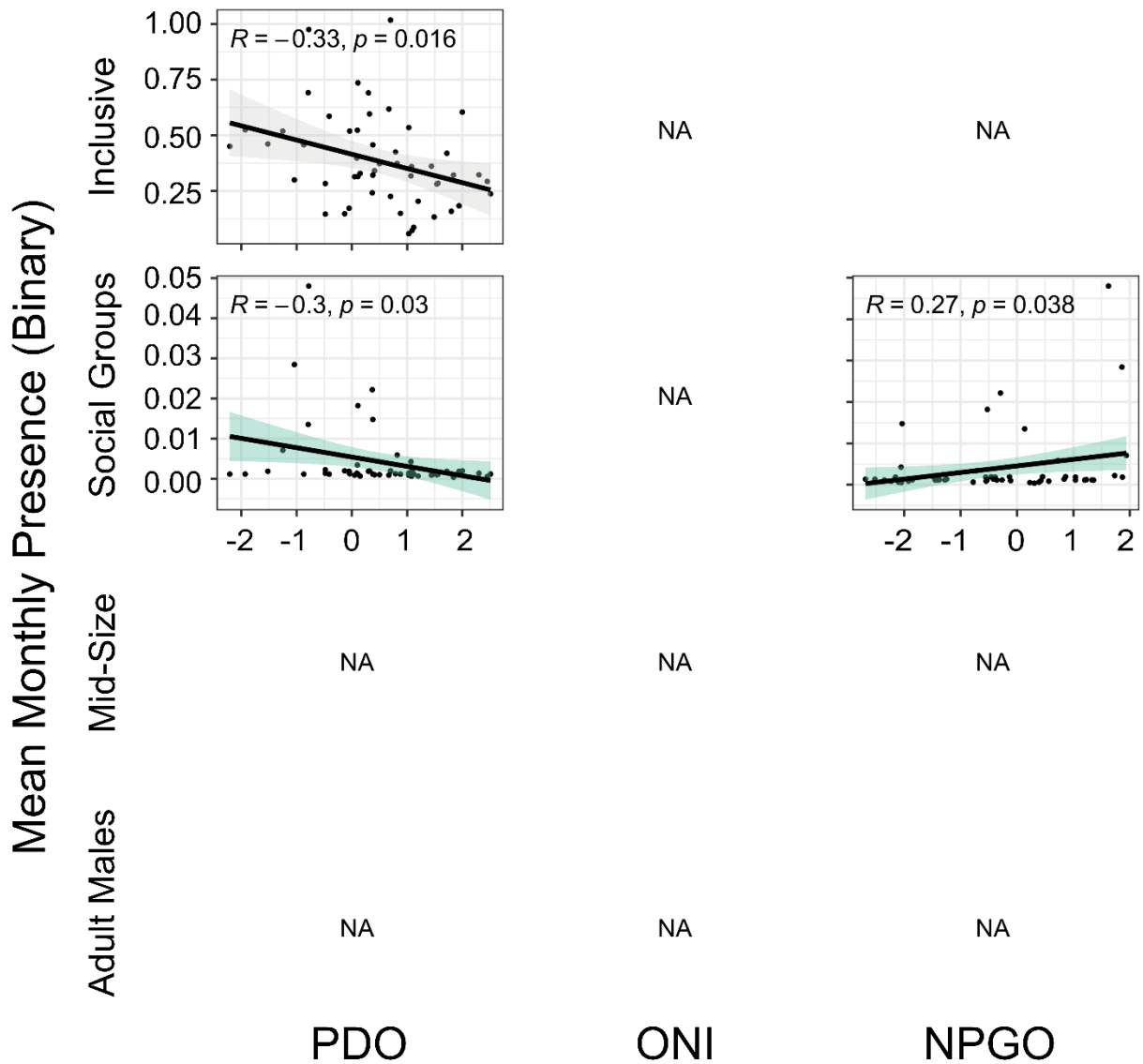
Figure S2.9. GLM plots displaying the relationship between mean monthly presence of sperm whales for site CB and the PDO, ONI, and NPGO index. All PDO and NPGO plots represent an eight-month lag, except for the Social Groups which does not include a lag. All ONI plots represent a nine-month lag. Each row (and color) represents outputs from the different size class models for each variable: Inclusive, Social Groups, Mid-Size, and Adult Males. All plots include 95% confidence intervals represented by the grey shading surrounding the linear regression. The regression formula for each model is displayed in the top left-hand corner. Covariates that were not retained in the model or not significant are represented with 'NA'.
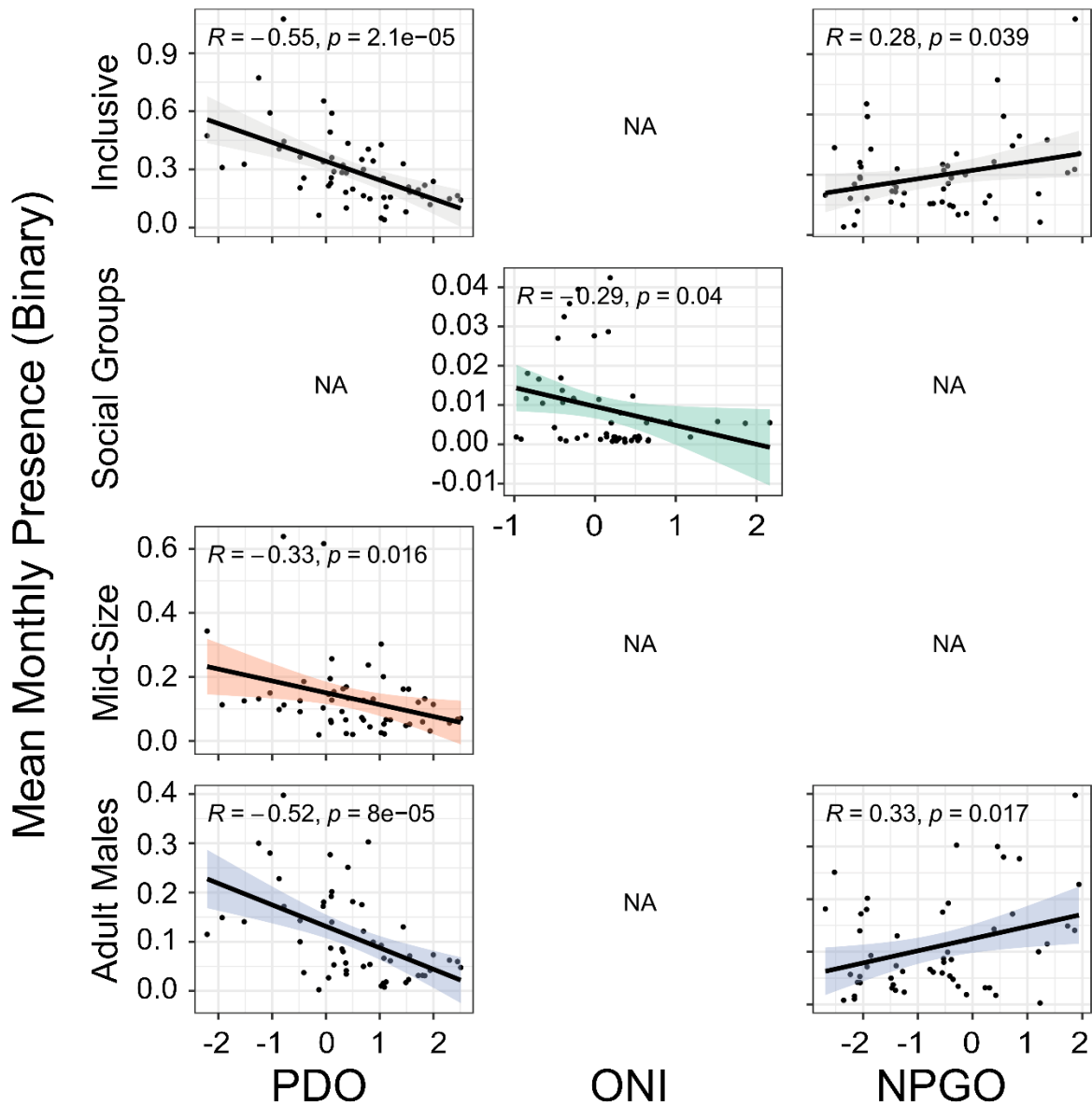
Figure S2.10. GLM plots displaying the relationship between mean monthly presence of sperm whales for the GOA region and the PDO, ONI, and NPGO index. All PDO and NPGO plots represent an eight-month lag, and all ONI plots represent a nine-month lag. Each row (and color) represents outputs from the different size class models for each variable: Inclusive, Social Groups, Mid-Size, and Adult Males. All plots include 95% confidence intervals represented by the grey shading surrounding the linear regression. The regression formula for each model is displayed in the top left-hand corner. Covariates that were not retained in the model or not significant are represented with 'NA'.

Table S2.2. Generalized linear model (GLM) summaries testing the relationship of sperm whale presence and the Pacific Decadal Oscillation (PDO), Oceanic Nino Index (ONI), North Pacific Gyre Oscillation (NPGO), and Marine Heat Wave (MHW) indices for all GAM/GEE models that included year as a variable (i.e., greater than 5 years of data). For each model and class, significance of the model with no lag is denoted with an asterisk (*) in the column 'Sig'. Significance of a model with a lag is denoted by a value from 8 to 12 representing the number of lags in months in the column 'Sig'. Respective p-values and R^2 values for each GLM is denoted for each significant model. Models that were not significant are denoted by 'NA'. Models where year was not significant in the corresponding GAM/GEE model are *italicized*.

	Class	PDO Sig	PDO P-Value	PDO R²	ONI Sig	ONI P-Value	ONI R²	NPGO Sig	NPGO P-Value	NPGO R²	MHW
CB	Inclusive	* 8	0.01 0.0016	-0.33 -0.33	NA	NA	NA	NA	NA	NA	NA
	Social Groups	* 8 9 10	0.045 0.03 0.012 0.047	-0.26 -0.3 -0.35 -0.28	NA	NA	NA	*	0.038	0.27	NA
	Mid-Size	*NA*			*NA*			*NA*			*NA*
	Adult Males	NA			NA			NA			NA
GOA	Inclusive	* 8 9 10	 0.007 2.1e-05 0.00023 0.01	-0.34 -0.55 -0.49 -0.36	NA	NA	NA	8	0.039	0.28	NA
	Social Groups	NA			9 10	0.04 0.049	-0.29 -0.28	NA	NA	NA	NA
	Mid-Size	8	0.016	-0.33	NA	NA	NA	NA	NA	NA	NA
	Adult Males	*** *8* *9* *10* *11* *12*	*0.025* *8e-05* *2.3e-05* *0.00051* *0.0034* *0.035*	*-0.29* *-0.52* *-0.55* *-0.47* *-0.41* *-0.3*	*9* *10*	*0.0396,* *0.0449*	*0.08196,* *0.0796*	*8* *9* *10*	*0.017* *0.0077* *0.014*	*0.33* *0.37* *0.34*	*NA*
All-Site	Inclusive	* 8 9 10 11 12	3e-05 1.1e-06 7.6e-07 2.4e-05 7.9e-05 8e-04	-0.46 -0.55 -0.57 -0.5 -0.47 -0.41	NA	NA	NA	8 9 10 11 12	1.6e-05 4e-05 0.00012 0.0014 0.0038	0.5 0.48 0.46 0.39 0.36	NA
	Social Groups	* 8 9 10 11 12	0.023 0.0022 0.012 0.015 0.047 0.015	-0.26 -0.37 -0.31 -0.3 -0.25 -0.3	9 10 11 12	0.027 0.007 0.012 0.016	-0.27 -0.33 -0.31 -0.3	8 9 10 1112	0.0049 0.037 0.0095 0.013 0.01	0.34 0.26 0.32 0.31 0.32	NA
	Mid-Size	* 8 9 10 12	0.014 0.0045 0.007 0.038 0.047	-0.28 -0.34 -0.33 -0.26 -0.25	NA	NA	NA	8	0.03	0.27	NA
	Adult Males	* 8 9 10 11 12	0.0053 9.7e-06 8.1e-07 1e-05 0.00021 0.02	-0.32 -0.51 -0.56 -0.52 -0.45 -0.29	8 9	0.021 0.047	-0.28 -0.25	8 9 10111 2	0.0018 3e-04 0.0028 0.0076 0.032	0.38 0.43 0.36 0.33 0.27	NA

Chapter 3: Demographic Specific Spatiotemporal Patterns and Density Trends for Sperm Whales in the Western North Atlantic

Natalie Posdaljian[1], W. Aaron Deans[1], Alba Solsona-Berga[1], John A. Hildebrand[1], Kaitlin E. Frasier[1], Samuel Murillo[1], Tiago Marques[2,3], Annamaria DeAngelis[4], Simone Baumann-Pickering[1]

[1] Scripps Institution of Oceanography, University of California San Diego, La Jolla, CA USA.

[2] Centre for Research into Ecological and Environmental Modelling, The Observatory, University of St. Andrews, St. Andrews, Scotland

[3] Centro de Estatística e Aplicações, Departamento de Estatística e Investigação Operacional, Faculdade de Ciências, Universidade de Lisboa, Lisboa, Portugal

[4] NOAA Northeast Fisheries Science Center, Woods Hole, MA USA.

3.1 Abstract

Sperm whales are sexually dimorphic with different body sizes, acoustic characteristics, and distribution patterns between males and females. Understanding sex- and age-specific spatiotemporal patterns is crucial for effective conservation and management of these animals. In the western North Atlantic (WNA), sperm whales are found throughout the ocean basin, particularly along the continental slope and further offshore. However, little is known about their population dynamics and seasonal presence of males and females. This study used acoustic data collected from 12 sites distributed along a latitudinal gradient in the WNA from 2015 to 2019. Demographic specific spatiotemporal patterns were investigated using differences in echolocation click characteristics to identify three distinct classes of sperm whales: Social Groups (females and their young), Mid-Size animals (including large females or juvenile males), and Adult Males. Sperm whale presence was significantly higher at the eight recording sites north of the Gulf Stream, with a notable proportion of Social Groups. Furthermore, the two regions exhibited marked differences in seasonal presence, with peaks in the spring and summer in the north and fall and winter in the south. This study also estimates the acoustic density of the three classes using two methods, one based on counting individual echolocation clicks and the other detecting animal groups in 5-minute time bins with at least one echolocation click. Both methods provided valuable insights in the acoustic density estimates for all three classes of sperm whales. Social Groups were the dominant group with a median density of over 80% across all sites, followed by the Mid-Size (+ 15%) and Adult Males (< 2%). The study also revealed an increase in density with a median annual change of 40% for Social Groups in the northern region over the recording effort. This could suggest a potential northern expansion of the population, possibly indicating ideal ecological conditions during our recording effort. These findings

emphasize the importance of considering specific demographic groups when analyzing spatiotemporal patterns particularly in revealing demographic specific population trends like seen with the increasing density of Social Groups in the WNA. Such knowledge is critical for the development of targeted conservation strategies and the sustainable management of sperm whale populations that could differ from one demographic group to another.

3.2 Introduction

Sperm whales face significant challenges that have contributed to their endangered status. One of the primary threats to their population was historical commercial whaling which started in the Atlantic Ocean and later expanded throughout the world, severely depleting sperm whale populations (Best 1983). Although there has been a cessation of commercial whaling activities, the population has been slow to recover (Whitehead 2003) and is still considered endangered under the U.S. Endangered Species Act, depleted under U.S. Marine Mammal Protection Act, and vulnerable under the International Union for the Conservation of Nature. In addition to historical impacts, sperm whales now face modern-day threats such as entanglement in fishing gear, underwater noise pollution, habitat degradation, and climate change (Sousa *et al.* 2019)

In the western North Atlantic (WNA), sperm whales are managed as one stock within the U.S. Exclusive Economic Zone by the National Oceanic Atmospheric Administration (NOAA) Northeast Fisheries Science Center (NEFSC). Comprehensive data on various aspects of animal biology and ecology are required to effectively conserve and manage sperm whales. Long-term monitoring programs that track spatial and temporal distribution patterns and estimate population size and trends are essential for identifying critical areas for conservation and implementing appropriate management measures. Furthermore, since sperm whales are highly sexually dimorphic and display differences in behavior and habitat preference, an understanding of their

demographic composition, including the proportions of males and females, is crucial for ensuring these measures are well equipped to protect the animals in the region.

In the WNA, sperm whales are concentrated over the continental slope and into mid-ocean regions over canyons and seamounts (Waring *et al.* 1993; Roberts *et al.* 2016), although they are also found in northern shelf waters, the continental shelf edge, and into deeper ocean waters, albeit in lower densities (Schmidly 1981; Roberts *et al.* 2016). Sperm whales are great candidates for acoustic monitoring since they spend more than 70% of their time in foraging dive cycles during which they produce echolocation clicks (Watwood *et al.* 2006). According to previously conducted acoustic studies by Stanistreet *et al.* (2018) sperm whales are acoustically detected more commonly north of the Gulf Stream with an almost constant presence in the mid-Atlantic Bight. A winter peak in presence occurs east and northeast of Cape Hatteras, North Carolina. In the spring, the peak is seen further northeast of Delaware and Virginia and the southeast portion of Georges Bank. In the summer, the distribution moves further north of Georges Bank and into the Northeast Channel and the continental shelf south of New England. In the fall, a peak occurs south of New England on the continental shelf. Abundance estimates have been conducted from NEFSC visual surveys in the WNA with the best estimate being 4,349 animals (CV = 0.28) (Hayes *et al.* 2022) and 5,353 animals (CV = 0.12) based on habitat cetacean density models from visual data (Roberts *et al.* 2016).

Despite the significant progress made in understanding the spatiotemporal patterns and abundance of animals in this region, notable gaps remain in our knowledge of demographic composition and any sex-specific differences. Male and female sperm whales are sexually dimorphic and exhibit distinct behaviors and habitat preferences, with variations in their distribution and seasonal patterns (Best 1979; Rice 1989; Gregr & Trites 2001). Females and

their young form social groups and are usually found in temperate and tropical latitudes, while males forage at higher latitudes. Visual sightings from NEFSC surveys included social groups in shelf-edge and off-shelf waters (CETAP 1982; Waring *et al.* 1992, 1993) as well as single animals, presumed to be males (Palka *et al.* 2017, 2021; NEFSC & SEFSC 2021). However, differences in seasonal trends or habitat use for males and females are unknown for this region. Although visual based abundance estimates exist for the entire WNA stock of sperm whales, they are outdated and do not incorporate acoustic data that could provide more insight into the presence of an easily acoustically detected animal with a high-amplitude echolocation click used for finding prey, communicating, and navigating their surroundings (Worthington & Schevill 1957; Norris & Harvey 1972; Watkins & Schevill 1977; Gordon 1987; Mullins *et al.* 1988)

Sperm whale sexual dimorphism in body size is also linked to differences in echolocation click characteristics and diving behaviors (Gordon 1991; Watwood *et al.* 2006; Growcott *et al.* 2011; Solsona-Berga *et al.* 2022). Not only do males produce echolocation clicks with higher source levels, but the time between clicks, or the interclick interval (ICI), is longer compared to the females likely as a result of their larger heads (Goold & Jones 1995; Solsona-Berga *et al.* 2022). Differences in click production and ICI would also greatly impact acoustic density estimation of sperm whales, a technique that relies on quantifying whale vocalizations within a designated timeframe in a given area, the cue rate (Marques *et al.* 2009). Calculating sex-specific acoustic density estimates could reduce the error in averaging values that are extremely different for each sex while allowing for analysis of population status trends for males and females separately. Long-term acoustic data can also be used to understand demographic composition and how it changes over time (Beslin *et al.* 2018; Solsona-Berga *et al.* 2022), particularly spatiotemporal or density trends for that subset of the population.

In this study, we used differences in sperm whale echolocation clicks to reveal spatiotemporal patterns for male and female sperm whales across 12 sites spanning a latitudinal gradient in the WNA from 2015 to 2019. Generalized additive models (GAMs) with generalized estimating equations (GEEs) were used to evaluate seasonal, interannual, and spatial trends for males and females in the region. Furthermore, we present demographic-specific acoustic density estimates using two distinct approaches—click counting and group counting—thereby enhancing our understanding of the density of sperm whales in the WNA. The knowledge gained from this study is crucial for the development of targeted conservation strategies and the sustainable management of sperm whale populations and highlights the significance of considering specific demographic groups in analyzing spatiotemporal patterns and population trends given differences in seasonal trends, spatial distribution, behavior, and acoustic characteristics that are used for acoustic density estimation. Ultimately, this research contributes to our broader understanding of sperm whale demographics, distribution, and density trends in the WNA.

3.3 Methods

3.3.1 Data Collection

Passive acoustic monitoring was carried out using High-frequency Acoustic Recording Packages (HARPs; Wiggins & Hildebrand 2007) at twelve sites in the WNA between April 2015 and June 2019 (Figure 3.1, Table 3.1). Henceforth, "the northern sites" or "North" collectively refers to sites north of the Gulf Stream (HZ, OC, NC, BC, WC, NFC, and HAT A/B) and includes the Georges Bank, Southern New England, and Mid-Atlantic Bight regions. The "southern sites" or "South" collectively refers to sites south of the Gulf Stream (GS, BP, BS, and JAX) and is within the South-Atlantic Bight. Except for JAX, all sites were located on the continental slope, an area of known high abundance for sperm whales (Waring *et al.* 1993, 2001;

Roberts *et al.* 2016). Each site had three to four deployments which resulted in 3-4 years of recordings at each site. Between all sites, nearly 36 years of cumulative recordings were included in this study. Each HARP sampled with a frequency of 200 kHz and recorded nearly continuously with intermittent gaps between deployments due to servicing schedules and limitations of battery life and data storage capacity (Table 3.1).

3.3.2 Detecting Sperm Whales

Sperm whale echolocation clicks were detected using the multi-step approach described in Solsona-Berga *et al.* 2020 (appendix) and applied in Posdaljian *et al.* (2022). The characteristic echolocation clicks of sperm whales have multiple pulses (Backus & Schevill 1966), 2-9 ms apart, depending upon the size of the animal (Norris & Harvey 1972). As a result, the detector had a lockout for clicks separated by less than 30 ms to avoid multiple detections of a single click. Bandpassing the data (5-95 kHz) minimized the effects of low-frequency noise from vessels, weather, or instrument self-noise on detections, but allowed for detection of the echolocation clicks of toothed whales. The Power Spectral Density (PSD) of detected signals was calculated with the Pwelch method (MATLAB, MathWorks, Natick, MA) using 4 ms of the waveform and a 512-point Hann window with 50% overlap (Welch 1967). Instrument-specific full-system transfer functions were applied to account for the hydrophone sensor response, signal conditioning electronics, and analog-to-digital conversion. To provide a consistent detection threshold, only clicks exceeding a peak-to-peak (pp) received level (RL) of at least 125 dBpp re 1 µPa were analyzed.

Sperm whale echolocation clicks can be confused with the impulsive signals from ship propeller cavitation. An automated vessel classifier developed by Solsona-Berga et al. 2020 (appendix) was used to exclude periods of ship passages during which it was not possible to

distinguish between sperm whale clicks and ship cavitation noise. The classifier identified potential ship passages from long-term spectral averages (LTSA), which are long duration spectrograms (Wiggins & Hildebrand 2007). Further averaging was calculated as Average Power Spectral Densities (APSD) per 2-hour blocks over low (1-5 kHz), medium (5-10 kHz), and high (10-50 kHz) frequency bands with 100 Hz bins and 50% overlap. Using received sound levels, transient ship passage signals were separated from odontocete echolocation clicks and weather events. Trained analysts manually reviewed identified ship passages using the MATLAB-based custom software program *Triton* (Wiggins & Hildebrand 2007). Ship passage times were removed from further analysis and considered time periods with no effort.

Instrument self-noise and the echolocation clicks of other odontocetes were also removed to reduce the number of false positive detections. A classifier using spectral click shape was implemented, taking advantage of a sperm whale click's distinct low-frequency spectral shape to remove dissimilar clicks by delphinid and beaked whales, which typically have higher frequencies (Solsona-Berga *et al.* 2020). The remaining acoustic encounters containing putative sperm whale echolocation clicks were manually reviewed with the MATLAB-based open-source *DetEdit* software program used to view, evaluate, and edit automatic detections (Solsona-Berga *et al.* 2020). After detections were edited, data was further analyzed on the click level as well as grouped into 5-min time bins. The proportion of false positive clicks and 5-min time bins was evaluated using *DetEdit*. The proportion of false positive clicks was calculated by evaluating every random 3,000[th] click in the entire dataset; the proportion of false positive 5-min time bins was calculated by evaluating the bin of the randomly selected clicks.

3.3.3 Inter-click Interval as a Proxy for Demographics

Histograms of ICI provide a visualization that can be used to indicate sperm whale size and sex (Solsona-Berga *et al.* 2022). A plot of concatenated histograms of 5-min time bins, referred to as ICIgrams, was annotated and categorized for each time period at each site. Examples of the ICIgram GUI can be found in Solsona-Berga *et al.* (2022). We used three ICI groups to correspond to three size classes as per Solsona-Berga *et al.* (2022). Detections with a modal ICI of 0.6 s or less were presumed to be females and their young, hereinafter referred to as Social Groups. Detections with a modal ICI of 0.8 s and greater were presumed to be adult males, hereinafter referred to as Adult Males. The detections with a modal ICI between the Social Groups and Adult Males (< 0.6 s and > 0.8 s) could be large females or juvenile males, hereinafter referred to as Mid-Size. To find the mean ICI of each class, a Gaussian mixture model (GMM) was fit to the distribution of ICI within a class and the mean of the distribution was used (Huang *et al.* 2001; Roch *et al.* 2007)

Each 5-min time bin was categorized into the appropriate size class. The class of each time bin was applied to all the clicks within that bin. If a 5-min time bin was categorized as one or more size class (2-7% of 5-min time bins), the clicks in that bin were proportionally assigned a class based on the proportion of the classes for that week.

For density estimation, the 5-min time bin data was binned by week. Some 5-min bins with clicks were not a candidate for categorization due to the low number of clicks or lack of neighboring time bins to inform categorization. As a result, not all clicks or 5-min time bins in a week were assigned a category. In this case, the unassigned clicks and bins were proportionally assigned to a class based on the proportion of the classes in that week.

3.3.4 Statistical Analysis

Sperm whale encounters lasted for many hours to days at all sites, indicating temporal autocorrelation whereby detections in a single one-hour bin increased the likelihood of detections in adjacent bins. To minimize the impacts of the temporal autocorrelation and to avoid data sub-sampling or using a coarse analysis resolution, Generalized Additive Models (GAMs; Hastie & Tibshirani 1987) were combined with Generalized Estimating Equations (GEEs; Liang & Zeger 1986) a method previously used to address autocorrelation in marine mammal presence data (Panigada *et al.* 2008; Pirotta *et al.* 2011; Benjamins *et al.* 2017; Merkens *et al.* 2019). The GAM/GEE model framework was used to test the significance of temporal predictors, or variables, of sperm whale presence, outlined by Pirotta *et al.* (2011), in the software R (R Core Team 2022). Patterns were explored for all sperm whales combined, hereinafter referred to as the Inclusive model, and for each of the three size classes, referenced as the Social Group, Mid-Size, and Adult Male models. The Inclusive model and class models were built for each site and region. The response variable was binomial presence-absence of sperm whale clicks in one-hour time bins (1 = presence and 0 = absence). The site-specific models included the explanatory variable Julian day and Year to describe seasonality and inter-annual variability in presence. The region-specific models included the explanatory variables Julian day and Year, as well as Site to account for the spatial variability.

Under the GAM/GEE approach, the data are grouped into blocks, within which residuals are allowed to be correlated, while independence is assumed between separate blocks. The R correlation function acf within the stats package (R Core Team 2022) was used to determine the time step for blocking. Blocks were defined by the value where the autocorrelation of the residuals of a Generalized Linear Model (GLM) dropped below 0.1. Block sizes varied between 226 – 1249 hours (9 – 52 days) for all 28 models. Although GEEs are considered robust against

correlation structure misclassification (Liang & Zeger 1986), an autoregressive order 1 (AR-1)

covariance structure was used to describe model error given the temporal autocorrelation in the

data (Panigada *et al.* 2008; Pirotta *et al.* 2011; Bailey *et al.* 2013b; Booth *et al.* 2013; Stimpert *et al.* 2015; Merkens *et al.* 2019).

The same GLM used to determine block size was also used to assess collinearity of

variables following Zuur (2012). The *vif* function in the R package *car* (Fox 2019) identified

potentially collinear variables. Because the variable Year is a factor, VIF was corrected by the

degrees of freedom of the predictor variable to calculate the Generalized Variance Inflation

Factor (*GVIF*):

$$GVIF = VIF^{\frac{1}{2*df}} \qquad (1)$$

where *VIF* is the variance inflation factor and *df* is the degrees of freedom of the predictor

variable (Fox & Monette 1992). None of the variables in the GLM model had a GVIF over 2.0

and all variables were retained for further modeling.

Models were built using the function geeglm in the *geepack* package (Halekoh *et al.*

2006) in R. Variables were treated differently within each model—as a spline, or as a factor—

based on the nature of the variable. Given the circular nature of the variable Julian day it was

included as a cyclic spline based on a variance-covariance matrix built using the *gam* function in

the *mgcv* package in R (Wood 2011) to fit a circular smooth in a GEE framework. Given the

small number of years for the time series, year was included as a factor to estimate year-specific

effects. Site and region were input into the models as factors given the categorical nature of both

variables.

For models with more than one variable, model selection used the Quasilikelihood under

Independence model Criterion (QICa) value, an alternative to Akaike's Information Criterion for

GEE models (Pan 2001), available through the function *QIC* in the *geepack* package in R (v.1.1-6; 58). Manual backwards stepwise model selection was carried out where the model with the lowest QICa was selected from among the full model (all variables) and a series of models containing all variables but one (Pirotta *et al.* 2011; Benjamins *et al.* 2017). This selection method continued until removing any of the remaining variables caused the QICa to increase. The order of the variables in the final model was determined by which variable, when removed, increased the QICa the most. A Wald's Test was conducted on the final model using the function *anova* in the *geepack* library to determine the significance of each variable in the model. Any non-significant variables were removed from the models using backwards stepwise model selection until all p-values of the remaining variables were greater than 0.05. Partial-fit plots for each variable in the final models were created using the approach described by Pirotta *et al.* (2011). The x-axis for Julian Day is represented by the months of the year and interpreted as sperm whale occurrence among seasons (winter: December - February, spring: March - May, summer: June – August, fall: September – November).

The goodness of fit of the models was evaluated using the *performance* package in R (Lüdecke *et al.* 2021). The coefficient of discrimination, also known as Tjur's R2 (Tjur 2009), was calculated for each model using the function *r2_tjur*. Binned residuals were also used to assess the fit of the models. Binned residual plots were obtained using the function *binnedplot* (Gelman & Hill 2007). A good fit was expected to have all residuals within the 95% confidence intervals (Gelman & Hill 2007).

3.3.4 Density Estimation

Sperm whale echolocation clicks were converted to acoustic density estimates using two approaches that work with fixed single-sensors (Buckland *et al.* 2001; Buckland 2006). The first

approach converts single echolocation clicks into density estimates, hereinafter referred to as

click counting. The click counting method uses echolocation clicks recorded from a fixed single

sensor at site k during week t to calculate animal density $\widehat{D}_{kt}$, based on the following equation

(Marques *et al.* 2009):

$$\widehat{D}_{kt} = \frac{n_{kt}\left(1 - \hat{c}_{pk}\right)(1 + \hat{c}_{nk})}{\pi\,w^2 \widehat{P}_k\,T_{kt}\,\hat{r}} \tag{2}$$

where n_{kt} is the number of clicks detected, $\hat{c}_{pk}$ is the false positive click rate, w is the detection

radius, P_k is the click detection probability, T_{kt} is the effort time, $\hat{r}$ is the cue rate, and $\hat{c}_{nk}$ is the

proportion of missed click detections (Figure 3.2).

The second approach converts the absence or presence of detections in a 5-min time bin

into density estimates, hereinafter referred to as group counting. The group counting method

converts 5-min time bin presence of acoustic cues recorded from a fixed single sensor at site k

during week t to calculate animal density $\widehat{D}_{kt}$, based on the following equation (Hildebrand *et al.*

2015):

$$\widehat{D}_{kt} = \frac{n_{kt}\left(1 - \hat{c}_k\right)(1 + \hat{c}_{nk})\,\hat{s}}{\pi\;w^2 \widehat{P}_k\;\widehat{P}_v\;T_{kt}} \tag{3}$$

where n_{kt} is the number of time bins detected, $\hat{c}_{pk}$ is the false positive bin rate, w is the detection

radius, P_k is the bin detection probability, T_{kt} is the effort time, $\hat{s}$ is the group size, $\widehat{P}_v$ is the

probability of the group being vocally active in a time bin, and $\hat{c}_{nk}$ is the proportion of missed

bin detections (Figure 3.2).

Delta method approximation was used to obtain the variance of estimated acoustic

densities using the following equation (Seber 1982):

$$\hat{v}ar(\hat{D}_{kt}) = \hat{D}_{kt}^2\{CV^2(\hat{c}_k) + CV^2(\hat{P}_k)\} \qquad (4)$$

where $CV_{(x)}$ represents the modified coefficient of variance, or the standard error of the mean

divided by the mean.

To differentiate between seasonal and non-seasonal trends in the time series, a parametric

model was employed. To detrend the data, the raw time series data underwent linear regression

analysis using the Theil-Sen estimator (Sen 1968) and the resulting seasonal pattern was

subtracted from the original data. To find an increasing or decreasing trend in density the

detrended data underwent regression analysis with a set of monthly indicators which were

subtracted from the original time series. The density trend was estimated using a least-square

linear regression approach, which also provided estimates for the trend's 95% confidence

intervals.

3.3.4a Propagation Modeling

Both click and group counting approaches to density estimation require understanding sound

propagation to calculate the probability of detecting acoustic cues. Sound propagation depends

on several variables including sound speed, local bathymetry, and sediment properties (Helble *et

al.* 2013b). This study developed a software repository with multiple packages to generate sound

speed profiles (SSPs) and model sound propagation at each of the respective sites. These

programs are globally applicable and are publicly accessible on GitHub as the *PropaMod*

repository (https://github.com/nposdalj/PropaMod).

To generate SSPs for each site, monthly samples of temperature and salinity data were taken

from the Hybrid Coordinate Ocean Model (HYCOM; https://www.hycom.org/) (Bleck 2002) for

July 2015 through June 2019. The HYCOM model has a temporal resolution of 3 hours, with

some gaps. Each sample included midnight and noon data from the earliest day in the month that

had both, downloaded as 3-dimensional matrices of temperature and salinity spanning the region 24-44°N, 82-63°W. To account for diel fluctuation, the midnight and noon data were averaged. For each month, a matrix of sound speeds was calculated for the region from the resulting averaged temperature and salinity matrices and the matrix of corresponding depths, using the nine-term equation developed by (Mackenzie 1981) and adapted for MATLAB by Koptenko (2023) as the function *salt_water_c*.

HYCOM includes no data under the sea floor; however, because each study site's SSP in water is applied to areas deeper than the study site during propagation modeling, it must be artificially calculated deeper than the study site. To enable this, the function *inpaint_nans.m* (D'Errico 2023) was applied to the monthly sound speed matrices to fill in each missing value by extrapolating from the nearest points at the same depth that had data.

The finalized monthly sound speed matrices were interpolated to the average coordinates of each study to obtain the site SSPs for each month. These SSPs were averaged across years to obtain twelve monthly averages (for January through December); these were in turn averaged to obtain the overall mean SSP at each study site.

Using these SSPs, the sound propagation around the study sites was modeled with the ray-tracing program bellhopcxx/bellhopcuda (Pisha *et al.* 2023),, originally written in Fortran by Dr. Michael B. Porter in 1983 and known as BELLHOP (Porter & Bucker 1987). Three propagation models, one for each size class, were generated for each site with frequencies specific to each size class. To account for sound absorption (Francois & Garrison 1982), peak frequencies were calculated for each class from the acoustic data itself by fitting a Gaussian mixture model (GMM) to the distribution of peak frequencies for each click within a class and taking the mean (Huang *et al.* 2001; Roch *et al.* 2007).

For each site and each class, propagation models were calculated using two-dimensional profiles (range vs. depth) at 10-degree azimuthal increments, or radials, with the receiver in the center. Each model included 36 evenly spaced radials with a radius of 40 km, and with depth-wise and range-wise data resolutions of 10 m.

To account for the impact of interaction with the sea floor on the propagation of sound, sediment type data was obtained from the Bottom Sediment Type (BST) database (Naval Oceanographic Office 2003). The BST database assigns sediment types as numbers 1-23. The function *getGrainSize* in *PropaMod*, extracts the numeric codes and replaces them with the phi grain size associated with each sediment as detailed by the APL-UW (1994) High-Frequency Ocean Environmental Acoustics Models Handbook in Section IV, Table 2. For each radial, the most important grain size was determined and applied to the entire radial, as allowing for range-dependent sediment type would be computationally expensive.

For each radial the assigned source frequency and grain size were used to calculate the compressional speed (CS), shear speed (SS), compressional attenuation (C-att), and shear attenuation of sound (S-att) in the sea floor along the radial. Calculations for CS, C-att, and S-att were done through bellhopcxx/bellhopcuda based on grain size. A program for modeling the interaction of sound with the sea floor, included within *PropaMod* as the MATLAB function *hamilton_aehs*, was adapted from programs developed by Miller and Potty and uses values and relationships detailed by Hamilton (1976, 1980) and Bowles (1997) to calculate S-att based on whether the sediment was "sand-type" or "clay-type" (Potty *et al.* 2006; Hillson *et al.* 2007).

3.3.4b Probability of Detection

Distance sampling-based methods (Buckland *et al.* 2001) using a Monte Carlo simulation approach (Küsel *et al.* 2011) have been used to estimate the probability of detecting marine

mammal sounds from a fixed single sensor (Küsel *et al.* 2011; Helble *et al.* 2013; Frasier 2015; Hildebrand *et al.* 2019; Solsona Berga 2019). In this study, two types of simulations were conducted at each site and for each class to model demographic specific detection probabilities. In the first type of simulation, the detection probability for an individual echolocation click was determined based on its horizontal range from the hydrophone. In the second type of simulation, the detection probability of a group of clicking sperm whales was determined based on the clicks received in a finite time window (5-min), with detection of the group dependent upon the highest amplitude received click within the window. To determine the probabilities of click and group detection at each site, both models consider various elements including echolocation signal characteristics (e.g., frequency, source level), sound propagation models (see above section), animal behavior, and receiver characteristics.

The model input parameters specific to each class were derived from the data itself when possible and otherwise obtained from relevant literature. Click characteristics such as frequency, beam pattern, and source level were required for the simulation approach. Frequency was derived from the data itself as described in the previous section. Source levels and directivity for on-axis clicks have only been measured for male sperm whales in the Mediterranean and Norway, reaching as high as 245 ± 3 dB$_{pp}$ re: 1µPa @ 1m with a directivity of 27 dB (Møhl *et al.* 2003; Zimmer *et al.* 2005). Source levels for Social Groups and Mid-Size are expected to be lower than the reported values for males given their smaller head size. For off-axis clicks, the circular piston model was employed to account for attenuation of source levels (Møhl *et al.* 2003, Zimmer *et al.* 2005) and the off-axis beam shape was interpolated based on two distinct beam patterns reported by Zimmer *et al.* (2005), varying click levels both forward and backward in direction.

Metrics of sperm whale dive behavior such as dive depth, clicking start depth, and body orientation were also required for the simulation approach. Since sperm whales display a bimodal mean dive altitude above the seafloor (Watwood *et al.* 2006; Irvine *et al.* 2017; Mate *et al.* 2017), 50% of the simulated dives were characterized by search and foraging phases in the mid-water column, while the other 50% involved traveling along the seafloor (10 m above). Based on existing literature, the start depth for clicking was set at 200 m (Watwood *et al.* 2006). Two dimensions were considered for body orientations, vertical (pitch) and horizontal (yaw) planes. During the foraging phase of the dive, the body was assumed to be parallel to the seafloor (mean body pitch angle of 0°), with a left-truncated normal, and standard deviation of 0-50° (Watwood *et al.* 2006). The yaw angle has not been documented in literature so azimuthal symmetry with respect to the sensor site was assumed and all orientations were given equal likelihood (0-360°).

The simulation approach also requires an understanding of whether a click would be detected within the maximum range (40 km). This can be calculated using the sonar equation:

$$RL = SL - TL \qquad\qquad (5)$$

where the click received level (RL) is derived by subtracting the transmission loss (TL, generated during propagation modeling as described in the section above) from the on-axis click source level.

For both the click and group approaches, 100,000 randomly placed animal positions vocalizing within 40 km radius of the sensor were simulated 500 times. Variability and uncertainty of model parameters were incorporated into the estimates over the 500 iterations. A received level threshold of 125 dB$_{pp}$ re: 1μPa was applied, and only individual clicks or groups above the threshold were used in the analysis. The ratio of detected clicks or groups to the

number of simulations was used to calculate the detection probability, and the mean probability

of detection and its variance were obtained using the Monte Carlo framework established in

Frasier *et al.* (2016).

A distribution of measured received levels of clicks for each class was used to determine the

parameters that best fit the model output (Hildebrand *et al.* 2019; Solsona Berga 2019). The sum

of the squared misfit for received level bins above the 125 dB$_{pp}$ was used as a goodness-of-fit

metric when selecting the model parameters. A grid search, testing over 200 potential parameter

values and combinations, was conducted to determine the parameters that optimized the

goodness-of-fit metric. By contrasting the model results with the actual data, the grid search

method facilitated the fine-tuning of parameters and enhanced the alignment between the

simulated and observed detection patterns. Once the model parameters were selected and the

final model was derived, the percentage of missed detections (false negatives) was estimated by

taking the sum of the misfit between the model and the measured data for the first five received

level bins above the threshold (125-130 dB$_{pp}$). This method is built on the fundamental concept

that as the received level increases, the distance between animal and receiver decreases, and with

it the radius and observed area. This results in a decrease of the number of detectable clicks

given even distribution of animals within the detectable area.

3.3.4c Vocal Activity

Both the click and group counting methods require an understanding of sperm whale vocal

activity, particularly the proportion of time spent clicking versus the time spent silent. This was

calculated by multiplying the proportion of time in a foraging dive spent in the search phase

producing echolocation clicks by the total time spent in a foraging dive. These parameters were

obtained from tag data in the literature. For the Social Groups and Mid-Size, tag data from the

northwestern Atlantic Ocean was used where whales spent 80.7% (SD = 3.7) of their time in a foraging dive in the search phase (Watwood *et al.* 2006). For the Adult Males, tag data from northern Norway was used where whales spent 91% (SD = 10) of their time in a foraging dive in the search phase (Teloni *et al.* 2008). The total time spent in a foraging dive cycle was 72% (SD = 32.7) and was obtained from tag data in the Gulf of Mexico and northwestern Atlantic Ocean (Watwood *et al.* 2006). Once the aerobic dive limit is surpassed, the duration of sperm whale dives is restricted by physiological constraints due to the rising expense of anaerobic metabolism (Kooyman *et al.* 1981; Watwood *et al.* 2006). As a result, both males and females likely spend similar proportions of time in foraging dive cycles given their physiological need to recover after a series of dives. It is possible that males might require longer to recover since they often dive longer than females (Clarke 1976; Schreer & Kovacs 1997; Watkins *et al.* 2002), but since the estimate by Watwood *et al.* (2006) was the best existing estimate, it was used for all classes.

For the click counting method, a cue rate, or sperm whale sound production rate, is needed for sperm whales of each class. The cue rate was simulated for each class and for each site and calculated by dividing the proportion of time whales spend clicking (see above for dive parameters) by their ICI. The ICI was obtained for each class by finding the time between detections. ICIs less than 0.3 s and greater than 2.0 s were removed from the calculation to reduce error from instances when the ICI appears faster because of multiple animals clicking at once and when the ICI appears slower because the time between detections spans two encounters with a larger gap or because of missed consecutive clicks.

For each class at each site, 100,000 cue rates were calculated by randomly choosing the dive parameters and ICI from a distribution of potential values. The cue rate was rounded to the second decimal place and the mode of the distribution was retained. This simulation was

repeated 100 times to create a distribution of modal cue rates. The mean and standard deviation of the modal cue rate distribution for each class and each site was used for density estimation.

For the group counting approach, an understanding of click synchronicity among members of a group is required to estimate the probability of detecting a group of animals. The probability of a group being vocally active, P_v, within a 5-min time bin increases with group size expressed as:

$$Pv = Pcyc \ (\ s - (s - 1) * o) \qquad (6)$$

where P_{cyc} is the proportion of time spent clicking by an individual sperm whale, s is the group size, and o is the pair-wise overlap, or synchrony, between bouts of echolocation between two animals. Equation (6) is more suitable for moderate group sizes, comprised of less than 10, and will result in 100% probability of vocalization for large groups of animals. This equation also assumed that all animals in a group contribute overlapped and non-overlapped echolocation time to the bout.

Ideally, simultaneously tagged animals from the same population would be used to calculate group synchronicity (o). However, this data is rare so the group synchronicity calculation in this study is based on an instance from the Gulf of Mexico where three female sperm whales from the same group were simultaneously tagged (Jochens *et al.* 2008). Pairwise analysis of their echolocation timing suggested a synchrony level of 77% ± 4% among pairs of whales within the group (Hildebrand *et al.* 2012, Solsona-Berga 2019).

3.3.4d Group Size

In this study, visual and aerial sighting data from several NOAA Southeast Fisheries Science Center (SEFSC) surveys were used to calculate group sizes for Social Groups necessary for the group counting density estimation approach. The surveys included four Atlantic Marine

Assessment Program for Protected Species (AMAPPS) surveys from 2011-2021 (Palka *et al.* 2017, 2021; NEFSC & SEFSC 2021) one Mid-Atlantic Cetacean Habitat (MACH) survey in 2006 (SEFSC, unpublished data), and data from 30 aerial surveys from 2002-2021 (SEFSC, unpublished data). Only data between 28.53^{o}N and 42.28^{o}N and -78.50^{o}W and -63.14^{o}W and from the shelf break to 1500 m water depth were considered. Data across the years spanned the summer months of June to September.

The three survey types had different methods for estimating group size. For the AMAPPS and MACH surveys, group sizes were collected as the minimum, best, and maximum group size estimates according to independent observer entries (SEFSC, unpublished data). The best estimate value was used for further group size calculations. For the aerial surveys, group size estimates were conducted by two teams and categorized as either being an 'Original' sighting, meaning the original group size estimate when the animal(s) was first sighted, or a 'Follow On' sighting when the group size estimate was repeated after following the animal(s). If more than one estimate existed for a unique sighting and both were categorized as 'Original' sightings, the average group size estimate between the two sightings was used as the best estimate value for further group size calculations. If more than one estimate existed for a unique sighting and one of them was categorized as 'Follow On', the 'Follow On' group size estimate for that sighting was considered the best estimate value and used for further group size calculations. A minimum group size threshold of 3 animals was used to exclude solitary males and bachelor juvenile groups. The average group size was calculated by averaging the best guess group size estimate across all surveys.

For Adult Males, which are thought to generally be solitary (Best 1979; Whitehead 2003), this study assumed a group size of 1.5 (SD = 0.5) to account for instances where there

could be pairs of males (Christal & Whitehead 1997; Kobayashi *et al.* 2020). For the Mid-Size group, which is likely juvenile males but could also include larger females, this study assumed a group size of 2 (SD = 1) to account for bachelor groups formed by juvenile males (Best 1979) or female sperm whales in smaller groups that were not categorized as Social Group based on their modal ICI.

3.3.4e Sensitivity Analysis

This study aimed to assess the sensitivity of the mean acoustic density estimate of sperm whales to various demographic specific parameters used to calculate vocal activity using both the click and group counting approaches, similar to the sensitivity analysis conducted in Frasier *et al.* (2016). The analysis focused on demonstrating how using demographic-specific parameters for density estimation can reduce variability and error in the calculations. The analysis was conducted at one representative site (HZ), and the following parameters were tested for the (1) click counting approach: ICI, proportion of time spent clicking in a dive, and proportion of time in a foraging dive; and for the (2) group counting approach: group size, synchronicity (overlap), proportion of time spent clicking in a dive, and proportion of time in a foraging dive. A systematic parameter variation approach was employed to evaluate the sensitivity of the mean acoustic density to each parameter. All variables, except for the parameter being tested, were held constant at their mean values either retrieved from existing literature (proportion of time spent clicking and proportion of time in a foraging dive, and synchronicity) or from the data itself (ICI and group size). For the parameter under investigation, 10,000 random values were generated from a normal distribution with the mean and standard deviation of the original variable. For each randomly chosen value of the parameter, the mean acoustic density estimate was calculated for the entire time period at the study site for a specific class of sperm whales.

This process was repeated for all randomly chosen parameter values, resulting in a dataset of mean density estimates corresponding to the 10,000 parameter values. Following Frasier et al. (2016), sensitivity of the mean density to parameter variations was assessed by plotting the parameter value against the corresponding mean density estimate. The slope of this plot was calculated to determine the magnitude of sensitivity to parameter changes. Furthermore, Z-scores were calculated for each of the 10,000 parameter values and mean density estimates. The Z-score, which normalizes the values, was plotted against the mean density estimate. The slope of this plot was calculated to compare sensitivity between the parameters and the higher the value the more sensitive density estimation was to that parameter. A linear regression analysis was performed to fit a line to the Z-score versus mean density plot, and the coefficient of determination (R^2) was calculated to evaluate the goodness of fit. The R^2 value provided a measure of how well the linear model explained the relationship between the Z-score and mean density. The relationship between the absolute value of the Z-score and the R^2 value was plotted to examine the relationship between importance (Z-score) and goodness of fit (R^2). A parameter with a steeper Z-score slope and a higher R^2 was considered more influential in explaining the variability of mean density.

3.4 Results

3.4.1 Sperm Whale Detection and Discrimination

The proportion of individual class presence and class overlap was evaluated on the 5-min time bin, hourly, and daily time scales and reported as the median in percentage and interquartile range (IQR). Sperm whales were present year-round in 17.5% (IQR = 13%) of 5-min time bins in the North and 1.5% (IQR = 1.5%) of 5-min time bins in the South (Table 3.2, Figure 3.3-5). Social Groups were present in 66.5% (IQR = 8.5%) of 5-min time bins, 70% (IQR = 12%) of

107

hourly time bins, and 39% (IQR = 12.5%) of daily time bins in the North (Figure 3.6, Table 3.1).

Social Groups were present in 40.5% (IQR = 31.5%) of 5-min time bins, 39% (IQR = 27.3%) of

hourly time bins, and 28% (IQR = 18.3%) of daily time bins in the South (Figure 3.6, Table 3.1).

Mid-Size were present in 17% (IQR = 10.5%) of 5-min time bins, 22% (IQR = 9.8%) of hourly

time bins, and 14% (IQR = 10%) of daily time bins in the North (Figure 3.6, Table 3.1). Mid-

Size were present in 34.5% (IQR = 21%) of 5-min time bins, 43% (IQR = 19.8%) of hourly time

bins, and 41% (IQR = 7%) of daily time bins in the South (Figure 3.6, Table 3.1). Adult Males

were present in 1% (IQR = 2%) of 5-min time bins, 2% (IQR = 1.3%) of hourly time bins, and

1% (IQR = 0) of daily time bins in the North (Figure 3.6, Table 3.1). Adult Males were present

in 7% (IQR = 7%) of 5-min time bins, 12% (IQR = 6.3%) of hourly time bins, and 15% (IQR =

8%) of daily time bins in the South (Figure 3.6, Table 3.1).

Overlap of the classes were detected across all sites, with temporal overlap observed on

5-min time bins, hourly, and daily time scales. The highest proportion of overlap at all sites was

between Social Groups and Mid-Size, particularly in the northern sites where they were present

together in 4% (IQR = 2%) of 5-min time bins, 8% (IQR = 2.5%) of hourly time bins, and 31%

(IQR = 8%) of daily time bins (Figure 3.6, Table 3.1). The proportions became more uniform

among the southern sites where they were present together in 3% (IQR = 0.5%) of 5-min time

bins, 5% (IQR = 0.5%) of hourly time bins, and 9% (IQR = 2%) of daily time bins. Social

Groups and Adult Males were present together in 0.25% (IQR = 0.15%) of 5-min time bins, 1%

(IQR = 0%) of hourly time bins, and 2% (IQR = 0.5%) of daily time bins in the North (Figure

3.6, Table 3.1). Social Groups and Adult Males were present together in 0.08% (IQR = 0.07%)

of 5-min time bins, 1% (IQR = 0.3%) of hourly time bins, and 1.5% (IQR = 1.3) of daily time

bins in the South. Mid-Size and Adult Males were present in 0.75% (IQR = 0.7%) of 5-min time

bins, 1.5% (IQR = 2%) of hourly time bins, and 3% (IQR = 1.5%) of daily time bins in the North (Figure 3.6, Table 3.1). Mid-Size and Adult Males were present in 2% (IQR= 1.1%) of 5-min time bins, 4% (IQR = 0.8%) of hourly time bins, and 7% (IQR = 2%) of daily time bins in the South. As expected, encounters with all three classes were rare, particularly on the 5-min time bin scale with simultaneous presence in 0.1% (IQR = 0.22%) of time bins in the North and 0.03% (IQR = 0.07%) of time bins in the South (Table 3.2). On the hourly and daily scale, overlap was less rare with overlap of all classes in 1% (IQR = 0%) of hourly time bins and 5.5% (IQR = 6.3%) of daily time bins in the North and 0.5% (IQR = 1%) of hourly time bins and 1% (IQR = 2%) of daily time bins in the South (Figure 3.6). In the North, 10% (IQR = 3%) of 5-min time bins were not assigned a class, while in the South, 12.5% (IQR = 3.5%) of 5-min time bins were not assigned a class (Table 3.2).

The median false positive click rate was 4.12% (IQR = 1.65%) in the North and 4.21% (IQR = 3.89%) in the South (Table 3.3). The median false positive bin rate was 0.49% (IQR = 0.23%) in the North and 0.23% (IQR = 0.72%) in the South.

3.4.2 Seasonal Patterns

Distinct and significant seasonal patterns were found in the majority (53 out of the 56) models (Table 3.4, Table 3.5). In the North, the peak in Inclusive, Social Group and Mid-Size was presence was in the late spring/early summer, while the dip was in late fall/early winter (Figure 3.7). Adult Males were almost exclusively present in the spring months with a large dip in the fall. The Social Group pattern at site OC was the only exception to the regional trend, with peak presence in the winter and the dip in late summer/early fall (Figure 3.10). In the South, the peak of each class was slightly offset with Social Group presence peaking early fall, followed by Adult Males in late fall, and Mid-Size in late fall/early winter (Figure 3.7). In the South, the dip

in presence for all classes was in the spring. The pattern at site BS was the only exception to the regional trend, with peak presence in spring for all classes and a dip in the fall/winter (Figure 3.11).

3.4.3 Spatial Patterns

Overall, the probability of presence for each of the classes decreased latitudinally in the North (Figure 3.8). The only exceptions were the two Hatteras sites found in the Gulf Stream, which had equivalent presence to the northernmost sites for Mid-Size (HAT_A and HAT_B) and Adult Males (HAT_B only). In the South, the presence of the classes among the sites were relatively consistent minus a few exceptions. On the extremes, for Social Groups, site BP had the relatively lowest amount of presence. For Mid-Size, site GS had the relatively highest amount of presence. For Adult Males, site JAX had the relatively lowest amount of presence.

3.4.4 Interannual trends

In the North, presence increased over the recording duration for all classes, apart from a small decrease for Mid-Size and Adult Males in 2019 (Figure 3.9). A consistent increase in presence was seen at sites HZ, WC, NFC, and HAT_A for Mid-Size and at site HAT_A for Adult Males (Figure 3.12). A decrease over the recording duration was seen for Mid-Size at site HAT_B. In the south, the interannual trend varied for each class and site. At site GS, presence remained constant except for an increase in 2017 and 2019 for Social Groups and a decrease in 2017 for Inclusive and Mid-Size (Figure 3.13). At site BP, presence increased over time for the Inclusive model with a dip in 2019. Social Group presence at site BP remained constant with a dip in 2019. At site BS, presence remained constant for all models with a dip in 2019 and an additional dip only for Adult Males in 2017. For site JAX, presence decreased over time for

110

Inclusive and Social Groups, with an increase in 2019; for Mid-Size and Adult Males, presence remained steady with a dip in 2017 and 2018 respectively.

The models had low Tjur's R2 values and percent of residuals within the 95% confidence intervals suggesting that the temporal (Julian day and year) and spatial (site) variables included in the models are not the main predictors of animal presence (Table 3.6, Table 3.7). The median percent of residuals within the 95% confidence intervals for Inclusive, Social Group, Mid-Size, and Adult Males models was 41.5% (IQR = 17.5%), 44% (IQR = 5.5%), 53.5% (IQR = 16.5%), and 26.5% (IQR = 16%), respectively.

3.4.5 Probability of Detection

Social Groups had the highest mean peak frequency of 10.5 kHz, followed by the Mid-Size (10 kHz), and the Adult Males (9.5 kHz) (Table 3.8, Figure 3.14). More variability was seen for the southern sites and the Adult Males likely due to less click detections. These frequencies were used to generate propagation models and derive Monte Carlo simulations for modeling the probability of detecting each size class.

The grid search to test different parameters resulted in the parameters that optimized the goodness-of-fit metric (Table 3.9). Dive altitude above the seafloor and the benthic dive altitude varied between sites and classes, likely based on the variability of depth for each site (563m – 1218m). Foraging occurred equally in the mid-water column and near the seafloor.

Echolocation source levels and directivity varied between Social Groups/Mid-Size and Adult Males, but not between sites. The grid search revealed a source level of 233-243 dB$_{pp}$ for Social Groups and Mid-Size and a source level of 238-248 dB$_{pp}$ for Adult Males. Click directivity of 25-30 dB was estimated for Social Groups and Mid-Size, while a directivity of 27-32 dB was estimated for Adult Males.

For both the click and group counting approaches, a distribution of measured received click amplitudes for each class was used to determine the parameters that best fit the model output (Figure 3.15-20). The model and the data, in most cases, reveal a decrease in the number of clicks detected as the received level increases. This is because with the assumption of even animal distribution across the observed area, the number of animals increases with increasing distance away from the sensor (area $= \pi r^2$), hence resulting in a larger number of low amplitude clicks detected. For the click counting approach, the data exhibits a high level of agreement with the model from 125-150 dB_{pp}. For the group counting approach, the data displays a reasonable alignment with the model from 130-150 dB_{pp}. Above 150 dB_{pp} for both approaches, the poor fit between the data and the model is likely a result of too few detected clicks and time bins. Below and near the detection threshold for the group counting approach (130 dB_{pp}), the data drops to numbers below the model prediction; this is also likely a result of too few detected time bins and suggests that group detections are missed when only low amplitude clicks are detected during that time window. The deviation can also be seen in the larger percentage of false negatives for the group versus the click counting approach (Table 3.10). Overall, the highest level of agreement between the data and the model was seen for the northern sites and the Social Group class, where number of click and bin detections were sufficient.

The probability of detection over the horizontal range (40 km) varied for the three size classes but had very little variability between the sites (Figure 3.21). The probability of detecting an individual click and time bin was 100% near the sensor. The detectability of an echolocation click dropped off rapidly 2-6 km away from the sensor and reached zero between 10-14 km depending on the size class (Figure 3.21). The area beneath the curve resulted in a mean detection probability of 1.58% (SD = 0.29), 1.84% (SD = 0.57), and 2.61% (SD = 0.66) for

Social Groups, Mid-Size, and Adult Males, respectively (Table 3.11). The probability of detecting a group had a more gradual decline and reached zero between 24-30 km depending on the size class (Figure 3.21). The area beneath the curve resulted in a mean group detection probability of 11.43% (SD = 2.73), 12.83% and 17.19% (SD = 5.44) for Social Groups, Mid-Size, and Adult Males, respectively (Table 3.11).

3.4.6 Group Size & Vocal Activity

Using the dive parameters from Watwood *et al.* (2006) and Teloni *et al.* (2008), the proportion of time spent clicking was 58% for Social Groups/Mid-Size and 66% for Adult Males. For the click counting approach, the proportion of time spent clicking was divided by the interclick interval (ICI) to calculate cue rate for each class at each site. ICI distributions and the peak of the GMM distribution fit to the data for Social Groups and Mid-Size were relatively consistent across sites (Figure 3.22). The mean peak of the GMM distribution fit for Social Groups and Mid-Size at all sites was 494 ms (SD = 18) and 642 ms (SD = 28), respectively (Table 3.12). The ICI distribution and peak of the GMM distribution fit for Adult Males was more variable with a mean at all sites of 864 ms (SD = 49), likely a result of less Adult Male clicks (Figure 3.22, Table 3.12).

The simulated cue rate for Social Groups and Mid-Size was larger than that of the Adult Males (Table 3.13). The mean cue rate across all sites for Social Groups, Mid-Size, and Adult Males was 1.29 clicks/s (SD = 0.04), 1.00 clicks/s (SD = 0.05), and 0.81 clicks/s (SD = 0.08) respectively.

For the group counting approach, understanding the probability of a group vocalizing relies on knowing the proportion of time spent clicking (derived from tag data as previously described), synchronicity (77 ± 4 %; Hildebrand *et al.* 2012), and group size. The average group

size estimate for Social Groups within the study region calculated from several visual/aerial surveys was 4.8 (SD = 2.4), composed of 267 unique sightings with three or more animals. Using equation 6, sperm whale groups with greater than 4 animals yield a vocal activity rate of 100%. Thus, with a group size of 4.8 animals, synchronicity of 77%, and a proportion of time spent clicking of 58%, the probability of a Social Group being vocally active was greater than 100% (CV = 0.06). For Mid-Size, assuming a group size of 2 animals, synchronicity of 77%, and a proportion of time spent clicking of 58%, the probability of vocal activity was 71% (CV = 0.04). For Adult Males, assuming a group size of 1.5 animals, synchronicity of 77%, and a proportion of time spent clicking of 66%, the probability of vocal activity was 73% (CV = 0.04).

3.4.7 Sperm Whale Density Estimates

Mean sperm whale density estimates by size were calculated using the click counting (Table 3.14) and group counting (Table 3.15) methods. In general, the two methods agree with a mean difference for Social Groups, Mid-Size, and Adult Males of 0.225 ± 0.371, 0.025 ± 0.021, and 0.006 ± 0.006 animals/1000 km^2, respectively. For Social Groups and Mid-Size, both approaches were equally greater or less than one another, but for Adult Males, the group counting approach was almost always higher except for HZ where the click counting approach was slightly greater. Click and group counting density estimates had similar uncertainties for Social Groups and Mid-Size, but less certainty for Adult Males, likely a result of less data overall (Table 3.14, Table 3.15).

Social groups were the dominant size class making up 84% (IQR = 22) of the animals in the region based on the click counting approach and 81% (IQR = 21) based on group counting (Table 3.14, Table 3.15). The second most dominant class was Mid-Size making up 16% (IQR = 19) of the animals in the region based on click counting and 25% (IQR = 17) based on group

counting. Adult Males were considered rare only making up 0.7% (IQR = 2) of the animals in

the region based on click counting and 1.4% (IQR = 3) based on group counting.

3.4.8 Spatial Variation

All classes had higher click and group densities at the northern sites, with the highest

total animal density estimated at site NC (3.086 and 2.9 animals/1000 km^2) and the lowest

estimated at site BP (0.071 and 0.063 animals/1000 km^2) (Table 3.14, Table 3.15). For Social

Groups, the highest densities were observed at sites NC (2.622 and 2.352 animals/1000 km^2), HZ

(1.877 and 1.932 animals/1000 km^2), and (NFC 2.691 and 1.386 animals/1000 km^2) and the

lowest densities at sites BP (0.022 and 0.018 animals/1000 km^2) and JAX (0.091 and 0.101

animals/1000 km^2). For Mid-Size, the highest densities were observed at sites NC (0.450 and

0.504 animals/1000 km^2) and OC (0.224 and 0.239 animals/1000 km^2) and the lesser densities at

sites BP (0.053 and 0.037 animals/1000 km^2) and JAX (0.021 and 0.027 animals/1000 km^2). For

Adult Males, the highest densities were observed at sites NC (0.014 and 0.039 animals/1000

km^2) and HZ (0.037 and 0.033 animals/1000 km^2) and the lesser densities at NFC (0.002 and

0.006 animals/1000 km^2) and JAX (0.001 and 0.002 animals/1000 km^2).

3.4.9 Trends

Sperm whale weekly densities are presented for the northern and southern sites for Social

Groups (Figure 3.23, Figure 3.26), Mid-Size (Figure 3.24, Figure 3.27), and Adult Males (Figure

3.25, Figure 3.28). Both the click and group counting approaches depict similar trends in density

across sites and size classes, with larger week-to-week variability for click counting. Long-term

density trends are only reported for Social Groups (Table 3.16. Annual trends in click % (left)

and group % (right) change per year for Social Groups at all sites (rows) with the 95%

confidence intervals represented by the respective minimum and maximum values.) since the

other two classes had low densities with no discernible trend. For the sites north of Cape Hatteras (HAT_A/HAT_B), Social Group density had an increase in density with a median annual change of 59% (IQR = 34) for the click counting approach and 43% (IQR = 12) for the group counting approach. Site NFC had the largest annual change per year of 84% and 78% for the click and group counting approaches respectively. At the two Hatteras sites, Social Group density declined with a median annual change of -2% and -23% for the click counting approach at HAT_A and HAT_B, respectively. The group counting approach also revealed a decline in density with an annual change of -4% at site HAT_A, and with no change (0.4%) at site HAT_B.

3.4.10 Sensitivity Analysis

The proportion of time spent in a foraging dive had the highest Z-score for all classes and for both the click and group counting approaches, making it the most important variable (Table 3.17-18). However, the fit was also the poorest with the lowest R^2 values (Table 3.17-18, Figure 3.29), indicating that although mean density is very sensitive to this parameter, the relationship is not linear. For the click counting approach, ICI was the second most important variable and proportion of time spent in a dive clicking was the least important for all classes (Table 3.17). For the group counting approach, the order of importance for the remaining variables varied by class. For Social Groups, group size was the second most important variable followed by overlap and proportion of time spent clicking in a dive (Table 3.18). For Mid-Size, group size was the second most important variable followed by proportion of time spent clicking in a dive and overlap (Table 3.18). For Adult Males, proportion of time spent clicking in a dive was the second most important variable followed by group size and overlap (Table 3.18). The proportion of time spent clicking in a dive had one of the lowest Z-score slopes for both approaches and for all

116

classes but had an R^2 ranging between 0.97 and 0.99 (Table 3.17-18, Figure 3.29). Although this variable has a linear relationship with mean density, there is also low sensitivity to the parameter.

3.5 Discussion

This study used acoustic differences between male and female sperm whales to better understand differences in their distribution, seasonal patterns, and acoustic density at 12 sites in the WNA. Three distinct classes were categorized using interclick interval as a proxy for sex: Social Groups, Mid-Size, and Adult Males. These classes demonstrated variations in the proportion of presence, seasonal patterns, and interannual trends across the different sites, highlighting the importance of considering demographic differences within regions when determining best conservation and management practices.

Socials Groups were the predominant class across all sites, making up over 80% of the animal density. This was surprising for some of the higher latitude sites like Heezen Canyon (HZ), Oceanographer's Canyon (OC), and Nantucket Canyon (NC) where a more proportionate ratio, or even one more dominated by males, would be expected. There are only a few studies of demography in the WNA, a study aiming to tag sperm whales in the same region of the WNA only reported tagging 8 females/juvenile sperm whales and no males (Watwood *et al.* 2006) although they do not report whether this bias was the result of a strategic decision to target females/juveniles or was strictly based on the animals encountered during the study. A second study looking at female philopatry and male dispersion in the WNA determined the sex of 58 out of 66 individuals tested and provided a sex ratio of 66% females to 35% males (Engelhaupt *et al.* 2009), with no specifications of the presumed age or maturity of the males. The very low density ($< 2\%$) of Adult Males in this study could be a result of a shifted sex ratio because of large mature males being heavily targeted and exploited during commercial whaling (Whitehead *et al.*

1997, 2012)It is also possible that Adult Males are found in higher proportions further north or offshore from this study's recording sites that span the continental slope and have a maximum latitude of 41° N (Lefort *et al.* 2022). Mid-Size and Social Groups overlapped in 4% of time bins. When Mid-Size and Social Groups were present at the same time, we hypothesized the animals categorized as Mid-Size were likely large females, although visual observations would be needed to corroborate this hypothesis. We hypothesized the remaining 17% of time bins with Mid-Size are juvenile males likely in bachelor groups because of their larger ICI, a peak frequency between the two other classes, and different seasonal patterns.

Across all classes, sperm whale presence demonstrates a clear latitudinal gradient, with comparatively higher presence at the sites north of the Gulf Stream compared to those to the south. This disparity is likely attributed to oceanographic features and higher prey availability influencing the distribution of sperm whales. North of the Gulf Stream, high presence is not surprising given the strategic placement of the recording sites along the continental slope, in and around submarine canyons, and near seamounts that provide cold and productive waters (Waring *et al.* 2001; Moors-Murphy 2014; Roberts *et al.* 2016). The two sites near Cape Hatteras (HAT_A & HAT_B) are particularly interesting given their situation within a very important oceanographic area, where the Gulf Stream separates from the continental slope (Tracey & Watts 1986). Although the exact location of the Gulf Stream can change dramatically throughout the year, one would expect both recording sites to be in a region of higher productivity given its proximity to Gulf Stream circulation features (Lohrenz *et al.* 2002). And although both sites are within 20 km of one another, sperm whale presence and demographic composition differed between them, highlighting the complex bathymetry and convergence of water masses that enhance biological productivity (Stanistreet *et al.* 2018) and impact detection probability of

sperm whales over very short distances. Increased sperm whale presence in this region has been reported in whaling data as the 'Hatteras Ground', an important habitat for sperm whales prior to the 20th century (Goode 1887). Sperm whales have also been documented associated with the Gulf Stream, and it has been hypothesized that Gulf Stream features are high-use habitats for sperm whales due to their high productivity (Nash *et al.* 1989; Waring *et al.* 1992). This is supported by recent acoustic surveys and density modeling near Cape Hatteras (Roberts *et al.* 2016, Stanistreet *et al.* 2018). South of the Gulf Stream, presence decreases dramatically, likely due to a difference in bathymetry and resulting oceanographic conditions. Although the southern sites are at a comparable depth to the northern ones, they are either located on the continental slope (JAX) or are not steeply followed by the abyssal plain, such as in the case of site BP, where the Blake Plateau extends hundreds of kms offshore before dropping off (Stanistreet *et al.* 2018). This type of bathymetry is not suitable habitat for sperm whales who prefer deeper slope waters (Stanistreet *et al*. 2018). Low presence and density have been previously reported for this region, suggesting a more offshore distribution south of the Gulf Stream (Roberts *et al.* 2016, Stanistreet *et al.* 2018).

The peaks and dips in sperm whale presence of all classes reversed between the northern and southern region of this study. Observed seasonal patterns are likely associated with changes in foraging opportunities based on small- and large-scale oceanographic features. The peak in the late spring early/summer in the north for all classes could highlight a lag in improved foraging conditions because of frontal regions formed after the spring bloom (Camphuysen *et al.* 2007) and perhaps warmer, and more ideal water temperatures for Social Groups (Kasuya & Miyashita 1988; Pierce *et al.* 2007) and their prey, although they are present year-round. The northern dip in the late fall/early winter is mirrored by a peak during the same time in the southern sites where

slightly cooled water temperatures and high chlorophyll production (Martins & Pelegrí 2006) can favor their preferred squid prey. Although sperm whales do not have clear migration patterns, it is understood that Adult Males travel poleward in the summer to take advantage of improved foraging conditions and travel equatorward in the winter for breeding (Best 1979). If Adult Males used the continental slope in the WNA as a travel route, we would expect a peak in presence in the spring and fall when they are traveling north and south. However, this study reveals an almost exclusive presence of Adult Males in the spring months in the northern region. This could indicate a potential breeding ground for sperm whales as is seen in the Pacific during the spring at similarly high latitudes, although this study did not have enough spatial coverage with single sensor passive acoustic monitoring to identify significant overlap of Social Groups and Adult Males (Gregr & Trites 2001). It's also possible that the continental slope in the WNA is their travel route going north, but their return trip in the fall is further offshore. Although the statistical models identifying spatiotemporal trends were useful in revealing seasonal, spatial and interannual patterns, the models had low predictive power and were not successful at explaining the variability in sperm whale presence. For future models aimed at predicting sperm whale presence rather than simply revealing spatiotemporal trends, additional environmental variables describing the habitat and oceanographic conditions should be included.

Modeling the probability of detecting each class at each site individually revealed differences in the range of detections and whale behavior for classes and acoustic propagation between sites. Comparing the predicted detections with measured received levels for each class allowed the determination of the best diving and acoustic parameters for each model. And although the fit was acceptable between the data and the model, improvements can be made by including more acoustic data and consequently more detected echolocation clicks and time bins.

Dive depth showed some differences between sites and classes. However, no significant correlation was observed between the depth of the hydrophone at a site and the dive depth of the whales. This suggests that other factors, such as prey distribution or social behaviors, might influence the whales' diving patterns. The source level and directivity of the vocalizations also exhibited differences between Social Groups/Mid-Size and Adult Males with important implications for determining the detection range of echolocation clicks. The source level of Social Groups/Mid-Size ranged between 233-244 dB$_{pp}$ and for Adult Males ranged between 238-248 dB$_{pp}$. Findings for Adult Males are consistent with the previously measured source level of 245 dB$_{pp}$ (236 dB$_{rms}$ Møhl *et al.* 2003) but there are no direct measurements for Social Groups or Mid-Size, although expectations would have them lower than those of males given their smaller body sizes (Jensen *et al.* 2018). The directivity of Social Groups/Mid-Size ranged between 25-30 dB and for Adult Males ranged between 27-32 dB. Findings for Adult Males are consistent with the previously measured directivity of 27 dB for males (Møhl *et al.* 2003, Zimmer *et al.* 2005), and similarly to source level, don't exist for Social Groups or Mid-Size.

For both the click and group counting approaches, understanding dive behavior and vocalization probability was crucial for estimating acoustic densities. The proportion of time spent in a foraging dive cycle had a high Z-score slope, but a lower R^2 value compared to the proportion of a dive spent clicking which had a lower Z-score slope but a higher R^2. Multiplying those two values together resulted in the proportion of time sperm whales spend clicking versus silent. This study used tag data from sperm whales in the WNA for Social Groups and Mid-Size (Watwood *et al.* 2006) and tag data from northern Norway for Adult Males (Teloni *et al.* 2008). A limitation of this study was the lack of tag data for Adult Males in the WNA region. Incorporating Adult Male tag data would offer valuable insights into their dive behavior in

temperate latitudes and provide a more comprehensive understanding of their distribution and habitat use. For the group counting approach, tag data of several animals in one group could provide a better estimate for group synchrony, or overlap, in the WNA. This study uses an estimate from a group of three females in the Gulf of Mexico, which is known to be its own population with smaller animal sizes and behavior (Jaquet 2006) that could affect the group synchrony estimate.

For the group counting approach, group size was also an important factor in estimating acoustic density, with a very high R^2 value and a higher Z-score slope for Social Groups, due to greater variability around the mean, compared to Mid-Size and Adult Males. Group sizes are not well documented for the WNA, and further visual observations of Mid-Size and Adult Males would be useful in corroborating the group size of 2 (SD = 1) and 1.5 (SD = 0.5), respectively. Using visual survey data, this study's findings indicate that sperm whale group sizes for Social Groups in the WNA (4.8 (SD = 2.4) animals), are smaller than those observed in the Pacific. Although sperm whale group size has not been defined for the WNA, in other regions of the Atlantic Ocean like the Gulf of Mexico (12.0; Jaquet & Gendron 2009), Caribbean Sea (6.4; Gero 2005), and the Sargasso Sea (6.9; Gero 2005), group sizes have been significantly smaller than in the Pacific where group sizes range from 18-30 individuals (Jaquet & Gendron 2009). Geographical differences may be attributed to variations in social organization, prey availabilities, predation pressure, whaling history, or other environmental factors specific to the Atlantic Ocean (Alexander 1974; Jaquet & Gendron 2009; Whitehead *et al.* 2012).

Estimating acoustic densities for each class separately revealed that Social Groups were the dominant class with a median density of over 80%, followed by the Mid-Size with a median density of 16-25% and the Adult Males accounting for less than 2% of the total density. The

highest total animal density was seen at site Nantucket Canyon (NC) and Norfolk Canyon (NFC) likely explained by the canyon bathymetry that attracts sperm whales and their preferred prey (Waring *et al.* 1993, 2001; Roberts *et al.* 2016). Demographic specific density estimation also revealed a generally consistent presence for the Mid-Size and Adult Males, with an increasing trend for Social Groups in the northern sites above Cape Hatteras (HAT_A, HAT_B) of 40-60% change per year. Although the trend analysis only encompasses 3-4 years, this increase could be a sign of changes in the ecosystem. This study encompassed some of the warmest ocean temperatures in the Northeast US shelf and the most northerly position of the Gulf Stream on record (Yang & Chen 2021). Ocean circulation in the Northeast US shelf ecosystem has experienced big changes in the last decade, including rising instability of the Gulf Stream leading to greater warm core rings (National Marine Fisheries Service 2021) which have been hypothesized to attract sperm whales (Griffin 1999). When scaling ecosystem productivity to total commercial fishery landings, it becomes clear that the primary production required to support landings north of the Gulf Stream has been declining for the last several decades (National Marine Fisheries Service 2021), supporting a potential expansion of Social Group range further north into the Georges Bank region. The increasing density of Social Groups in the northern region could also be a sign of recovering populations, although a longer time series extending beyond 4 years would be necessary to make that determination.

By converting abundance estimates from ship and aerial visual surveys (Palka 2020; Hayes *et al.* 2022) into a density, (Whitehead & Shin 2022) estimated 10.55 whales/1000 km^2 off the U.S. continental shelf in the Northwest Atlantic, about five times greater than the density estimated in this study. Although the region included in the Whitehead *et al.* (2022) estimate extends to similar latitudes, it only included more offshore waters deeper than 1000 m while this

study's recording sites ranged in depth from 560 to 1200 m and included waters much shallower than 1000 m along the slope. The density estimates produced in this study are more in line with the density estimate for the entire North Atlantic basin of 2.47 whales/1000 km (Whitehead & Shin 2022).

3.6 Conclusion

This study provides valuable insights into the spatiotemporal patterns and population dynamics of sexually dimorphic sperm whales in the Western North Atlantic (WNA). By analyzing acoustic data collected from 12 sites along a latitudinal gradient over a four-year period, this study evaluated three distinct classes of sperm whales: Social Groups (females and their young), Mid-Size animals (large females or juvenile males), and Adult Males. The presence of sperm whales was significantly higher in the northern recording sites, particularly north of the Gulf Stream, with a notably large proportion of Social Groups. Seasonal patterns of presence also differed between regions, with peaks in the spring and summer in the north and fall and winter in the south.

Acoustic density estimates were calculated, revealing that Social Groups were the dominant group across all sites, followed by Mid-Size animals and Adult Males. A significant increase in density of Social Groups in the northern region over the recording effort suggests a potential recovery or range expansion in this area which may be indicative of favorable ecological conditions or successful conservation measures.

The study underscores the importance of considering specific demographic groups when analyzing spatiotemporal patterns in marine mammal research. The observed differences in presence, seasonal patterns, and dive behavior highlight the complexity of the factors influencing the distribution and ecology of sperm whales in this region. These findings reveal the potential

for population recovery in certain regions and emphasize the need for targeted conservation strategies to ensure the sustainable management of sperm whale populations in the crucial oceanic ecosystem of the WNA. Understanding sex- and age-specific patterns is vital for effective conservation and management efforts, especially for sperm whales, and this research contributes to the knowledge base required to protect and preserve these magnificent creatures in their natural habitat.

3.7 Acknowledgements

Ocean Partnership Program and the Office of Naval Research. Data assimilative products using HYCOM are funded by the U.S. Navy. Computer time was made available by the DoD High Performance Computing Modernization Program. The output is publicly available at https://hycom.org.

Chapter 3, in full is currently being prepared for submission for publication of the material. Posdaljian, N., Deans, A., Solsona-Berga, A., Hildebrand, J., Frasier, K.E., Murillo, S., Marques, T., DeAngelis, A., & Baumann-Pickering, S. "Demographic Specific Spatiotemporal Patterns and Density Trends for Sperm Whales in the Western North Atlantic". The dissertation author was the primary researcher and author of this material.

3.8 Figures and Tables
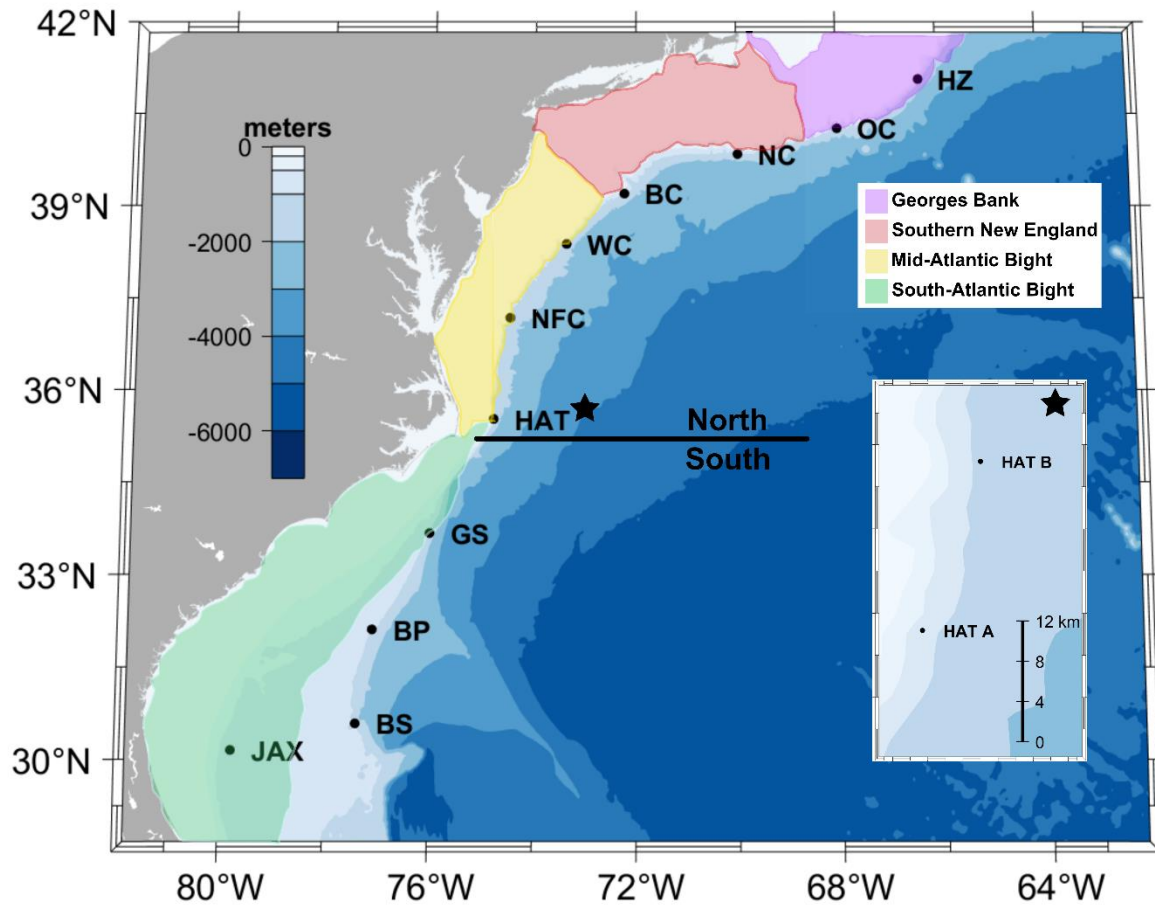
Figure 3.1. The western North Atlantic study region with HARP locations represented by circle markers and labeled with the site abbreviation. Bathymetry is represented with a blue color scale and is given in meters. The inset map shows the two HAT locations. Site abbreviations: Heezen Canyon – HZ, Oceanographer Canyon – OC, Nantucket Canyon – NC, Babylon Canyon – BC, Wilmington Canyon – WC, Norfolk Canyon – NFC, Hatteras – HAT, Gulf Stream – GS, Blake Plateau – BP, Blake Spur – BS, Jacksonville – JAX. The black line represents the division between the northern and southern regions as referred to in this study. The shaded regions represent the four Western North Atlantic regions: Georges Bank, Southern New England, Mid-Atlantic Bight, and South-Atlantic Bight.

Table 3.1. Summary of high-frequency acoustic recording packages (HARP) in the western North Atlantic from 2015 to 2019. Each row represents a new deployment. Recording effort includes site name (abbreviation), location (latitude, longitude), depth in meters (sourced from Google Earth), recording dates (MM/DD/YY), and total number of recording days. All deployments were sampled continuously at a rate of 200 kHz.

Site	Location	Depth (m)	Recording dates	Duration (days)
Heezen Canyon (HZ)	41.062° N, 66.352° W	898	06/27/15–03/25/16	271
	41.062° N, 66.352° W	901	05/22/16–06/19/17	423
	41.062° N, 66.352° W	906	07/09/17–01/13/18	189
	41.062° N, 66.352° W	906	06/11/18–05/10/19	333
Oceanographer's Canyon (OC)	40.263° N, 67.986° W	563	04/26/15–02/09/16	289
	40.263° N, 67.986° W	563	04/24/16–05/18/17	389
	40.263° N, 67.986° W	563	07/06/17–04/16/18	283
	40.230° N, 67.978° W	563	06/10/18–05/19/19	343
Nantucket Canyon (NC)	39.832° N, 69.982° W	946	04/27/15–09/18/15	145
	39.832° N, 69.982° W	946	04/21/16–05/24/17	398
	39.833° N, 69.982° W	945	07/16/17–06/09/18	328
	39.833° N, 69.982° W	945	06/10/18–06/03/19	358
Babylon Canyon (BC)	39.191° N, 72.229° W	994	04/20/16–06/10/17	416
	39.191° N, 72.227° W	1002	06/30/17–06/03/18	338
	39.192° N, 72.227° W	996	06/03/18–05/19/19	350
Wilmington Canyon (WC)	38.374° N, 73.371° W	929	04/20/16–06/29/17	436
	38.374° N, 73.370° W	944	06/30/17–06/02/18	338
	38.373° N, 73.370° W	962	06/02/18–05/19/19	350
Norfolk Canyon (NFC)	37.167° N, 74.467° W	1022	04/30/16–06/29/17	424
	37.167° N, 74.466° W	1019	06/29/17–06/02/18	337
	37.165° N, 74.466° W	1048	06/02/18–05/18/19	350
Cape Hatteras (HAT A)	35.342° N, 74.857° W	994	4/07/15-01/21/16	282
	35.302° N, 74.879° W	1173	04/29/16-02/06/17	283

Table 3.1. Summary of high-frequency acoustic recording packages (HARP) in the western North Atlantic from 2015 to 2019. Each row represents a new deployment. Recording effort includes site name (abbreviation), location (latitude, longitude), depth in meters (sourced from Google Earth), recording dates (MM/DD/YY), and total number of recording days. All deployments were sampled continuously at a rate of 200 kHz.

	35.584° N, 74.750° W	1124	05/09/17-10/17/17	169
Cape Hatteras	35.584° N, 74.743° W	1207	10/25/17-06/01/18	217
(HAT B)	35.590° N, 74.748° W	1218	06/01/18-12/14/18	196
	35.589° N, 74.755° W	1088	12/13/18-05/17/19	155
Gulf Stream	33.666° N, 76.001° W	951	04/29/16–06/27/17	425
	33.667° N, 75.999° W	958	06/28/17–06/26/18	363
(GS)	33.670° N, 75.998° W	962	06/28/18–06/18/19	355
Blake Plateau	32.106° N, 77.094° W	936	04/28/16–06/27/17	425
	32.107° N, 77.090° W	940	06/27/17–06/28/18	366
(BP)	32.105° N, 77.091° W	939	06/28/18–05/28/19	334
Blake Spur	30.584° N, 77.391° W	1012	04/27/16–06/26/17	425
	30.583° N, 77.390° W	1013	06/26/17–06/23/18	362
(BS)	30.583° N, 77.390° W	1014	06/28/18–06/16/19	354
Jacksonville	30.152° N, 79.770° W	759	04/26/16–06/25/17	425
	30.153° N, 79.770° W	760	06/25/17–10/28/17	125
(JAX)	30.152° N, 79.771° W	758	06/27/18–06/15/19	353
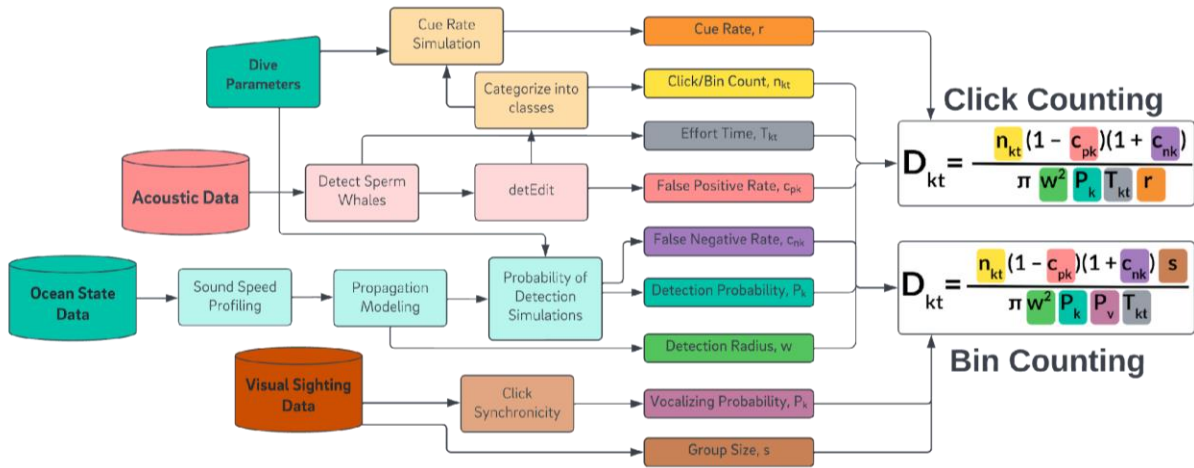
Figure 3.2. Acoustic density estimation workflow for click and group counting approaches.

Table 3.2. Number of five-minute bins assigned to each class (SG = Social Groups, MS = Mid-Size, AM = Adult Male) for each site, bins that include more than one size class (SG/MS, SG/AM, MS/AM, SG/MS/AM), bins where classification was not possible (NA = No assignment), and total bins of monitoring effort as number of 5-minute bins. The percentage in parenthesis represents the proportion of five-minute bins that fall into each category.

Site	SG	MS	AM	SG/MS	SG/AM	MS/AM	SG/MS/AM	NA	Total Bins Detected	Total Effort Bins
HZ	54112 (68%)	7847 (10%)	2297 (4%)	4112 (5%)	990 (1%)	846 (1%)	239 (0.3%)	8979 (11%)	79422	344947
OC	45858 (65%)	11905 (17%)	929 (1%)	3961 (6%)	156 (0.2%)	896 (1%)	103 (0.1%)	6778 (10%)	70586	368025
NC	56824 (62%)	19282 (21%)	1896 (2%)	3499 (4%)	392 (0.4%)	1147 (1%)	85 (0.1%)	9029 (10%)	92154	349498
BC	34389 (70%)	8549 (17%)	446 (0.9%)	1270 (3%)	139 (0.3%)	230 (0.5%)	16 (0.03%)	3835 (8%)	48874	307343
WC	25199 (71%)	5419 (15%)	410 (1%)	741 (2%)	64 (0.2%)	89 (0.3%)	9 (0.03%)	3566 (10%)	35497	305359
NFC	25720 (75%)	4135 (12%)	203 (0.6%)	1723 (5%)	105 (0.3%)	97 (0.3%)	12 (0.03%)	2529 (7%)	34524	396124
HAT_A	1687 (21%)	4271 (53%)	498 (6%)	226 (3%)	13 (0.2%)	242 (3%)	28 (0.3%)	1113 (14%)	8078	194853
HAT_B	22799 (62%)	9864 (27%)	376 (1%)	1613 (4%)	12 (0.03%)	107 (0.3%)	44 (0.1%)	1981 (5%)	36796	154705
GS	3151 (31%)	4343 (43%)	838 (8%)	313 (3%)	6 (0.06%)	218 (2%)	6 (0.06%)	1227 (12%)	10102	322606
BP	408 (14%)	1432 (50%)	430 (15%)	80 (3%)	4 (0.1%)	90 (3%)	0 (0%)	460 (16%)	2904	324475
BS	3061 (50%)	1588 (26%)	350 (6%)	165 (3%)	8 (0.1%)	125 (2%)	5 (0.08%)	760 (13%)	6062	324828
JAX	1643 (58%)	711 (25%)	89 (3%)	66 (2%)	0 (0%)	23 (0.8%)	0 (0%)	277 (10%)	2809	252175
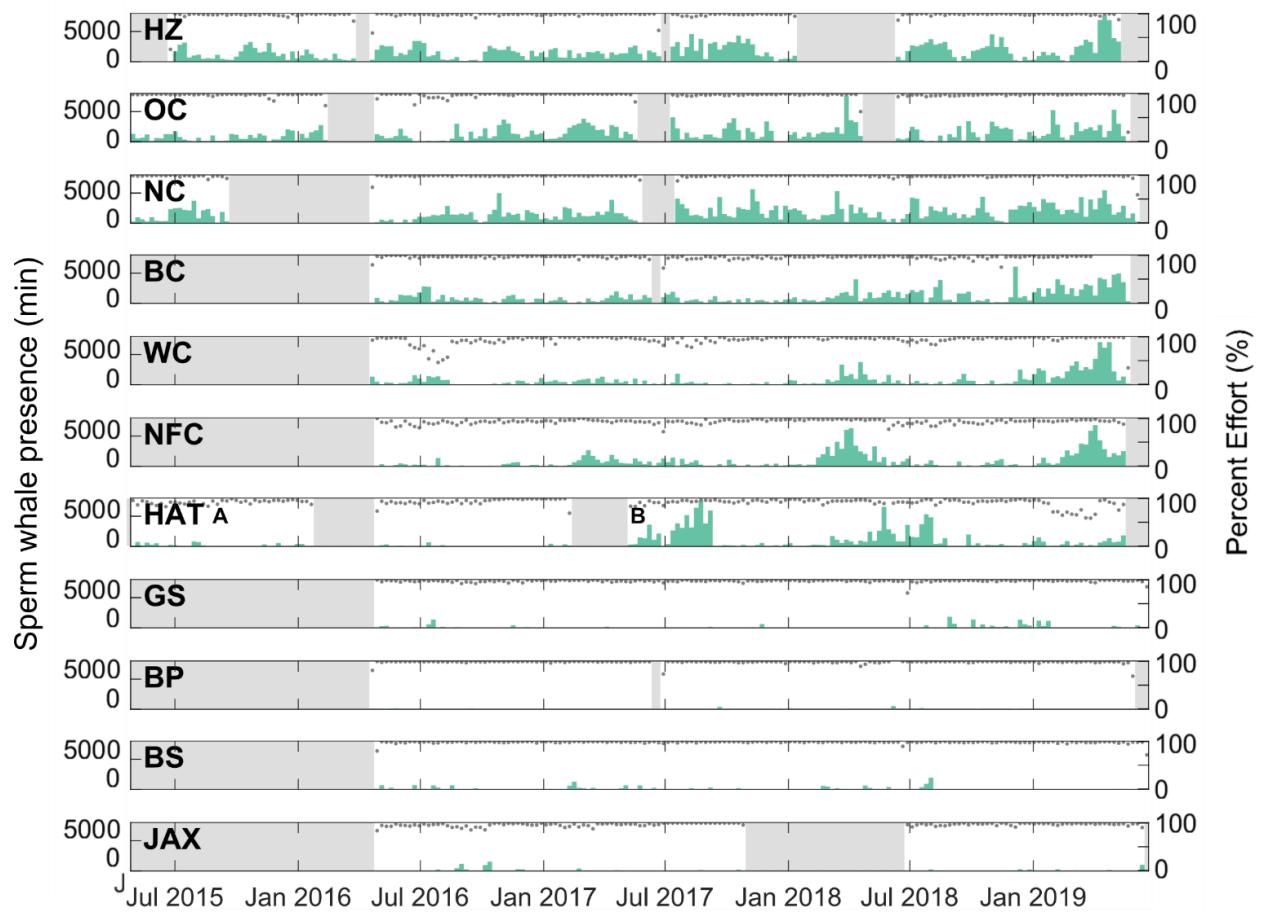
Figure 3.3. Time-series of acoustic presence of Social Groups (green bars). Percent effort during each week is indicated on the right vertical axis (gray dots) and the gray blocks represent gaps between deployments.
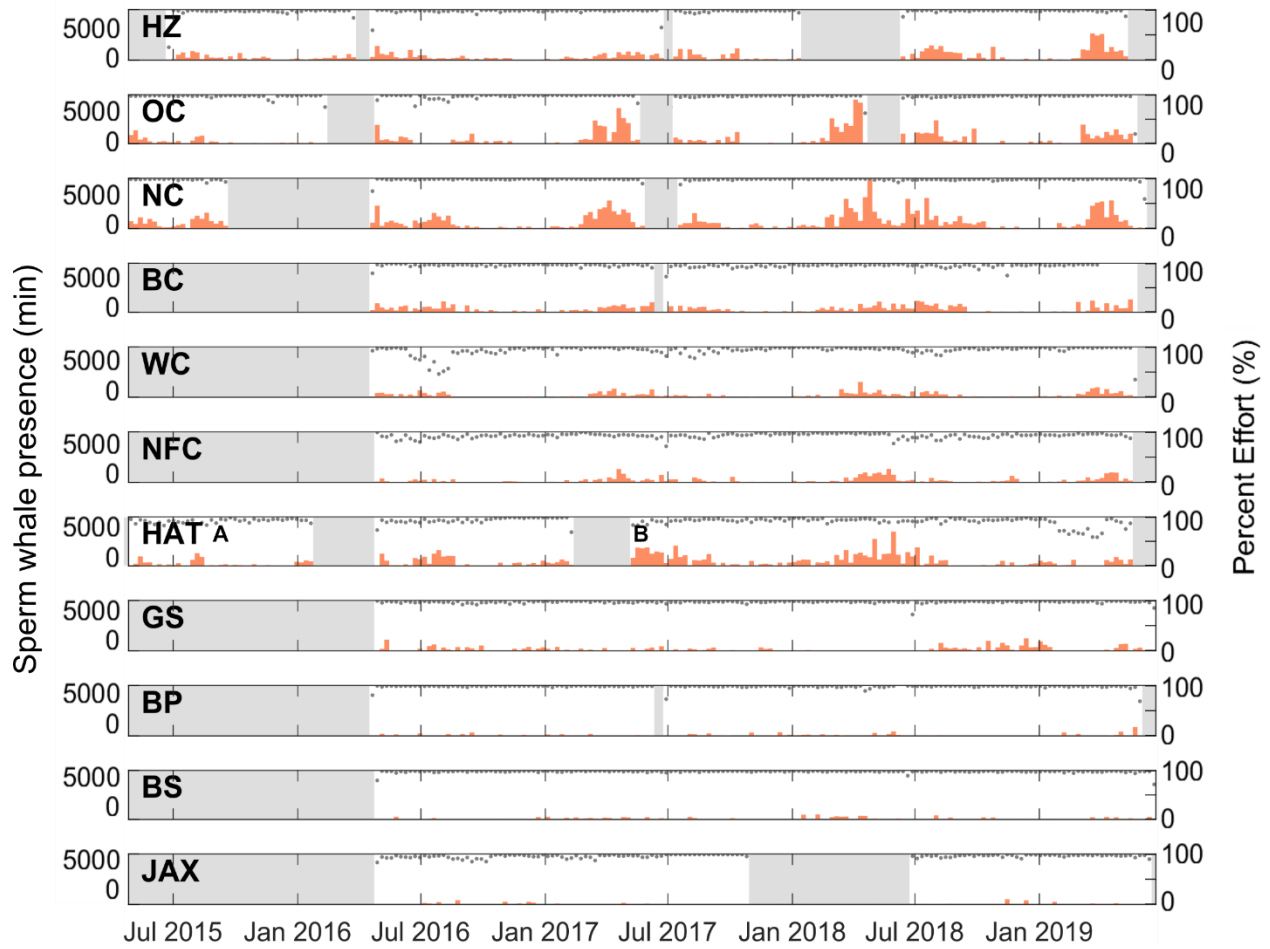
Figure 3.4. Time-series of acoustic presence of Mid-Size sperm whales (orange bars). Percent effort during each week is indicated on the right vertical axis (gray dots) and the gray blocks represent gaps between deployments.
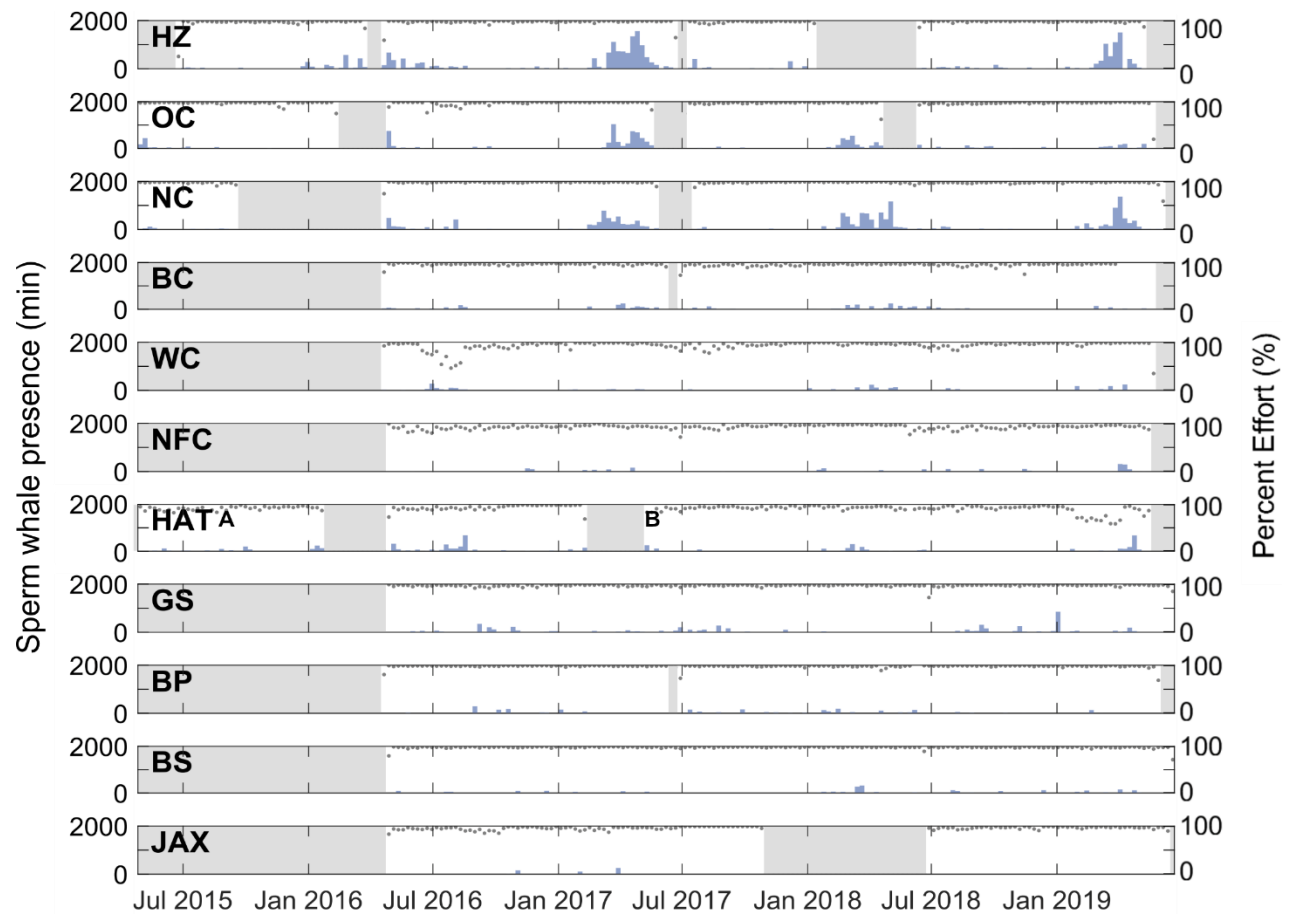
Figure 3.5. Time-series of acoustic presence of Adult Males (blue bars). Percent effort during each week is indicated on the right vertical axis (gray dots) and the gray blocks represent gaps between deployments.

134
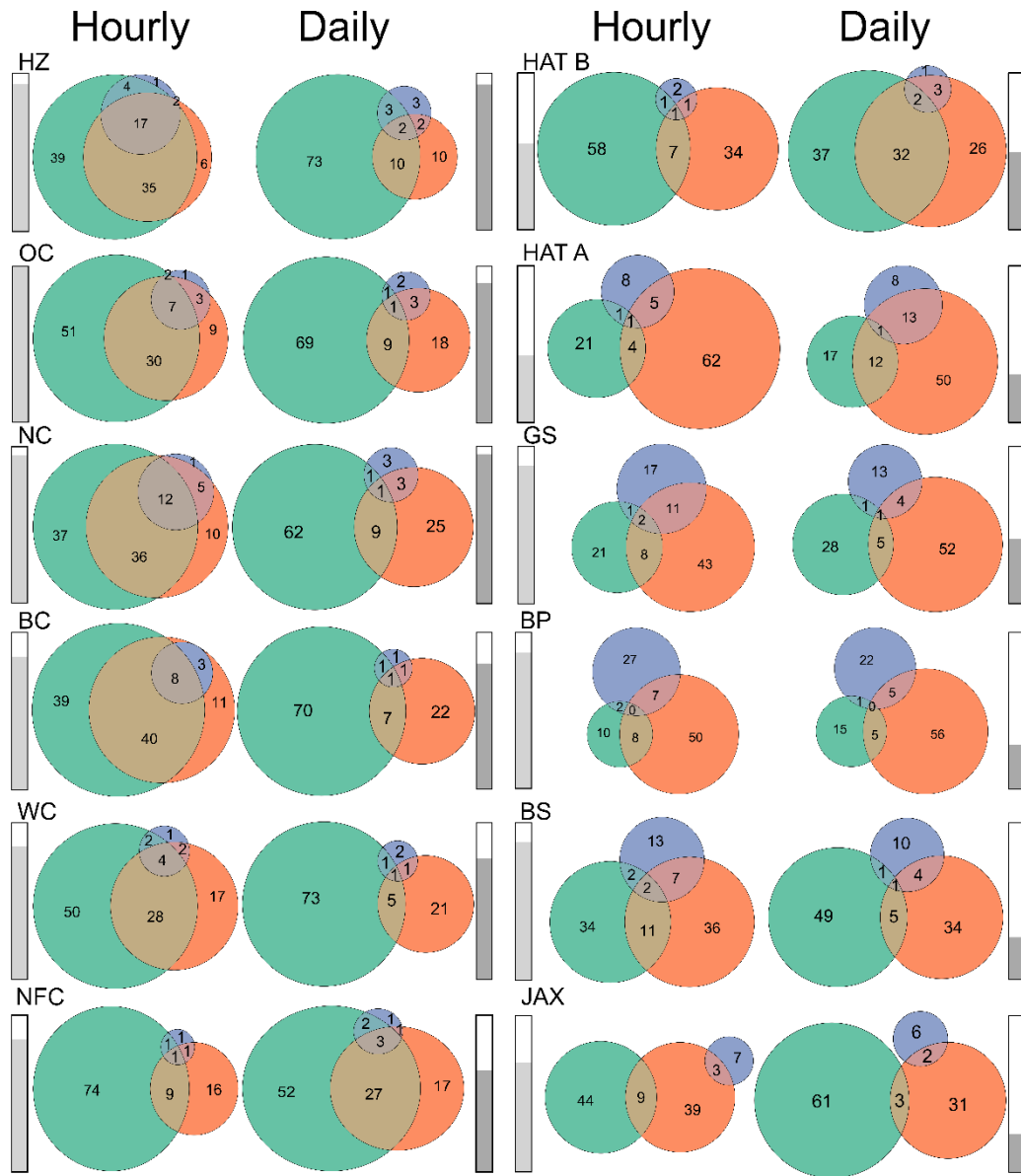
Figure 3.6. The demographic composition as the ratio of hourly (on the left) and daily (on the right) presence of each size class at each recording site displayed as Venn diagrams. Social Groups are represented in green, Mid-Size in orange, and Adult Males with blue. Overlap between groups represents presence of those groups in the same hour or day. The bars on the left of the Venn diagrams (light grey) represent normalized sperm whale presence at that site. The northern sites (HZ, OC, NC, WC, BC, NFC, HAT A/B) had the most presence while the southern sites (GS, BP, BS, JAX) had the least. The bars on the right of the Venn diagrams (dark grey) represent normalized recording effort at that site. OC had the highest recording effort (1); JAX, the least (< 0.3). The bars on the right of the Venn diagrams (dark grey) represent normalized sperm whale presence at that site.

Table 3.3. Mean false positive rates c_k for sperm whale detections at each site and their associated coefficients of variation $CV(c_k)$ for the click and group counting approaches.

Site	Click Counting		Group Counting	
	c_k (%)	$CV(c_k)$	c_k (%)	$CV(c_k)$
HZ	5.31	0.0066	0.41	0.022
OC	4.94	0.012	0.47	0.032
NC	3.50	0.0076	0.31	0.019
BC	4.15	0.0066	0.51	0.018
WC	2.94	0.018	0.53	0.028
NFC	5.76	0.017	0.70	0.012
HAT_A	3.46	0.049	0.77	0.086
HAT_B	4.08	0.052	0.36	0.071
GS	2.46	0.041	0.45	0.059
BP	2.14	0.13	0	0
BS	5.96	0.056	0.99	0.070
JAX	6.41	0.067	0	0

Table 3.4. Site model output summaries, including the p-value (P), degrees freedom (Df), and the Chi-square statistic (X^2). The significance of the p-value is indicated by the following significance codes: '***' 0.001, '**' 0.01, and '*' 0.05. If a model had more than one variable, the listed order of the variables represents the order they were inputted into the model. Models that had different input orders have superscripts for the p-values indicating the order each variable was inputted into the model.

Site	Variable	Model Output	General	Social Groups	Mid-Size	Males
HZ	Julian Day	P	1.7e-05 ***	0.00058***	< 2e-16 ***	<2e-16***
		Df	2	2	2	2
		X^2	21.9	14.9	193.5	160.2
	Year	P			5.8e-07***	
		Df	NA	NA	4	NA
		X^2			34.5	
OC	Julian Day	P	8.12e-07 ***	0.00062 ***	< 2.2e-16 ***	1.65e-11 ***
		Df	2	2	2	2
		X^2	28.1	14.8	117.0	49.7
	Year	P	0.027*		2.44e-08 ***	1.40e-06 ***
		Df	4	NA	4	4
		X^2	11.0		41.2	32.7
NC	Julian Day	P	0.011 *	0.0039 **	<2e-16 ***	3.8e-12 ***
		Df	2	2	2	2
		X^2	9.0	11.1	94.2	52.6
	Year	P	0.0037**	2.1e-12 ***	0.015 *	0.0079 **
		Df	4	4	4	4
		X^2	15.5	60.7	12.3	13.8

Table 3.4. Site model output summaries, including the p-value (P), degrees freedom (Df), and the Chi-square statistic (X^2). The significance of the p-value is indicated by the following significance codes: '***' 0.001, '**' 0.01, and '*' 0.05. If a model had more than one variable, the listed order of the variables represents the order they were inputted into the model. Models that had different input orders have superscripts for the p-values indicating the order each variable was inputted into the model.

BC	Julian Day	P	2.1e-15 ***	8.09e-06[2] ***	<2e-16 ***	1.22e-15 ***
		Df	2	2	2	2
		X^2	67.5	223.5	255.6	68.6
	Year	P	< 2e-16 ***	<2.2e-16[1] ***		0.038 *
		Df	3	3	NA	3
		X^2	109.2	109.4		8.4
WC	Year	P	5.7e-10 ***	7.6e-13 ***	0.027[2] *	
		Df	3	3	3	NA
		X^2	46.0	59.5	9.2	
	Julian Day	P	2.9e-08 ***	1.1e-05 ***	<2e-16[1] ***	0.00062 ***
		Df	2	2	2	2
		X^2	34.7	22.8	200.7	14.8
NFC	Julian Day	P	< 2e-16 ***	7.8e-12 ***	< 2e-16 ***	
		Df	2	2	2	NA
		X^2	151	51.1	78.1	
	Year	P	3.1e-11 ***	0.00011 ***	0.00015 ***	
		Df	3	3	3	NA
		X^2	52	21.0	20.2	
HAT_A	Julian Day	P	4.7e-06 ***	8.3e-05 ***	8.7e-06[2] ***	0.020[2] *
		Df	2	2	2	2
		X^2	24.5	18.8	23.3	7.9
	Year	P	0.014 *		0.00024[1] ***	0.0016[1] **
		Df	2	NA	2	2
		X^2	8.5		16.6	12.9

Table 3.4. Site model output summaries, including the p-value (P), degrees freedom (Df), and the Chi-square statistic (X^2). The significance of the p-value is indicated by the following significance codes: '***' 0.001, '**' 0.01, and '*' 0.05. If a model had more than one variable, the listed order of the variables represents the order they were inputted into the model. Models that had different input orders have superscripts for the p-values indicating the order each variable was inputted into the model.

Site	Variable	Stat				
HAT_B	Julian Day	P	<2e-16 ***	1.7e-08 ***	<2e-16 ***	9.7e-05 ***
		Df	2	2	2	2
		X^2	103	35.7	109.2	18.5
	Year	P			3e-08 ***	
		Df	NA	NA	2	NA
		X^2			34.7	
GS	Julian Day	P	1.9e-05 ***	8.12e-06^2 ***	0.00051 ***	0.0021 **
		Df	2	2	2	2
		X^2	21.8	23.4	15.2	12.3
	Year	P	1.4e-05 ***	0.0035^1 **	0.00097 ***	
		Df	3	3	3	NA
		X^2	25.1	13.6	16.3	
BP	Year	P	1.4e-07 ***	0.024*		
		Df	3	3	NA	NA
		X^2	34.8	9.41		
	Julian Day	P	3.6e-06 ***			
		Df	2	NA	NA	NA
		X^2	25.1			
BS	Year	P	0.00066***	0.025^2 *	0.049^2 *	0.0052^2 **
		Df	3	3	3	3
		X^2	17.1	9.34	7.8	12.8
	Julian Day	P	1e-10***	0.00059^1 ***	5.5e-05^1 ***	0.050^1 *
		Df	2	2	2	2
		X^2	46.0	14.9	19.6	6.0
JAX	Julian Day	P	3.6e-05 ***	0.019 *		
		Df	2	2	NA	NA
		X^2	20.5	7.9		
	Year	P	0.00062 ***	0.029 *	0.022 *	<2e-16 ***
		Df	3	3	3	3
		X^2	17.3	9.02	9.7	232

Table 3.5. Regional model output summaries include the p-value (P), degrees freedom (Df), and the Chi-square statistic (X2). The significance of the p-value is indicated by the following significance codes: '***' 0.001, '**' 0.01, and '*' 0.05. If a model had more than one variable, the listed order of the variables represents the order they were inputted into the model. Models that had different input orders have a superscript for the p-value indicating the order it was inputted into the model.

Region	Variable	Model Output	General	Social Groups	Mid-Size	Males
North	Site	P	2.2e-16 ***	$<$2.2e-16^1 ***	$<$2.2e-16^2 ***	$<$2.2e-16^2 ***
		Df	7	7	7	7
		X^2	6742	755	207	199.4
	Julian Day	P	2.2e-16 ***	7.7e-14^3 ***	$<$2.2e-16^1 ***	$<$2.2e-16^1 ***
		Df	2	2	2	2
		X^2	2604	60	1712	150.2
	Year	P	2.2e-16 ***	$<$2.2e-16^2 ***	$<$2.2e-16^3 ***	1.7e-06^3 ***
		Df	4	4	4	4
		X^2	1092	163	207	32.2
South	Site	P	2.2e-16 ***	$<$ 2e-16^1 ***	$<$ 2e-16^1 ***	4.4e-16^1 ***
		Df	3	3	3	3
		X^2	577	100	342	74.6
	Julian Day	P	2.2e-16 ***	0.0024^3 **	0.042^3 *	0.0038^1 **
		Df	2	2	2	2
		X^2	78	12.1	6	11.2
	Year	P	1.1e-07***	1.8e-07^2 ***	2.9e-06^2 ***	
		Df	3	3	3	NA
		X^2	35	34.2	28	
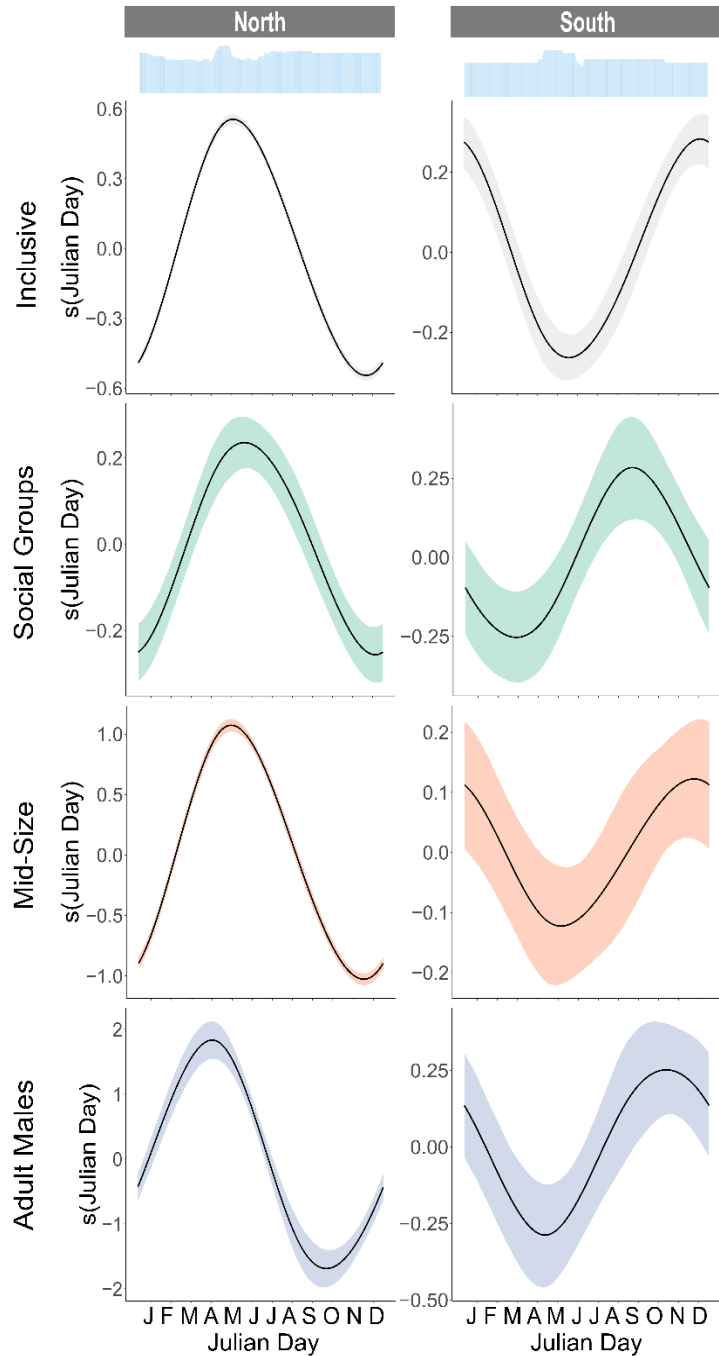
Figure 3.7. Seasonal plots for the northern sites (left) and the southern sites (right). Each row represents outputs from the different class models for each region: a) Inclusive (grey), b) Social Groups (green), c) Mid-Size (orange), and d) Adult Males (blue). Julian day is represented as months. The blue histograms at the top denote effort. All plots include 95% confidence intervals represented by the shading surrounding the smooth.
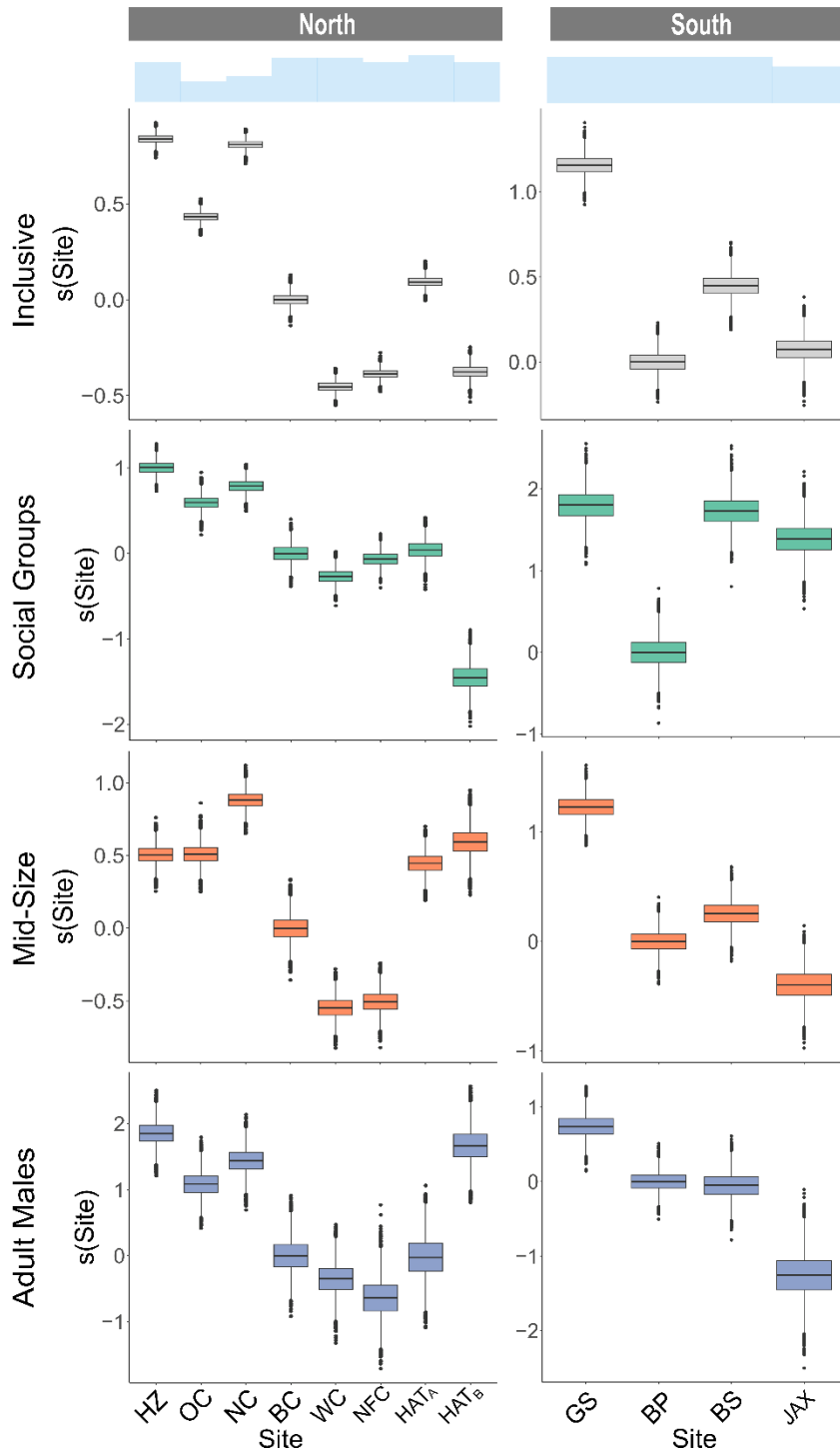
Figure 3.8. Presence by site for the northern sites (left) and southern sites (right). Each row represents outputs from the different class models for each region: a) Inclusive (grey), b) Social Groups (green), c) Mid-Size (orange), and d) Adult Males (blue). Site is a categorical variable displayed as box plots with the first level centered on zero.
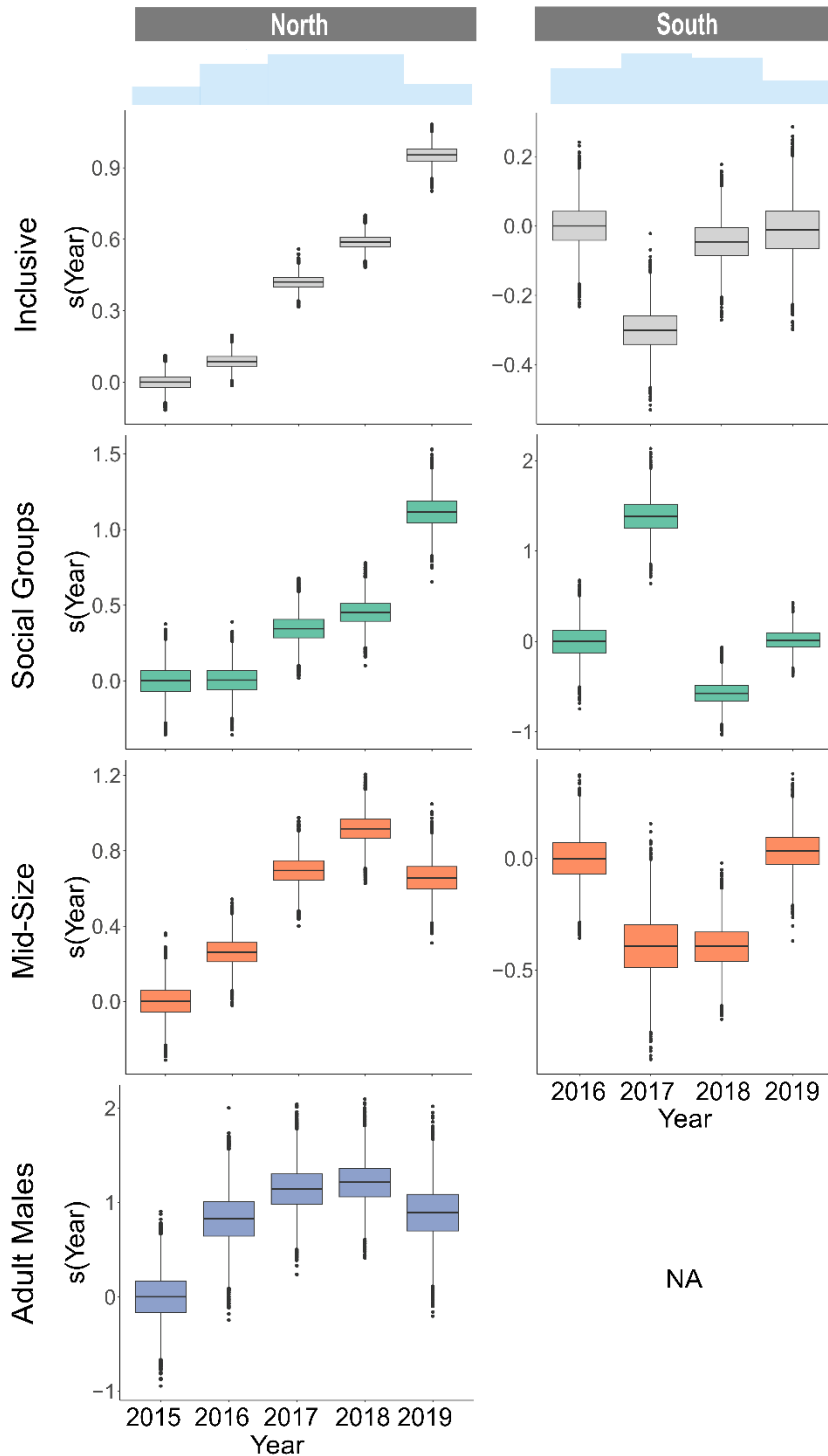
Figure 3.9. Presence by year for the northern sites (left) and southern sites (right). Each row represents outputs from the different class models for each region: a) Inclusive (grey), b) Social Groups (green), c) Mid-Size (orange), and d) Adult Males (blue). Year is a categorical variable displayed as box plots with the first level centered on zero. Year was not retained or not significant for the Adult Male model and is represented with 'NA'.
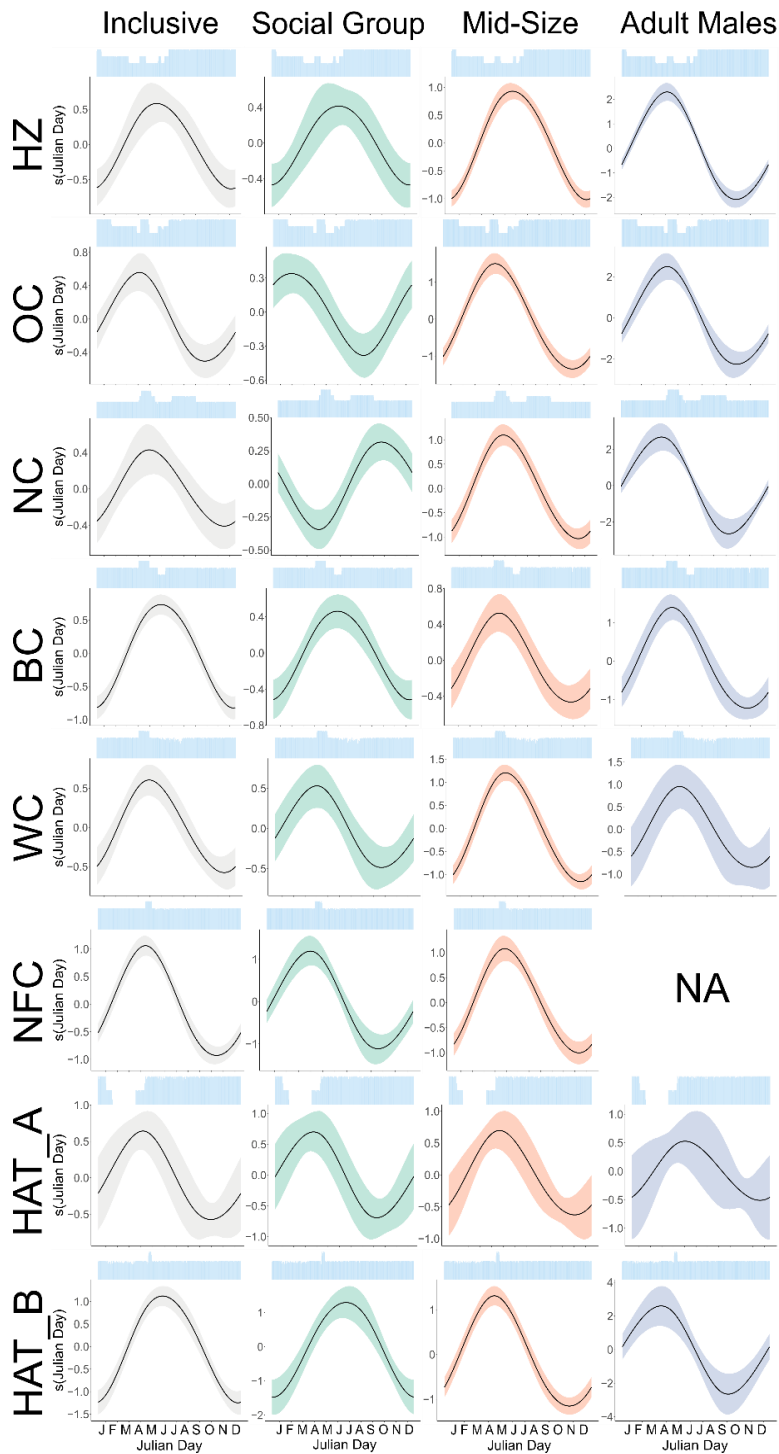
Figure 3.10. Seasonal plots for all northern sites (rows). Each column represents outputs from the different class models for each region: a) Inclusive (grey), b) Social Groups (green), c) Mid-Size (orange), and d) Adult Males (blue). Julian day is represented as months. The blue histograms at the top denote effort. All plots include 95% confidence intervals represented by the shading surrounding the smooth. Variables that were not retained in the model or not significant are represented with 'NA'.
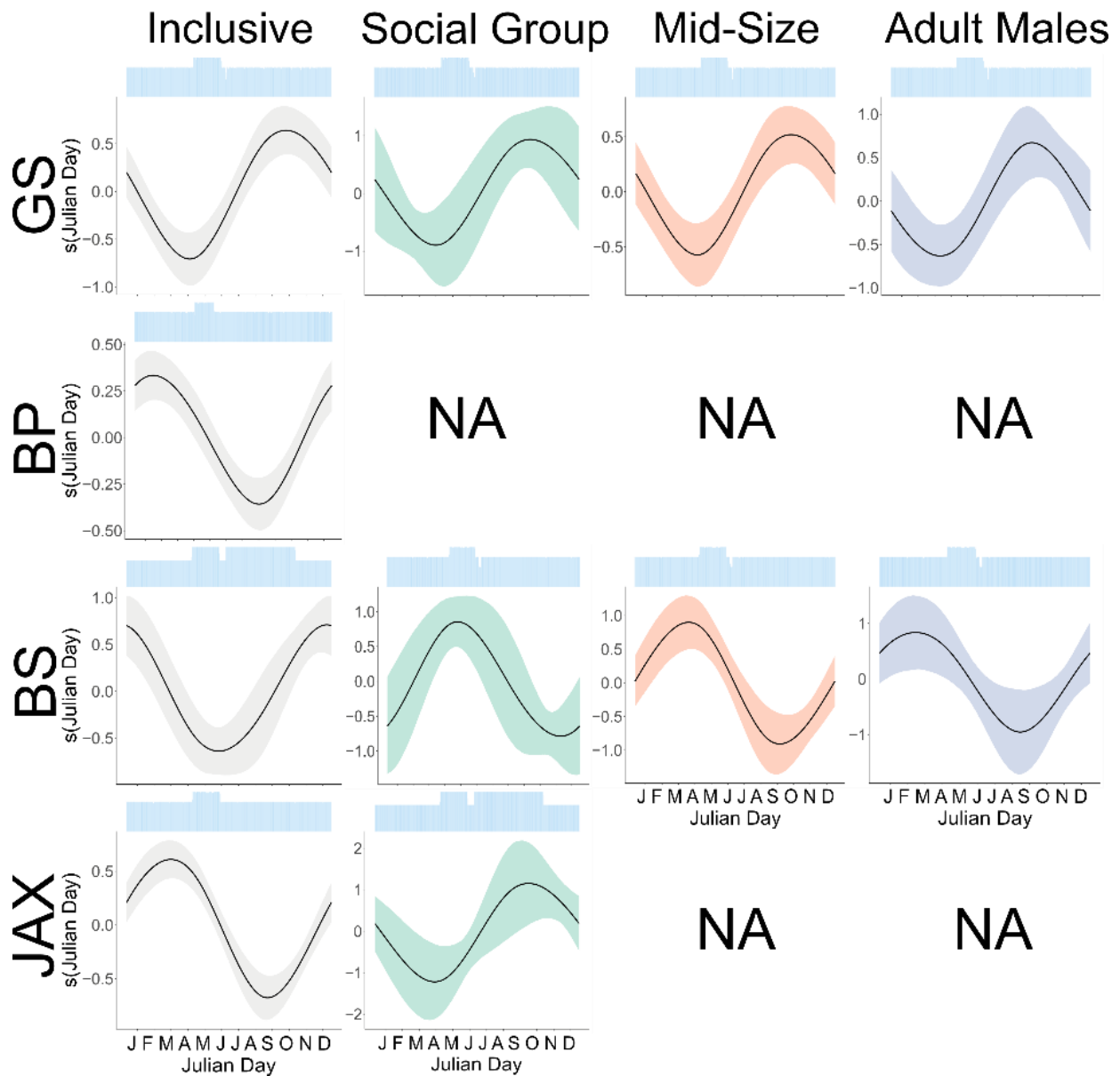
Figure 3.11. Seasonal plots for all northern sites (rows). Each column represents outputs from the different class models for each region: a) Inclusive (grey), b) Social Groups (green), c) Mid-Size (orange), and d) Adult Males (blue). Julian day is represented as months. The blue histograms at the top denote effort. All plots include 95% confidence intervals represented by the shading surrounding the smooth. Variables that were not retained in the model or not significant are represented with 'NA'.
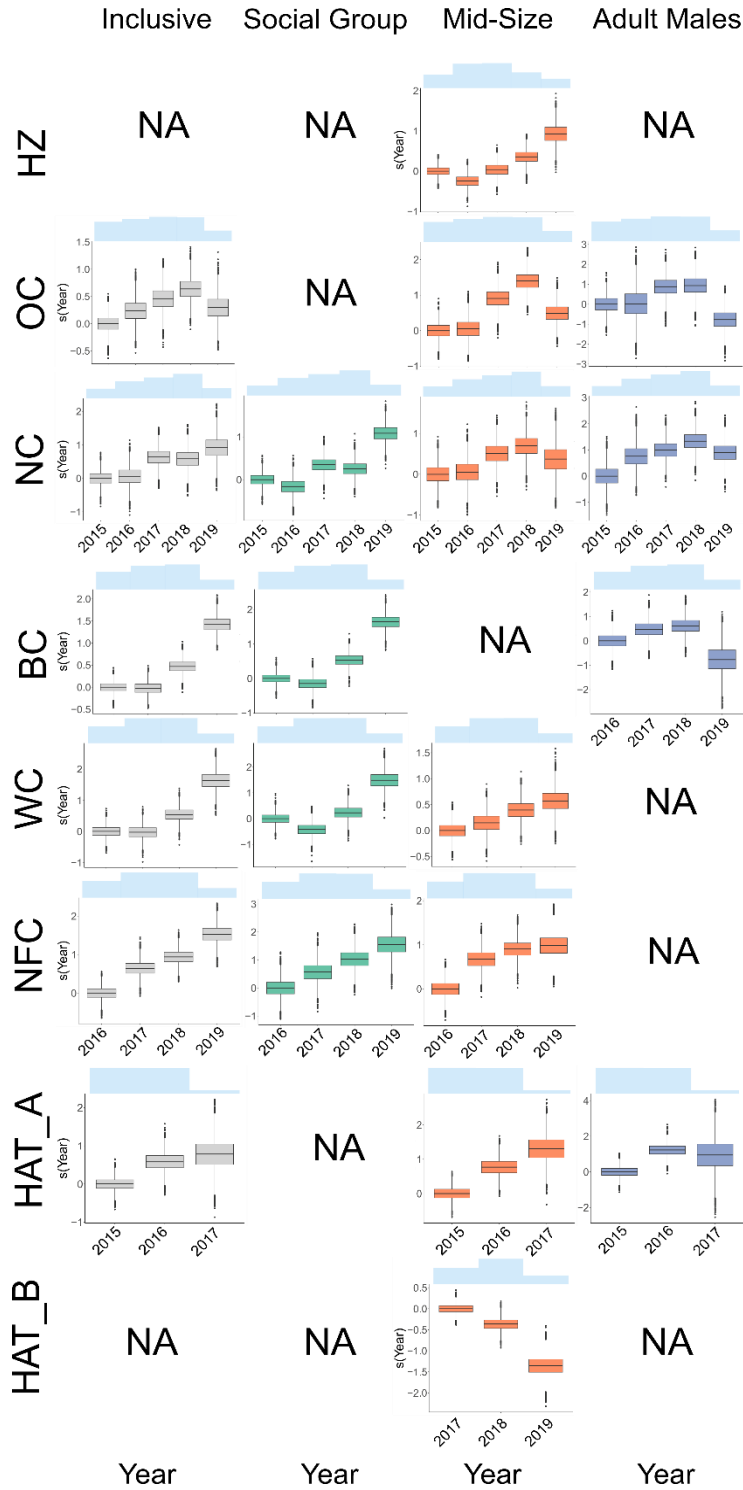
Figure 3.12. Presence by year for all northern sites (rows). Each column represents outputs from the different class models for each region: a) Inclusive (grey), b) Social Groups (green), c) Mid-Size (orange), and d) Adult Males (blue). Year is a categorical variable displayed as box plots with the first level centered on zero. Variables that were not retained in the model or not significant are represented with 'NA'.
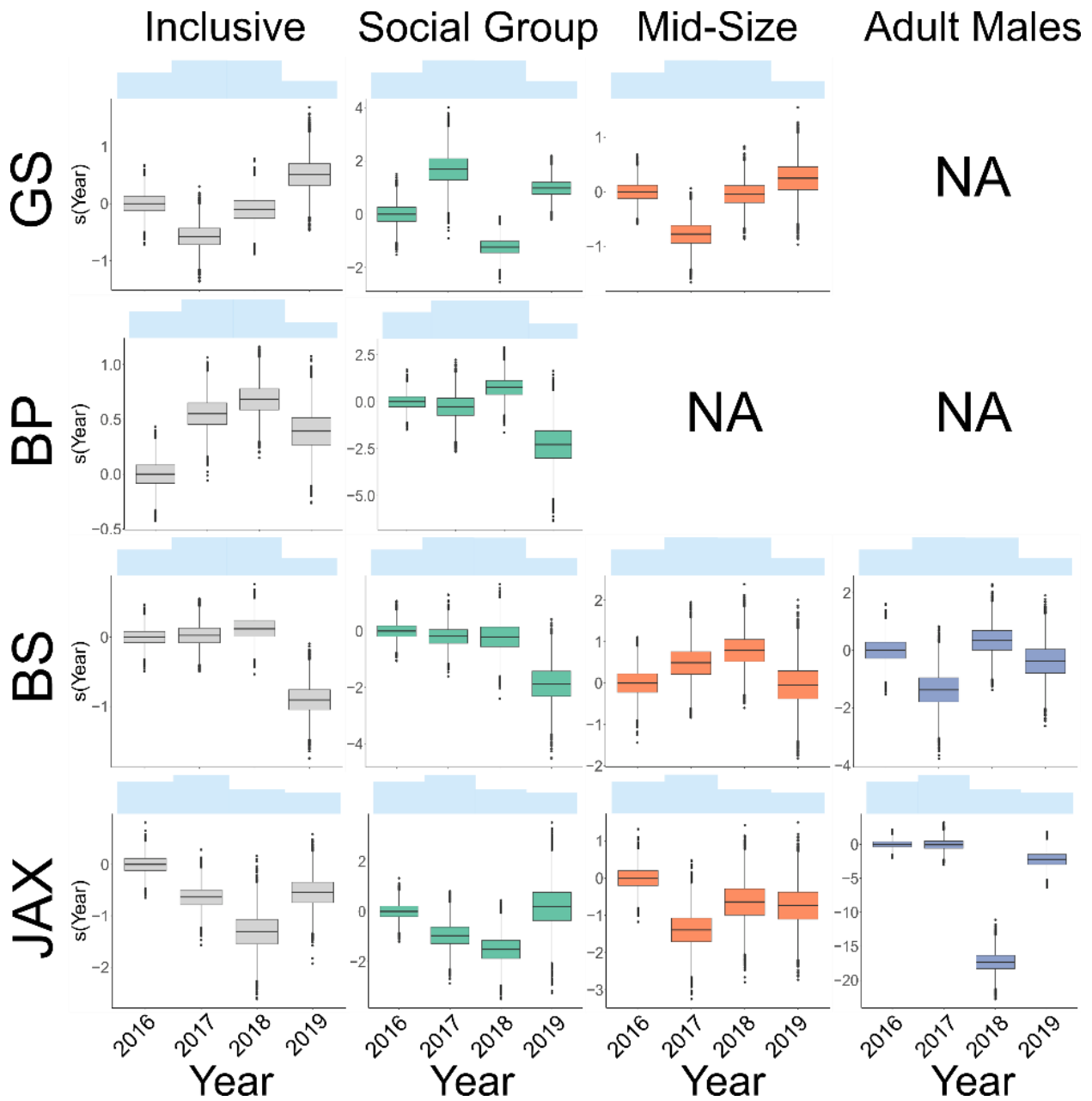
Figure 3.13. Presence by year for all southern sites (rows). Each column represents outputs from the different class models for each region: a) Inclusive (grey), b) Social Groups (green), c) Mid-Size (orange), and d) Adult Males (blue). Year is a categorical variable displayed as box plots with the first level centered on zero. Variables that were not retained in the model or not significant are represented with 'NA'.

147

Table 3.6. Site model evaluation summaries with Tjur's R2 values and the % of residuals within the 95% confidence intervals.

Site	Sex	Tjur's R2	% of Residuals
HZ	Inclusive	0.042	38%
	Social Groups	0.019	49%
	Mid-Size	0.039	66%
	Adult Males	0.052	45%
OC	Inclusive	0.043	44%
	Social Groups	0.011	47%
	Mid-Size	0.087	56%
	Adult Males	0.038	26%
NC	Inclusive	0.039	32%
	Social Groups	0.025	43%
	Mid-Size	0.054	46%
	Adult Males	0.048	35%
BC	Inclusive	0.091	41%
	Social Groups	0.070	38%
	Mid-Size	0.018	53%
	Adult Males	0.006	36%
WC	Inclusive	0.099	42%
	Social Groups	0.102	45%
	Mid-Size	0.023	56%
	Adult Males	0.001	23%
NFC	Inclusive	0.139	44%
	Social Groups	0.130	45%
	Mid-Size	0.027	53%
	Adult Males	0.001	12%

Table 3.6. Site model evaluation summaries with Tjur's R2 values and the % of residuals within the 95% confidence intervals.

HAT_A	Inclusive	0.030	44%
	Social Groups	0.007	33%
	Mid-Size	0.019	43%
	Adult Males	0.005	27%
HAT_B	Inclusive	0.133	47%
	Social Groups	0.102	40%
	Mid-Size	0.073	54%
	Adult Males	0.011	16%
GS	Inclusive	0.021	45%
	Social Groups	0.014	24%
	Mid-Size	0.007	38%
	Adult Males	0.002	32%
BP	Inclusive	0.007	66%
	Social Groups	0.001	100%
	Mid-Size	0.001	100%
	Adult Males	0.000	21%
BS	Inclusive	0.013	59%
	Social Groups	0.006	19%
	Mid-Size	0.005	33%
	Adult Males	0.002	18%
JAX	Inclusive	0.012	47%
	Social Groups	0.011	14%
	Mid-Size	0.002	100%
	Adult Males	0.001	75%

Table 3.7. Regional model evaluation summaries with Tjur's R2 values and the % of residuals within the 95% confidence intervals.

Region	Sex	Tjur's R2	% of Residuals
North	Inclusive	0.083	45%
	Social Groups	0.043	34%
	Mid-Size	0.056	56%
	Adult Males	0.042	47%
South	Inclusive	0.016	49%
	Social Groups	0.004	30%
	Mid-Size	0.007	40%
	Adult Males	0.002	32%
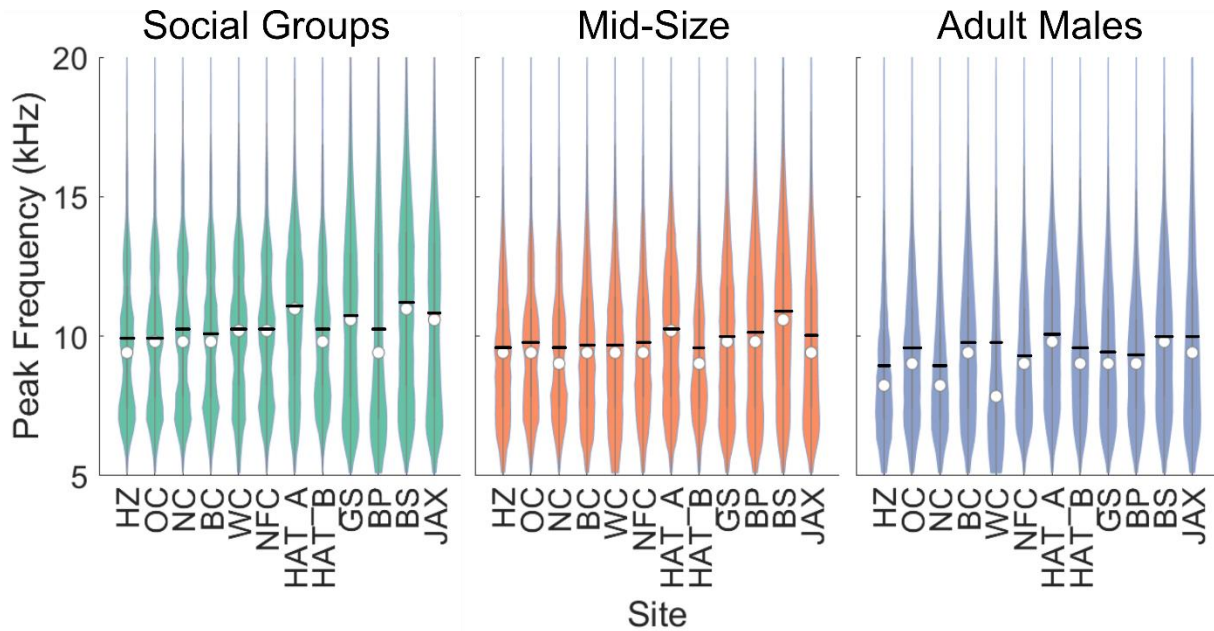
Figure 3.14. Violin plots of the peak frequency distribution for each class at each site. The white marker represents the mean of the distribution, and the black line represents the peak of the GMM distribution fit to the data.

Table 3.8. Peak frequency (kHz) and CV for each class (column) at each site (row). The mean value and CV for each class is displayed in the last row.

Site	Social Groups		Mid-Size Animals		Males	
	f	CV(*f*)	*f*	CV(*f*)	*f*	CV(*f*)
HZ	9.92	0.0001	9.60	0.0003	8.96	0.0006
OC	9.92	0.0001	9.75	0.0003	9.58	0.0010
NC	10.25	0.0002	9.58	0.0003	8.97	0.0009
BC	10.08	0.0002	9.68	0.0004	9.81	0.002
WC	10.25	0.0002	9.68	0.0005	9.81	0.002
NFC	10.25	0.0001	9.75	0.0006	9.29	0.002
HAT_A	11.07	0.0008	10.25	0.0007	10.08	0.002
HAT_B	10.25	0.0002	9.58	0.0004	9.58	0.002
GS	10.72	0.0005	10.02	0.0006	9.41	0.001
BP	10.27	0.001	10.15	0.0009	9.31	0.002
BS	11.19	0.0006	10.91	0.001	10.01	0.002
JAX	10.78	0.0008	10.03	0.002	10.02	0.006
Mean	10.41	0.0004	9.92	0.0007	9.57	0.002

Table 3.9. Acoustic data derived and literature-based signal and behavior parameters used in Monte Carlo simulations to model the probability of detecting sperm whales. If the parameter was not consistent for each location or class, the site and sex to which it applies to is listed to the right of the parameter. If there were class differences at an individual site, the relevant class is displayed as a superscript to the site. The units, mean value, standard deviation, and distribution are also included. The reference is displayed numerically or symbolically with the respective reference at the bottom of the table.

Parameter		Units	Mean	Standard Deviation	Distribution	Ref
Dive altitude above seafloor	OC^{AM}, BC$^{MS/AM}$, WC, HAT_A^{AM}	m	500 – 600	10 – 30	Uniform	*
	OC^{SG}, BC^{SG}, BP		450 – 500			
	HZ, OC^{MS}, NC, NFC, HAT_A$^{SG/MS}$, HAT_B, BS, JAX		400 – 500			
	GS		350 – 450			
Water column dive fraction		%	50 – 60§	1 – 2	Uniform	1, *
Benthic dive altitude	NC, BC^{MS}, WC$^{SG/AM}$, NFC, HAT_A, BP	m	2 – 7	10 – 20	Uniform	1, 2, *
	HZ, OC, BC$^{SG/AM}$, WC^{MS}, HAT_B		1 – 6			
	GS, BS, JAX		0 – 5			
Benthic dive altitude fraction		%	50 – 40	1 – 2	Uniform	1, 2, *
Start clicking depth		m	200 – 220	65 – 75	Uniform	1
Orientation: Elevation		deg	0	0 – 50	Normal, 0° truncated	1
Orientation: Azimuth		deg	0 – 359	n/a	Uniform	*
Source level	Social Group	dB$_{rn}$	233 – 243	2 – 5	Normal	*
	Mid-Size		233 – 243			
	Adult Male		238 – 248			

152

Table 3.9. Acoustic data derived and literature-based signal and behavior parameters used in Monte Carlo simulations to model the probability of detecting sperm whales. If the parameter was not consistent for each location or class, the site and sex to which it applies to is listed to the right of the parameter. If there were class differences at an individual site, the relevant class is displayed as a superscript to the site. The units, mean value, standard deviation, and distribution are also included. The reference is displayed numerically or symbolically with the respective reference at the bottom of the table.

Directivity	Social Group & Mid-Size	dB	25 – 30	n/a	Uniform	3, 4, *
	Adult Male		27 – 32			
90° off-axis TL		dB	35 – 40	n/a	Uniform	4
180° off-axis TL		dB	25 – 30	n/a	Uniform	4
Peak freq.	Social Group	kHz	10.5	n/a	None	^
	Mid-Size		10			
	Adult Male		9.5			
Maximum detection range		km	40	n/a	None	*

[1.] Watwood et al. 2006, [2.] Irvine et al. 2017, [3.] Møhl et al. 2003, [4.] Zimmer et al., 2005b, * Simulated in this study, ^ Directly estimated from this study
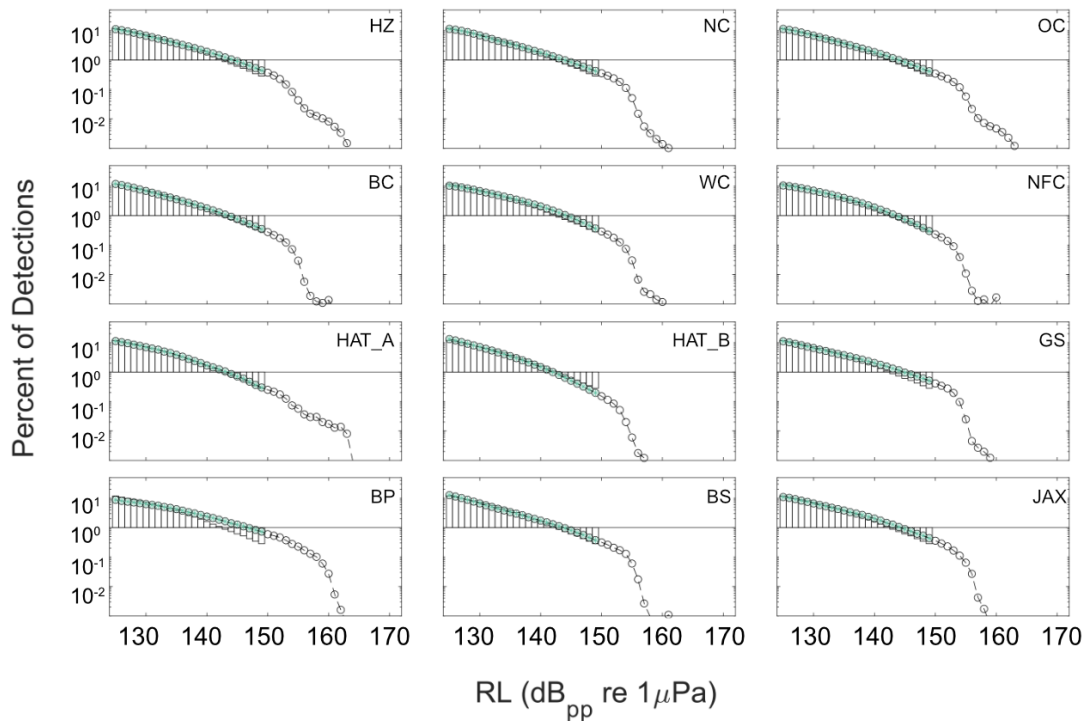
Figure 3.15. Comparison between measured received levels (points) for Social Group clicks at each site with the predicted received level (bars) displayed with a log scale. The acoustic data that was included in the models have been filled in green.
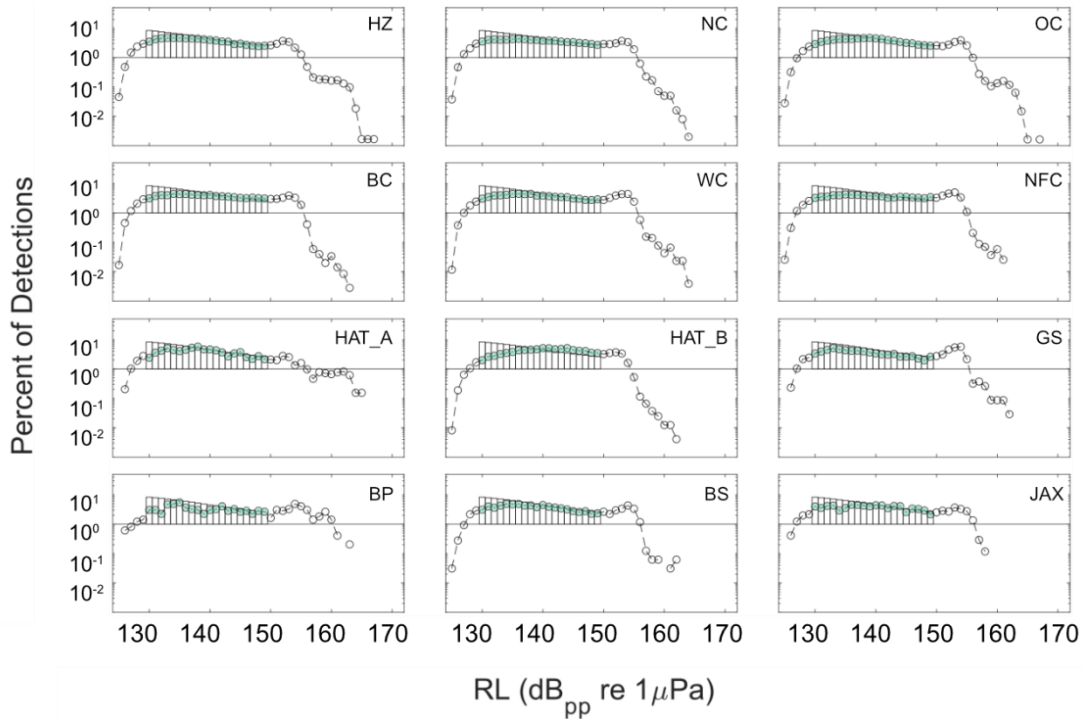
Figure 3.16. Comparison between measured received levels (points) for Social Group 5-min bins at each site with the predicted received level (bars) displayed with a log scale. The acoustic data that was included in the models have been filled in green.
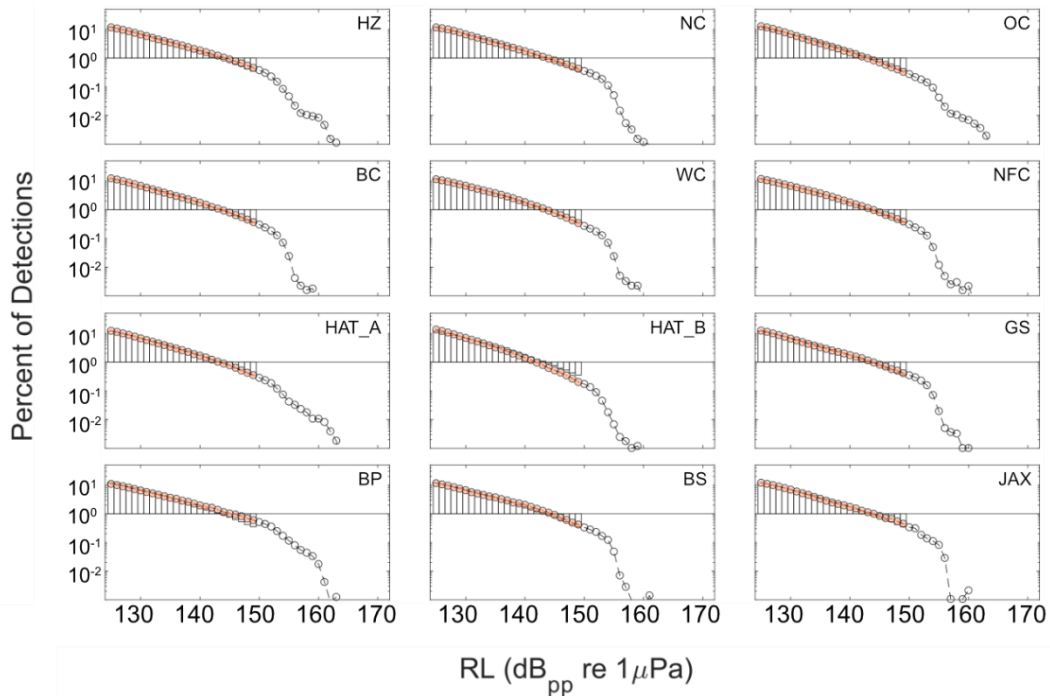
Figure 3.17. Comparison between measured received levels (points) for Mid-Size clicks at each site with the predicted received level (bars) displayed with a log scale. The acoustic data that was included in the models have been filled in orange.
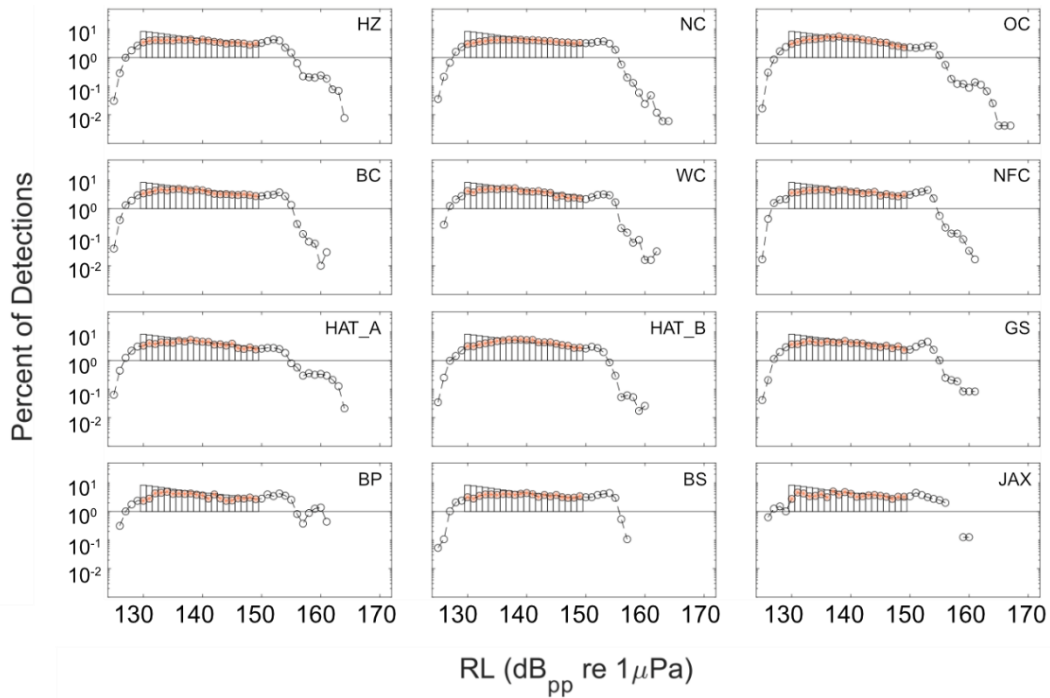
Figure 3.18. Comparison between measured received levels (points) for Mid-Size 5-min bins at each site with the predicted received level (bars) displayed with a log scale. The acoustic data that was included in the models have been filled in orange.
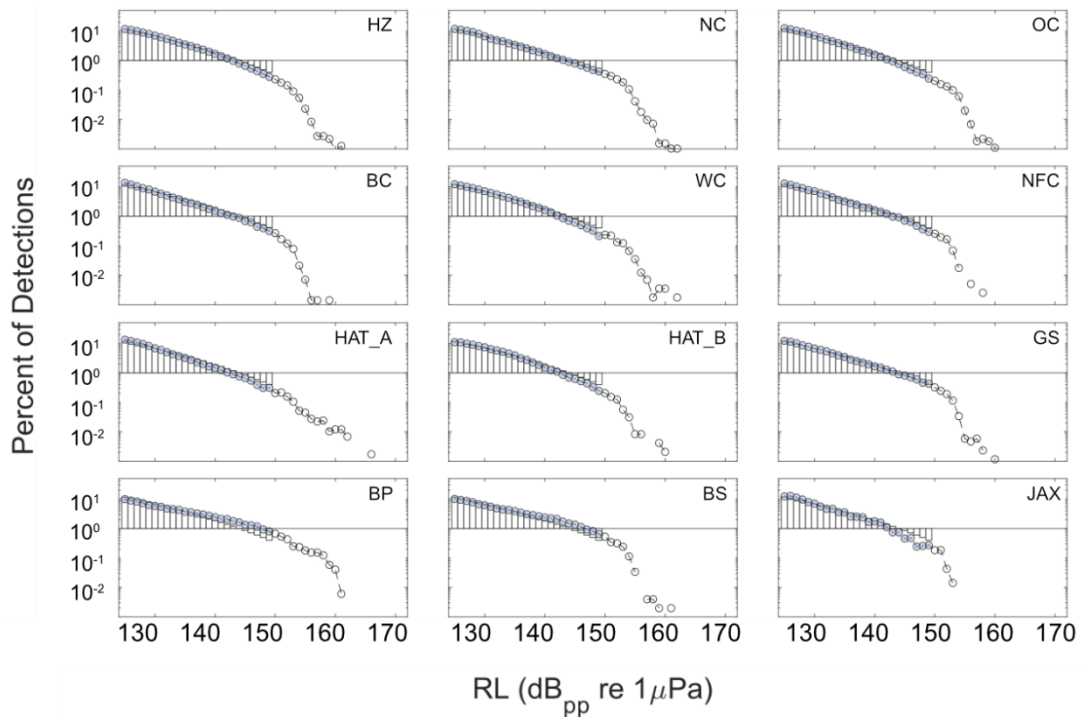
Figure 3.19. Comparison between measured received levels (points) for Adult Male clicks at each site with the predicted received level (bars) displayed with a log scale. The acoustic data that was included in the models have been filled in blue.

155
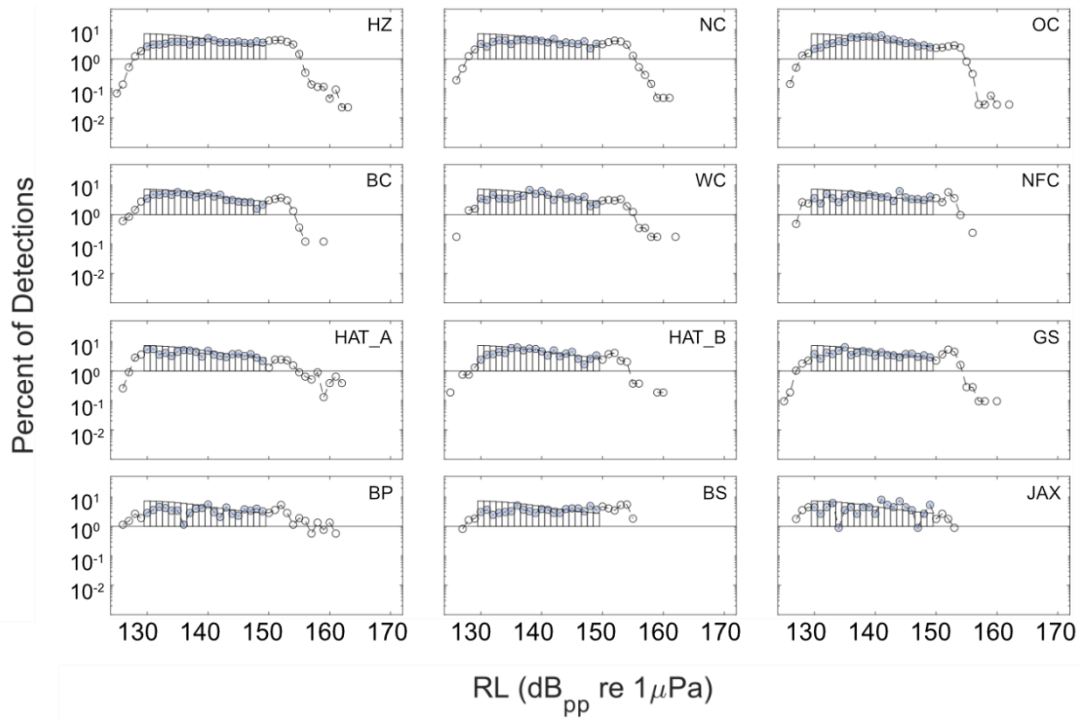
Figure 3.20. Comparison between measured received levels (points) for Adult Male 5-min bins at each site with the predicted received level (bars) displayed with a log scale. The acoustic data that was included in the models have been filled in blue.

Table 3.10. The percentage of missed clicks, or false negatives (c_x), and associated coefficients of variation CV(c_x) for each site and class for the click and group counting approaches.

Site	Class	Click Counting		Group Counting	
		c_x (%)	CV(c_x)	c_x (%)	CV(c_x)
HZ	Social Group	2.69	0.01	10.20	0.01
	Mid-Size	0.90	0.01	11.18	0.01
	Adult Male	0	0.01	17.28	0.01
OC	Social Group	0.810	0.01	11.89	0.01
	Mid-Size	0	0.01	13.09	0.01
	Adult Male	0	0.01	14.88	0.01
NC	Social Group	1.63	0.01	13.93	0.01
	Mid-Size	0	0.01	11.43	0.01
	Adult Male	0	0.01	18.35	0.01
BC	Social Group	0.31	0.01	12.54	0.01
	Mid-Size	0	0.01	9.97	0.01
	Adult Male	0	0.01	9.62	0.01
WC	Social Group	4.27	0.01	13.81	0.01
	Mid-Size	1.34	0.01	8.45	0.01
	Adult Male	0	0.01	15.44	0.01
NFC	Social Group	3.34	0.01	13.89	0.01
	Mid-Size	1.14	0.01	11.02	0.01
	Adult Male	0	0.01	15.71	0.01
HAT_A	Social Group	2.02	0.01	12.29	0.01
	Mid-Size	0	0.01	10.55	0.01
	Adult Male	0	0.01	10.02	0.01

Table 3.10. The percentage of missed clicks, or false negatives (c_x), and associated coefficients of variation $CV(c_x)$ for each site and class for the click and group counting approaches.

HAT_B	Social Group	0	0.01	18.91	0.01
	Mid-Size	0	0.01	12.86	0.01
	Adult Male	0	0.01	15.89	0.01
GS	Social Group	3.47	0.01	10.77	0.01
	Mid-Size	0	0.01	9.50	0.01
	Adult Male	0	0.01	13.93	0.01
BP	Social Group	11.08	0.01	15.40	0.01
	Mid-Size	3.85	0.01	11.98	0.01
	Adult Male	7.27	0.01	14.76	0.01
BS	Social Group	0	0.01	11.92	0.01
	Mid-Size	1.78	0.01	13.50	0.01
	Adult Male	5.23	0.01	18.36	0.01
JAX	Social Group	3.40	0.01	13.64	0.01
	Mid-Size	0	0.01	13.71	0.01
	Adult Male	0	0.01	12.16	0.01
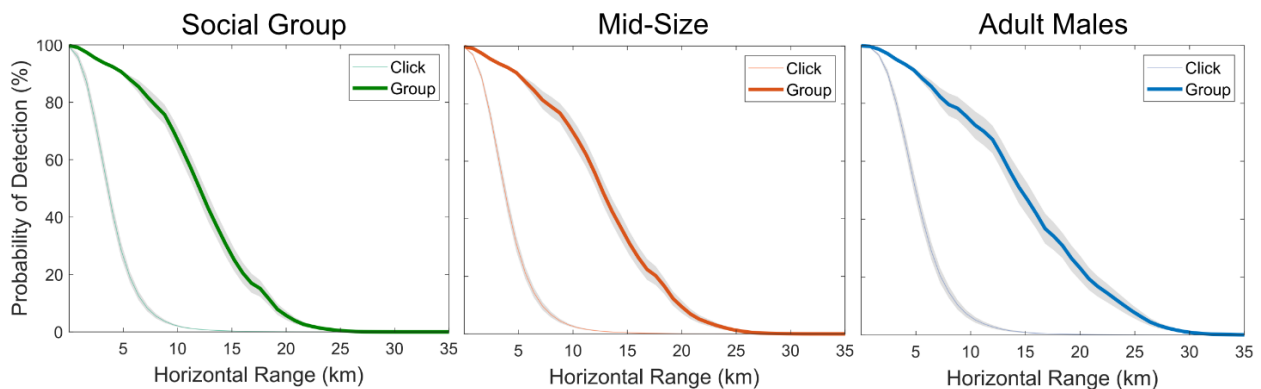
Figure 3.21. Average detection probability across sites (dark line) with confidence intervals represented in the shaded area for each class for the click and group counting approach.

Table 3.11. Probability of click and bin detection, and the respective CVs, for all classes at each site.

Site	Class	Click Counting		Group Counting	
		c_x (%)	CV(c_x)	c_x (%)	CV(c_x)
HZ	Social Group	0.78	0.017	11.60	0.0087
	Mid-Size	1.01	0.018	15.45	0.0090
	Adult Male	2.18	0.016	23.53	0.0076
OC	Social Group	1.21	0.015	13.14	0.0070
	Mid-Size	1.39	0.016	14.64	0.0071
	Adult Male	2.75	0.014	20.20	0.0062
NC	Social Group	0.66	0.018	9.70	0.0081
	Mid-Size	0.75	0.017	10.71	0.0080
	Adult Male	1.89	0.015	16.02	0.0068
BC	Social Group	0.77	0.017	10.25	0.0079
	Mid-Size	0.88	0.017	11.19	0.0081
	Adult Male	1.14	0.015	10.72	0.0078
WC	Social Group	0.7	0.017	10.02	0.0078
	Mid-Size	0.75	0.017	10.90	0.0078
	Adult Male	1.27	0.016	14.22	0.0071
NFC	Social Group	0.51	0.016	7.64	0.0082
	Mid-Size	0.6	0.017	8.52	0.0083
	Adult Male	1.28	0.014	12.13	0.0076
HAT_A	Social Group	1.48	0.016	17.03	0.0078
	Mid-Size	1.66	0.017	19.15	0.0082
	Adult Male	2.72	0.016	26.32	0.0078
HAT_B	Social Group	1.29	0.017	15.93	0.0076
	Mid-Size	1.53	0.017	18.01	0.0078
	Adult Male	3.1	0.014	25.37	0.0072

Table 3.11. Probability of click and bin detection, and the respective CVs, for all classes at each site.

GS	Social Group	1.07	0.016	10.61	0.0064
	Mid-Size	1.22	0.016	11.61	0.0071
	Adult Male	1.54	0.016	14.06	0.0079
BP	Social Group	1.04	0.014	10.88	0.0053
	Mid-Size	1.16	0.015	11.53	0.0052
	Adult Male	2.28	0.013	14.18	0.0041
BS	Social Group	0.76	0.016	11.34	0.0082
	Mid-Size	0.87	0.016	12.58	0.0080
	Adult Male	1.99	0.013	17.68	0.0061
JAX	Social Group	0.91	0.016	9.00	0.0066
	Mid-Size	0.97	0.017	9.64	0.0069
	Adult Male	1.42	0.016	11.81	0.0072
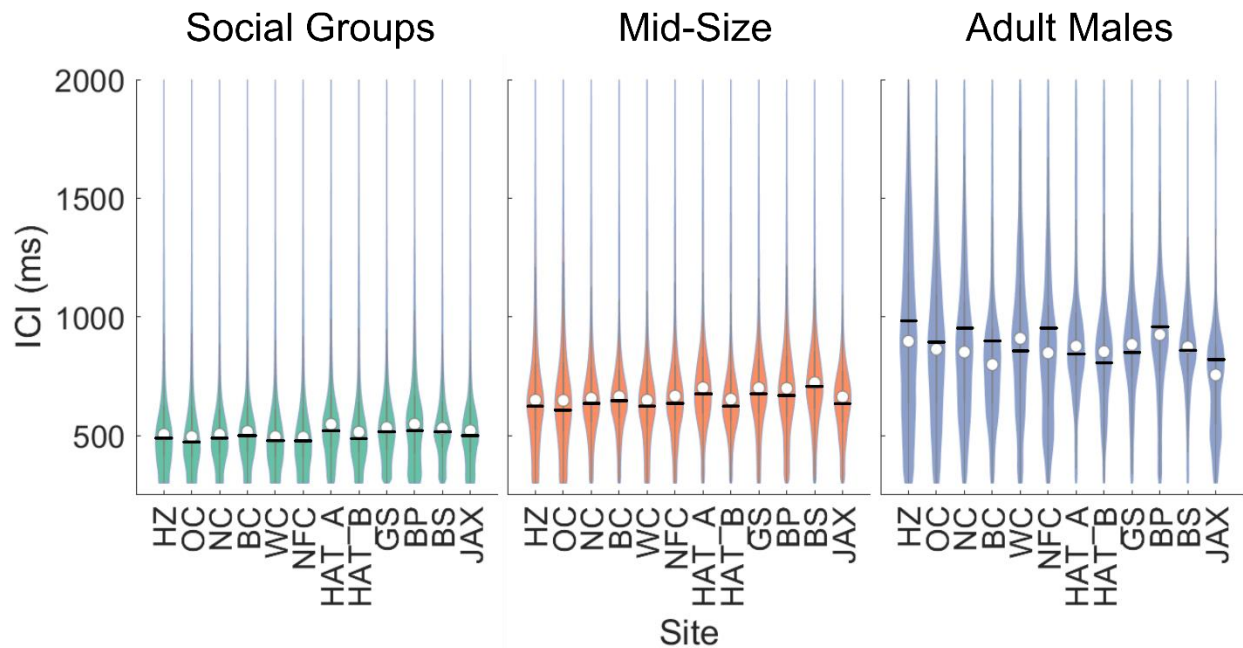
Figure 3.22. Violin plots reveal interclick interval distribution for each class at each site. The white marker represents the mean of the distribution, and the black line represents the peak of the GMM distribution fit to the data.

Table 3.12. Interclick interval (ms) and CV for each class (column) at each site (row).

Site	Social Groups		Mid-Size Animals		Males	
	f	CV(f)	f	CV(f)	f	CV(f)
HZ	483	0.0001	609	0.0003	934	0.001
OC	471	0.0001	609	0.0003	892	0.002
NC	483	0.0001	627	0.0003	892	0.001
BC	495	0.0002	639	0.0004	832	0.002
WC	477	0.0002	621	0.0005	808	0.002
NFC	471	0.0002	633	0.0005	880	0.003
HAT_A	519	0.0007	676	0.0006	844	0.002
HAT_B	489	0.0002	621	0.0004	808	0.002
GS	513	0.0005	670	0.0006	838	0.001
BP	519	0.001	670	0.0009	959	0.001
BS	513	0.0006	694	0.0009	862	0.001
JAX	501	0.0008	633	0.001	820	0.003

Table 3.13. Cue rate (clicks/s) and CV for each class (column) at each site (row).

Site	Social Groups		Mid-Size		Adult Males	
	r	CV(*r*)	*r*	CV(*r*)	*r*	CV(*r*)
HZ	1.38	0.06	1.02	0.06	0.65	0.09
OC	1.32	0.06	0.96	0.06	0.73	0.09
NC	1.31	0.06	1.01	0.06	0.75	0.09
BC	1.27	0.06	0.99	0.06	0.88	0.09
WC	1.32	0.06	1.03	0.06	0.76	0.09
NFC	1.31	0.06	1.01	0.06	0.82	0.09
HAT_A	1.29	0.06	0.99	0.06	0.85	0.09
HAT_B	1.27	0.06	1.10	0.06	0.86	0.09
GS	1.27	0.06	0.96	0.06	0.84	0.09
BP	1.21	0.06	0.94	0.06	0.79	0.09
BS	1.28	0.06	0.93	0.06	0.85	0.09
JAX	1.29	0.06	1.02	0.06	0.93	0.09

Table 3.14. Average sperm whale densities derived from click counting for each class (column) at each site (row) given in # of animals per 1000 km^2 ± standard deviation.

Site	Social Group Density (#/1000 km^2) ± st dev	Mid-Size Density (#/1000 km^2) ± st dev	Adult Male Density (#/1000 km^2) ± st dev	Total Animal Density (#/1000 km^2) ± st dev
HZ	1.877 ± 0.200	0.207 ± 0.027	0.037 ± 0.010	2.121 ± 0.202
OC	1.060 ± 0.122	0.224 ± 0.042	0.006 ± 0.002	1.290 ± 0.129
NC	2.622 ± 0.245	0.450 ± 0.049	0.014 ± 0.003	3.086 ± 0.249
BC	1.416 ± 0.147	0.210 ± 0.023	0.006 ± 0.002	1.632 ± 0.148
WC	1.792 ± 0.309	0.181 ± 0.023	0.009 ± 0.003	1.982 ± 0.310
NFC	2.691 ± 0.459	0.123 ± 0.017	0.002 ± 0.001	2.816 ± 0.459
HAT_A	0.076 ± 0.014	0.111 ± 0.016	0.007 ± 0.002	0.194 ± 0.021
HAT_B	1.091 ± 0.190	0.171 ± 0.022	0.004 ± 0.001	1.266 ± 0.192
GS	0.121 ± 0.033	0.079 ± 0.013	0.010 ± 0.004	0.210 ± 0.035
BP	0.022 ± 0.019	0.044 ± 0.019	0.005 ± 0.003	0.071 ± 0.027
BS	0.126 ± 0.039	0.053 ± 0.010	0.004 ± 0.002	0.183 ± 0.040
JAX	0.091 ± 0.039	0.021 ± 0.007	0.001 ± 0.001	0.113 ± 0.040

Table 3.15. Average sperm whale densities derived from group counting for each class (row) at each site (column) given in # of animals per 1000 km^2 ± standard deviation.

Site	Social Group Density (#/1000 km^2) ± st dev	Mid-Size Density (#/1000 km^2) ± st dev	Adult Male Density (#/1000 km^2) ± st dev	Total Animal Density (#/1000 km^2) ± st dev
HZ	1.932 ± 0.171	0.194 ± 0.075	0.033 ± 0.020	2.159 ± 0.188
OC	1.354 ± 0.130	0.239 ± 0.112	0.017 ± 0.012	1.610 ± 0.172
NC	2.352 ± 0.198	0.504 ± 0.193	0.039 ± 0.023	2.900 ± 0.278
BC	1.381 ± 0.128	0.213 ± 0.076	0.014 ± 0.007	1.608 ± 0.149
WC	1.173 ± 0.138	0.155 ± 0.062	0.009 ± 0.006	1.329 ± 0.151
NFC	1.385 ± 0.170	0.163 ± 0.072	0.006 ± 0.005	1.554 ± 0.184
HAT_A	0.114 ± 0.023	0.133 ± 0.056	0.013 ± 0.008	0.260 ± 0.061
HAT_B	1.043 ± 0.169	0.248 ± 0.094	0.007 ± 0.006	1.298 ± 0.193
GS	0.132 ± 0.033	0.107 ± 0.048	0.016 ± 0.011	0.255 ± 0.059
BP	0.018 ± 0.015	0.037 ± 0.020	0.008 ± 0.005	0.063 ± 0.021
BS	0.116 ± 0.029	0.043 ± 0.022	0.006 ± 0.004	0.165 ± 0.037
JAX	0.101 ± 0.023	0.027 ± 0.018	0.002 ± 0.004	0.130 ± 0.029

Table 3.16. Annual trends in click % (left) and group % (right) change per year for Social Groups at all sites (rows) with the 95% confidence intervals represented by the respective minimum and maximum values.

Site	Click % Change per year	Min (%)	Max (%)	Group % Change per year	Min (%)	Max (%)
HZ	52	39	65	37	30	44
OC	24	19	27	14	9	17
NC	68	52	79	44	34	54
BC	66	58	76	52	43	57
WC	28	18	42	41	33	52
NFC	84	62	100	78	62	95
HAT_A	-2	-3	-1	-4	-5	-3
HAT_B	-23	-33	-17	0.4	-7	7
GS	2	1	5	6	5	8
BP	0	0	0	0.2	0.01	0.3
BS	-5	-7	-4	-4	-5	-3
JAX	-0.4	-1	0.01	-0.5	-2	0.01
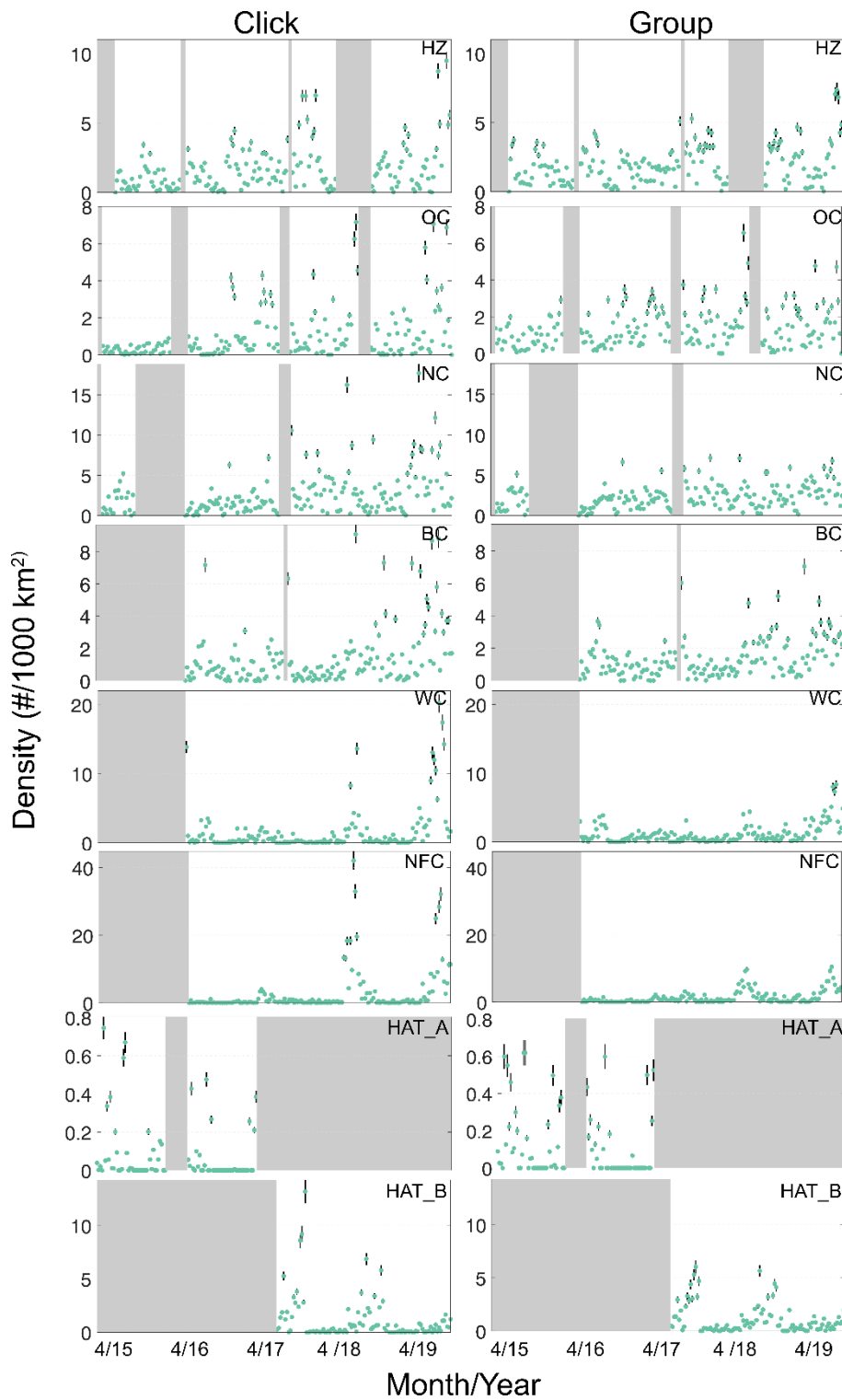
Figure 3.23. Weekly density estimates for Social Groups at the northern sites based on the click (left) and group (right) counting approaches. The circles denote mean density estimates, the vertical lines represent plus and minus one standard error, and shaded areas show gaps in recording effort.
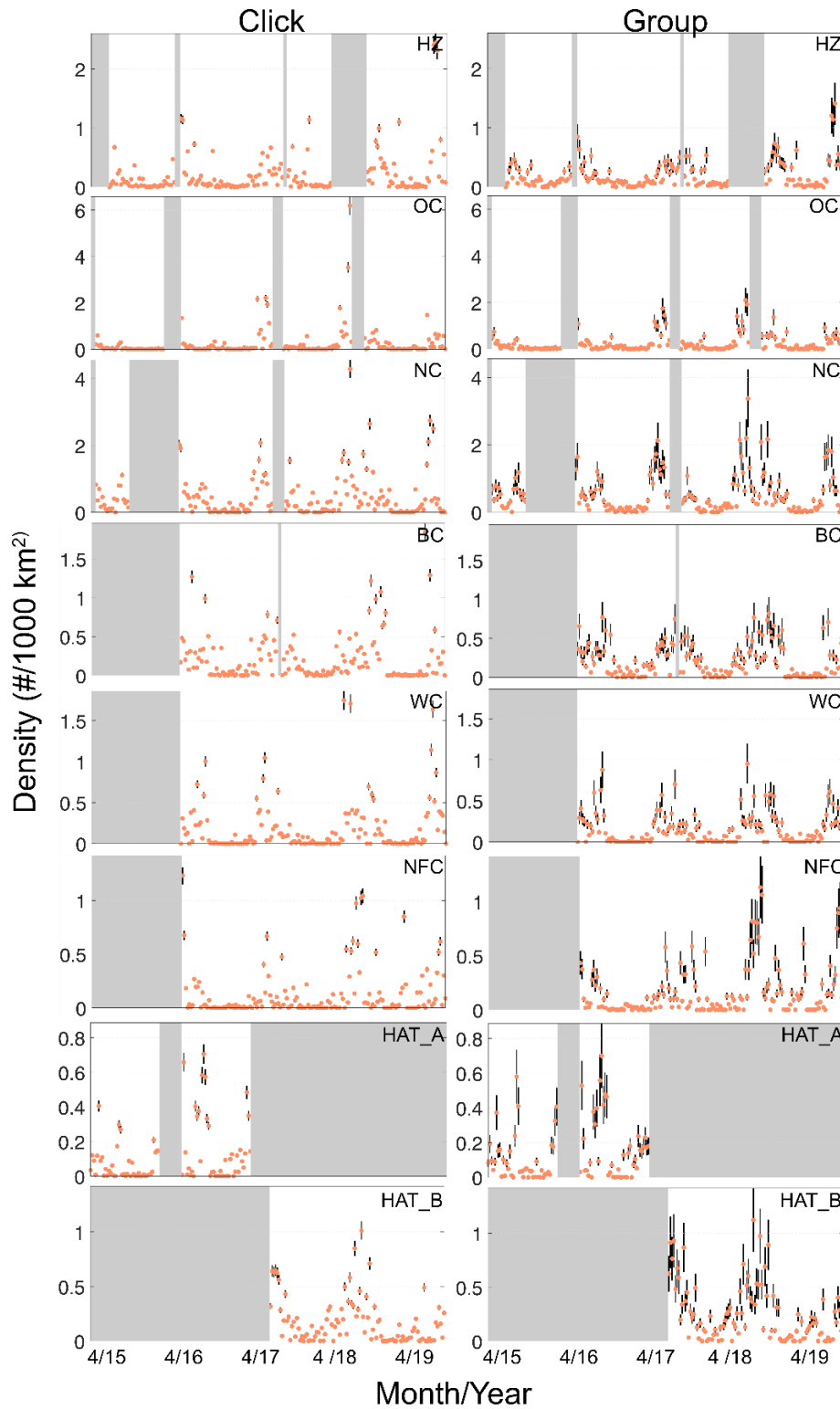
Figure 3.24. Weekly density estimates for Mid-Size at the northern sites based on the click (left) and group (right) counting approaches. The circles denote mean density estimates, the vertical lines represent +/- one standard error, and shaded areas show gaps in recording effort.
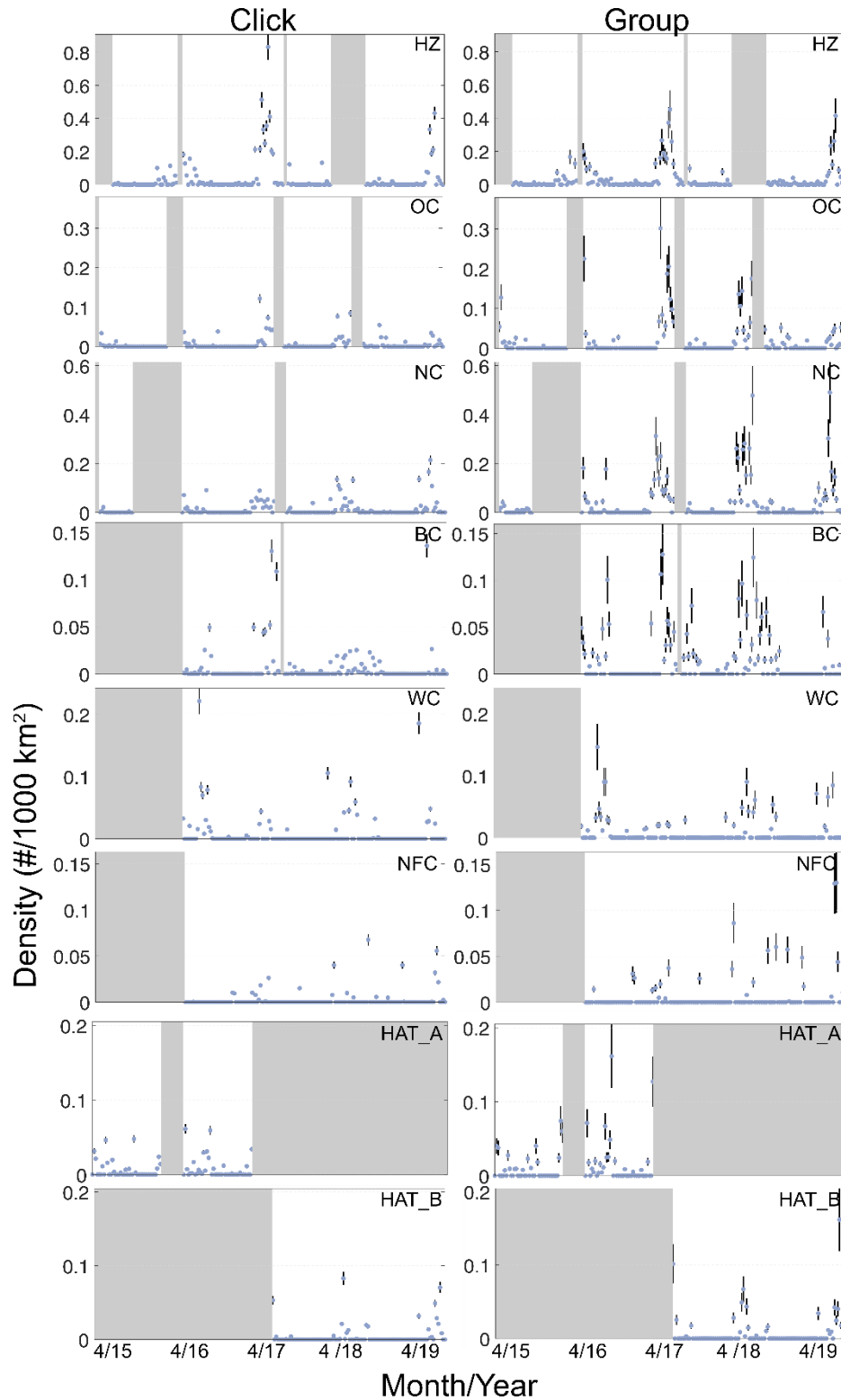
Figure 3.25. Weekly density estimates for Adult Males at the northern sites based on the click (left) and group (right) counting approaches. The circles denote mean density estimates, the vertical lines represent +/- one standard error, and shaded areas show gaps in recording effort.
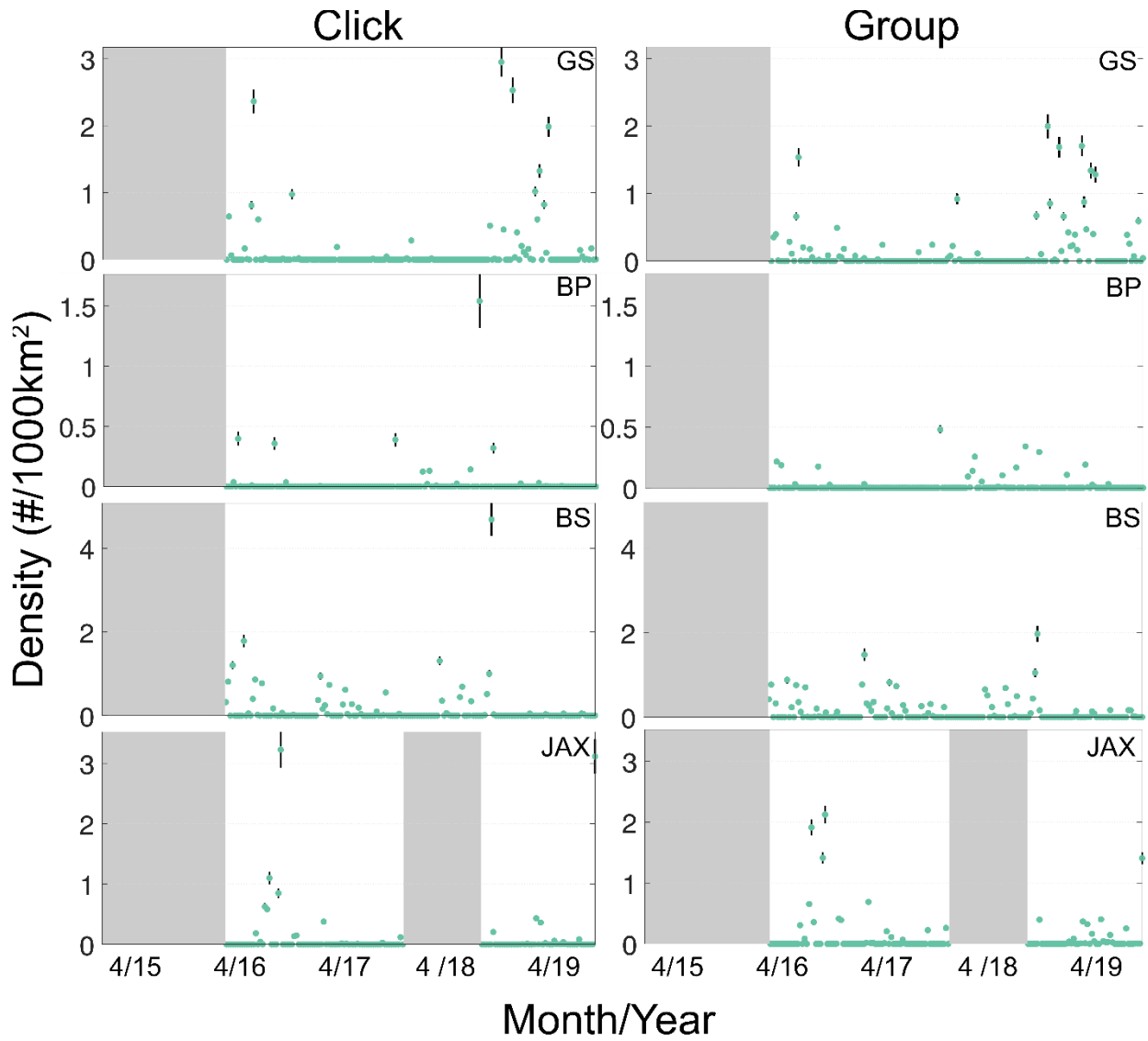
Figure 3.26. Weekly density estimates for Social Groups at the southern sites based on the click (left) and group (right) counting approaches. The circles denote mean density estimates, the vertical lines represent +/- one standard error, and shaded areas show gaps in recording effort.
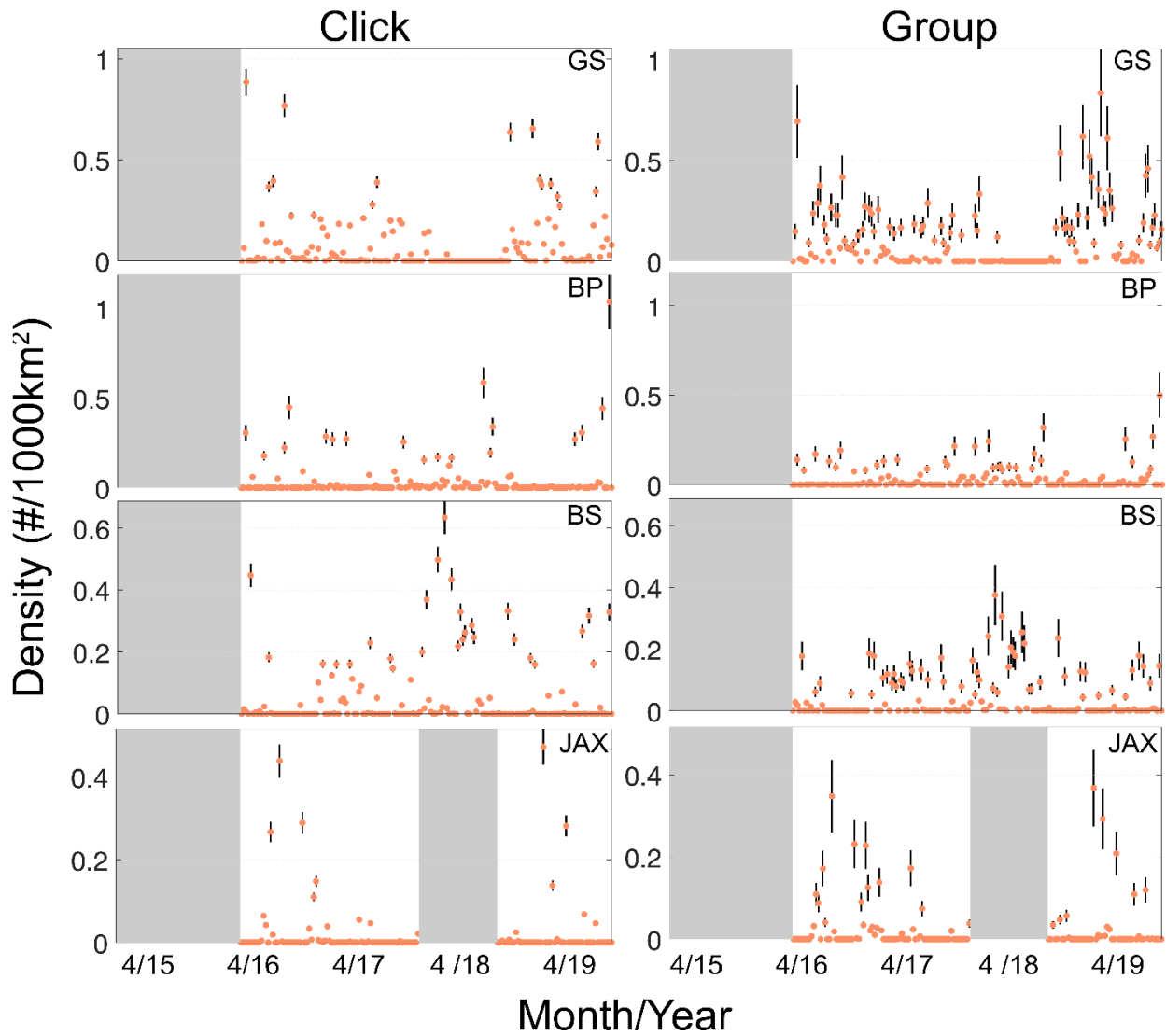
Figure 3.27. Weekly density estimates for Mid-Size at the southern sites based on the click (left) and group (right) counting approaches. The circles denote mean density estimates, the vertical lines represent +/- one standard error, and shaded areas show gaps in recording effort.

170
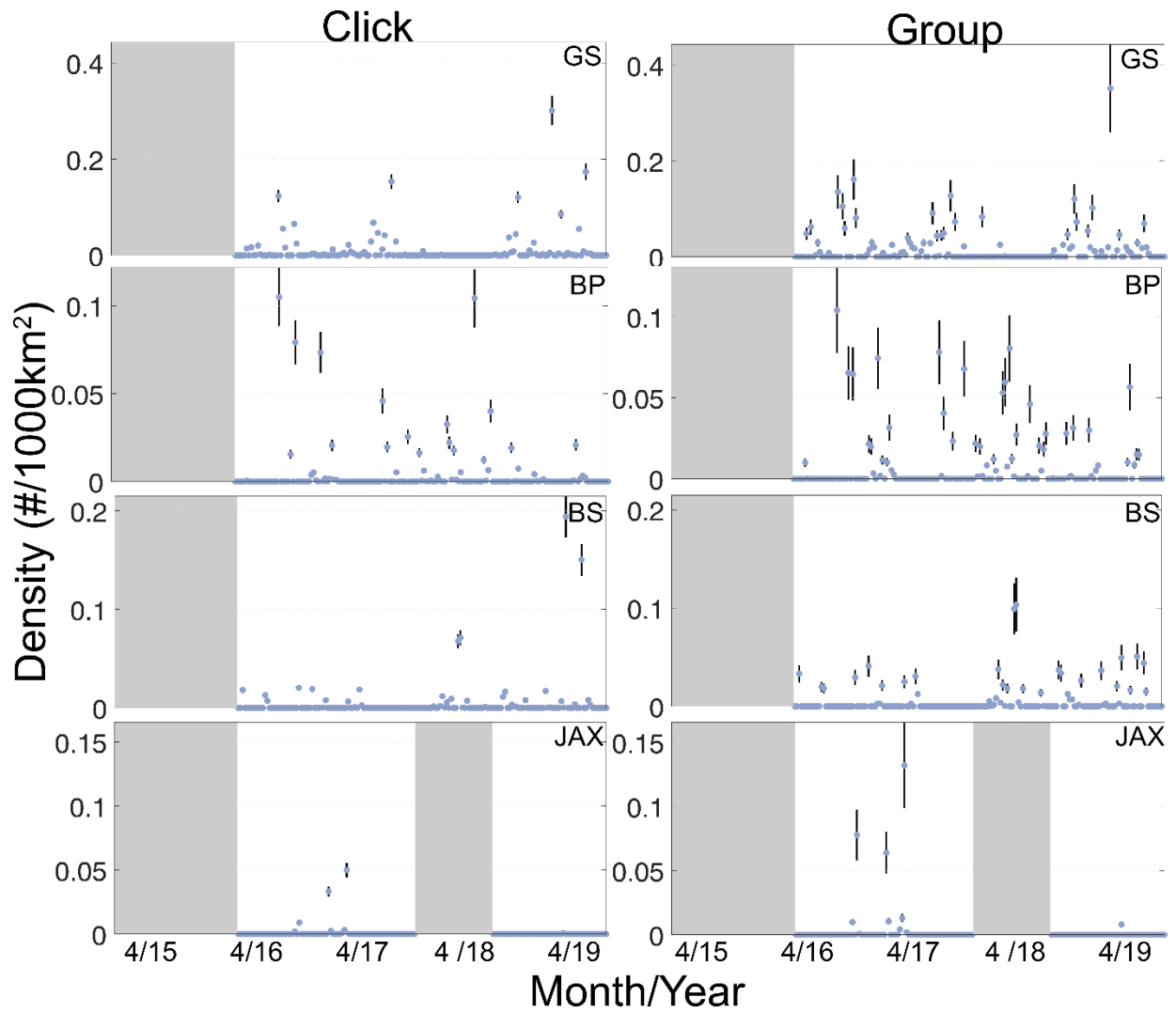
Figure 3.28. Weekly density estimates for Adult Males at the southern sites based on the click (left) and group (right) counting approaches. The circles denote mean density estimates, the vertical lines represent +/- one standard error, and shaded areas show gaps in recording effort.

171

Table 3.17. Output of sensitivity analysis of dive parameters and interclick interval on mean density using the click counting approach displaying the parameter that was tested, the slope of the variable versus density plot, the slope of the Z-score versus density plot, and the R^2 value of the line fit to the Z-score versus density plot.

Parameter	Variable vs. Density Slope			Z-Score vs. Density Slope			R^2		
	Social Groups	Mid-Size	Adult Males	Social Groups	Mid-Size	Adult Males	Social Groups	Mid-Size	Adult Males
Proportion of Dive Clicking	-2.79	-0.32	-0.038	-0.10	-0.011	-0.0038	0.99	0.99	0.97
Proportion of Time in Foraging Dive	-8.36	-0.95	-0.13	-1.66	-0.19	0.025	0.72	0.72	0.72
Interclick Interval	0.0045	3.64E-04	3.71E-05	0.72	0.059	0.0060	1	1	1

Table 3.18. Output of sensitivity analysis of dive parameters, group size, and synchrony on mean density using the group counting approach displaying the parameter that was tested, the slope of the variable versus density plot, the slope of the Z-score versus density plot, and the R^2 value of the line fit to the Z-score versus density plot.

Parameter	Variable vs. Density Slope			Z-Score vs. Density Slope			R^2		
	Social Groups	Mid-Size	Adult Males	Social Groups	Mid-Size	Adult Males	Social Groups	Mid-Size	Adult Males
Proportion of Dive Clicking	-2.21	-0.24	-0.038	-0.082	-0.0089	-0.0038	0.99	0.99	0.97
Proportion of Time in Foraging Dive	-6.57	-0.72	-0.12	-1.31	-0.143	-0.0238	0.72	0.72	0.71
Overlap	3.67	0.16	0.015	0.15	0.0064	5.94E-04	0.99	0.99	0.99
Group Size	-0.22	-0.031	-0.0069	-0.47	-0.025	-0.0032	0.91	0.97	0.98
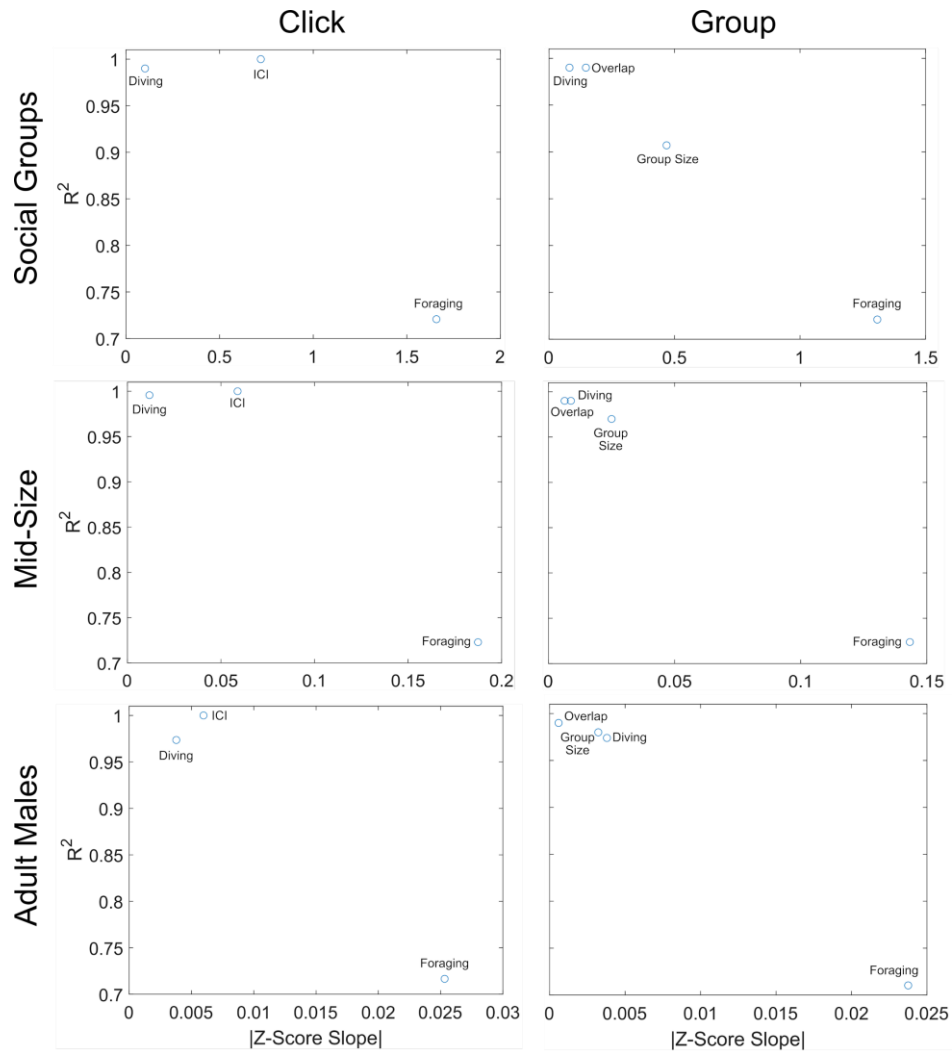
Figure 3.29. The relationship between the absolute value of the Z-score Slope and the R^2 value for the click and group counting approaches (column) for each class (rows). For the click counting approach, the proportion of a dive spent clicking ('Diving'), interclick interval ('ICI'), and proportion of time spent in a foraging dive cycle ('Foraging') were tested. For the group counting approach, the proportion of a dive spent clicking ('Diving'), proportion of time spent in a foraging dive cycle ('Foraging'), group size ('Group Size'), and synchronicity or overlap of vocalizing animals ('Overlap') were tested. Acoustic density estimation is more sensitive to the values with the higher Z-score slope and R^2 values.

Chapter 4: Demographic Dependent Habitat Associations and High Use Areas of Sperm Whales in the North Pacific

Natalie Posdaljian[1], Alba Solsona-Berga[1], Erin M. Oleson[2], John A. Hildebrand[1], Simone Baumann-Pickering[1]

[1] Scripps Institution of Oceanography, University of California San Diego, La Jolla, CA USA.

[2] NOAA Fisheries Pacific Islands Fisheries Science Center, Honolulu, Hawaii, United States of America

4.1 Abstract

Although a cosmopolitan species, sperm whale distribution varies latitudinally and across different demographic groups. Females and their young form lasting bonds, or social groups, and are thought to mostly remain in lower latitudes. As male sperm whales mature, they eventually leave their social group and at higher latitudes, juvenile male sperm whales can form bachelor schools consisting of males about the same age. But as they grow older and reach sexual maturity, they become increasingly solitary and begin traveling between temperate latitudes for increased foraging opportunities and tropical latitudes for breeding. Sperm whale habitat preferences and associations also vary latitudinally and across demographic groups and, yet understanding these nuances remains a challenge. This study provides foundational insight into demographic-dependent habitat associations and high use areas of sperm whales in the North Pacific using passive acoustic data collected from 27 sites. Leveraging differences in click characteristics, this study characterizes the demographic composition at each site, providing insights into the spatial distribution of different groups. By employing a two-sample permutation test, this study also identifies significant demographic-dependent associations within three regions: Eastern North Pacific, California Current Ecosystem, and the Central Pacific. Our results reveal that habitat preferences not only varied between regions but also exhibited significant differences among demographic groups, reflecting varying ecological requirements. Furthermore, we pinpoint seasonal high use areas for demographic groups, shedding light on potential ecological hotspots critical for the North Pacific sperm whale population. This study emphasizes the importance of considering demographic variations when assessing habitat associations and highlights the utility of passive acoustic data in deciphering complex patterns of species-habitat interactions. The findings have implications for the conservation and

management of sperm whales in the North Pacific by providing a foundation for targeted

conservation efforts that account for the diverse needs of different demographic groups within

the same ocean basin.

4.2 Introduction

Sperm whales are a cosmopolitan species renowned for their sexual dimorphism (Rice

1989). Even with a global distribution, sperm whales exhibit diverse patterns in their geographic

range based on the demographic group, or sex and social behavior of the animal. Female sperm

whales and their young form lasting bonds within tightly knit social groups, fostering maternal

care and cooperative behaviors (Ohsumi 1966; Best 1979; Rice 1989). Social groups are most

often found inhabiting lower latitudes, a preference attributed to their maternal and social

responsibilities, as well as the relatively abundant resources available in these warmer waters

(Best 1979; Whitehead & Weilgart 1991; Whitehead *et al.* 1991). Conversely, male sperm

whales undergo a distinct behavioral trajectory towards a solitary lifestyle as they mature. Upon

reaching juvenile age, young males leave their social group and begin traveling to higher

latitudes for improved foraging opportunities (Best 1979). Here they form bachelor schools,

representing a transitional phase between their initial social affiliations and eventual solitary

lifestyles (Best 1979). These groups of similarly aged males engage in social interactions and

play critical roles in the development of social skills and behavior patterns (Kobayashi *et al.*

2020). As they continue to mature, male sperm whales gradually shift towards solitary behaviors,

becoming increasingly solitary as they approach sexual maturity (Caldwell *et al.* 1966; Best

1979; Rice 1989). This transition prompts their migration between temperate latitudes, where

they seek enhanced foraging opportunities, and tropical latitudes, which serve as breeding

grounds (Best 1979). The dynamic movement patterns of male sperm whales underscore the

intricate balance between biological imperatives and environmental influences, shaping their distribution and demographic associations.

In the North Pacific, understanding of sperm whale distribution and demographics has been shaped by a combination of historical whaling records, contemporary visual and acoustic studies, and advanced monitoring techniques such as tagging and genetic analysis. The Eastern North Pacific (ENP), specifically the Gulf of Alaska (GOA) and Bering Sea/Aleutian Islands (BSAI), maintains year-round presence of sexually mature and juvenile male sperm whales with a peak presence in the summer (Mellinger *et al.* 2004; Diogou *et al.* 2019a; Chapter 2). More recent studies have shown that this region may be an overlooked habitat for social groups as well (Fearnbach *et al.* 2014; Rone *et al.* 2017; Chapter 2) with peaks in the GOA in spring and in the BSAI in winter (Chapter 2). The California Current Ecosystem (CCE) region also has year-round sperm whale presence (Dohl 1983; Barlow 1995; Forney *et al.* 1995), with a peak abundance in the spring and fall months (Rice 1974). Demographic composition in the CCE is not well understood, although sightings of all groups have been made throughout the region (Jaquet 2006; Mesnick *et al.* 2011) and there is evidence that the region supports a demographically independent population from the rest of the Pacific (Mesnick *et al.* 2011). The Central Pacific (CP) also maintains a year-round presence of social groups with a dip in presence during the summer and fall and subtle temporal patterns in acoustic activity throughout the region (Merkens *et al.* 2019). It has been hypothesized that sexually mature males return to these latitudes seasonally for mating (Best 1979), however there isn't clear evidence about when they return and if it's random or seasonal in nature.

Understanding sperm whale habitat preference in the North Pacific is important for identifying the areas of critical importance by knowing which environmental characteristics

influence their choice of habitat and how this choice changes seasonally. Studies have found that biological productivity at the base of the food chain partially explains sperm whale distributions (Wong & Whitehead 2014; Baumann-Pickering *et al.* 2016). However, sperm whales are the end of a long food chain and most correlations become obscure with the large temporal and spatial lags between increases in chlorophyll concentration and sperm whale occurrence (Jaquet 1996; Jaquet & Gendron 2002). There is also evidence of a positive relationship between sperm whale occurrence and increased ocean heating, vertical stratification, and circulation (Diogou *et al.* 2019b). On smaller scales, studies have found association with distinct mesoscale oceanographic features such as thermal fronts (Griffin 1999) and eddies (Wong & Whitehead 2014), although these associations are not always consistent between regions. A relationship between bathymetry features and sperm whale presence has also been established, with areas close to the continental shelf break and steep underwater topography such as seamounts identified as prime habitat (Waring *et al.* 2001; Drouot *et al.* 2004; Pirotta *et al.* 2011; Hann *et al.* 2016; Diogou *et al.* 2019a) particularly for groups of female sperm whales (Jaquet & Whitehead 1996). Bathymetric features can result in vertical water circulation that redistributes nutrients and can lead to an aggregation of sperm whale prey (Biggs *et al.* 2000; Praca *et al.* 2009). Prey availability is likely the main determining factor of marine mammal habitat use (Gregr *et al.* 2013; Palacios *et al.* 2013), and sperm whales are no exception. However, prey abundance is very difficult to measure (Guisan & Zimmermann 2000; Jaquet & Gendron 2002), particularly in the case of sperm whales who prefer deep sea cephalopods and certain fish species, including rock fishes, cod, sharks, rag fish, skate, lingcod, etc. with importance varying by region (Clarke 1956, 1966, 1980; Kawakami 1980). Obtaining environmental variables that serve as proxies to prey availability is often used to explain observed variability in animal presence. Although environmental variables usually

only explain a small proportion of the variability and are difficult to extrapolate to other areas since the relationship between presence and a specific variable (or combination of variables) might vary in different regions (Guisan & Zimmermann 2000). For sperm whales, this issue is further complicated by the fact that they are deep diving species who target high-tropic level deep diving prey that might not have a clear or direct relationship to sea surface variables that are often easier to retrieve (Jaquet & Whitehead 1996). A study using a combination of in-situ and remotely sensed environmental variables reported improvements in the amount of sperm whale presence variability the habitat modeling explained (Redfern *et al.* 2006; Diogou *et al.* 2019b). However, in-situ environmental monitoring over long time periods is extremely difficult, particularly in remote areas and over large spatial scales. Habitat association modeling provides insight into habitat preference and can serve as a foundational step for traditional habitat modeling. By knowing which variables sperm whales are associated with, future studies can incorporate in-situ measurements at depths where sperm whales forage with the goal of bridging the gap between the environment and prey availability which is the ultimate driver of sperm whale presence.

In this study we use passive acoustic data from 27 recording sites in the North Pacific to understand sperm whale demographic composition and spatiotemporal habitat use in three regions: Eastern North Pacific, California Current Ecosystem, and Central Pacific. We use the acoustic data to create a time series of demographic specific sperm whale presence at each site ranging from less than a year to nearly 10 years of data from one site to another. These time series were then used to describe temporal and spatial overlap of males and females at each site. Additionally, we recognized seasonal high-use areas of males and females throughout the North Pacific that informs management and conservation efforts to critical sperm whale habitat.

Finally, we identified demographic dependent habitat associations and preferences to serve as foundational insight for future habitat modeling. This study is the first known effort to understand demographic specific habitat associations to identify which environmental variables have the potential to predict different demographic compositions within geographic regions.

4.3 Methods

4.3.1 Data Collection

Passive acoustic monitoring was carried out using High-frequency Acoustic Recording Packages (HARPs; Wiggins & Hildebrand 2007) at 27 sites in the North Pacific Ocean between 2005 and 2002 (Figure 4.1-2, Table 4.1). The 27 sites were among three regions: the Eastern North Pacific (ENP), the California Current Ecosystem (CCE), and the Central Pacific (CP). The ENP contained seven sites among two subregions, the Gulf of Alaska (GOA) and the Bering Sea/Aleutian Islands (BSA). The CCE contained 8 sites among three subregions, the northern CCE (N.CCE), the central CCE (C.CCE), and the southern CCE (S.CCE). The CP contained 11 sites among five regions, the Northern Mariana Islands (NMI), Northwest Hawaiian Islands (NWHI), Main Hawaiian Islands (MHI), Marcus-Wake Seamount Group (MWSG), and the Northern Line Islands (NLI). The Equator (EQ) site was not part of a subregion. Each site varied in the number of deployments ranging from 1 to 19 deployments which resulted in anywhere from four months to 10 years of recordings at each site. Each HARP sampled with a frequency of 200 kHz. Some deployments recorded continuously while others had duty cycles to preserve battery life. Intermittent or long gaps between deployments were due to servicing schedules and limitations of battery life and data storage capacity. For three sites (PS, PHR, Palmyra), the instrument changed locations during the monitoring period. For PS, the two locations were considered differently and referred to as PS1 and PS2. For PHR and Palmyra, the location shift

was marked, however the location change was not considered as individual sites due to the lack of difference in sperm whale detections and demographic composition.

4.3.2 Detecting Sperm Whales

Sperm whale echolocation clicks were detected using the multi-step approach described in Solsona-Berga *et al.* (2020) (appendix) and applied in Chapter 2. The characteristic echolocation clicks of sperm whales have multiple pulses (Backus & Schevill 1966), 2-9 ms apart, depending upon the size of the animal (Norris & Harvey 1972). As a result, the detector had a lockout for clicks separated by less than 30 ms to avoid multiple detections of a single click. Bandpassing the data (5-95 kHz) minimized the effects of low-frequency noise from vessels, weather, or instrument self-noise on detections, but allowed for detection of the echolocation clicks of toothed whales. The Power Spectral Density (PSD) of detected signals was calculated with the Pwelch method (MATLAB, MathWorks, Natick, MA) using 4 ms of the waveform and a 512-point Hann window with 50% overlap (Welch 1967). Instrument-specific full-system transfer functions were applied to account for the hydrophone sensor response, signal conditioning electronics, and analog-to-digital conversion. To provide a consistent detection threshold, only clicks exceeding a peak-to-peak (pp) received level (RL) of at least 125 dBpp re 1 µPa were analyzed.

Sperm whale echolocation clicks can be confused with the impulsive signals from ship propeller cavitation. An automated vessel classifier developed by Solsona-Berga *et al.* (2020) (appendix) was used to exclude periods of ship passages during which it was not possible to distinguish between sperm whale clicks and ship cavitation noise. The classifier identified potential ship passages from long-term spectral averages (LTSA), which are long duration spectrograms (Wiggins & Hildebrand 2007). Further averaging was calculated as Average Power

Spectral Densities (APSD) per 2-hour blocks over low (1-5 kHz), medium (5-10 kHz), and high (10-50 kHz) frequency bands with 100 Hz bins and 50% overlap. Using received sound levels, transient ship passage signals were separated from odontocete echolocation clicks and weather events. Trained analysts manually reviewed identified ship passages using the MATLAB-based custom software program *Triton* (Wiggins & Hildebrand 2007). Ship passage times were removed from further analysis and considered time periods with no effort.

Instrument self-noise and the echolocation clicks of other odontocetes were also removed to reduce the number of false positive detections. A classifier using spectral click shape was implemented, taking advantage of a sperm whale click's distinct low-frequency spectral shape to remove dissimilar clicks by delphinid and beaked whales, which typically have higher frequencies (Solsona-Berga *et al*. 2020). The remaining acoustic encounters containing putative sperm whale echolocation clicks were manually reviewed with the MATLAB-based open-source *DetEdit* software program used to view, evaluate, and edit automatic detections (Solsona-Berga *et al.* 2020). After detections were edited, data was further analyzed on the click level as well as grouped into 5-min time bins. The proportion of false positive clicks and 5-min time bins was evaluated using *DetEdit.* The proportion of false positive clicks was calculated by evaluating every random 3,000[th] click in the entire dataset; the proportion of false positive 5-min time bins was calculated by evaluating the bin of the randomly selected clicks.

4.3.3 Interclick Interval as a Proxy for Demographics

Histograms of ICI provide a visualization that can be used to indicate sperm whale size and sex (Solsona-Berga *et al.* 2022). A plot of concatenated histograms of 5-min time bins, referred to as ICIgrams, was annotated and categorized for each time period at each site. Examples of the ICIgram GUI can be found in Solsona-Berga *et al*. (2022). We used three ICI

groups to correspond to three size classes as per Solsona-Berga *et al.* (2022). Detections with a modal ICI of 0.6 s or less were presumed to be females and their young, hereinafter referred to as Social Groups. Detections with a modal ICI of 0.8 s and greater were presumed to be adult males, hereinafter referred to as Adult Males. The detections with a modal ICI between the Social Groups and Adult Males (< 0.6 s and > 0.8 s) could be large females or juvenile males, hereinafter referred to as Mid-Size. Each 5-min time bin was categorized into the appropriate size class. The class of each time bin was applied to all the clicks within that bin.

4.3.4 Click Detection Processing and Accounting for the Duty Cycle

Duty cycle regimes, or the process of turning an acoustic recorder on at specified intervals, are implemented to maximize the deployment duration by conserving battery power and storage space of the instrument (Wiggins & Hildebrand 2007; Au *et al.* 2013). Duty cycle regimes can widely vary based on the desired deployment duration, the sampling rate, and the recording instrument.

Sperm whale click detections were binned into 5-min time bins. To account for deployments that were duty cycled, the number of 5-min bins in a day with presence were scaled by the amount of effort for that day. For example, one of the most common duty cycle regimes in this study was the 5/20, meaning there was a 5-min recording duration in a 20-min cycle. In one day, you would expect 288 5-min recording bins with potential to contain sperm whale detections. But if you apply a 5/20 duty cycle, there would only be 72 5-min bins with potential to contain sperm whale detections. If there were 30 5-min bins with sperm whale clicks, after scaling for lower effort because of the duty cycle, you would expect 120 5-min bins with sperm whale detections if there was full recording effort.

For plotting time series of presence and identifying high-use areas of sperm whale presence, the proportion of hours per week and per season were used. For understanding demographic composition at each site, the proportion of binary (1/0) hourly and daily presence was used. And finally, for habitat association analysis, binary (1/0) daily presence was used for statistical analysis (see next section). Time series were not plotted for the ENP region since they are already available in Chapter 2 of this dissertation.

4.3.5 Identifying Habitat Association for Sperm Whale Classes

This study used a suite of habitat variables that have previously been linked to the distribution of sperm whales (Jaquet 1996; Jaquet & Gendron 2002; Wong & Whitehead 2014; Baumann-Pickering *et al.* 2016; Diogou *et al.* 2019b) including sea surface temperature (SST), Chlorophyll-a concentration (CHL), sea surface height (SSH) variation, eddy kinetic energy (EKE), potential temperature (PT), ocean mixed layer thickness (MLT), and salinity (SAL). Variables were averaged across the entire region of interest. For the ENP the bounding box was -140 to -180 (longitude) and 50 to 60 (latitude). For the CCE, the bounding box was -113 to -127 (longitude) and 28 to 48 (latitude). For the CP, the bounding box was -145 to -215 (longitude) and 5 to 30 (latitude). The equator site (EQ) was not included in the bounding box since the recording site only contributed 3 months of sperm whale presence data to the analysis and was located in a very different pelagic habitat than the remaining CP sites. Daily CHL averages were obtained from the Aqua Moderate Resolution Imaging Spectrometer (MODIS) (NASA/GSFC/OBPG 2023) using ERDDAP and averaged for each region of interest (ENP, CCE, CP). Daily SST averages were also obtained from the Aqua MODIS (NOAA NMFS SWFSC ERD 2023) using ERDDAP and averaged for each region of interest (ENP, CCE, CP). The remaining habitat variables were obtained from the CMEMS Global Ocean Ensemble

Physics Reanalysis (CMEMS GOEPR) (E.U. Copernicus Marine Service Information (CMEMS) 2023) using Copernicus Marine and averaged for each region of interest (ENP, CCE, CP). This dataset only extended until December 31, 2020, so even though SST and CHL extended beyond that date, this study only conducted habitat association modeling until the year 2020, or up to the length of the acoustic time series for that region. EKE was calculated as $\frac{1}{2}(U^2 + V^2)$, where U and V are meridional and zonal geostrophic current components, respectively (Ducet *et al.* 2000) obtained from the CMEMS GOEPR dataset.

To identify habitat variables that are associated with sperm whale presence of each class within each region, this study followed methods similar to Benson *et al.*(2011). Using a two-sample permutation test (Efron & Tibshirani 1993), differences in the mean values of each variable were compared between times with and without daily presence. This test offers a straightforward approach to assess the significance of patterns in the data without many of the assumptions tied to parametric tests. The permutation test was conducted in the software R (R Core Team 2022) using the function *perm2* (Helsel *et al.* 2020). Permutation samples for all times within each region (n = 10,000) were generated by randomly shuffling the values of day without presence among all available times. The mean value for each habitat variable for the permuted times with presence to provide a distribution of the expected means if presence occurred randomly among all available times. For this study's two-sided alternative hypothesis, the p-value was calculated by determining the proportion of instances where the absolute differences between means in the permutation distribution were equal to or exceeded the absolute difference observed in the actual means. A p-value of 0.05 was considered significant and provides reasonably strong evidence of a significantly non-random association between sperm whale presence and the habitat variable of interest. Permuted distributions were plotted

with the mean values for sperm whale presence for each region and variable to show whether

sperm whale presence was associated with high or low values of each variable of interest.

Correlation Analysis was conducted in the software R (R Core Team 2022) using the R

package *corrplot* to explore if there was a relationship between two or more variables and how

strong that relationship was within each region.

4.4 Results

At the Quinault Canyon (QC) site in the CCE, sperm whales were present year-round

with more Mid-Size and Adult Male presence compared to Social Groups who were only present

for a few weeks in 2011 (Figure 4.3). Presence appears to decline over time, with the least

amount of presence from mid-2013 to mid-2014. At the Point Sur 1 (PS1) site in the CCE, sperm

whales were present year-round, with Adult Male presence increasing over the study period

(Figure 4.4). At the Point Sure 2 (PS2) site in the CCE, sperm whale presence appeared more

seasonal, with a consistent presence throughout the study period (Figure 4.5). The recording

period at the Diablo Canyon Power Plant (DCPP) site in the CCE only lasted from November

2012 to March 2013, but there did appear to be temporal partitioning of the three classes during

the study period, with little weekly overlap (Figure 4.6). Sperm whales of all size classes were

present year-round at the California Current Ecosystem (CCE) recording site in the CCE region

(Figure 4.7). A peak in presence was seen in the spring months for the Mid-Size and Adult

Males. There was less than a year of acoustic data from Hoke Seamount (Hoke) recording site,

however there were only two weeks with Social Group presence in the fall and winter of 2008

(Figure 4.8). The offshore mooring recording site (CORC) in the CCE had sperm whale presence

year-round with a peak in presence in the summer months for the Mid-Size and Adult Males and

sporadic presence of the Social Groups (Figure 4.9). The Guadalupe Island (GI) site in the CCE

had year-round sperm whale presence, particularly of Mid-Size and Adult Males (Figure 4.10). Social Groups were present very sporadic in 2019 with increased presence in 2020 and 2022. The Gulf of California (CA) site in the CCE had relatively low sperm whale presence except for a few weeks in the winter of 2009 where presence of all classes increased (Figure 4.11).

There was year-round sperm whale presence at the Saipan site in the CP, with Social Group presence reaching above 0.2 proportions of hours per week for several weeks throughout the study period (Figure 4.12). The nearby Tinian recording site had more sporadic sperm whale presence, particularly for Social Groups (Figure 4.13). The Ladd Seamount (LSM) recording site only recorded from mid-May to mid-August of 2009 with higher presence in May and June for Social Groups and June and July for Adult Males (Figure 4.14). The Pearl and Hermes (PHR) site had year-round presence of all classes, with more presence by Social Groups and presence for all classes decreasing beginning in 2016. (Figure 4.15). The Wake Seamount (Wake) site also had year-round presence for all classes, with a decrease across all classes, but mostly Mid-Size and Adult Males beginning in 2015 (Figure 4.16). Adult Males were present most often at the Kauai site in the CP, with only sporadic presence by Social Groups and Mid-Size (Figure 4.17). The Kona time series was the longest, with Social Groups presence reaching proportions of 0.1 hours per week throughout the study period (Figure 4.18). The Cross Seamount (CSM) site only had very sporadic Social Group presence, with no Mid-Size or Adult Male presence from March 2005 to May 2006 (Figure 4.19). The Pagan recording site had presence of all classes with peaks in September of 2016 and March of 2017 (Figure 4.20). The Kingman Reef (KR) site only had Social Group and Adult Male presence for only a few weeks during the study period in the beginning of 2012 (Figure 4.21). The Palmyra Atoll (Palmyra) site had very low and sporadic presence of all classes, particularly Mid-Size and Adult Males (Figure 4.22). The Equator (EQ)

187

site only had three weeks of sperm whale presence, with no Mid-Size presence throughout the study region (Figure 4.23).

The proportion of individual class presence and class overlap was evaluated on the hourly and daily time scales and reported as the median in percentage and interquartile range (IQR) (Figure 4.24-25). In the ENP, Social Groups were present in 7% (IQR = 7%) of hourly time bins and 8% (IQR = 9%) of daily time bins. Mid-Size were present in 38% (IQR = 10%) of hourly time bins and 47% (IQR = 11%) of daily time bins. Adult Males were present in 32% (IQR = 8%) of hourly time bins and 43% (IQR = 15%) of daily time bins. Social Groups and Mid-Size overlapped in 3% (IQR = 3%) of hourly time bins and 1% (IQR = 1%) of daily time bins. Social Groups and Adult Males overlapped in 3% (IQR = 2%) of hourly time bins and 0.2% (IQR = 0.05%) of daily time bins. Adult Males and Mid-Size overlapped in 16% (IQR = 5%) of hourly time bins and 4% (IQR = 5%) of daily time bins. All three classes overlapped in 1% (IQR = 2%) of hourly time bins and 0.01% (IQR = 0.1%) of daily time bins.

In the CCE, Social Groups were present in 17% (IQR = 18%) of hourly time bins and 24% (IQR = 22%) of daily time bins. Mid-Size were present in 36% (IQR = 22%) of hourly time bins and 40% (IQR = 19%) of daily time bins. Adult Males were present in 35% (IQR = 14%) of hourly time bins and 37% (IQR = 14%) of daily time bins. Social Groups and Mid-Size overlapped in 3% (IQR = 7%) of hourly time bins and 0.06% (IQR = 1%) of daily time bins. Social Groups and Adult Males overlapped in 0% (IQR = 3%) of hourly time bins and 0% (IQR = 0.7%) of daily time bins. Adult Males and Mid-Size overlapped in 7% (IQR = 4%) of hourly time bins and 2% (IQR = 5%) of daily time bins. All three classes overlapped in 0% (IQR = 1%) of hourly time bins and 0% (IQR = 0.2%) of daily time bins.

In the CP, Social Groups were present in 46% (IQR = 14%) of hourly time bins and 75% (IQR = 20%) of daily time bins. Mid-Size were present in 21% (IQR = 9%) of hourly time bins and 9% (IQR = 14%) of daily time bins. Adult Males were present in 7% (IQR = 11%) of hourly time bins and 11% (IQR = 22%) of daily time bins. Social Groups and Mid-Size overlapped in 21% (IQR = 9%) of hourly time bins and 2% (IQR = 4%) of daily time bins. Social Groups and Adult Males overlapped in 7% (IQR = 11%) of hourly time bins and 0.2% (IQR = 0.7%) of daily time bins. Adult Males and Mid-Size overlapped in 0.6% (IQR = 1%) of hourly time bins and 0.3% (IQR = 1%) of daily time bins. All three classes overlapped in 0.6% (IQR = 1%) of hourly time bins and 0% (IQR = 0.2%) of daily time bins.

High use areas of each class were identified by plotting the mean proportion of hours with presence in each season across all sites. The CP was a high use area for Social Groups across all seasons (Figure 4.26). The other two regions showed seasonal use by Social Groups, with the GOA serving as a high use area in the Spring and the BSAI in winter. The CCE had a larger proportion of Social Group presence in the fall months, particularly in the S.CCE. The ENP and CP were both high use areas for Mid-Size, with very little relative presence in the CP (Figure 4.27). In the spring and summer, the ENP had higher use of Mid-Size while the CCE had higher use in fall and winter. For Adult Males, the high use areas were the ENP and CCE, with lower use in the winter in the GOA and in the fall in the CCE (Figure 4.28).

Habitat associations were identified for all classes within all regions, except for Mid-Size in the CCE (Table 4.2). For the Social Groups in the ENP, sea surface height (SSH), ocean mixed layer thickness (MLT), salinity (SAL), and Chlorophyll-a (CHL) means were higher than the random mean while sea surface temperature (SST) was lower (Table 4.2, Figure 4.29). For Mid-Size in the ENP and SST were higher than the random mean while SSH, MLT, and SAL

were lower (Table 4.2, Figure 4.29). For Adult Males in the ENP, SSH, SST, and CHL means were higher than the random mean while SAL and EKE were lower (Table 4.2, Figure 4.29). For Social Groups in the CCE, SSH, MLT, and SAL were lower than the random mean (Table 4.2, Figure 4.30). For Mid-Size in the CCE, there were no significant habitat associations. For Adult Males in the CCE, MLT, SAL, and EKE were lower than the random mean (Table 4.2, Figure 4.30). For Social Groups and Mid-Size in the CP, SAL was higher than the random mean while SSH and CHL were lower (Table 4.2, Figure 4.31). For Adult Males in the CP, MLT, SAL, EKE, and CHL were higher than the random mean while SSH and SST were lower (Table 4.2, Figure 4.31).

Correlations among all variables within a region were tested and were considered too correlated to include in future habitat modeling if the correlation value was less than or greater than -0.5 and 0.5. In the ENP, MLT, SAL, SSH, and SST were all correlated (Figure 4.32). In the CCE, MLT was correlated with SAL, SST, and EKE (Figure 4.33). SAL was also correlated with EKE and SSH was correlated with SST. In the CP, SST was correlated with MLT, SAL, and CHL (Figure 4.34).

Three site pairs were identified as being close in proximity but with different demographic compositions. The two Point Sur sites (PS1 and PS2) were only 12 km apart (Figure 4.35). PS1 had an average depth of 1390 m between deployments and was located west of a ridge, facing the open ocean. PS2 had an average depth of 840 m between deployments and was located between the same ridge (east and downslope) and the coast of California. The daily proportion of Social Groups vs. Adult Males at PS1 was 30% to 27% while at PS2 the proportion was 40% to 17%. The Kauai and Kona sites are both located within the Main Hawaiian Islands region and were 500 km apart (Figure 4.36). Kauai had an average depth of 715 m between

deployments and faced the open ocean. Kona had an average depth of 660 m between deployments and had a cluster of seamounts directly west of the recording site. The daily proportion of Social Groups vs. Adult Males at Kauai was 20 to 56% while at Kona the proportion was 76% to 5%. The Tinian and Saipan sites were only 44 km apart and both located within the Northern Mariana Islands Region (Figure 4.37). Saipan had an average depth of 720 m between deployments and was located west of the Mariana active arc, facing the Mariana Trough. Tinian had an average depth of 1000 m between deployments and was located east of the Mariana active arc, facing the Mariana trench. The daily proportion of Social Groups vs. Adult Males at Saipan was 81% to 4% while at Tinian the proportion was 32% to 41%.

4.5 Discussion

Sperm whales are found throughout the North Pacific and appear to be nomadic, with widespread movements between areas of concentration where their preferred prey can be found (Mizroch & Rice 2012). Whaling data provides a historical picture of distribution in the region, including seasonal high-use areas, referred to as 'grounds' by whalers, and concentrations of demographic groups (Mizroch & Rice 2012). It is important to note that although whaling data is a crucial part of creating a baseline understanding of sperm whale distribution, it is biased to seasons that are conducive to whaling. Contemporary studies using visual observations, satellite tags, genetics, and acoustic data, like from this study, often corroborate historic distributions or provide insight into how distributions might have changed after whaling or as a result of contemporary threats such as climate change.

The ENP was a prominent whaling ground for males and females, with estimates for female sperm whale catches ranging from 6% of total catch above 50N to 80% in the western Aleutians, western Bering Sea, and the USSR defined Gulf of Alaska (Berzin & Rovnin 1966;

Nishiwaki 1966; Tomlin 1967; Berzin 1971, 1972; Mizroch & Rice 2013; Fearnbach *et al.* 2014; Ivashchenko *et al.* 2014). Contemporary presence of Social Groups in the GOA and BSAI in acoustic data from this study reveals a potential return to pre-whaling distributions of sperm whales (Chapter 2). In the CCE, modern whaling data highlights pelagic concentrations of sperm whales near the United States and Canadian west coasts between 40ºN and 55ºN and between 150W and 122W (Mizroch & Rice 2012). In the N.CCE from the coast of Washington down to Monterey Bay, sperm whales were historically caught in the summer (Maury 1851) which matches the pattern seen by Adult Males in this study within this region. Gilmore (1959) world map of the distribution of sperm whales also reveals a concentration of males near Baja California in the summer (Smith *et al.* 2012), which aligns with this study's findings from the GI site in the same region. Sperm whales were also reported in this region in the fall and winter months according to a whaling map by Maury (1851) which aligns with the peak in presence seen by Social Groups and Mid-Size at the GI recording site.

In the CP, Yankee whaling data (1761-1920) revealed that the equatorial Pacific had high concentrations of sperm whales (Townsend 1935), with a very concentrated band along and slightly south of the equator with very little seasonal shift in latitude (Smith *et al.* 2012). However, our study found an almost negligible presence at the Equator recording site during the three-month recording period (03/05/12 - 06/17/12), with no Mid-Size presence. The site is situated directly in the previously described equatorial grounds and the lack of presence could be a result of the short, three-month recording period or the inability of the population to recover following the decline noted in this region after 1850 (Smith *et al.* 2012). Whaling data highlighted pelagic concentrations of sperm whales along the North Pacific Subtropical Frontal Zone (NPSFZ) as well, with peak presence in the summer and fall (Maury 1851; Roden 1991;

Mizroch & Rice 2013). The PHR and LSM recording sites are located in the NPSFZ and both

sites had a high presence of all three classes, aligning with historical distributions, however those

two sites were most used in the spring months by Social Groups. The MHI region containing the

Kona and Kauai recording sites were also part of historical whaling grounds where sperm whales

were reported year-round but did appear to prefer one side of the islands over the other

depending on the season (Maury 1851). According to whaling data, the NMI region containing

the Saipan and Tinian recording sites also had high concentrations of sperm whales,

corroborating our study's findings, with a peak in the summer and fall months that was not

noticeable in our data (Maury 1851).

Historically, both whaling records and contemporary research have often depicted the

distribution of female and male sperm whales in a binary manner, with females confined to lower

latitudes and males venturing to higher latitudes. While this narrative holds true for most

recording sites in this study, an important revelation arises from data collected in the ENP and

select site pairs within the CCE and CP. In the ENP, Chapter 2 of this dissertation has already

shown how we may be overlooking important habitats for Social Groups by assuming animals in

this region are strictly males. There are also instances of discord between geographic proximity

and demographic composition which underscore the nuanced nature of sperm whale

distributions. This study identified three site pairs, one in the CCE and two in the CP, that are

very near to one another in proximity yet have very different demographic composition. These

site pairs ranged in proximity to one another from 12 km to 500 km and ranged in difference of

depth from 55 m to 550 m. The site pairs with a larger Social Group composition (PS2, Kona,

Saipan) were always shallower and protected by bathymetric features such as ridges, seamounts,

or a trough. The site pairs with larger Adult Male composition (PS1, Kauai, Tinian) were always

deeper and faced the open ocean with no protection of bathymetric features, or in the case of

Tinian faced the Mariana Trench. The comparison of demographic compositions between site

pairs in close proximity highlights the remarkable variability that can exist within a relatively

small spatial area. These findings underscore the complex social dynamics and habitat

preferences of sperm whales, which can be influenced by subtle differences in environmental

conditions. While passive acoustic monitoring proves invaluable in deciphering such variations,

it is important to recognize that relying solely on stationary recording sites might provide an

incomplete perspective. Sperm whale movement may be influenced by factors not captured at a

single site, such as local prey distribution or underwater topography. Furthermore, the

consideration of depth and bathymetry is pivotal when selecting recording sites for acoustic

studies. The interaction between sperm whales and their environment is intricately linked to

water depth and seafloor topography, which can impact prey availability, diving behavior, and

vocalization patterns. Neglecting these factors in site selection might lead to biased or

incomplete insights into the species' habitat associations and distribution. Such findings suggest

that adhering strictly to the traditional narrative of latitudinal segregation might lead us to

overlook crucial habitats that host diverse demographic groups. Thus, this study underscores the

need to challenge and expand upon established notions of spatial distribution, urging a more

holistic consideration of the multifaceted dynamics that govern sperm whale habitat preferences

and group compositions.

Although there was no difference in demographic composition, the PHR site is another

example where hydrophone placement can make a big impact on animal detections. Over the

recording period (2009-2019), PHR was moved primarily to combat-low frequency hydrophone

cable strumming from strong currents at depth (Ziegenhorn *et al.* 2023). The first recording

location (~ 750 m) was on average 200 m shallower than the second recording location (~ 950m). Sperm whale detections significantly dropped beginning in 2014 coinciding with the site relocation, likely a result of the animals preferring the shallower recording site that was also more protected by the reef. Although the amount of sperm whale presence dropped, demographic composition did not change.

It has been hypothesized that sperm whales do not conduct timed or seasonal movements throughout their home ranges, but rather as nomads, move between concentrations of their prey. However, this study identified clear seasonal high-use areas for the three classes. For Social Groups, while CP was a year-round high-use area, the ENP and CCE showed seasonal use, in the spring/winter and fall respectively. Social Group use of the high-latitudes and the CCE is not well described, but it is possible they could be traveling to these areas to increase their chances for breeding (Gregr & Trites 2001). The ENP and CCE were high-use areas for Mid-Size, which is defined as either large females or juvenile males. There is evidence that small-group abundance, likely representing adult males traveling alone or in pairs has increased in the CCE based on visual surveys from 1991 to 2008 (Moore & Barlow 2014), which would support our study's findings. However, there was very little Mid-Size presence in the CP. This provides some evidence that the Mid-Size group might consist of juvenile males who are not sexually mature enough for breeding and decide to stay in their foraging grounds year-round. If this is the case, it is possible that Mid-Size detections at the CP sites are in fact large females that were detected at the same time as Social Groups but still stood out with a longer interclick interval, leading to a different classification. Bachelor schools of juvenile males have been most often described in higher latitude or temperate regions like the waters of New Zealand, Japan, and in the Mediterranean (Gaskin 1970; Drouot *et al.* 2004; Kobayashi *et al.* 2020), supporting the

findings of this study. For Social Groups and Mid-Size, it is possible that the sperm whales are not moving between these regions seasonally, but rather moving within a region as they follow their prey as hypothesized by Merkens *et al.* (2019). Especially Social Groups who do not appear to range over great distances like Adult Males (Mizroch & Rice 2013; Moore & Barlow 2014). However, Adult Males show a very clear increase in the ENP in the summer when productivity is higher and an increase in the CP in the winter where they breed. This pattern provides evidence that movement between breeding and foraging grounds are timed and are not completely sporadic as previously hypothesized.

Habitat association analysis yielded valuable insights into the complex interactions between environmental variables and sperm whale presence across different regions and demographic groups. Significant habitat associations were identified for almost all classes within each of the studied regions, with some variations. Sea surface height (SSH) serves as a dynamic link between atmospheric drivers and their corresponding oceanic responses (Hauri *et al.* 2021)where areas of low and high SSH are characterized by regional upwelling and downwelling, respectively. When SSH was significant, almost all classes within all regions displayed an association with lower SSH, except for Social Groups and Adult Males in the ENP. Lower SSH is often associated with a shallower thermocline that increases the availability of nutrients to the euphotic zone for biological uptake and increases chlorophyll production (Wilson & Adamec 2001). For the Social Groups and Adult Males in the ENP, the association with higher SSH could be a result of the relationship between SSH and the Pacific Decadal Oscillation (PDO). Sperm whales were negatively correlated with the PDO in the ENP (Chapter 2), meaning they were present in higher numbers during a negative PDO. Higher SSH with a warmer, fresher surface layer is associated with negative phases of the PDO in the North Pacific

(Gordon & Giulivi 2004), possibly explaining the association of Social Groups and Adult Males in the ENP with higher SSH. When ocean mixed layer thickness (MLT) was significant, almost all classes within all regions displayed an association with thinner MLT, except for Social Groups at ENP and Adult Males at CP. In the northern hemisphere, MLT becomes thinner in the summer and fall, causing the energy flux to inertial motions to increase which can amplify certain ocean currents and shift water masses (Watanabe & Hibiya 2002). The relationship between MLT and higher trophic level predators is not well understood, however in the equatorial Pacific, heat accumulation due to higher abundance of chlorophyll leads to a thinning of the mixed layer (Nakamoto *et al.* 2001) potentially explaining the association with thinner MLT for most regions and classes. Associations with thicker MLT for Social Groups in the ENP and Adult Males in the CP could be indicative of an external variable beyond environment and prey availability, such as breeding, in the case of the males, and site fidelity. There is evidence from females in the Eastern Caribbean (Gero *et al.* 2007; Vachon *et al.* 2022), North Atlantic (Engelhaupt *et al.* 2009), western Mediterranean (Carpinelli *et al.* 2014), and males in the GOA (Straley *et al.* 2014) that site fidelity is a factor in their habitat choice. In the ENP and CCE, all classes except Social Groups in the ENP, were associated with lower salinity (SAL). Lower SAL is often associated with cooler temperatures, particularly at high latitudes (Olson *et al.* 2022), however the connection between SAL and higher trophic level predators in pelagic waters is not well understood. In the CP, all classes were associated with higher SAL, this is likely a result of averaging SAL over the entire region which is characterized as the salinity maximum in the Pacific (Reid 1973), masking potentially lower salinity areas with cooler waters. In the ENP, Mid-Size and Adult Males, were associated with higher sea surface temperatures (SST) while in the CP, Social Groups and Mid-Size were not associated at all with SST and Adult Males were

197

associated with lower SST. In the ENP, SST had low evidence of significance in explaining sperm whale presence, however, their presence was highly explained by increased ocean heating (Diogou *et al.* 2019b). Overall, increase in SST or ocean heating could reflect periods in the summer when increased solar radiation at higher latitudes could result in increased biological productivity (Diogou *et al.* 2019b). This also supports the association with higher chlorophyll-a concentrations (CHL) of Social Groups and Adult Males in the ENP and Adult Males in the CP. In lower latitudes and in the Mediterranean Sea, sperm whale presence was associated with lower SST (Jaquet 1996; Rendell *et al.* 2004; Praca *et al.* 2009; Pirotta *et al.* 2011) since cooler waters in these regions likely indicate stronger mixing and upwelling that increases primary productivity by injecting the upper layer with nutrients (Diogou *et al.* 2019b). Eddy Kinetic Energy (EKE) was only associated with Adult Males (in all regions); however, the relationship was not consistent. Eddies are prominent oceanographic features in the North Pacific and have been associated with marine apex predators (Palacios *et al.* 2006) including a positive association with sperm whales in the North Atlantic (Wong & Whitehead 2014) and North Pacific (Diogou *et al.* 2019b). However, in this study, Adult Males in the ENP were associated with lower EKE but in the CCE and CP they were associated with higher EKE. Association with lower EKE in could be a result of a previously described phenomenon in the GOA where as eddies decay, nutrients get injected up towards the surface layer enhancing marine productivity in an otherwise iron-poor basin (Crawford *et al.* 2007).

The inclusive pattern, including all sperm whales, usually mirrored the habitat associations of the dominant class. This reveals how considering the classes separately in habitat models could result in different relationships between environmental variables and presence. Grouping all the animals together convolutes the variable relationship each class has with its

environment potentially because of their different prey preferences, as well as other behavioral states beyond feeding. Potential temperature (PT) was initially also included in the analysis, however since it is extremely correlated with SST, it was ultimately left out of final analysis. However, it is important to note that the patterns were the same for PT and SST, highlighting that PT could be used instead of SST if that data was not available due to cloud cover.

While these findings provide valuable insights, it is important to acknowledge the limitations of the approach and the potential for more intricate relationships beyond the scope of this study. By averaging environmental variables across entire regions, the analysis might mask more localized relationships between variables and sperm whale presence. This coarse approach might lead to overlooking finer-scale preferences and potentially important habitats within the regions. Considering potential time lags in surface variables and those that describe primary productivity could be crucial, as the influence of environmental conditions on prey availability and sperm whale distribution might not be immediate. Further refinement of the analysis by considering subregions or individual sites could reveal more nuanced patterns of habitat associations. Additionally, future studies should strive to integrate a broader array of environmental variables, particularly those that characterize the environment at depth, where sperm whales spend a significant portion of their time foraging. Furthermore, incorporating in-situ variables could improve the accuracy of habitat associations by capturing the intricate ecological interactions that influence sperm whale distribution as seen in Diogou *et al.* (2019b), although it is important to acknowledge the challenges associated with acquiring in-situ data.

4.6 Conclusion

In conclusion, this study sheds light on the complex habitat associations and distribution patterns of sperm whales in the North Pacific, offering insights that have implications for their

conservation and management. By integrating historical whaling data with contemporary research methodologies, we have gained a deeper understanding of sperm whale movements, demographic compositions, and their relationships with environmental variables. Visual observations, satellite tagging, genetic analyses, and acoustic data, such as the data collected in this study, provide essential context to understand how distributions have changed over time due to factors like whaling and contemporary threats, including climate change.

This research reveals the dynamic nature of sperm whale distribution across various regions in the North Pacific. In the Eastern North Pacific, we observe potential returns to pre-whaling distribution patterns, suggesting a degree of recovery in some demographic groups. In the California Current Ecosystem and Central Pacific, the alignment of our findings with historical whaling data and other studies showcases the value of multiple data sources in capturing accurate distribution trends. However, the study also uncovers nuances that challenge the traditional narrative of latitudinal segregation between male and female sperm whales. The presence of Social Groups in the Gulf of Alaska and Bering Sea highlights the importance of considering female distributions in regions previously assumed to be predominantly male. And contrasting the demographic compositions among site pairs situated in close proximity underscores the striking variability that can prevail within a compact spatial region.

Furthermore, our analysis of habitat associations provides valuable insights into the interplay between environmental variables and sperm whale presence. While certain trends emerge across regions, demographic groups, and variables, the complexity of these relationships brings awareness to the limitations of averaging environmental conditions over broad areas. Localized relationships between variables and sperm whale presence might be obscured, emphasizing the need for more refined analyses that consider subregions and individual sites.

In summary, this study illuminates the diverse habitat associations and demographic dynamics of sperm whales in the North Pacific, emphasizing the need for a holistic approach to their conservation and management. By considering historical context, modern research techniques, and the intricate interplay between environmental variables, we lay the groundwork for targeted conservation efforts that account for the unique requirements of different demographic groups and contribute to the preservation of this iconic species.

4.7 Acknowledgements

Chapter 4, in full, is currently being prepared for submission for publication of the material. Posdaljian, N., Solsona-Berga, A., Oleson, E.M., Hildebrand, J. A., & Baumann-Pickering, S. "Demographic Dependent Habitat Associations and High Use Areas of Sperm Whales in the North Pacific". The dissertation author was the primary researcher and author of this material.

4.8 Figures and Tables
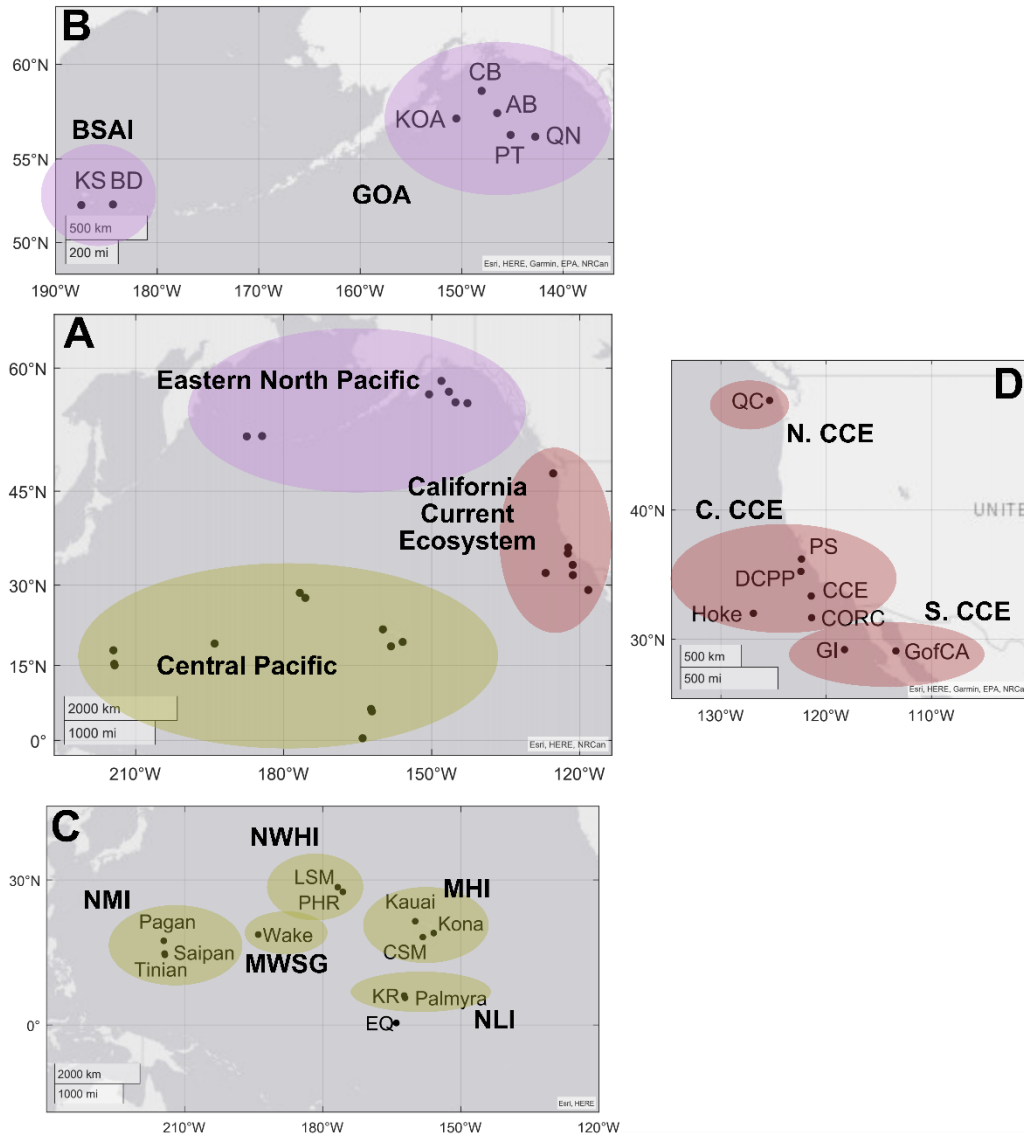
Figure 4.1. Site map showing (A) all 27 recording sites in the Pacific Ocean with colors representing the three regions: Eastern North Pacific (purple), California Current Ecosystem (red), and the Central Pacific (yellow). Site map showing (B) the seven recording sites in the Eastern North Pacific, five in the Gulf of Alaska (GOA) and two in the Bering Sea/Aleutian Islands (BSA). Site map showing (C) all nine recording sites in the California Current Ecosystem (CCE), one in the north (N.CCE), six in the central region (C.CCE), and two in the south (S. CCE). Site map showing (D) all 11 sites in the Central Pacific, two in the Northern Mariana Islands, two in the Northwestern Hawaiian Islands, three in the Main Hawaiian Islands, one in the Marcus-Wake Seamount Group, two in the Northern Line Islands, and one that was not part of a subregion (EQ).
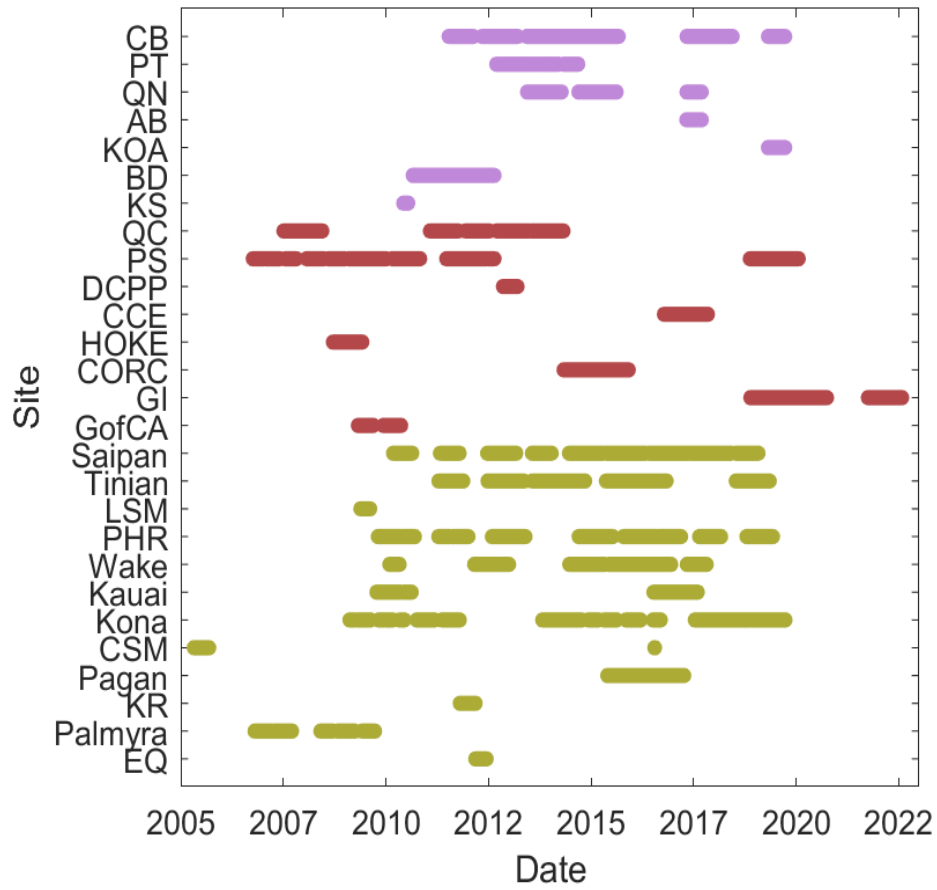
Figure 4.2. Recording effort for each site (row) within each region (color) from 2005 to 2022.

Table 4.1. Recording effort for each site within each subregion displaying the latitude (N), longitude (W; unless specified as E), depth (m), recording dates (mm/dd/YYYY), duty cycle if applicable (recording duration/recording interval) and total duration (days). Dark line between deployments of PHR and Palmyra represents when instrument location changed.

Subregion	Site	Latitude (N)	Longitude (W*)	Depth (m)	Recording Dates	Duty Cycle (Duration/ Interval)	Duration (days)
Gulf of Alaska (GOA)	Continental Slope (CB)	58° 38.74'	148° 04.13'	1000	07/13/11 – 02/19/12	--	221
		58° 40.28'	148° 01.25'	900	05/03/12 – 02/21/13	10/12	294
		58° 40.41'	148° 00.55'	877	06/06/13 – 09/05/13	--	91
		58° 40.31'	148° 01.31'	858	09/05/13 – 04/28/14	--	235
		58° 40.26'	148° 01.46'	914	04/29/14 – 09/09/14	--	133
		58° 40.25'	148° 01.46'	900	09/09/14 – 05/02/15	--	235
		58° 39.32'	148° 05.48'	931	05/01/15 – 09/06/15	--	128
		58° 40.26'	148° 01.45'	874	04/30/17 – 09/12/17	--	135
		58° 40.22'	148° 01.62'	900	09/14/17 – 06/16/18	--	275
		58° 40.18'	148° 01.57'	972	04/25/19 – 09/27/19	--	155
	Pratt Seamount (PT)	56° 14.61'	142° 45.44'	989	09/09/12 - 06/10/13	--	275
		56° 14.64'	142° 45.43'	987	06/11/13 - 08/20/13	--	70
		56° 14.58'	142° 45.41'	988	09/03/13 - 03/21/14	--	199
		56° 14.60'	142° 45.46'	998	04/30/14 - 09/10/14	--	134
	Quinn Seamount (QN)	56° 20.36'	145° 11.24'	930	09/11/13 - 04/16/14	--	217
		56° 20.48'	145° 10.99'	900	09/10/14 - 05/2/15	--	234
		56° 20.44'	145° 11.11'	945	05/02/15 - 08/18/15	--	109
		56° 20.48'	145° 10.99'	964	04/30/17 - 09/14/17	--	138

Table 4.1. Recording effort for each site within each subregion displaying the latitude (N), longitude (W; unless specified as E), depth (m), recording dates (mm/dd/YYYY), duty cycle if applicable (recording duration/recording interval) and total duration (days). Dark line between deployments of PHR and Palmyra represents when instrument location changed.

	Abyssal Deep (AB)	57° 30.82'	146° 30.05'	1200	04/28/17 - 09/14/17	--	139
	Kodiak Shelf (KOA)	57° 13.44'	150° 31.70'	1000	04/24/19 - 09/27/19	--	157
Bering Sea Aleutian Islands (BSAI)	Buldir Island (BD)	52° 38.00'	175° 37.99'	783	08/27/10 - 05/26/11	--	272
		52° 04.56'	175° 38.39'	777	05/31/11 - 08/26/12	5/10	438
	Kiska Island (KS)	52° 19.01'	178° 31.24'	1092	06/3/10 - 07/20/10	--	84
North - California Current Ecosystem (N. CCE)	Quinault Canyon (QC)	47° 27.96'	125° 09.20'	653	07/05/07- 06/15/08	5/35	346
		47° 30.00'	125° 21.20'	650	01/27/11 - 10/07/11	--	253
		47° 30.03'	125° 21.21'	1394	12/07/11 - 07/11/12	--	217
		47° 30.03'	125° 21.22'	1394	09/14/12 - 06/30/12	--	289
		47° 30.02'	125° 39.00'	1384	07/17/13 - 05/02/14	--	289
Central – California Current Ecosystem (C. CCE)	Point Sur 1 (PS1)	36° 17.95'	122° 23.63	1392	10/03/06 – 01/16/07	5/15	105
		36° 17.92'	122° 23.58	1390	07/01/25 – 07/06/04	5/15	130
		36° 17.92'	122° 23.60	1386	07/19/07 – 10/29/07	5/20	102
		36° 18.88'	122° 23.47	1386	01/25/08 – 07/08/08	5/20	165
		36° 17.94'	122° 23.63	1412	11/30/11 – 05/24/12	--	207
		36° 17.94'	122° 23.63	1370	07/03/12 – 08/26/12	--	54
	Point Sur 2 (PS2)	36° 23.42'	122° 18.35	833	08/04/08 – 01/06/09	5/15	155
		36° 23.33'	122° 18.40	835	02/01/09 – 05/07/09	5/10	95
		36° 23.33'	122° 18.41	847	05/01/09 – 09/22/09	5/15	144
		36° 23.37'	122° 18.46	843	09/23/09 – 01/06/10	5/10	105
		36° 23.48'	122° 18.45	837	02/26/10 – 11/03/10	5/25	250

Table 4.1. Recording effort for each site within each subregion displaying the latitude (N), longitude (W; unless specified as E), depth (m), recording dates (mm/dd/YYYY), duty cycle if applicable (recording duration/recording interval) and total duration (days). Dark line between deployments of PHR and Palmyra represents when instrument location changed.

Subregion	Site	Latitude	Longitude	Depth	Recording dates	Duty cycle	Duration
		36° 23.47'	122° 18.42	850	06/21/11 – 04/07/12	5/10	291
		36° 22.22'	122° 18.89'	845	11/14/18 – 06/10/19	--	208
		36° 22.21'	122° 18.86	858	06/11/19 – 01/25/20	5/10	228
	Diablo Canyon Power Plant (DCPP)	35° 23.60'	121° 33.75'	1000	11/07/12 – 03/19/13	--	133
	California Current Ecosystem (CCE)	33° 28.97'	122° 34.56'	812	10/10/16 – 11/08/17	--	395
	Hoke Seamount (Hoke)	32° 6.37'	126° 54.58'	770	09/15/08 – 06/06/09	5/25	265
	Offshore Mooring (CORC)	31° 44.49'	121°22.68'	948	04/30/14 – 12/04/15	15/30	583
South – California Current Ecosystem (S. CCE)	Guadalupe Island (GI)	29° 8.46'	118° 15.66'	1113	11/19/18 – 10/22/19	--	338
		29° 8.55'	118° 15.50'	1187	10/23/19 – 10/03/20	--	345
		29° 8.55'	118° 15.66'	1074	09/30/21 – 08/03/22	--	307
	Gulf of California (GofCA)	29° 1.64'	113° 22.54'	694	04/26/09 – 09/12/09 ~	5/15	139
		29° 1.65'	113° 22.53'	600	12/07/09 – 05/18/10 ~	5/15	163
Northern Mariana Islands (NMI)	Saipan	15° 19.00'	145° 27.54' E	689	03/10/10 - 04/02/11	5/40	174
		15° 19.03'	145° 27.46' E	696	04/30/11 - 06/18/12	5/20	176
		15° 19.07'	145° 27.42' E	700	08/19/12 - 07/14/13	5/6	262
		15° 19.28'	145° 27.26' E	600	07/13/13 - 06/14/14	5/7	179
		15° 19.28'	145° 27.26' E	786	06/18/14 - 04/17/15	5/7	304
		15° 19.05'	145° 27.43' E	786	05/11/15 - 05/18/16	5/7	356
		15° 19.00'	145° 27.26' E	786	05/30/16 – 05/17/17	5/7	353

Table 4.1. Recording effort for each site within each subregion displaying the latitude (N), longitude (W; unless specified as E), depth (m), recording dates (mm/dd/YYYY), duty cycle if applicable (recording duration/recording interval) and total duration (days). Dark line between deployments of PHR and Palmyra represents when instrument location changed.

Subregion	Site	Latitude (N)	Longitude (W)	Depth	Recording dates	Duty cycle	Total duration
		15° 19.02'	145° 27.44' E	725	05/28/17 – 06/02/18	5/7	369
		15° 18.97'	145° 27.40' E	678	07/12/18 – 02/01/19	5/7	205
	Tinian	15° 2.34'	145° 45.13' E	995	04/12/11 - 06/22/12	5/20	224
		15° 2.39'	145° 45.32' E	998	06/23/12 - 07/14/13	5/6	326
		15° 2.40'	145° 45.38' E	1000	07/21/13 - 06/14/14	5/7	327
		15° 2.40'	145° 45.38' E	1000	06/16/14 - 11/11/14	5/7	137
		15° 0.04'	145° 45.38' E	1000	05/11/15 - 05/26/16	5/7	376
		15° 2.40'	145° 45.38' E	1000	05/27/16 - 05/23/17	5/7	160
		15° 2.40'	145° 45.46' E	1020	07/12/18 – 05/12/19	5/7	304
	Pagan	17° 57.79'	145° 28.87'	830	05/25/15 – 04/11/17	5/15	587
Northwestern Hawaiian Islands (NWHI)	Ladd Seamount (LSM)	28° 37.65'	176° 43.68'	1092	05/18/09 - 08/15/09	5/10	89
	Pearl and Hermes Reef (PHR)	27° 43.52'	175° 38.29'	753	10/20/09 – 05/24/10	5/20	216
		27° 43.62'	175° 37.95'	752	06/01/10 – 09/17/10	--	109
		27° 43.52'	175° 38.26'	550	04/12/11 – 07/29/11	--	108
		27° 43.52'	175° 38.25'	806	08/15/11 – 01/07/12	5/8	145
		27° 44.55'	175° 33.55'	945	09/12/14 – 07/16/15	5/20	308
		27° 44.51'	175° 33.59'	945	10/15/15 – 08/14/16	5/30	304
		27° 44.46'	175° 33.63'	915	08/20/16 – 03/04/17	5/30	207
		27° 43.77'	175° 33.22'	1100	08/20/17 – 03/05/18	5/30	198
		27° 43.05'	175° 33.28'	1100	10/15/18 – 06/10/19	5/30	238
Marshall Islands (MI)	Wake Seamount	19° 13.20'	166° 41.01' E	800	01/31/10 – 05/04/10	5/10	94
		19° 13.25'	166° 41.56' E	886	03/25/11 – 05/27/11	5/6	63

Table 4.1. Recording effort for each site within each subregion displaying the latitude (N), longitude (W; unless specified as E), depth (m), recording dates (mm/dd/YYYY), duty cycle if applicable (recording duration/recording interval) and total duration (days). Dark line between deployments of PHR and Palmyra represents when instrument location changed.

		19º 13.29'	166º 41.56' E	935	02/25/12 – 01/03/13	5/30	314
		19º 13.33'	166º 41.67' E	849	06/20/14 – 05/08/15	5/30	323
		19º 13.41'	166º 41.67' E	620	05/05/15 – 05/24/16	5/30	385
		19º 22.32'	166º 41.67' E	620	05/02/17 – 10/28/17	5/30	248
	Kauai	21º 57.16'	159º 53.24'	706	10/07/09 - 06/03/10	5/20	217
		21º 57.22'	159º 53.38'	720	06/03/10 - 08/20/10	--	77
		21º 56.95'	159º 53.27'	717	07/07/16 - 09/12/17	5/7	396
Main Hawaiian Islands (MHI)	Kona	19º 34.66'	156º 0.83'	460	02/10/09 – 04/01/09	--	51
		19º 34.96'	156º 0.95'	620	04/23/09 – 08/18/09	5/15	117
		19º 34.92'	156º 0.91'	620	10/25/09 – 12/15/09	--	52
		19º 34.89'	156º 0.93'	620	12/20/09 – 03/05/10	5/12	76
		19º 34.89'	156º 0.93'	620	05/01/10 – 06/16/10	5/25	47
		19º 34.94'	156º 0.91'	652	09/30/10 – 03/12/11	5/8	163
		19º 34.95'	156º 0.91'	650	05/12/11 – 10/22/11	5/8	163
		19º 34.98'	156º 0.94'	680	10/23/13 – 03/25/14	5/15	153
		19º 34.99'	156º 0.94'	716	03/25/14 – 07/14/14	--	111
		19º 34.98'	156º 0.94'	700	07/28/14 – 10/12/14	--	77
		19º 34.99'	156º 0.98'	648	12/06/14 – 03/06/15	--	91
		19º 34.99'	156º 0.98'	650	04/25/15 – 08/18/15	--	115
		19º34.97'	156º 0.97'	665	11/07/15 – 02/27/16	--	112
		19º 34.98'	156º 0.94'	665	07/04/16 – 09/14/16	--	72
		19º34.98'	156º0.95'	676	07/12/17 – 10/25/17	--	105
		19º 34.98'	156º 0.95'	730	10/26/17 – 04/25/18	--	181

Table 4.1. Recording effort for each site within each subregion displaying the latitude (N), longitude (W; unless specified as E), depth (m), recording dates (mm/dd/YYYY), duty cycle if applicable (recording duration/recording interval) and total duration (days). Dark line between deployments of PHR and Palmyra represents when instrument location changed.

		19° 34.98'	156° 0.95'	730	04/29/18 – 11/19/18	--	204
		19° 34.99	156° 0.95'	710	11/23/18 – 03/31/19	--	128
		19° 34.96	156° 0.91'	730	04/04/19 – 09/29/19	--	178
	Cross Seamount (CSM)	18° 43.33'	158° 15.23'	398	04/26/05 - 11/17/05*	5/25	139
		18° 43.34'	158° 15.22'	396	11/19/05 - 11/27/07	5/25	172
Northern Line Islands (LNI)	Kingman Reef (KR)	6° 21.91'	162° 17.54'	859	11/10/11 – 03/11/12	--	143
	Palmyra	5° 51.85'	162° 9.91'	620	10/19/06 – 03/23/07	5/20	155
		5° 51.88'	162° 9.36'	550	04/09/07 – 09/20/07	5/20	165
		5° 51.93'	162° 9.40'	550	05/27/08 – 09/17/08	5/20	145
		5° 51.91'	162° 9.49'	520	10/22/08 – 04/02/09	5/20	113
		5° 54.25'	162° 2.22'	1085	06/02/09 – 09/27/09	5/20	118
		5° 53.72'	162° 1.23'	718	10/05/09 – 11/12/09	5/20	38
	Equator (EQ)	0° 26.61'	164° 8.08'	1266	03/05/12 - 06/17/12	--	103

* Longitude is W unless specified with an E for Saipan, Tinian, Pagan, and Wake sites.
━ Black line between PHR and Palmyra deployments represents when instrument location changed.
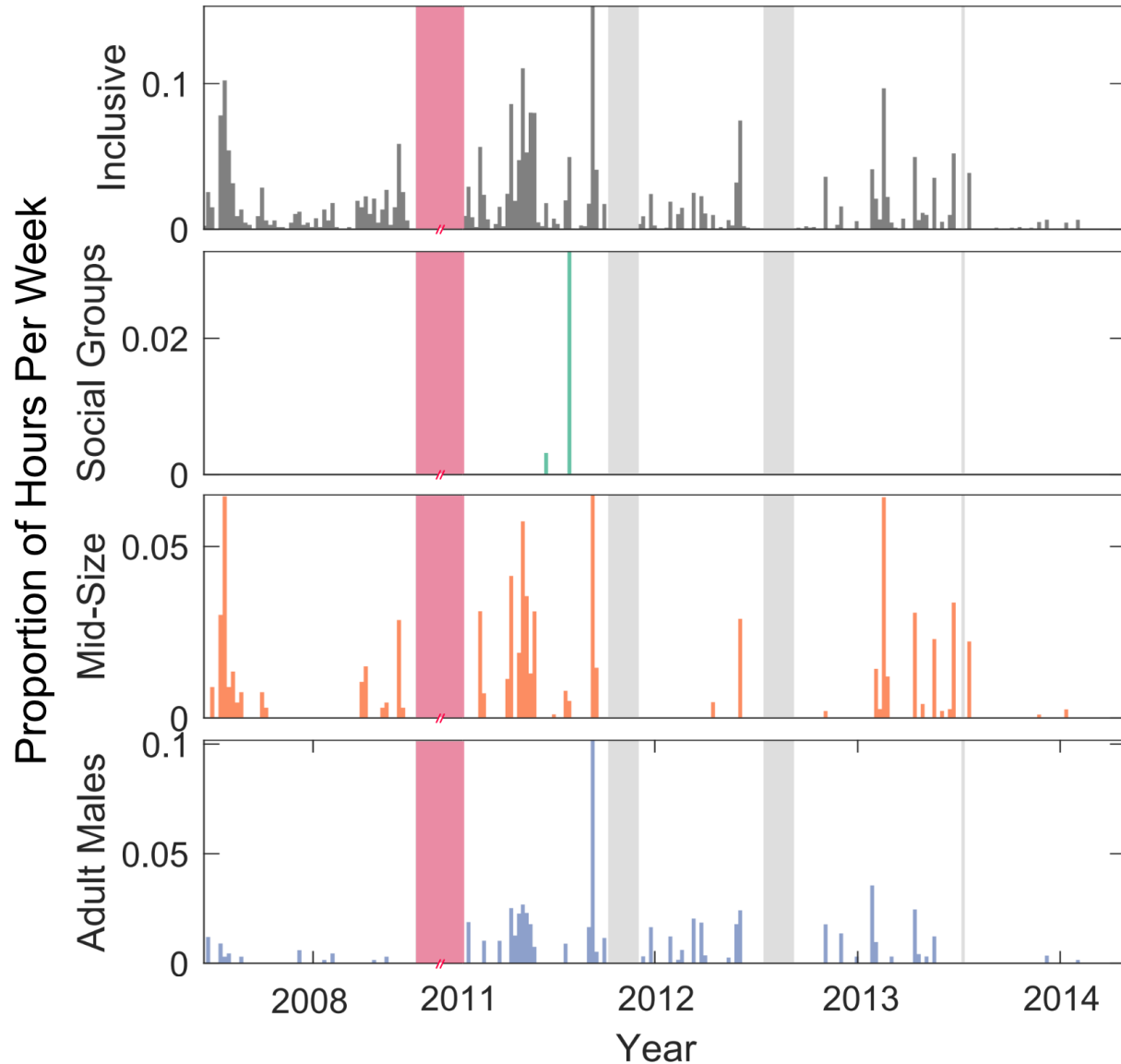
Figure 4.3. Time series of sperm whale presence at the Quinn Seamount (QC) site. The first row (dark gray) represents Inclusive, or all sperm whale, presence, the second row (green) represents Social Group presence, the third row (orange) represents Mid-Size presence, and the fourth row (blue) represents Adult Male presence. Sperm whale presence is represented as the proportion of hours per week with detections. Light gray spaces represent times with no effort. Red spaces represent times with no effort that extend beyond a year (06/16/2008 – 01/26/2011).

Figure 4.4. Time series of sperm whale presence at the Point Sur 1 (PS1) site. The first row (dark gray) represents Inclusive, or all sperm whale, presence, the second row (green) represents Social Group presence, the third row (orange) represents Mid-Size presence, and the fourth row (blue) represents Adult Male presence. Sperm whale presence is represented as the proportion of hours per week with detections. Light gray spaces represent times with no effort. Red spaces represent times with no effort that extend beyond a year (07/9/2008 – 11/19/2011).
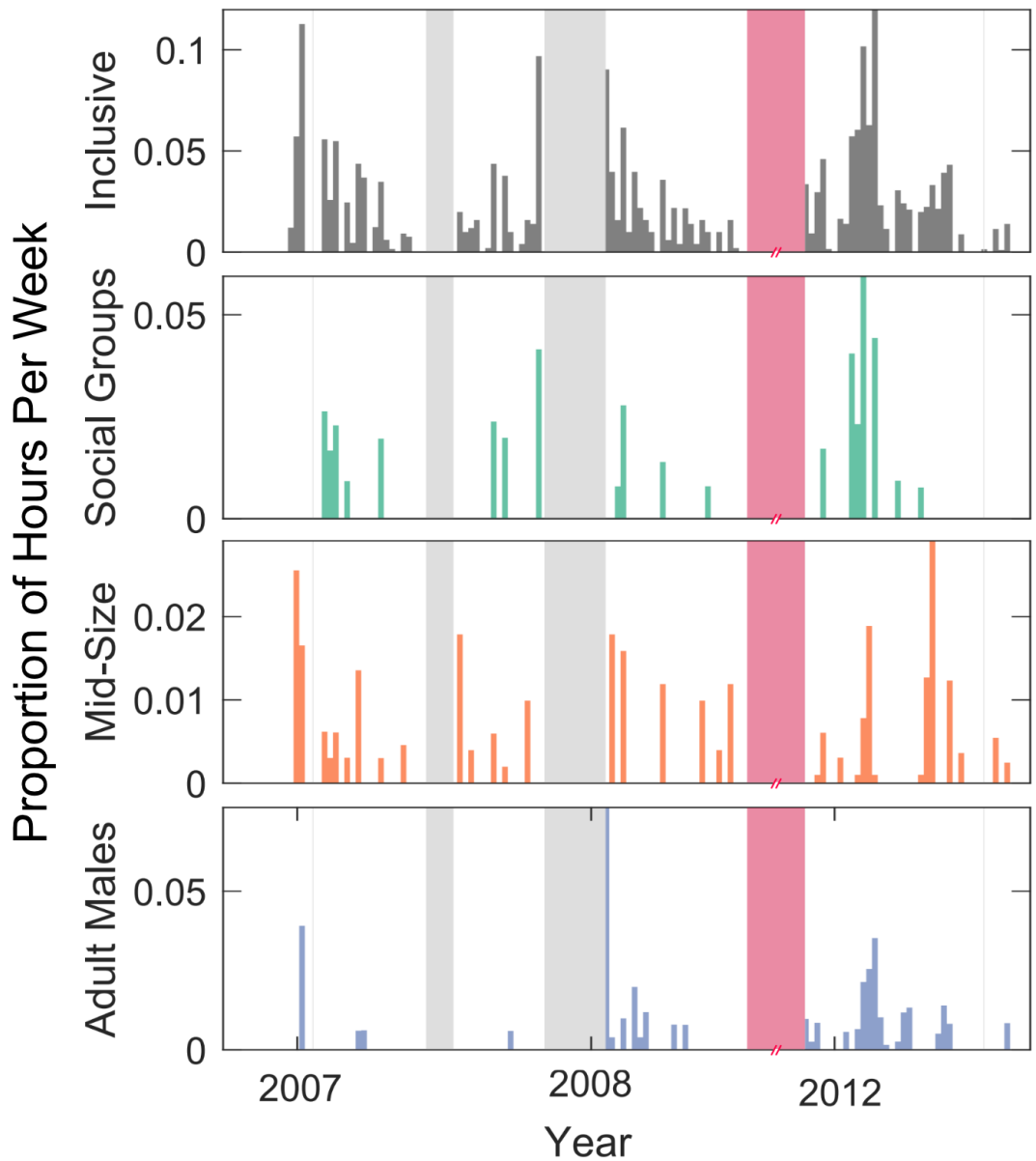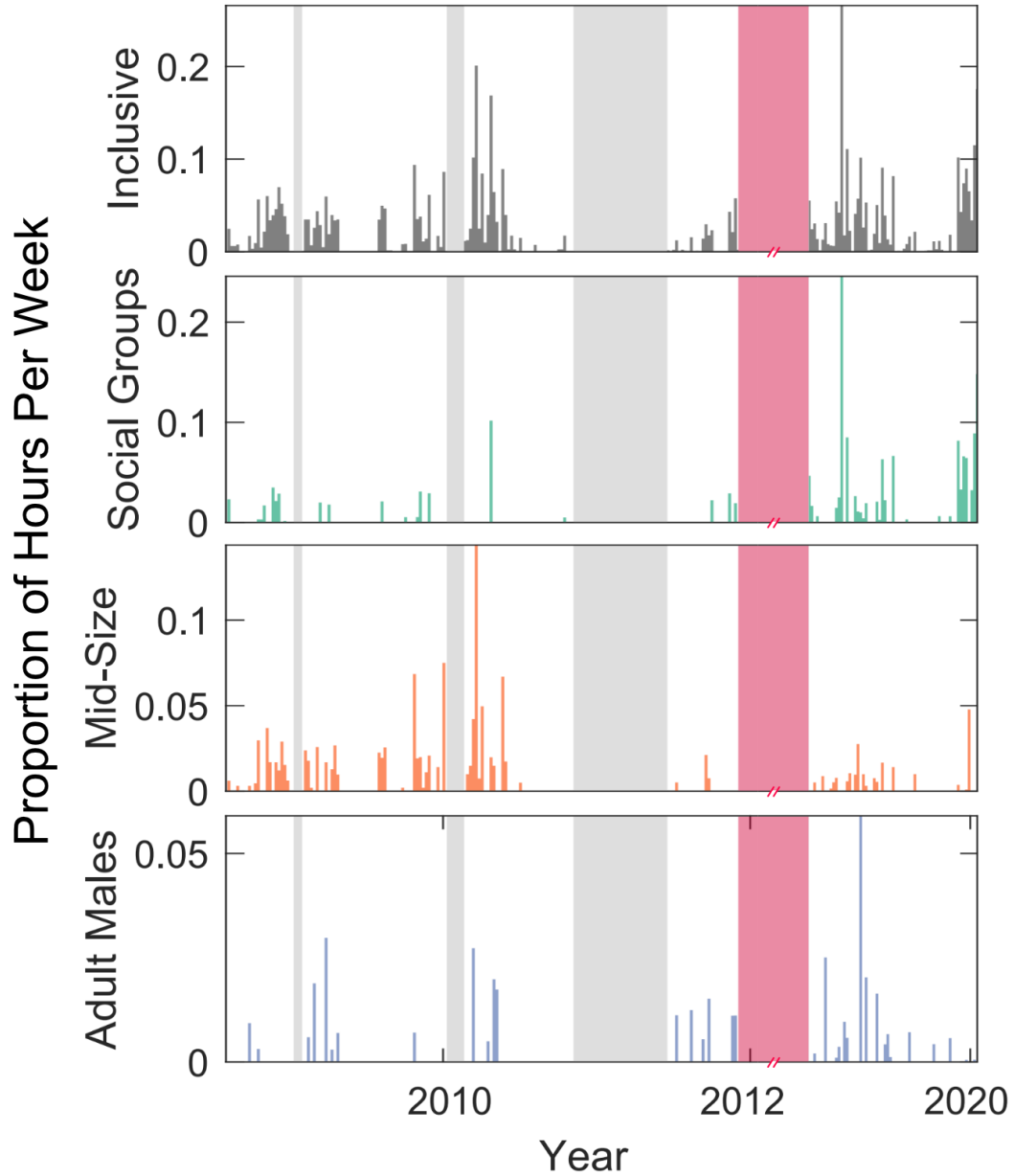
Figure 4.5. Time series of sperm whale presence at the Point Sur 2 (PS2) site. The first row (dark gray) represents Inclusive, or all sperm whale, presence, the second row (green) represents Social Group presence, the third row (orange) represents Mid-Size presence, and the fourth row (blue) represents Adult Male presence. Sperm whale presence is represented as the proportion of hours per week with detections. Light gray spaces represent times with no effort. Red spaces represent times with no effort that extend beyond a year (4/8/2012 – 11/13/2018).

Figure 4.6. Time series of sperm whale presence at the Diablo Canyon Power Plant (DCPP) site. The first row (dark gray) represents Inclusive, or all sperm whale, presence, the second row (green) represents Social Group presence, the third row (orange) represents Mid-Size presence, and the fourth row (blue) represents Adult Male presence. Sperm whale presence is represented as the proportion of hours per week with detections.
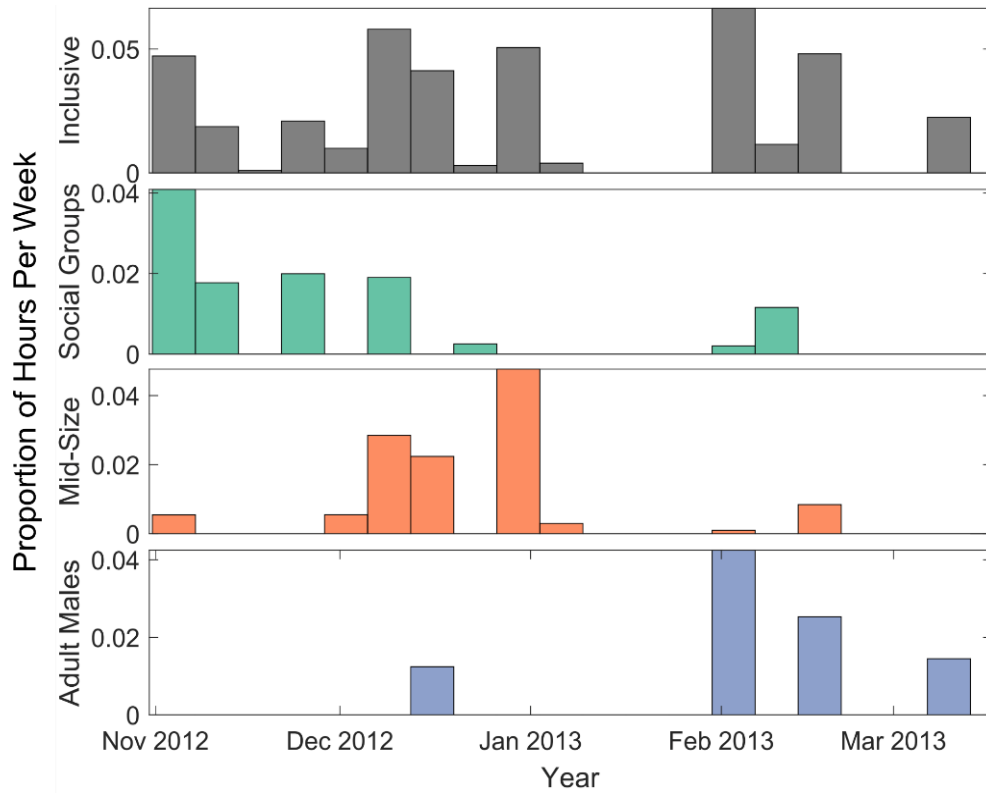
Figure 4.7. Time series of sperm whale presence at the California Current Ecosystem (CCE) site. The first row (dark gray) represents Inclusive, or all sperm whale, presence, the second row (green) represents Social Group presence, the third row (orange) represents Mid-Size presence, and the fourth row (blue) represents Adult Male presence. Sperm whale presence is represented as the proportion of hours per week with detections.
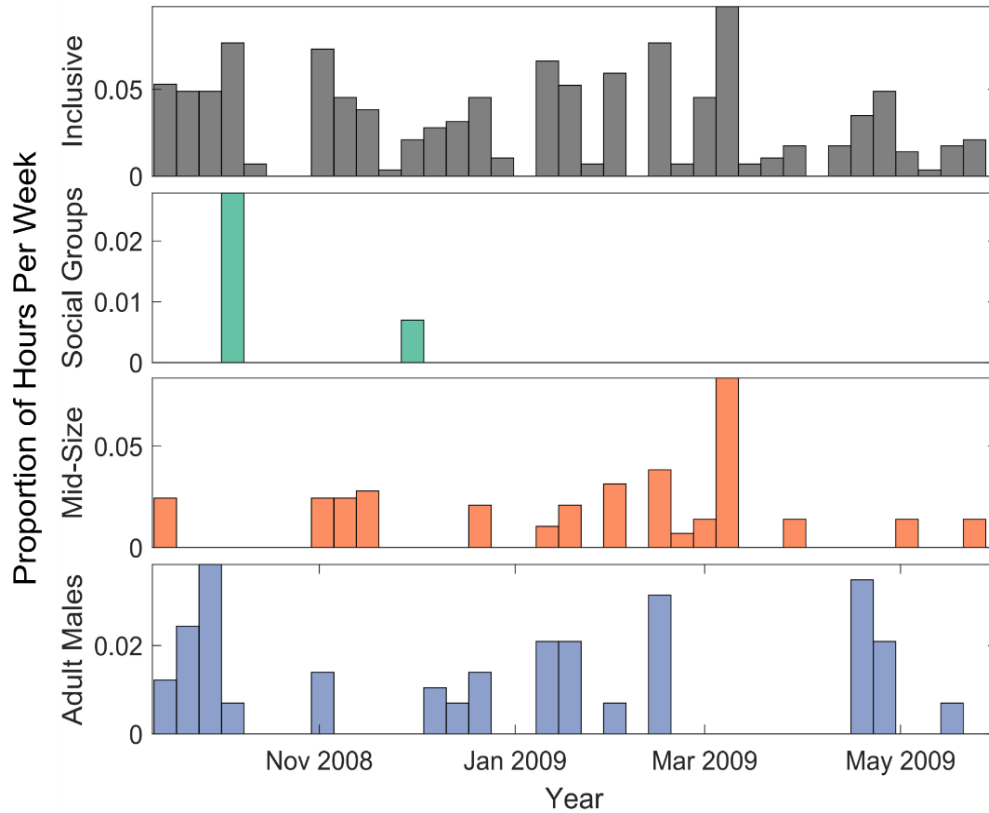
Figure 4.8. Time series of sperm whale presence at the Hoke Seamount (Hoke) site. The first row (dark gray) represents Inclusive, or all sperm whale, presence, the second row (green) represents Social Group presence, the third row (orange) represents Mid-Size presence, and the fourth row (blue) represents Adult Male presence. Sperm whale presence is represented as the proportion of hours per week with detections.
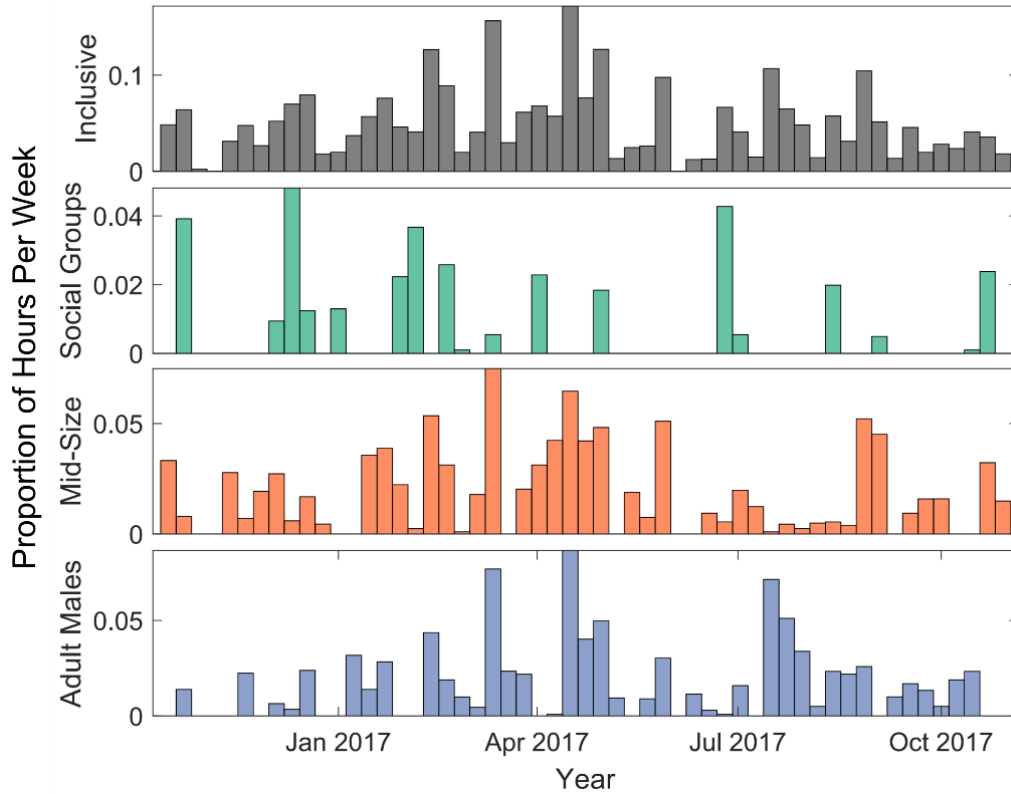
Figure 4.9. Time series of sperm whale presence at an offshore mooring (CORC) site. The first row (dark gray) represents Inclusive, or all sperm whale, presence, the second row (green) represents Social Group presence, the third row (orange) represents Mid-Size presence, and the fourth row (blue) represents Adult Male presence. Sperm whale presence is represented as the proportion of hours per week with detections.

Figure 4.10. Time series of sperm whale presence at the Guadalupe Islands (GI) site. The first row (dark gray) represents Inclusive, or all sperm whale, presence, the second row (green) represents Social Group presence, the third row (orange) represents Mid-Size presence, and the fourth row (blue) represents Adult Male presence. Sperm whale presence is represented as the proportion of hours per week with detections. Light gray spaces represent times with no effort. Red spaces represent times with no effort that extend beyond a year (10/04/2020 – 09/29/2021).

Figure 4.11. Time series of sperm whale presence at the Gulf of California (CA) site. The first row (dark gray) represents Inclusive, or all sperm whale, presence, the second row (green) represents Social Group presence, the third row (orange) represents Mid-Size presence, and the fourth row (blue) represents Adult Male presence. Sperm whale presence is represented as the proportion of hours per week with detections. Light gray spaces represent times with no effort.
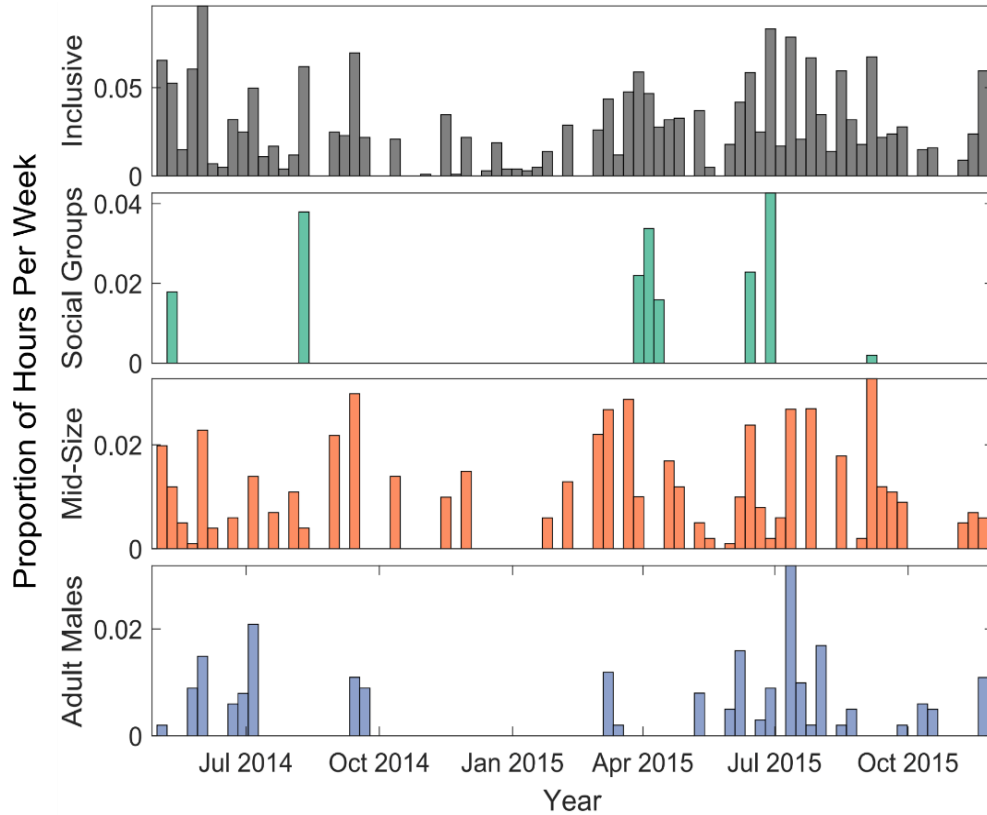
Figure 4.12. Time series of sperm whale presence at the Saipan site. The first row (dark gray) represents Inclusive, or all sperm whale, presence, the second row (green) represents Social Group presence, the third row (orange) represents Mid-Size presence, and the fourth row (blue) represents Adult Male presence. Sperm whale presence is represented as the proportion of hours per week with detections. Light gray spaces represent times with no effort.
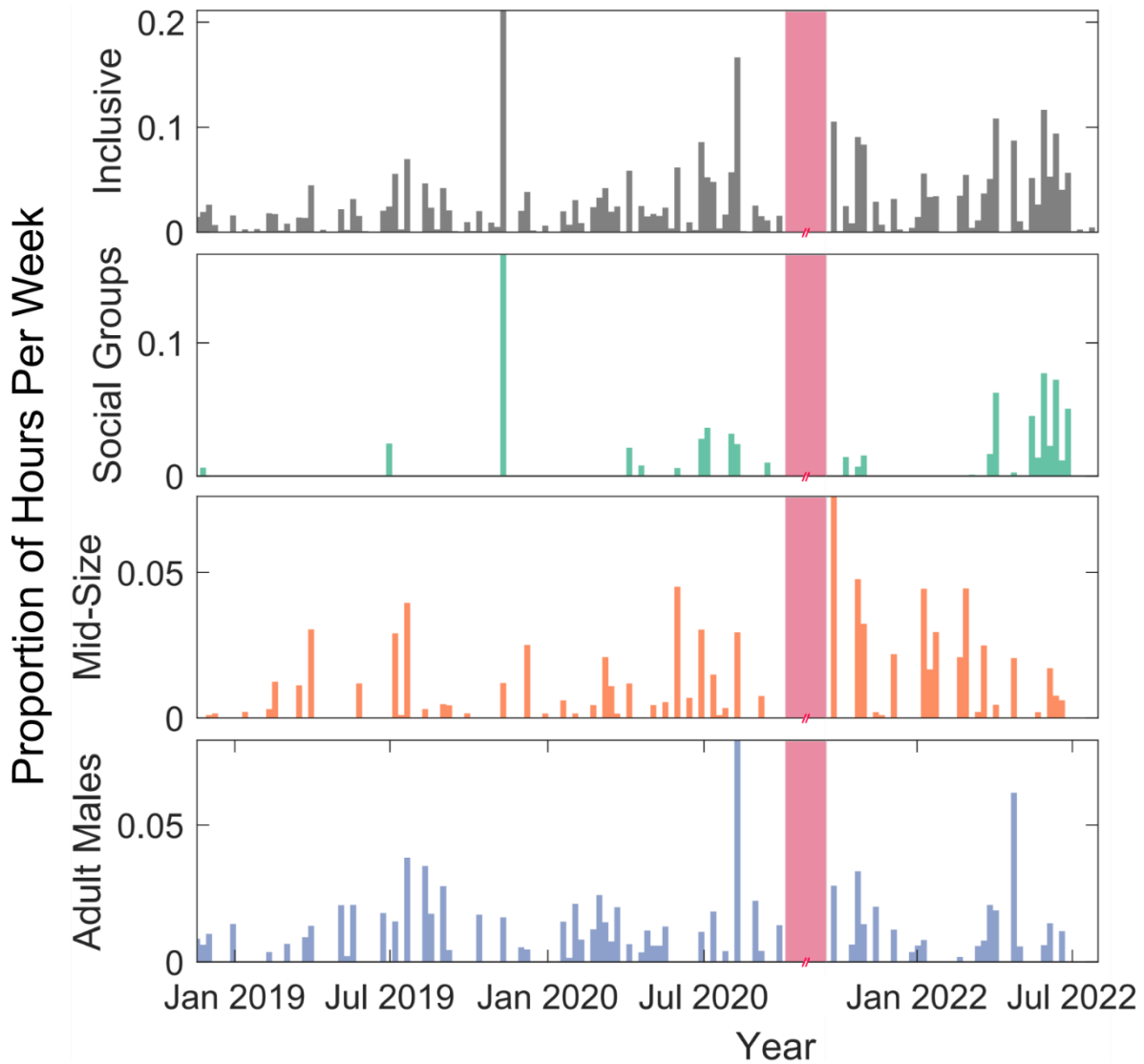
Figure 4.13. Time series of sperm whale presence at the Tinian site. The first row (dark gray) represents Inclusive, or all sperm whale, presence, the second row (green) represents Social Group presence, the third row (orange) represents Mid-Size presence, and the fourth row (blue) represents Adult Male presence. Sperm whale presence is represented as the proportion of hours per week with detections. Light gray spaces represent times with no effort. Red spaces represent times with no effort that extend beyond a year (11/06/2016 – 07/11/2018).
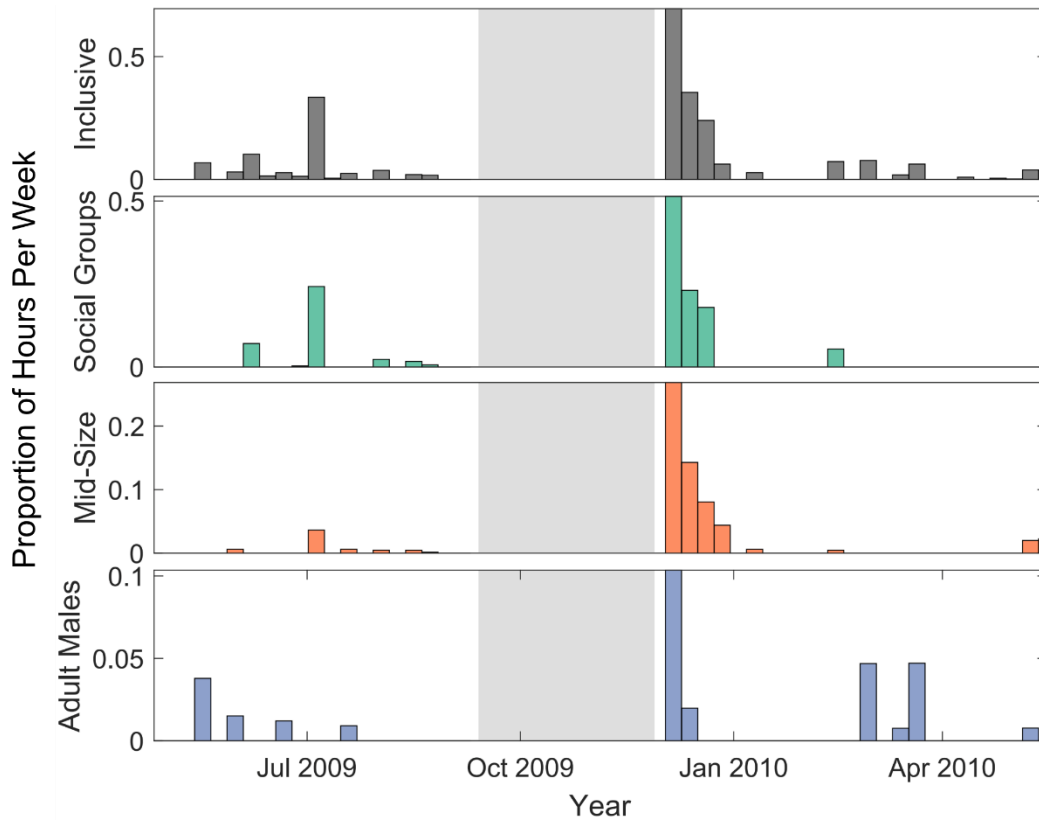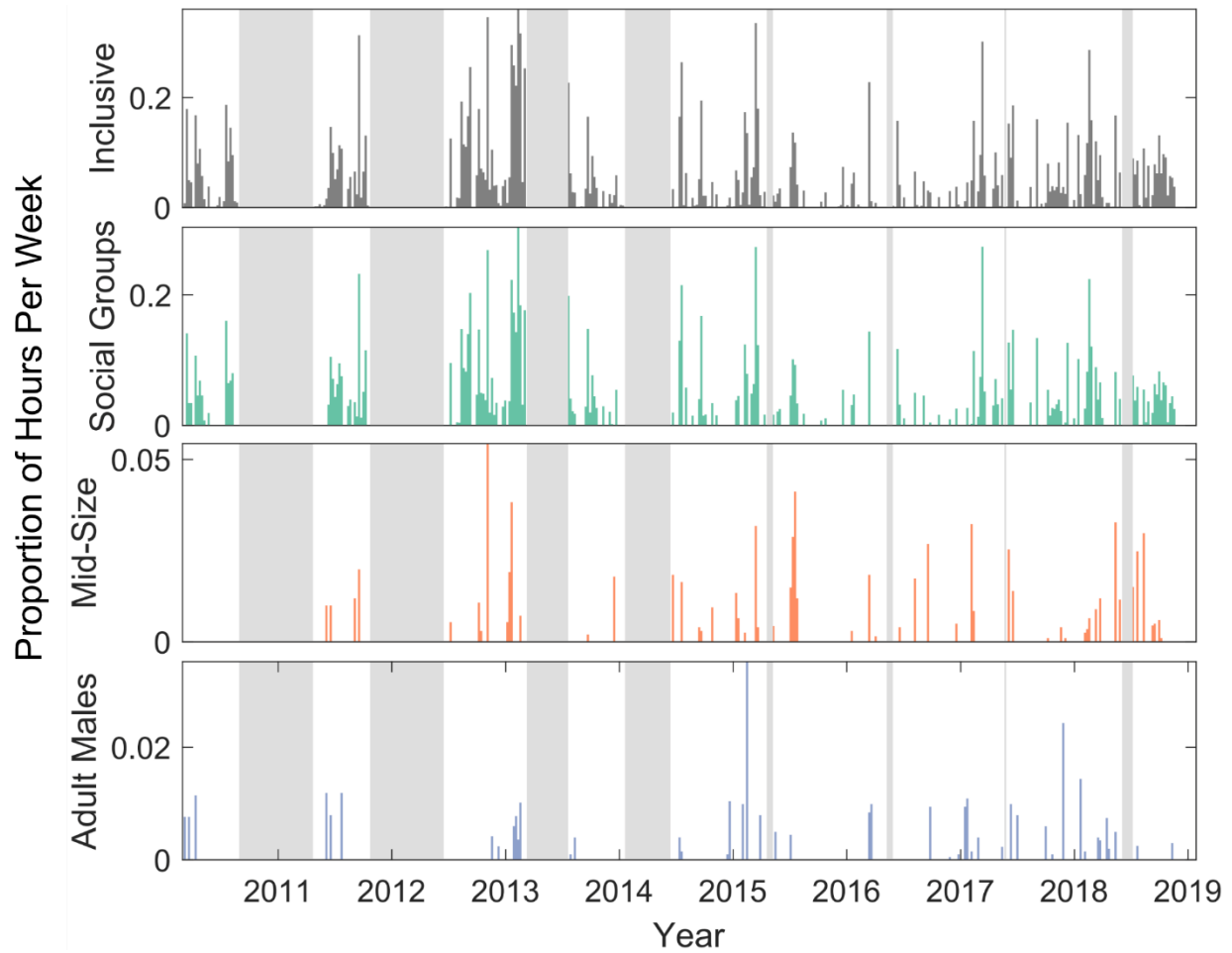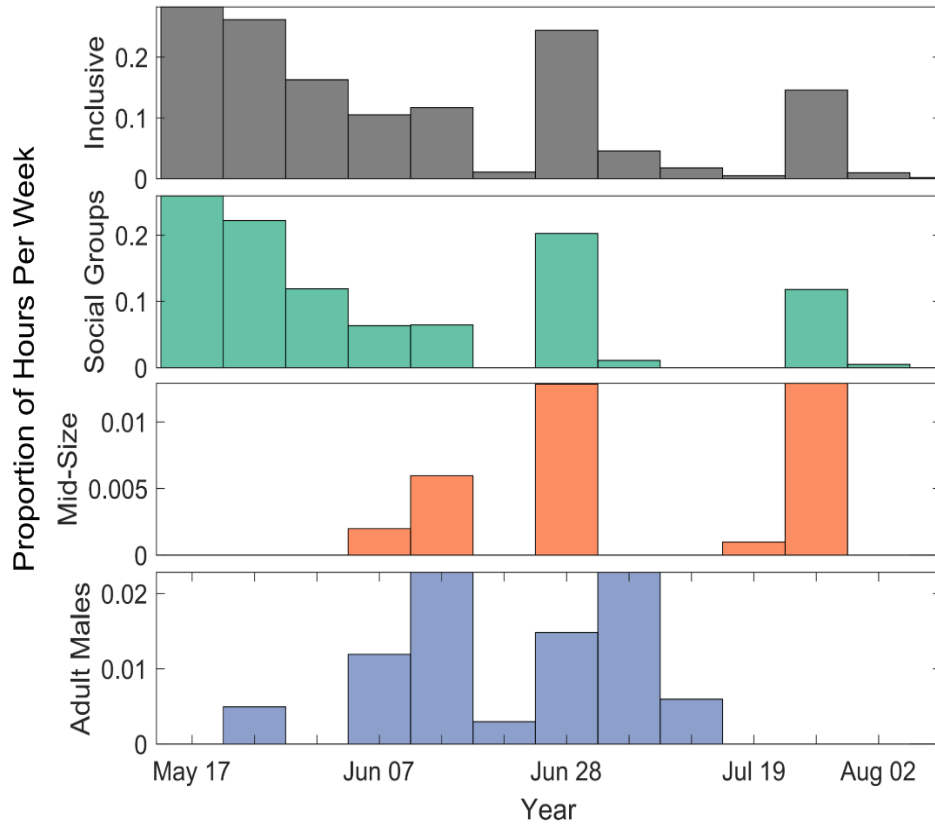
Figure 4.14. Time series of sperm whale presence at the Ladd Seamount (LSM) site. The first row (dark gray) represents Inclusive, or all sperm whale, presence, the second row (green) represents Social Group presence, the third row (orange) represents Mid-Size presence, and the fourth row (blue) represents Adult Male presence. Sperm whale presence is represented as the proportion of hours per week with detections.

Figure 4.15. Time series of sperm whale presence at the Pearl and Hermes (PHR) site. The first row (dark gray) represents Inclusive, or all sperm whale, presence, the second row (green) represents Social Group presence, the third row (orange) represents Mid-Size presence, and the fourth row (blue) represents Adult Male presence. Sperm whale presence is represented as the proportion of hours per week with de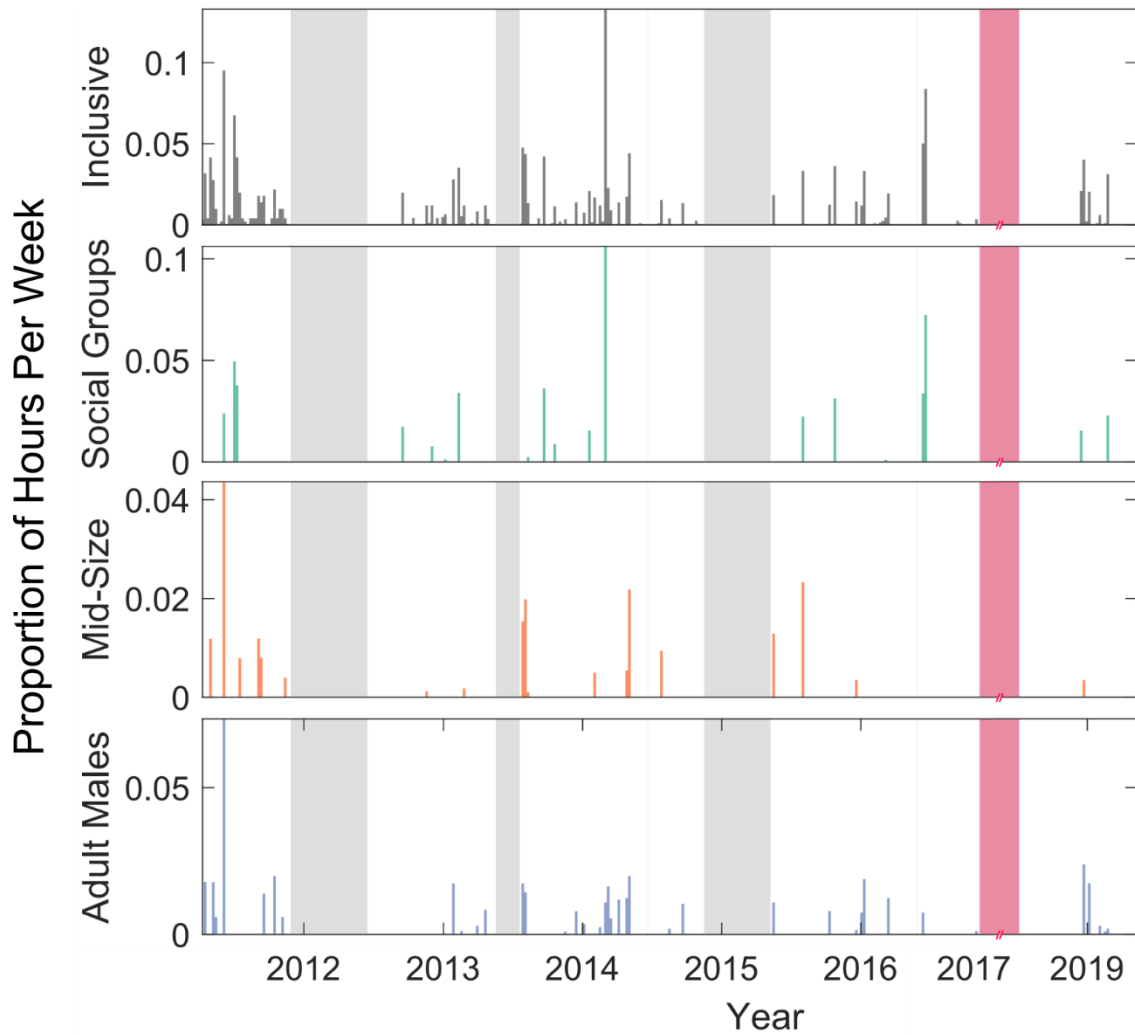tections. Light gray spaces represent times with no effort. Red spaces represent times with no effort that extend beyond a year (01/08/2012 – 09/11/2014). The black line represents the change in instrument location after 2014.

Figure 4.16. Time series of sperm whale presence at the Wake Seamount (Wake) site. The first row (dark gray) represents Inclusive, or all sperm whale, presence, the second row (green) represents Social Group presence, the third row (orange) represents Mid-Size presence, and the fourth row (blue) represents Adult Male presence. Sperm whale presence is represented as the proportion of hours per week with detections. Light gray spaces represent times with no effort. Red spaces represent times with no effort (05/05/2010 – 03/24/2011, 05/27/2011 – 02/24/2012, 01/02/2013 – 06/19/2014).

Figure 4.17. Time series of sperm whale presence at the Kauai site. The first row (dark gray) represents Inclusive, or all sperm whale, presence, the second row (green) represents Social Group presence, the third row (orange) represents Mid-Size presence, and the fourth row (blue) represents Adult Male presence. Sperm whale presence is represented 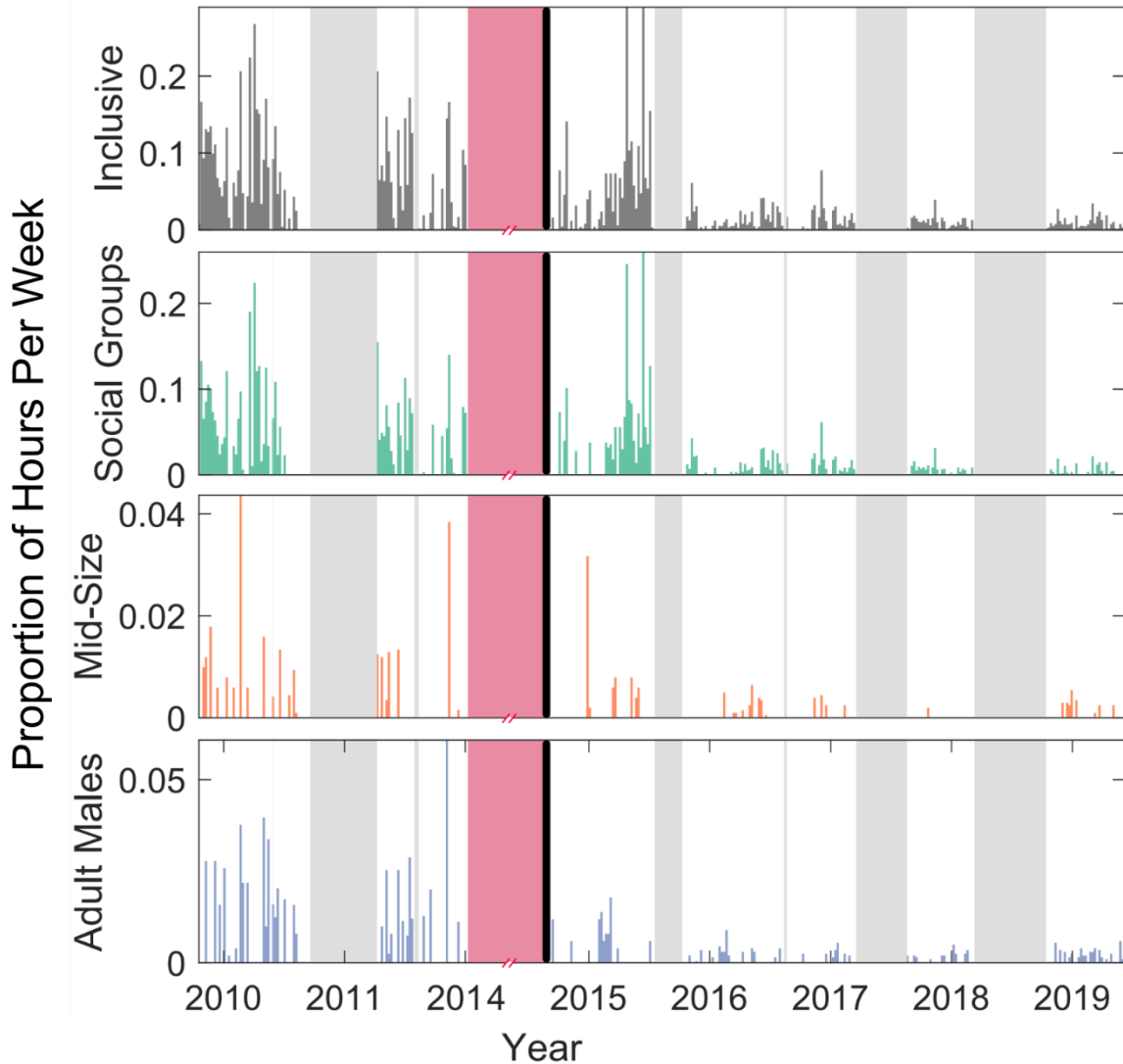as the proportion of hours per week with detections. Light gray spaces represent times with no effort. Red spaces represent times with no effort that extend beyond a year (08/21/2010 – 07/08/2016).

Figure 4.18. Time series of sperm whale presence at the Kona site. The first row (dark gray) represents Inclusive, or all sperm whale, presence, the second row (green) represents Social Group presence, the third row (orange) represents Mid-Size presence, and the fourth row (blue) represents Adult Male presence. Sperm whale presence is represented as the proportion of hours per week with detections. Light gray spaces represent times with no effort. Red spaces represent times with no effort that extend beyond a year (10/23/2011 – 10/22/2013).
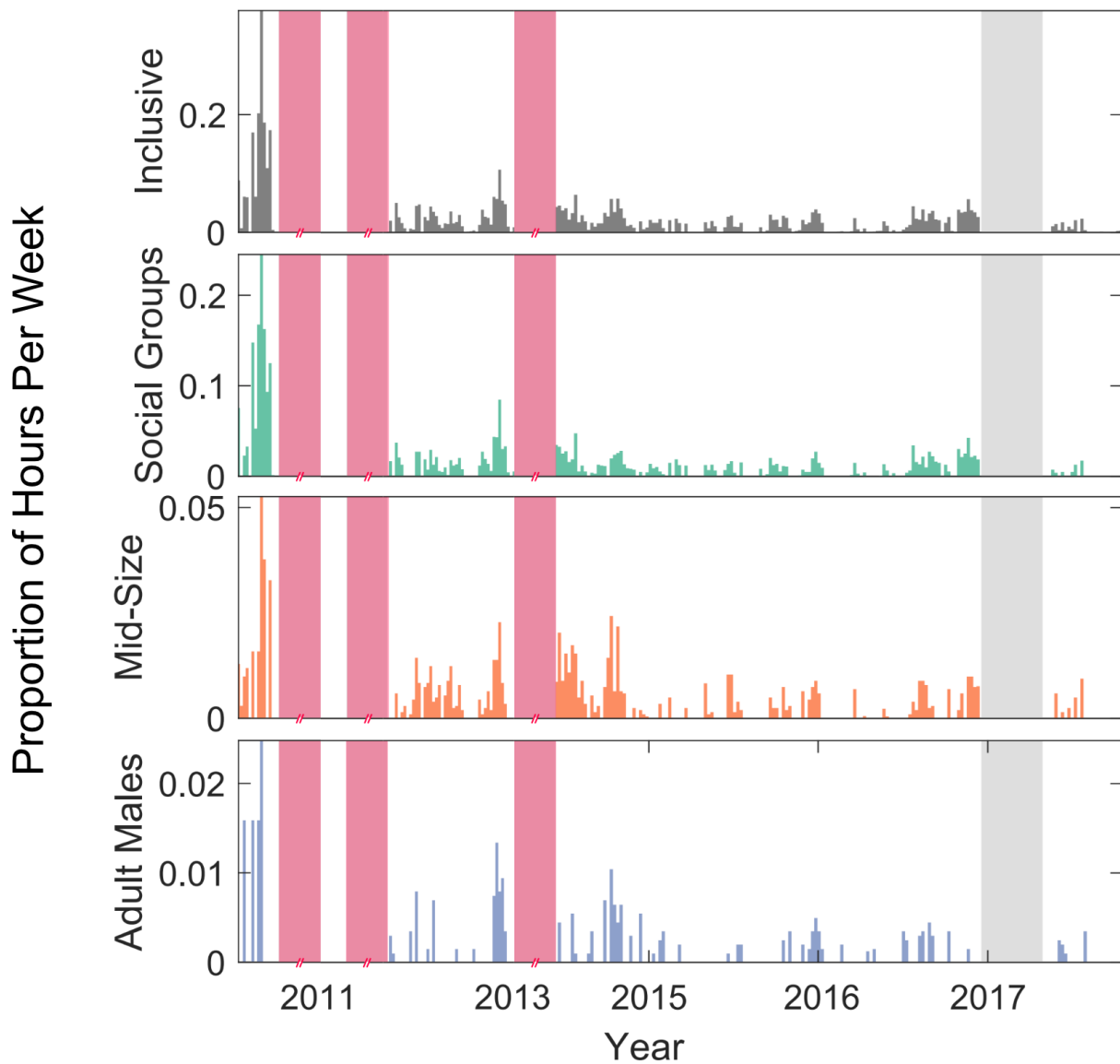
Figure 4.19. Time series of sperm whale presence at the Cross Seamount (CSM) site. The first row (dark gray) represents Inclusive, or all sperm whale, presence, the second row (green) represents Social Group presence, the third row (orange) represents Mid-Size presence, and the fourth row (blue) represents Adult Male presence. Sperm whale presence is represented as the proportion of hours per week with detections. Light gray spaces represent times with no effort.
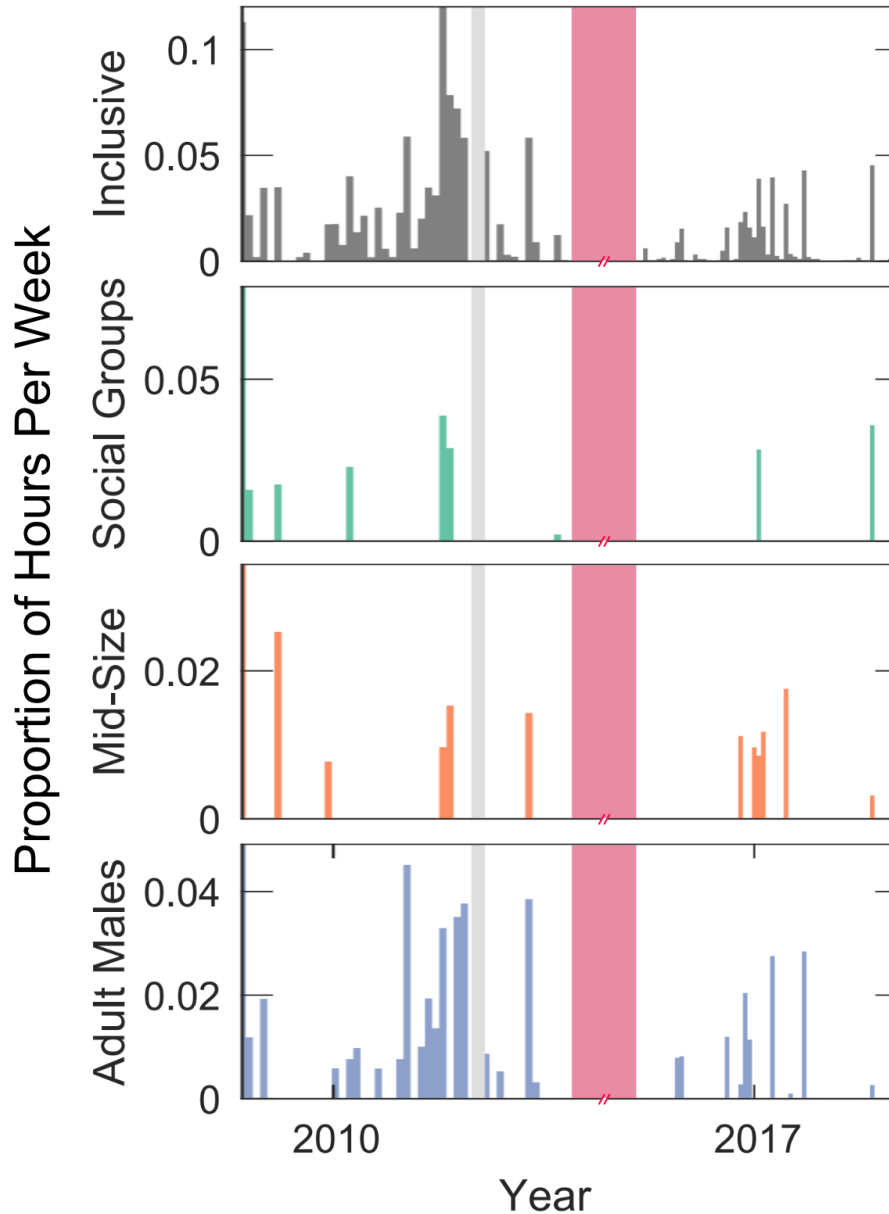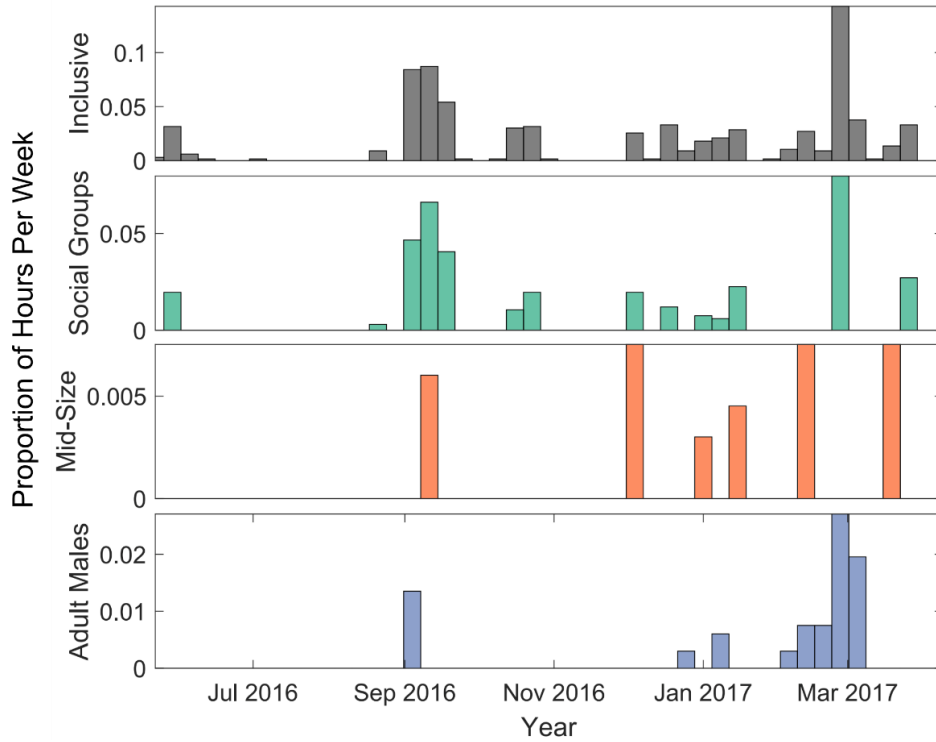
Figure 4.20. Time series of sperm whale presence at the Pagan site. The first row (dark gray) represents Inclusive, or all sperm whale, presence, the second row (green) represents Social Group presence, the third row (orange) represents Mid-Size presence, and the fourth row (blue) represents Adult Male presence. Sperm whale presence is represented as the proportion of hours per week with detections.
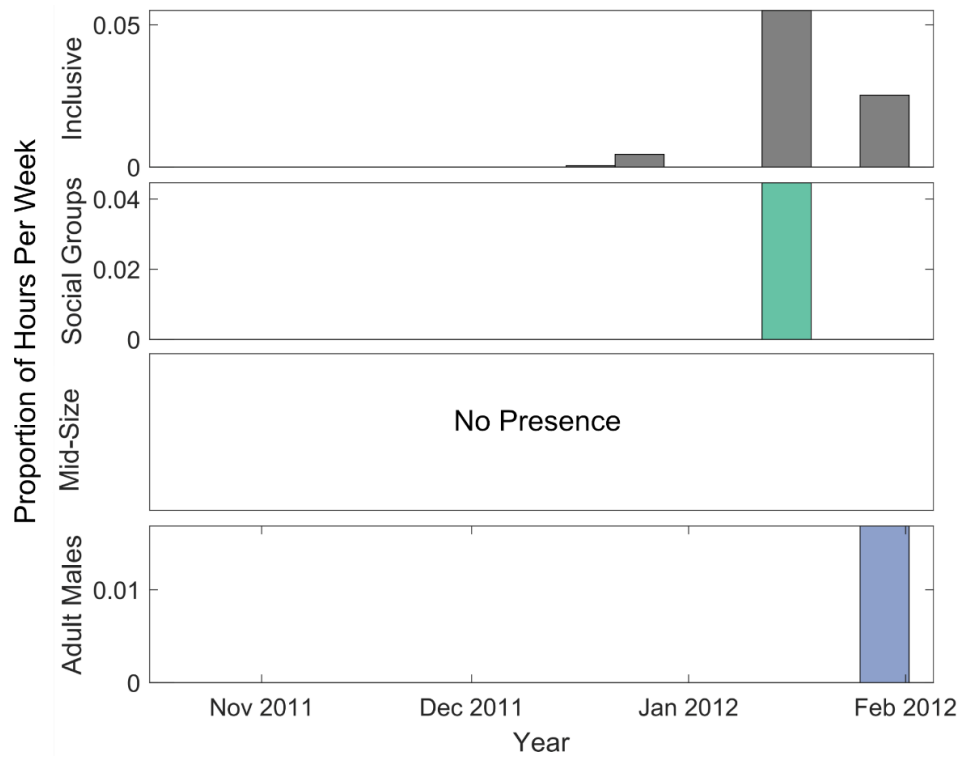
Figure 4.21. Time series of sperm whale presence at the Kingman Reef (KR) site. The first row (dark gray) represents Inclusive, or all sperm whale, presence, the second row (green) represents Social Group presence, the third row (orange) represents Mid-Size presence, and the fourth row (blue) represents Adult Male presence. Sperm whale presence is represented as the proportion of hours per week with detections.
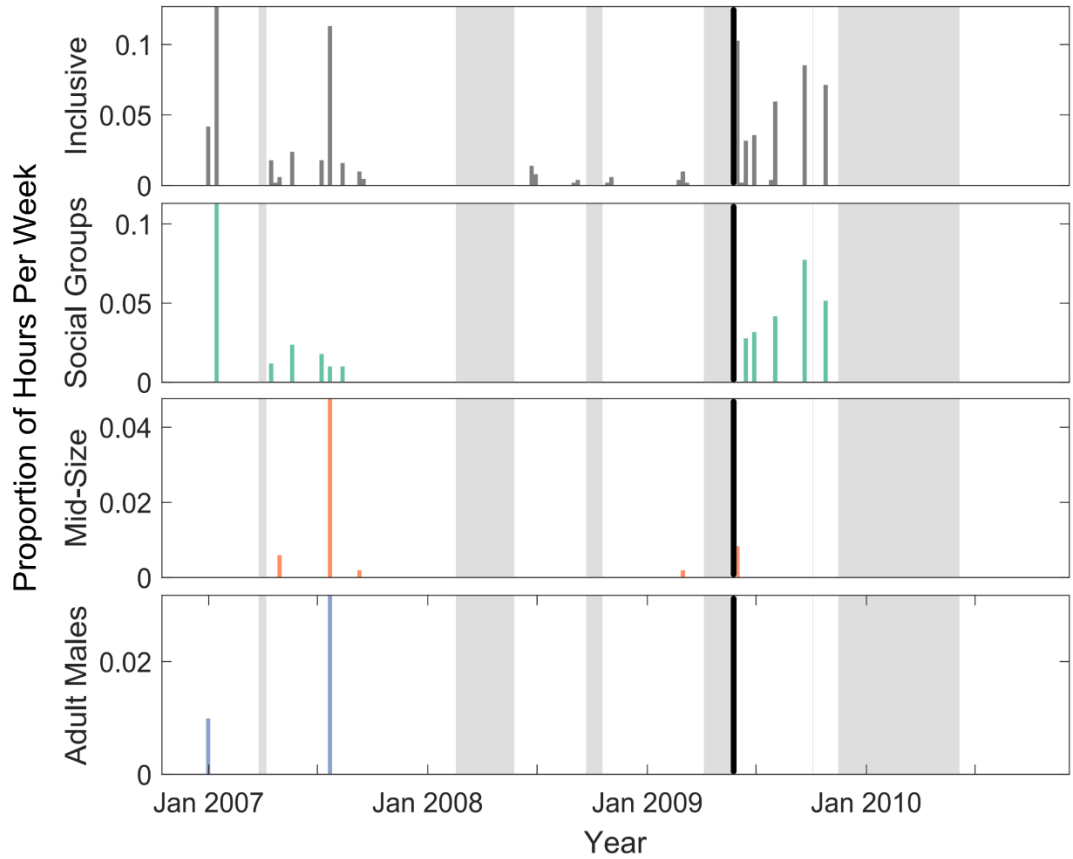
Figure 4.22. Time series of sperm whale presence at the Palmyra Atoll (Palmyra) site. The first row (dark gray) represents Inclusive, or all sperm whale, presence, the second row (green) represents Social Group presence, the third row (orange) represents Mid-Size presence, and the fourth row (blue) represents Adult Male presence. Sperm whale presence is represented as the proportion of hours per week with detections. Light gray spaces represent times with no effort. The black line represents the change in instrument location after June 2009.

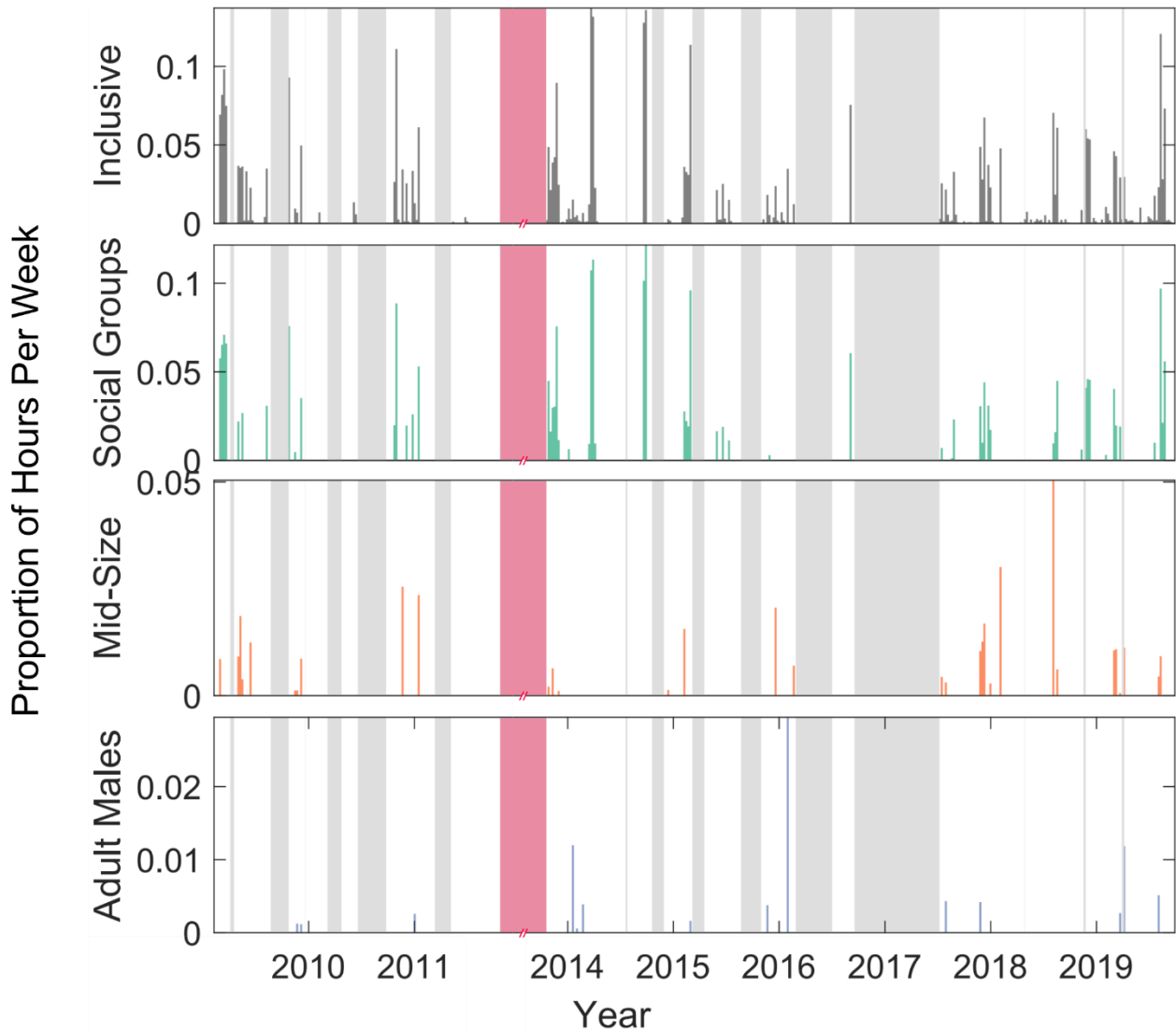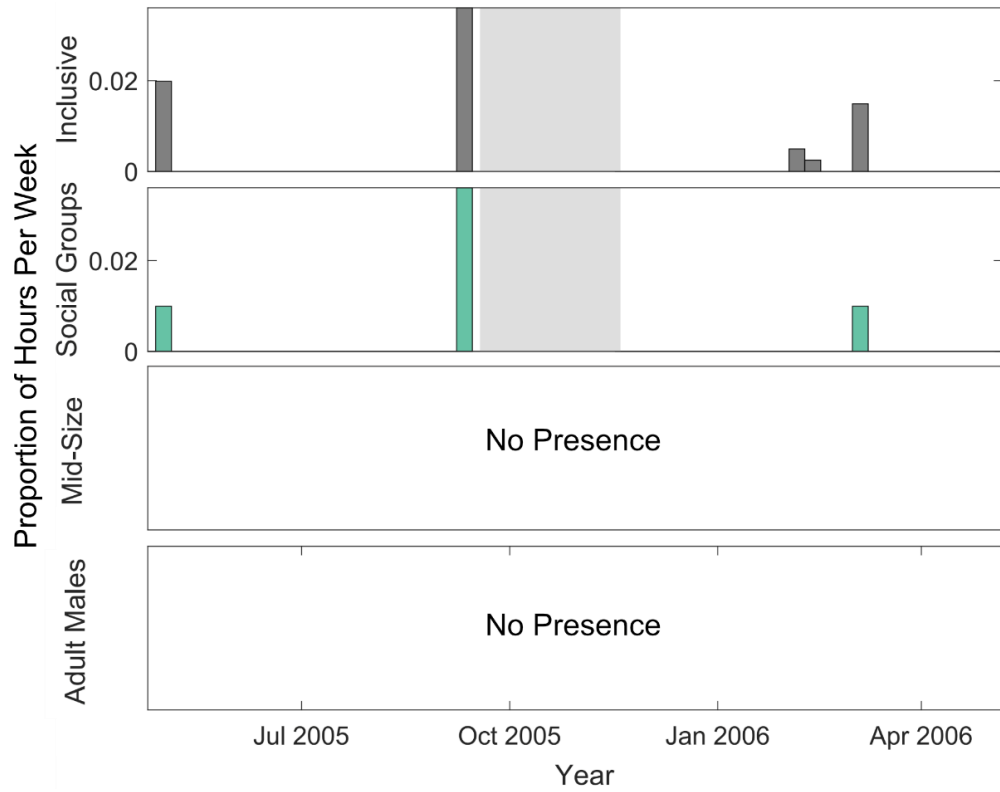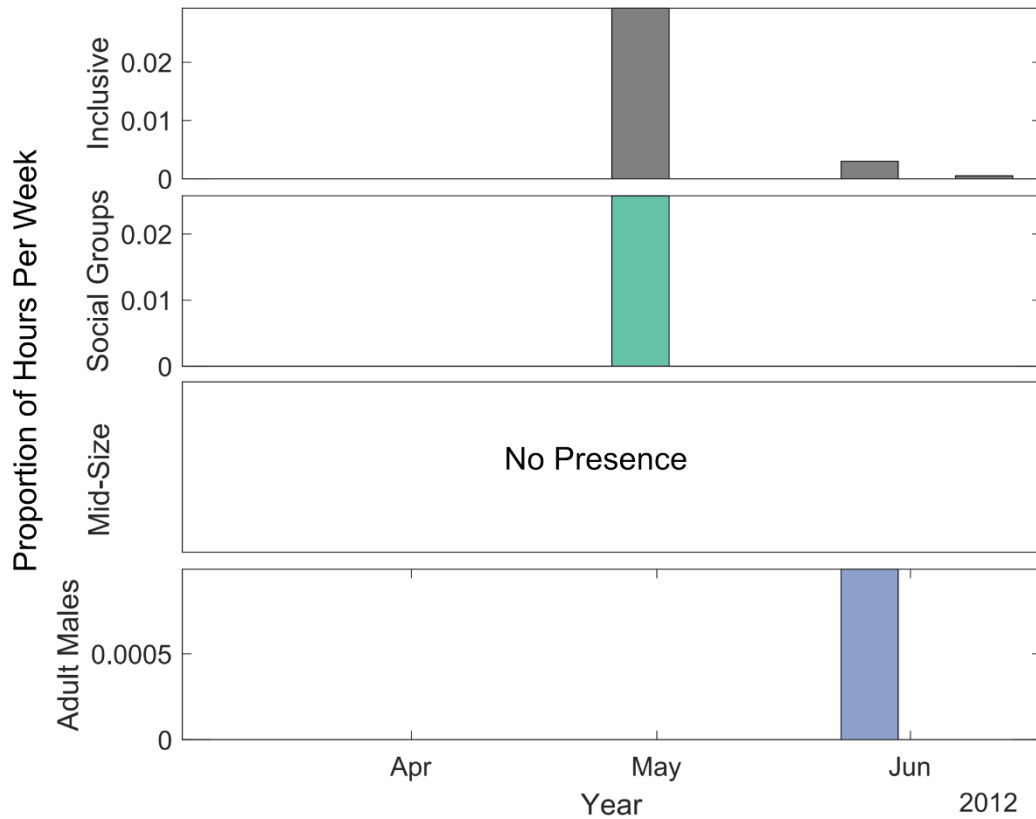Figure 4.23. Time series of sperm whale presence at the Equator (EQ) site. The first row (dark gray) represents Inclusive, or all sperm whale, presence, the second row (green) represents Social Group presence, the third row (orange) represents Mid-Size presence, and the fourth row (blue) represents Adult Male presence. Sperm whale presence is represented as the proportion of hours per week with detections.
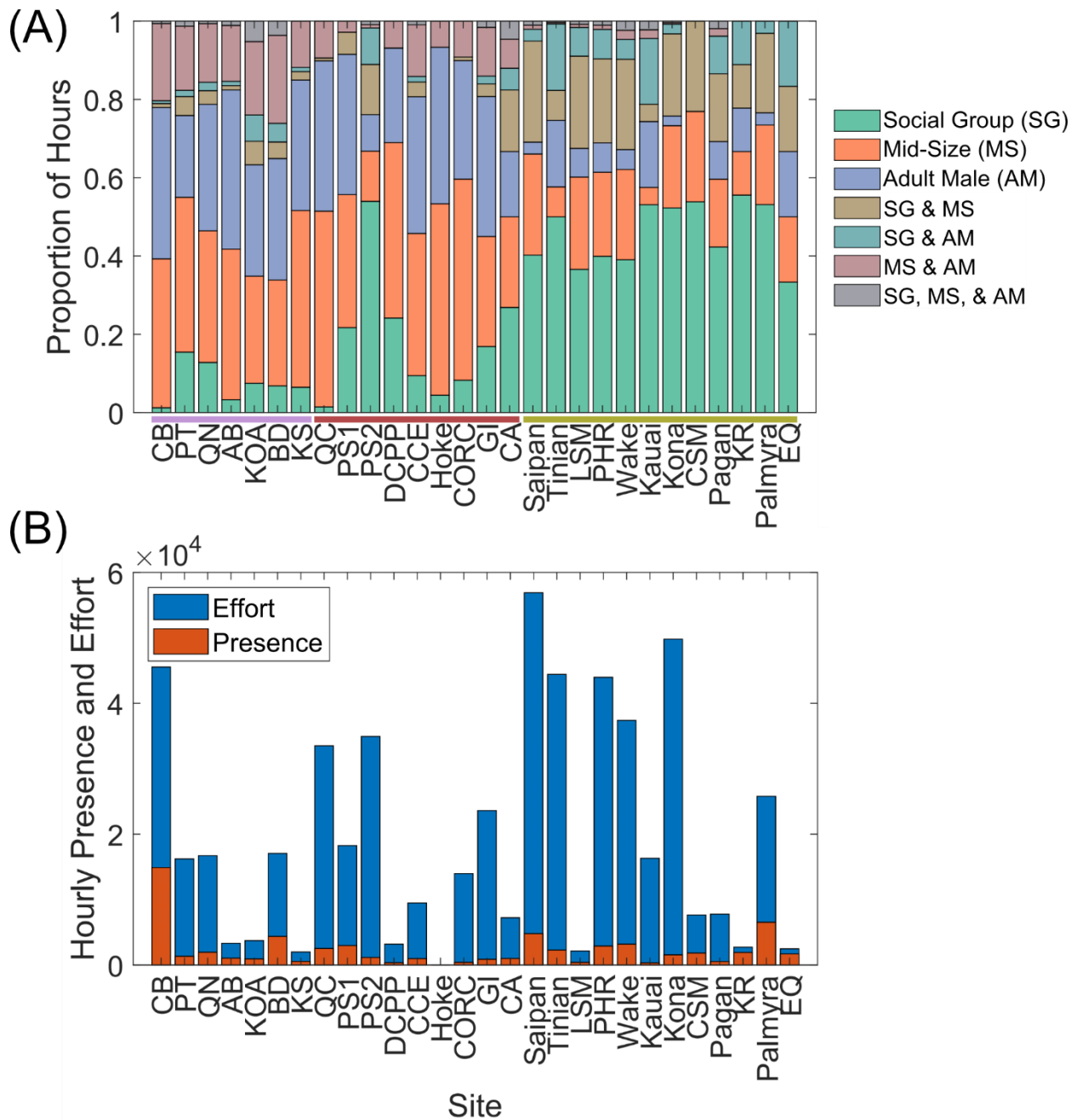
Figure 4.24. (A) Proportion of hours with sperm whale presence of each class (or combination of classes) at each site (bar) within each region (color bar along x-axis). (B) Number of hours with effort for each site (blue) and number of hours with presence for each site (red).
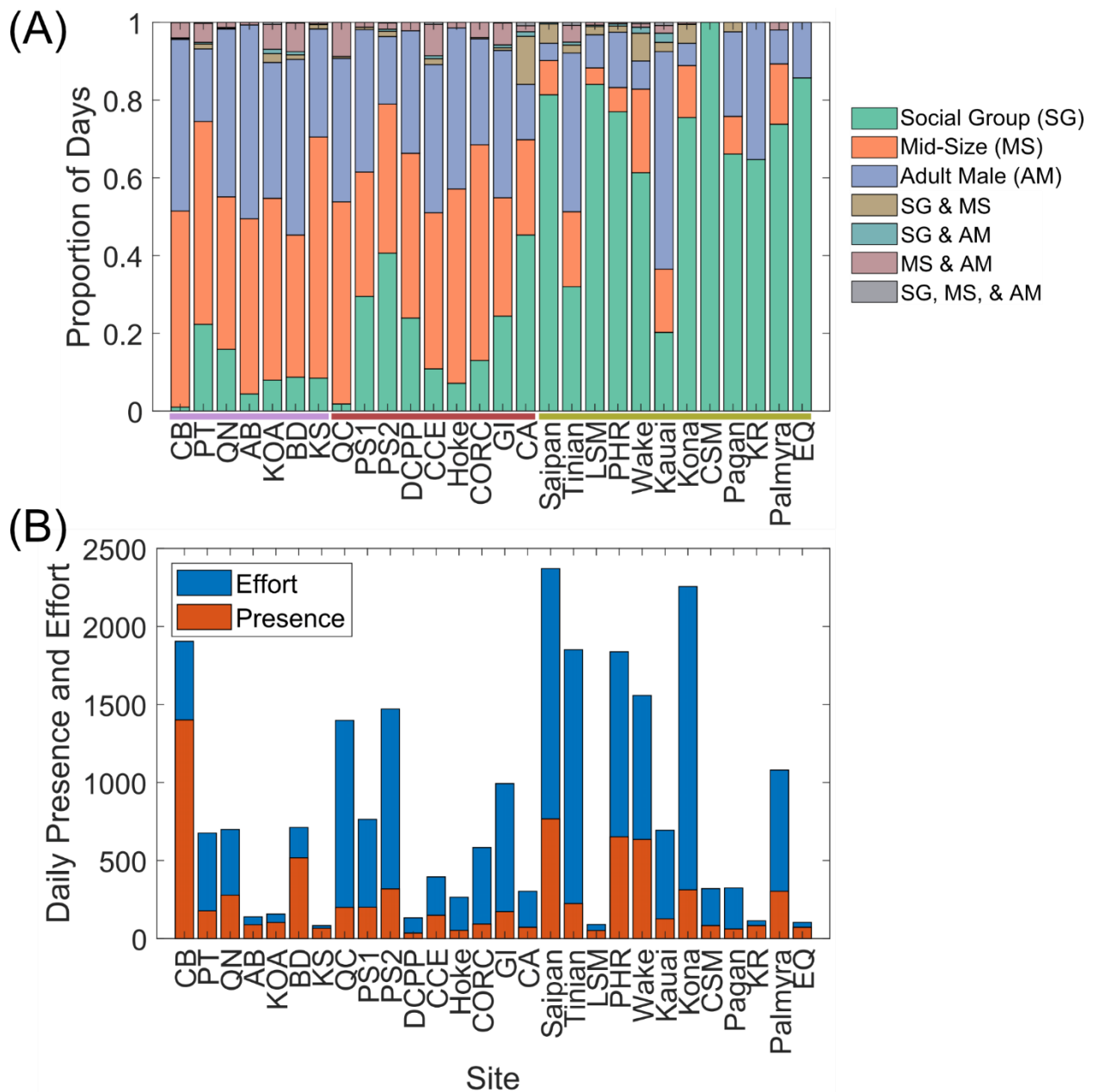
Figure 4.25. (A) Proportion of days with sperm whale presence of each class (or combination of classes) at each site (bar) within each region (color bar along x-axis). (B) Number of days with effort for each site (blue) and number of days with presence for each site (red).
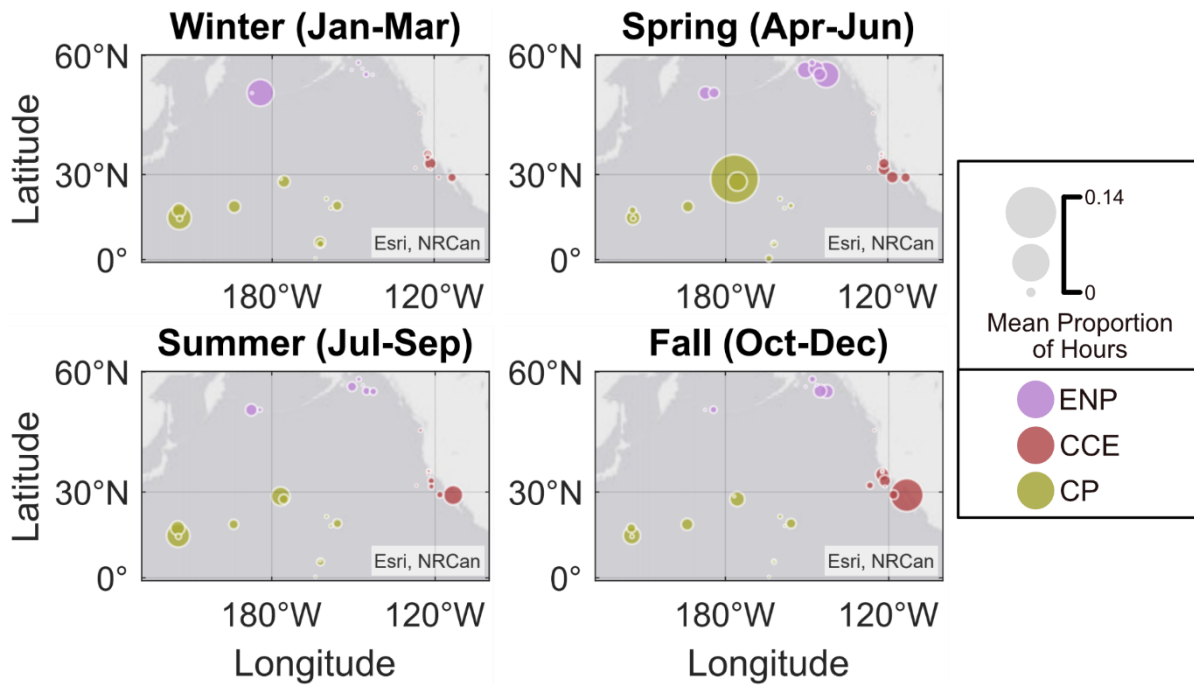
Figure 4.26. High-use areas of Social Groups for each season and within each region. Sperm whale use (or presence) is represented by the mean proportion of hours in that season (spanning three months).
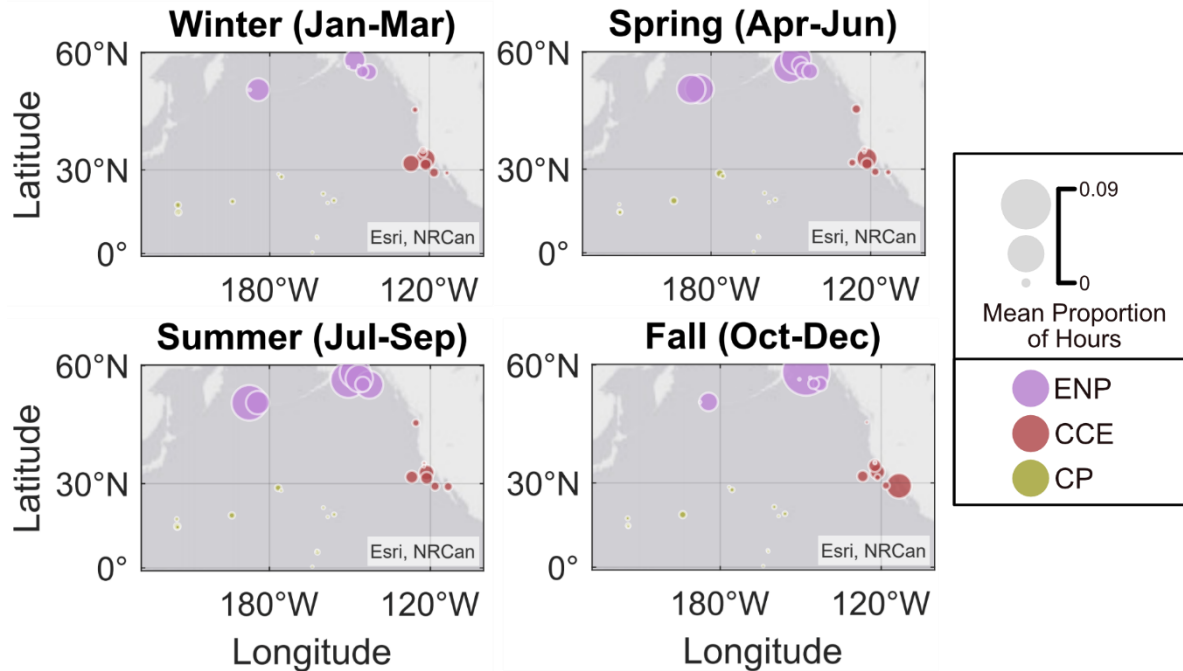
Figure 4.27. High-use areas of Mid-Size for each season and within each region. Sperm whale use (or presence) is represented by the mean proportion of hours in that season (spanning three months).
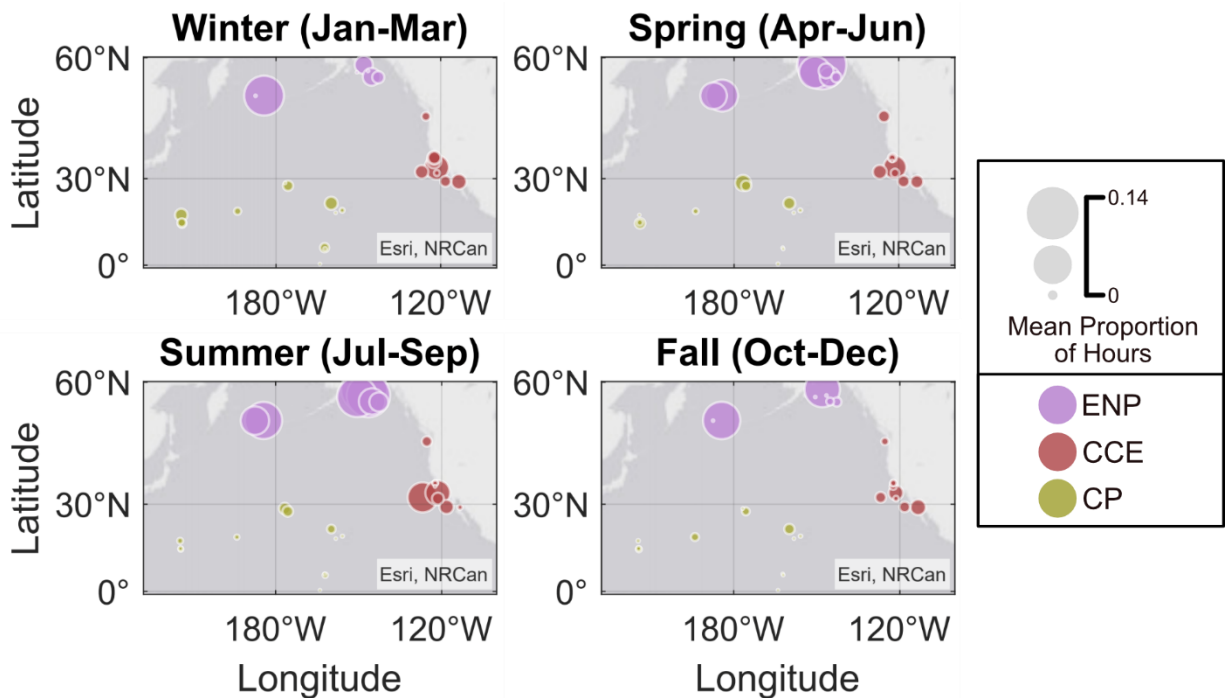
Figure 4.28. High-use areas of Adult Males for each season and within each region. Sperm whale use (or presence) is represented by the mean proportion of hours in that season (spanning three months).

Table 4.2. Habitat associations of each class (column) for each region (row). The proportion of each class is displayed as a percentage beneath each class name. The habitat variables are represented as acronyms as follows: chlorophyll-a (CHL), sea surface temperature (SST), sea surface height (SSH), ocean mixed layer thickness (MLT), salinity (Salinity), and EKE (eddy kinetic energy). The arrows following each habitat variable acronym represent whether presence of that group was associated with higher or lower values compared to the random distribution of that variable.

Region	Inclusive	Social Groups	Mid-Size	Adult Males
Eastern North Pacific	MLT↓, SAL↓, SST↑, CHL↑	SSH↑, MLT↑ SAL↑, SST↓, CHL ↑	SSH↓, MLT↓, SAL↓, SST↑	SSH↑, SAL↓, EKE↓, SST↑, CHL↑
California Current Ecosystem	MLT↑, EKE↑, SST↓, CHL↑	SSH↓, MLT↓, SAL↓	--	MLT↓, SAL↓, EKE↑,
Central Pacific	SSH↓, SAL↑,	SSH↓, MLT↓, SAL↑	SSH↓, MLT↓, SAL↑	SSH↓, MLT↑, SAL↑, EKE↑, SST↓, CHL↑
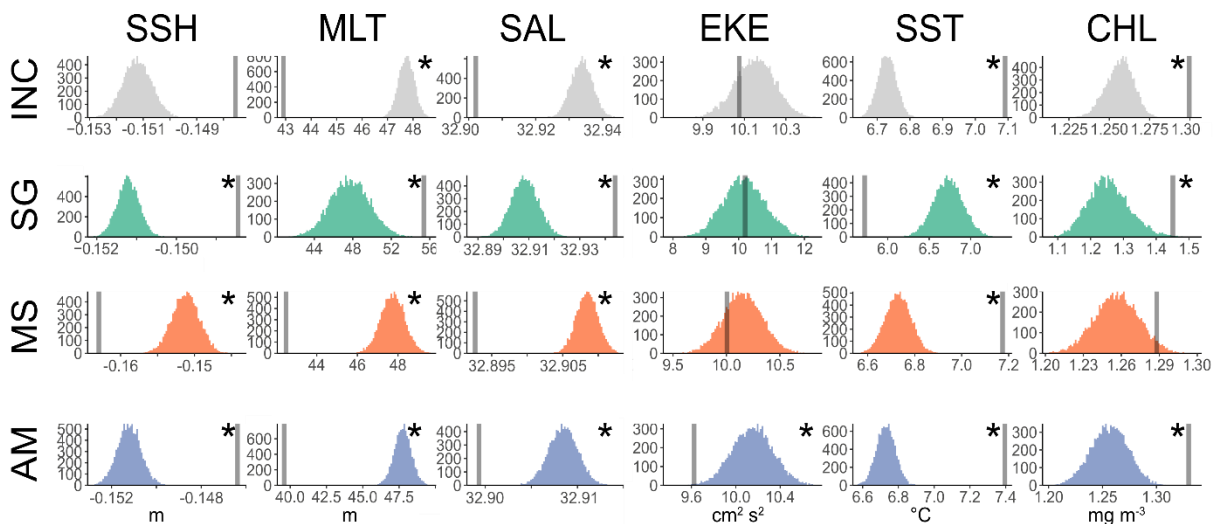
Figure 4.29. Habitat associations of each class (row and color) for each habitat variable (column) in the Eastern North Pacific. The random distribution of the mean (based on 10,000 permutations) for the variable is represented as a histogram and the mean during times of presence for that class is represented by the gray bar. The habitat variables are represented as acronyms as follows: sea surface height (SSH), ocean mixed layer thickness (MLT), salinity (SAL), eddy kinetic energy (EKE) sea surface temperature (SST), chlorophyll-a (CHL). The units for each habitat variable are displayed along the bottom most x-axis.
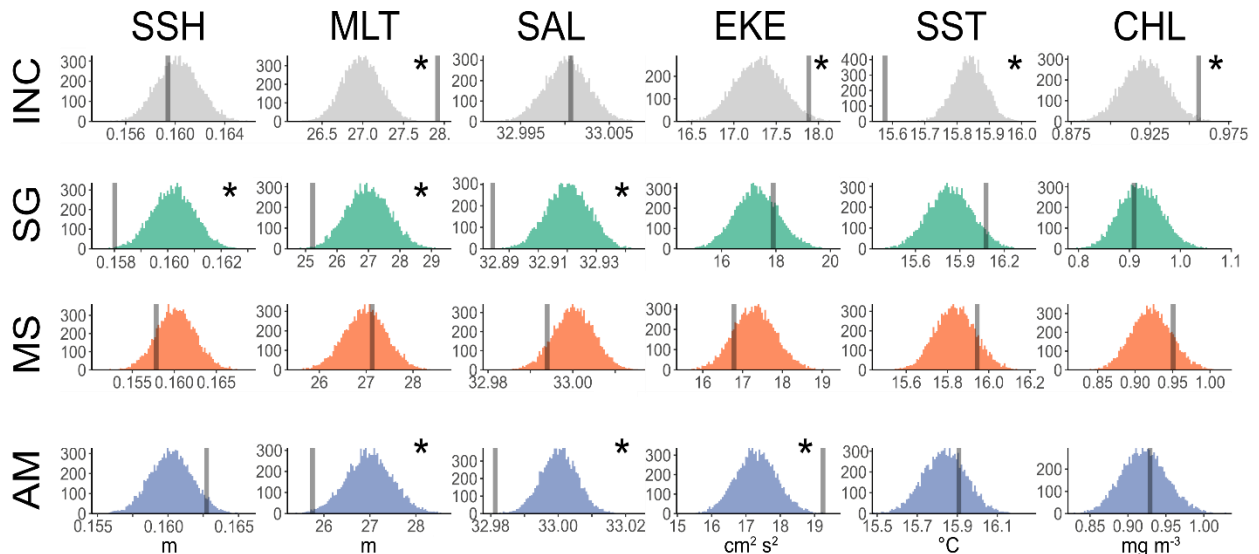
Figure 4.30. Habitat associations of each class (row and color) for each habitat variable (column) in the California Current Ecosystem. The random distribution of the mean (based on 10,000 permutations) for the variable is represented as a histogram and the mean during times of presence for that class is represented by the gray bar. The habitat variables are represented as acronyms as follows: sea surface height (SSH), ocean mixed layer thickness (MLT), salinity (SAL), eddy kinetic energy (EKE) sea surface temperature (SST), chlorophyll-a (CHL). The units for each habitat variable are displayed along the bottom most x-axis.
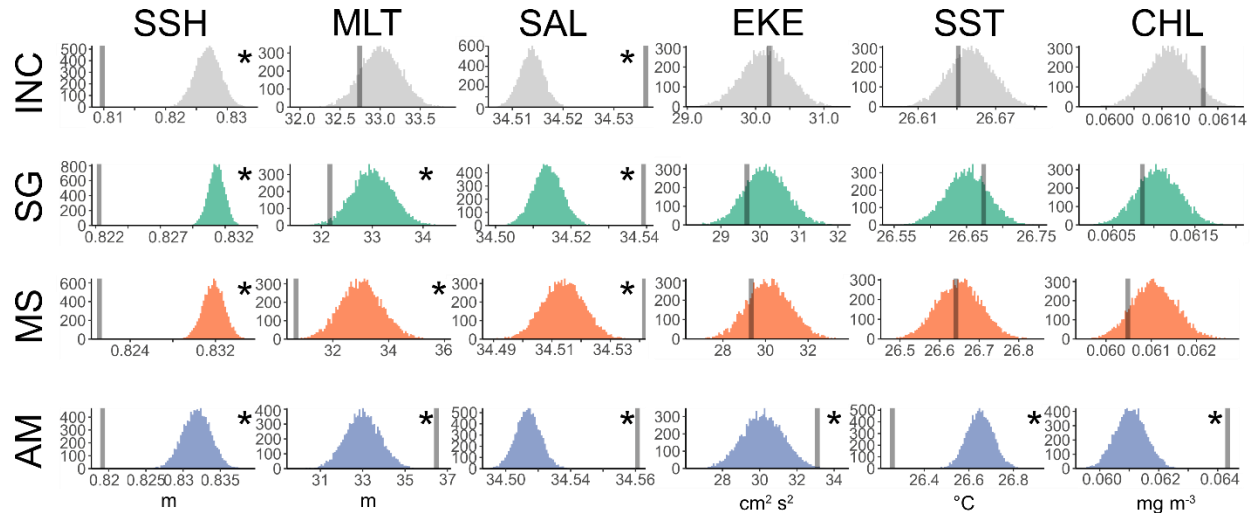
Figure 4.31. Habitat associations of each class (row and color) for each habitat variable (column) in the Central Pacific. The random distribution of the mean (based on 10,000 permutations) for the variable is represented as a histogram and the mean during times of presence for that class is represented by the gray bar. The habitat variables are represented as acronyms as follows: sea surface height (SSH), ocean mixed layer thickness (MLT), salinity (SAL), kinetic energy (EKE) sea surface temperature (SST), chlorophyll-a (CHL). The units for each habitat variable are displayed along the bottom most x-axis.

Figure 4.32. A correlation matrix plot for all variables (diagonal) within the Eastern North Pacific. The habitat variables are represented as acronyms as follows: ocean mixed layer thickness (MLT), salinity (SAL), sea surface height (SSH), sea surface temperature (SST), eddy kinetic energy (EKE), and chlorophyll-a (CHL). The size of the circle represents the amount of correlation between the two variables, the color represents the correlation value (red = negative/blue = positive), and the stars representing how significant the correlation is based on the p-value ('***' - 0.0001, '**' 0.01, '**' 0.05. Non-significant correlations are not displayed. The black rectangles around the plot of the correlation matrix is based on the results of hierarchical clustering.

Figure 4.33. A correlation matrix plot for all variables (diagonal) within the California Current Ecosystem. The habitat variables are represented as acronyms as follows: ocean mixed layer thickness (MLT), salinity (SAL), sea surface height (SSH), sea surface temperature (SST), eddy kinetic energy (EKE), and chlorophyll-a (CHL). The size of the circle represents the amount of correlation between the two variables, the color represents the correlation value (red = negative/blue = positive), and the stars representing how significant the correlation is based on the p-value ('***' - 0.0001, '**' 0.01, '**' 0.05. Non-significant correlations are not displayed. The black rectangles around the plot of the correlation matrix is based on the results of hierarchical clustering.
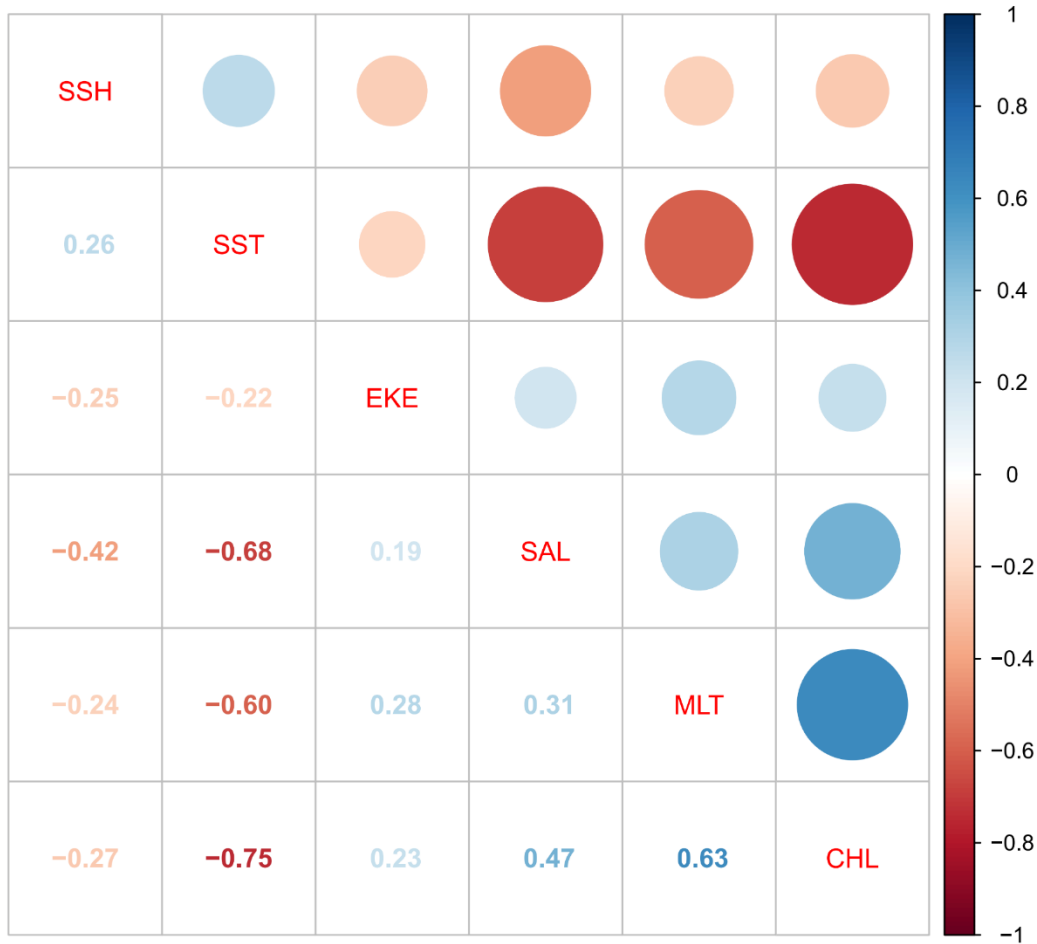
Figure 4.34. A correlation matrix plot for all variables (diagonal) within the Central Pacific. The habitat variables are represented as acronyms as follows: sea surface temperature (SST), ocean mixed layer thickness (MLT), salinity (SAL), eddy kinetic energy (EKE), sea surface height (SSH) and chlorophyll-a (CHL). The size of the circle represents the amount of correlation between the two variables, the color represents the correlation value (red = negative/blue = positive), and the stars representing how significant the correlation is based on the p-value ('***' - 0.0001, '**' 0.01, '**' 0.05. Non-significant correlations are not displayed. The black rectangles around the plot of the correlation matrix is based on the results of hierarchical clustering.
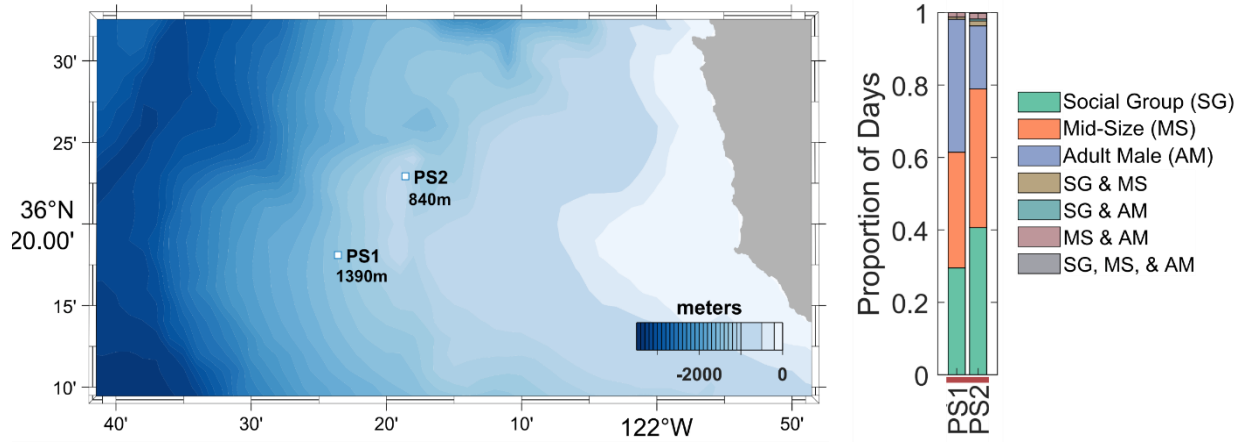
Figure 4.35. Map displaying the two Point Sur recording sites (PS1 and PS2) and their respective depths off the coast of Monterey California (left). Proportion of days with sperm whale presence of each class (or combination of classes) at each site (bar) (right). The PS1 site is west of the ridge, facing open ocean while the PS2 site is between the ridge (east, downslope) and the coast of California.
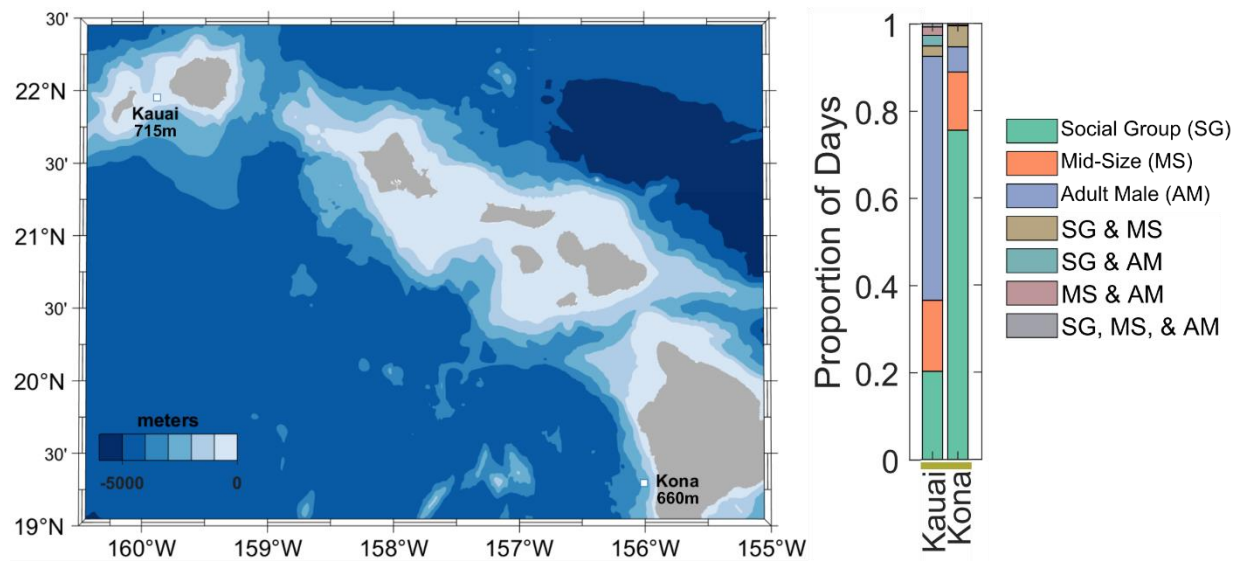
Figure 4.36. Map displaying the Kauai and Kona recording sites and their respective depths within the Main Hawaiian Islands region (left). Proportion of days with sperm whale presence of each class (or combination of classes) at each site (bar) (right). The Kauai site is facing open ocean while the Kona site is protected by a cluster of seamounts directly west of the site.

241
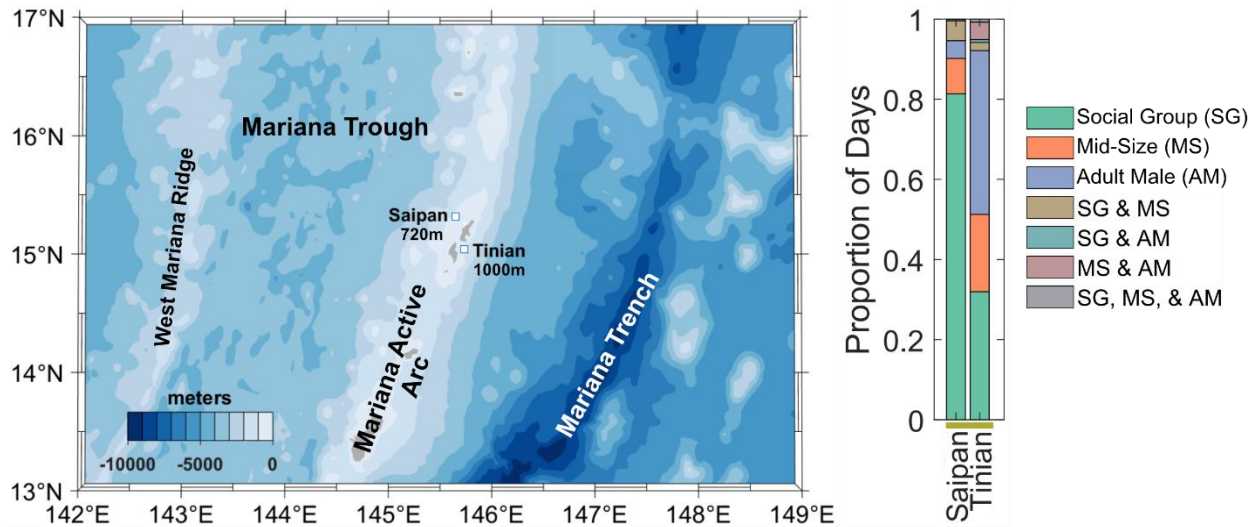
Figure 4.37. Map displaying Saipan and Tinian recording sites and their respective depths within the Northern Mariana Islands region, part of the Mariana Active Arc (left). The two sites are between the Mariana Trough and the West Mariana Ridge on the west and the Mariana Trench on the east. Proportion of days with sperm whale presence of each class (or combination of classes) at each site (bar) (right).

References

Albers, S. (2020). *Rsoi: Import Various Northern and Southern Hemisphere Climate Indices*. Available at: https://cran.r-project.org/package=rsoi. Last accessed .

Alexander, R.D. (1974). The Evolution of Social Behavior. *Annu. Rev. Ecol. Evol. Syst.*, 5, 325–383.

Anderson, P.J. (1997). Declines of forage species in the Gulf of Alaska, 1972-1995, as an indicator of regime shift. In: *Forage fishes in marine ecosystems*. University of Alaska.

Anderson, P.J. & Piatt, J.F. (1999). Community reorganization in the Gulf of Alaska following ocean climate regime shift. *Mar. Ecol. Prog. Ser.*, 189, 117–123.

APL-UW. (1994). *APL-UW High-Frequency Ocean Environmental Acoustic Models Handbook*.

Au, W.W.L., Giorli, G., Chen, J., Copeland, A., Lammers, M., Richlen, M., *et al.* (2013). Nighttime foraging by deep diving echolocating odontocetes off the Hawaiian islands of Kauai and Ni'ihau as determined by passive acoustic monitors. *J. Acoust. Soc. Am.*, 133, 3119–3127.

Backus, R.H. & Schevill, W.E. (1966). *Whales, dolphins and porpoises*. University of California Press.

Bailey, H., Corkrey, R., Cheney, B. & Thompson, P.M. (2013). Analyzing temporally correlated dolphin sightings data using generalized estimating equations. *Mar. Mammal Sci.*, 29, 123–141.

Barlow, J. (1995). The abundance of cetaceans in California waters. Part I: Ship surveys in summer and fall of 1991. *Oceanogr. Lit. Rev.*, 9, 784.

Barlow, J. & Taylor, B.L. (2005). Estimates of Sperm Whale Abundance in the Northeastern Temperate Pacific From a Combined Acoustic and Visual Survey. *Mar. Mammal Sci.*, 21, 429–445.

Baumann-Pickering, S., Trickey, J.S., Wiggins, S.M. & Oleson, E.M. (2016). Odontocete occurrence in relation to changes in oceanography at a remote equatorial Pacific seamount. *Mar. Mammal Sci.*, 32, 805–825.

Benjamins, S., van Geel, N., Hastie, G., Elliott, J. & Wilson, B. (2017). Harbour porpoise distribution can vary at small spatiotemporal scales in energetic habitats. *Deep. Res. Part II Top. Stud. Oceanogr.*, 141, 191–202.

Benson, S.R., Eguchi, T., Foley, D.G., Forney, K.A., Bailey, H., Hitipeuw, C., *et al.* (2011). Large-scale movements and high-use areas of western Pacific leatherback turtles, Dermochelys coriacea. *Ecosphere*, 2, 1–27.

Berzin, A.A. (1971). The Sperm Whale, Israel Program for Scientific Translation, Jerusalem.

Transl. from Russ. Berzin.

Berzin, A.A. (1972). *Kashalot (The sperm whale)*. Pischevaya Promyshlenmost, Moscow.

Berzin, A.A. & Rovnin, A.A. (1966). The distribution and migrations of whales in the northeastern part of the Pacific, Chukchi, and Bering Seas. *Iszv. Tikhookean. Nauchno. Issled. Inst. Ryb. Khoz. Okeanogr*, 58, 179–208.

Beslin, W.A.M., Whitehead, H. & Gero, S. (2018). Automatic acoustic estimation of sperm whale size distributions achieved through machine recognition of on-axis clicks. *J. Acoust. Soc. Am.*, 144, 3485–3495.

Best, P.B. (1979). Social organization in sperm whales, Physeter macrocephalus. In: *Behavior of marine animals*. Springer, pp. 227–289.

Best, P.B. (1983). Sperm whale stock assessments and the relevance of historical whaling records. *Rep. Int. Whal. Comm.*, 5, 41–55.

Biggs, D.C., Leben, R.R. & Ortega-Ortiz, J.G. (2000). Ship and satellite studies of mesoscale circulation and sperm whale habitats in the Northeast Gulf of Mexico during GulfCet II. *Gulf Mex. Sci.*, 18, 15–22.

Bleck, R. (2002). An oceanic general circulation model in pressure coordinates. *Ocean Model.*, 37, 55–88.

Bond, N.A., Cronin, M.F., Freeland, H. & Mantua, N. (2015). Causes and impacts of the 2014 warm anomaly in the NE Pacific. *Geophys. Res. Lett.*, 42, 3414–3420.

Booth, C.G., Embling, C., Gordon, J., Calderan, S. V. & Hammond, P.S. (2013). Habitat preferences and distribution of the harbour porpoise Phocoena phocoena west of Scotland. *Mar. Ecol. Prog. Ser.*, 478, 273–285.

Bowles, F.A. (1997). Observations on attenuation and shear-wave velocity in fine-grained, marine sediments. *J. Acoust. Soc. Am.*, 101, 3385–3397.

Boyd, P.W. (1995). The NE subarctic Pacific in winter: I. Biological standing stocks. *Mar. Ecol. Prog. Ser.*, 128, 11–24.

Brodeur, R.D. & Ware, D.M. (1992). Long-term variability in zooplankton biomass in the subarctic Pacific Ocean. *Fish. Oceanogr.*, 1, 32–38.

Buckland, S.T. (2006). Point-transect surveys for songbirds: Robust methodologies. *Auk*, 123, 345–357.

Buckland, S.T., Anderson, D.R., Burnham, K.P., Laake, J.L., Borchers, D.L. & Thomas, L. (2001). *Introduction to distance sampling: estimating abundance of biological populations*. Oxford (United Kingdom) Oxford Univ. Press.

Caldwell, D.K., Caldwell, M.C. & Rice, D.W. (1966). Behavior of the sperm whale, Physeter catodon L. *Whales, dolphins and porpoises*, 677–717.

Camphuysen, C.J., Scott, B. & Wanless, S. (2007). Distribution and foraging interactions of seabirds and marine mammals in the North Sea: a metapopulation analysis. *Top predators Mar. Ecosyst. Their role Monit. Manag. Conserv. Biol.*

Carmack, E. & McLaughlin, F. (2011). Towards recognition of physical and geochemical change in Subarctic and Arctic Seas. *Prog. Oceanogr.*, 90, 90–104.

Carpinelli, E., Gauffier, P., Verborgh, P., Airoldi, S., David, L., Di-Méglio, N., *et al.* (2014). Assessing sperm whale (Physeter macrocephalus) movements within the western Mediterranean Sea through photo-identification. *Aquat. Conserv. Mar. Freshw. Ecosyst.*, 24, 23–30.

Carretta, J. V, Forney, K.A., Oleson, E.M., Weller, D.W., Lang, A.R., Baker, J., *et al.* (2020). U.S. Pacific Marine Mammal Stock Assessments: 2019.

Caruso, F., Sciacca, V., Bellia, G., Domenico, E. De, Larosa, G., Papale, E., *et al.* (2015). Size Distribution of Sperm Whales Acoustically Identified during Long Term Deep-Sea Monitoring in the Ionian Sea Size Distribution of Sperm Whales Acoustically Identified during Long Term Deep-Sea Monitoring in the Ionian Sea. *PLoS One*, 1–16.

Cavole, L.M., Demko, A.M., Diner, R.E., Giddings, A., Koester, I., Pagniello, C.M.L.S., *et al.* (2016). Biological impacts of the 2013–2015 warm-water anomaly in the northeast Pacific: Winners, Losers, and the Future. *Oceanography*, 29, 273–285.

Cecco, L. (2018). *Sighting of sperm whales in Arctic a sign of changing ecosystem, say scientists*. Available at: https://www.theguardian.com/environment/2018/nov/05/sperm-whales-canadian-arctic. Last accessed 15 May 2021.

CETAP, A. (1982). characterization of marine mammals and turtles in the mid-and north Atlantic areas of the USA outer continental shelf. Cetacean and Turtle Assessment Program, University of Rhode Island. *Final Report, Contract AA51-C78-48*.

Christal, J. & Whitehead, H. (1997). Aggregations of mature male sperm whales on the Galapagos Islands breeding ground. *Mar. Mammal Sci.*, 13, 59–69.

Christensen, I., Haug, T. & Oien, N. (1992). A review of feeding and reproduction in large baleen whales (Mysticeti) and sperm whales Physeter macrocephalus in Norwegian and adjacent waters. *Fauna Nor. Ser. A*, 13, 39–48.

Clarke, M.R. (1966). A Review of the Systematics and Ecology of Oceanic Squids. *Adv. Mar. Biol.*, 4, 91–300.

Clarke, M.R. (1976). Observation On Sperm Whale Diving. *J. Mar. Biol. Assoc. United Kingdom*, 56, 809–810.

Clarke, M.R. (1980). Cephalopoda in the diet of sperm whales of the southern hemisphere and their bearing on sperm whale biology. *Discov. Rep.*, 37, 1–324.

Clarke, R. (1956). *Sperm Whales of the Azores, &c*. University Press.

Comiso, J.C., Parkinson, C.L., Gersten, R. & Stock, L. (2008). Accelerated decline in the Arctic sea ice cover. *Geophys. Res. Lett.*, 35, 1–6.

Crawford, W.; McKinnell, S.; and Freeland, H. (2012). News of the Northeast Pacific Ocean. *PICES Press*, 20, 1–3.

Crawford, W. & Mckinnell, S. (2013). Continuing Cool in the Northeast Pacific Ocean, 21, 2012–2013.

Crawford, W.R., Brickley, P.J. & Thomas, A.C. (2007). Mesoscale eddies dominate surface phytoplankton in northern Gulf of Alaska. *Prog. Oceanogr.*, 75, 287–303.

Cucknell, A.-C., Boisseau, O. & Moscrop, A. (2015). *A Review of the Impact of Seismic Survey Noise on Narwhals and other Arctic Cetaceans*.

Cummins, P.F. & Lagerloef, G.S.E. (2002). Low-frequency pycnocline depth variability at Ocean Weather Station P in the northeast Pacific. *J. Phys. Oceanogr.*, 32, 3207–3215.

CWS. (2021). *Environment and Climate Change Canada. East. Canada Seabirds Sea v. 3.64*.

D'Errico, J. (2023). *inpaint_nans*. *MATLAB Cent. File Exch.* Available at: https://www.mathworks.com/matlabcentral/fileexchange/4551-inpaint_nans. Last accessed 7 March 2023.

Das, K., Lepoint, G., Leroy, Y. & Bouquegneau, J.M. (2003). Marine mammals from the southern North Sea: Feeding ecology data from δ13C and δ15N measurements. *Mar. Ecol. Prog. Ser.*, 263, 287–298.

Davidson, E. (2016). Exploring the Characteristics of Spatial Distribution for Sperm Whales (Physeter macrocephalus) and Northern Bottlenose Whales (Hyperoodon ampullatus) in the Arctic: A Preliminary Study to Inform Conservation Management. *PhD Diss. Univ. Akureyri*.

Dawe, E.G., Bowering, W.R. & Joy, J.B. (1998). Predominance of squid (Gonatus spp.) in the diet of Greenland halibut (Reinhardtius hippoglossoides) on the deep slope of the northeast Newfoundland continental shelf. *Fish. Res.*, 36, 267–273.

Dede, A., Öztürk, A.A., Tonay, A.M., Uğur, Ö., Gönülal, O., Öztürk, B., *et al.* (2022). Cetacean sightings in the Finike Seamounts area and adjacent waters during the surveys in 2021. *J. Black Sea Mediterr. Environ.*, 28, 221–239.

Diogou, N., Palacios, D.M., Nieukirk, S.L., Nystuen, J.A., Papathanassiou, E., Katsanevakis, S., *et al.* (2019a). Sperm whale (Physeter macrocephalus) acoustic ecology at Ocean Station

PAPA in the Gulf of Alaska – Part 1: Detectability and seasonality. *Deep. Res. Part I Oceanogr. Res. Pap.*, 150, 103047.

Diogou, N., Palacios, D.M., Nystuen, J.A., Papathanassiou, E., Katsanevakis, S. & Klinck, H. (2019b). Sperm whale (Physeter macrocephalus)acoustic ecology at Ocean Station PAPA in the Gulf of Alaska – Part 2: Oceanographic drivers of interannual variability. *Deep. Res. Part I Oceanogr. Res. Pap.*, 150, 103044.

Dohl, T.P. (1983). *Cetaceans of central and northern California, 1980-1983: status, abundance, and distribution*. Pacific OCS Region, Minerals Management Service, US Department of the Interior.

Drouot, V., Gannier, A. & Goold, J.C. (2004). Summer social distribution of sperm whales (Physeter macrocephalus) in the Mediterranean Sea. *J. Mar. Biol. Assoc. United Kingdom*, 84, 675–680.

Ducet, N., Le Traon, P.Y. & Reverdin, G. (2000). Global high-resolution mapping of ocean circulation from TOPEX/Poseidon and ERS-1 and -2. *J. Geophys. Res. Ocean.*, 105, 19477–19498.

Dufault, S., Whitehead, H. & Dillon, M. (1999). An examination of the current knowledge on the stock structure of sperm whales (Physeter macrocephalus) worldwide. *J. Cetacean Res. Manag.*, 1, 1–10.

E.U. Copernicus Marine Service Information (CMEMS). (2023). *Global Ocean Ensemble Physics Reanalysis*. *Mar. Data Store*. Available at: https://data.marine.copernicus.eu/product/GLOBAL_REANALYSIS_PHY_001_031/description. Last accessed 8 January 2023.

Efron, B. & Tibshirani, R.J. (1993). Chapter 17: Cross-Validation. *An Introd. to Bootstrap*, 436.

Engelhaupt, D., Rus Hoelzel, A., Nicholson, C., Frantzis, A., Mesnick, S., Gero, S., *et al.* (2009). Female philopatry in coastal basins and male dispersion across the North Atlantic in a highly mobile marine species, the sperm whale (Physeter macrocephalus). *Mol. Ecol.*, 18, 4193–4205.

Evans, P.G.H. (1997). Ecology of sperm whales (Physeter macrocephalus) in the Eastern North Atlantic, with special reference to sightings & strandings records from the British Isles. *Bull. L'Institut R. Des Sci. Nat. Belgique*, 37–46.

Fearnbach, H., Durban, J.W., Mizroch, S.A., Barbeaux, S. & Wade, P.R. (2014). Winter observations of a group of female and immature sperm whales in the high-latitude waters near the Aleutian Islands, Alaska. *Mar. Biodivers. Rec.*, 5, 1–4.

Finley, K.J. & Gibb, E.J. (1982). Summer diet of the narwhal (Monodon monoceros) in Pond Inlet, northern Baffin Island. *Can. J. Zool.*, 60, 3353–3363.

Ford, J.D., Smit, B. & Wandel, J. (2006). Vulnerability to climate change in the Arctic: A case

study from Arctic Bay, Canada. *Glob. Environ. Chang.*, 16, 145–160.

Forney, K.A., Barlow, J. & Carretta, J. V. (1995). The abundance of cetaceans in California waters. Part II: Aerial surveys in winter and spring of 1991 and 1992. *Oceanogr. Lit. Rev.*, 9, 784–785.

Forsythe, J.W. (2004). Accounting for the effect of temperature on squid growth in nature: From hypothesis to practice. *Mar. Freshw. Res.*, 55, 331–339.

Fox, J. (2019). John Fox and Sanford Weisberg. *An R companion to Appl. regression, 3rd ed Sage Publ. Sch.*

Fox, J. & Monette, G. (1992). Generalized collinearity diagnostics. *J. Am. Stat. Assoc.*, 87, 178–183.

Francois, R.E. & Garrison, G.R. (1982). Sound absorption based on ocean measurements. Part II: Boric acid contribution and equation for total absorption. *J. Acoust. Soc. Am.*, 72, 1879–1890.

Frasier, K.E. (2015). Density estimation of delphinids using passive acoustics: A case study in the Gulf of Mexico. University of California, San Diego.

Fristrup, K.M. & Harbison, G.R. (2002). How do sperm whales catch squids? *Mar. Mammal Sci.*, 18, 42–54.

Frouin-Mouy, H., Kowarski, K., Martin, B. & Bröker, K. (2017). Seasonal Trends in Acoustic Detection of Marine Mammals in Baffin Bay and Melville Bay , Northwest Greenland. *Arctic*, 70, 59–76.

Gardiner, K. & Dick, T.A. (2010). Arctic cephalopod distributions and their associated predators. *Polar Res.*, 29, 209–227.

Gaskin, D.E. (1970). Composition of schools of sperm whales physeter catodon linn. East of New Zealand. *New Zeal. J. Mar. Freshw. Res.*, 4, 456–471.

Gaskin, D.E. & MW, C. (1973). Sperm whales (Physeter catodon L.) in the Cook Strait region of New Zealand: some data on age, growth and mortality.

Gelman, A. & Hill, J. (2007). *Data analysis using regression and multilevel/hierarchical models*. Cambridge University Press.

Gero, S. (2005). Fundamentals of sperm whale societies, care for calves.

Gero, S., Gordon, J.C.D., Carlson, C., Evans, P. & Whitehead, H. (2007). Population estimate and inter-island movement of sperm whales, *Physeter macrocephalus*, in the Eastern Caribbean. *J. Cetacean Res. Manag.*

Gershunov, A. & Barnett, T.P. (1998). Interdecadal Modulation of ENSO Teleconnections. *Bull.*

Am. Meteorol. Soc., 79, 2715–2725.

Gilmore, R.M. (1959). On the mass strandings of sperm whales. *Pacific Nat.*, 1, 9–16.

Gjerdrum, C., Fifield, D.A. & Wilhelm, S.I. (2012). *Eastern Canada Seabirds at Sea (ECSAS) standardized protocol for pelagic seabird surveys from moving and stationary platforms*. *Can. Wilidlife Serv. Tech. Rep. Ser. No. 515*.

Goode, G.B. (1887). *The fisheries and fishery industries of the United States*. US Government Printing Office.

Goold, J.C. & Jones, S.E. (1995). Time and frequency domain characteristics of sperm whale clicks. *J. Acoust. Soc. Am.*, 98, 1279–1291.

Gordon, A.L. & Giulivi, C.F. (2004). Pacific decadal oscillation and sea level in the Japan/East sea. *Deep. Res. Part I Oceanogr. Res. Pap.*, 51, 653–663.

Gordon, J.C.D. (1987). Sperm whale groups and social behaviour observed off Sri Lanka. *Rep. Int. Whal. Comm.*, 37, 205–217.

Gordon, J.C.D. (1991). Evaluation of a method for determining the length of sperm whales (*Physeter catodon*) from their vocalizations. *J. Zool. London*, 224, 301–314.

Gregr, E.J., Baumgartner, M.F., Laidre, K.L. & Palacios, D.M. (2013). Marine mammal habitat models come of age: The emergence of ecological and management relevance. *Endanger. Species Res.*, 22, 205–212.

Gregr, E.J., Nichol, L., Ford, J.K.B., Ellis, G. & Trites, A.W. (2000). Migration and population structure of northeastern Pacific whales off coastal British Columbia: An analysis of commercial whaling records from 1908-1967. *Mar. Mammal Sci.*, 16, 699–727.

Gregr, E.J. & Trites, A.W. (2001). Predictions of critical habitat for five whale species in the waters of coastal British Columbia. *Can. J. Fish. Aquat. Sci.*, 58, 1265–1285.

Griffin, R.B. (1999). Sperm whale distributions and community ecology associated with a warm-core ring off Georges Bank. *Mar. Mammal Sci.*, 15, 33–51.

Growcott, A., Miller, B., Sirguey, P., Slooten, E. & Dawson, S. (2011). Measuring body length of male sperm whales from their clicks: The relationship between inter-pulse intervals and photogrammetrically measured lengths. *J. Acoust. Soc. Am.*, 130, 568–573.

Guisan, A. & Zimmermann, N.E. (2000). Predictive habitat distribution models in ecology. *Ecol. Modell.*, 135, 147–186.

Halekoh, U., Højsgaard, S. & Yan, J. (2006). The R package geepack for generalized estimating equations. *J. Stat. Softw.*, 15, 1–11.

Hamer, D.J., Childerhouse, S.J. & Gales, N.J. (2012). Odontocete bycatch and depredation in

longline fisheries: A review of available literature and of potential solutions. *Mar. Mammal Sci.*, 28, 345–374.

Hamilton, E.L. (1976). Shear-Wave Velocity Versus Depth in Marine Sediments: a Review. *Geophysics*, 41, 985–996.

Hamilton, E.L. (1980). Geoacoustic modeling of the sea floor. *J. Acoust. Soc. Am.*, 68, 1313–1340.

Hann, C.H., Smith, T.D. & Torres, L.G. (2016). A sperm whale's perspective: The importance of seasonality and seamount depth. *Mar. Mammal Sci.*, 32, 1470–1481.

Happywhale. (2021). *Happywhale - Sperm Whale in North Atlantic Ocean. Data downloaded from OBIS-SEAMAP*. Available at: http://seamap.env.duke.edu/dataset/1726. Last accessed 5 May 2021.

Hartvedt, S. (2020). *Incidental sightings of marine mammals. Data downloaded from OBIS-SEAMAP (http://seamap.env.duke.edu/dataset/103152572)*. Available at: https://obis.org/dataset/dd335e79-f580-44a1-bedc-1476437eb73e). Last accessed 5 May 2021.

Hassol, S.J. (2004). *Impacts of a warming Arctic-Arctic climate impact assessment*. Cambridge University Press, Canada.

Hastie, T. & Tibshirani, R. (1987). Generalized additive models: Some applications. *J. Am. Stat. Assoc.*, 82, 371–386.

Hatch, S.A. (2013). Kittiwake diets and chick production signal a 2008 regime shift in the Northeast Pacific. *Mar. Ecol. Prog. Ser.*, 477, 271–284.

Hauri, C., Pagès, R., McDonnell, A.M.P., Stuecker, M.F., Danielson, S.L., Hedstrom, K., *et al.* (2021). Modulation of ocean acidification by decadal climate variability in the Gulf of Alaska. *Commun. Earth Environ.*, 2, 191.

Hayes, S., Josephson, E., Maze-Foley, K., Rosel, P.E. & Wallace, J. (2022). U.S. Atlantic and Gulf of Mexico Marine Mammal Stock Assessments 2021. *NOAA Tech. Memo. NMFS-NE-288*, 380.

Hazen, E.L., Jorgensen, S., Rykaczewski, R.R., Bograd, S.J., Foley, D.G., Jonsen, I.D., *et al.* (2013). Predicted habitat shifts of Pacific top predators in a changing climate. *Nat. Clim. Chang.*, 3, 234–238.

Heide-Jørgensen, M.P. & Teilmann, J. (1994). Growth, reproduction, age structure, and feeding habits of white whales (Delphinapterus leucas) in West Greenland waters. *Bioscience*, 39, 195–212.

Helble, T. a, D'Spain, G.L., Hildebrand, J. a, Campbell, G.S., Campbell, R.L. & Heaney, K.D. (2013). Site specific probability of passive acoustic detection of humpback whale calls from

single fixed hydrophones. *J. Acoust. Soc. Am.*, 134, 2556–70.

Helsel, D.R., Hirsch, R.M., Ryberg, K.R., Archfield, S.A. & Gilroy, E.J. (2020). Statistical Methods in Water Resources Techniques and Methods 4 – A3. *USGS Tech. Methods*, 458.

Higdon, J.W. & Ferguson, S.H. (2009). *Loss of Arctic Sea Ice Causing Punctuated Change in Sightings of Killer Whales (Orcinus Orca) over the Past Century. Source Ecol. Appl.*

Higdon, J.W. & Ferguson, S.H. (2011). Reports of humpback and minke whales in the hudson bay region, Eastern Canadian arctic. *Northeast. Nat.*, 18, 370–377.

Higdon, J.W. & Ferguson, S.H. (2018). Reports of Humpback and Minke Whales in the Hudson Bay Region , Eastern Canadian Arctic Author (s): Jeff W . Higdon and Steven H . Ferguson Published by : Eagle Hill Institute Stable URL : http://www.jstor.org/stable/41315968 REFERENCES Linked reference, 18, 370–377.

Hildebrand, J.A., Frasier, K.E., Baumann-pickering, S., Wiggins, S.M., Merkens, K.P., Garrison, L.P., *et al.* (2019). Assessing Seasonality and Density From Passive Acoustic Monitoring of Signals Presumed to be From Pygmy and Dwarf Sperm Whales in the Gulf of Mexico, 6, 1–17.

Hildebrand, J., Merkens, K., Frasier, K., Bassett, H., Baumann-pickering, S., Ana, Š., *et al.* (2012). *Passive acoustic monitoring of cetaceans in the northern Gulf of Mexico during 2010-2011.*

Hillson, R., Shyu, H.J. & DC, N.R.L.A.B.W. (2007). Modeling and Simulation Architecture for the Effects of Sound on the Marine Environment (ESME).

Holland, M.M., Bitz, C.M. & Tremblay, B. (2006). Future abrupt reductions in the summer Arctic sea ice. *Geophys. Res. Lett.*, 33, 1–5.

Huang, X., Acero, A. & Hon, H.-W. (2001). *Spoken Languace Processing*. Prentice Hall PTR, Upper Saddle River, NJ.

Hyndman, R., Athanasopoulos, G., Bergmeir, C., Caceres, G., Chhay, L., O'Hara-Wild, M Petropoulos, F., *et al.* (2023). *forecast: Forecasting functions for time series and linear models. R Packag. version 8.21*. Available at: https://pkg.robjhyndman.com/forecast/. Last accessed .

Insley, S.J., Halliday, W.D., Mouy, X. & Diogou, N. (2021). Bowhead whales overwinter in the Amundsen Gulf and Eastern Beaufort Sea. *R. Soc. Open Sci.*, 8.

Irvine, L., Palacios, D.M., Urbán, J. & Mate, B. (2017). Sperm whale dive behavior characteristics derived from intermediate-duration archival tag data. *Ecol. Evol.*, 1–16.

Ivashchenko, Y. V., Brownell, R.L. & Clapham, P.J. (2014). Distribution of Soviet catches of sperm whales Physeter macrocephalus in the North Pacific. *Endanger. Species Res.*, 25, 249–263.

Jackson, J.M., Carmack, E.C., McLaughlin, F.A., Allen, S.E. & Ingram, R.G. (2010). Identification, characterization, and change of the near-surface temperature maximum in the Canada Basin, 1993-2008. *J. Geophys. Res. Ocean.*, 115, 1–16.

Jackson, J.M., Myers, P.G. & Ianson, D. (2006). An examination of advection in the northeast Pacific Ocean, 2001-2005. *Geophys. Res. Lett.*, 33, 2001–2005.

Jacox, M.G., Alexander, M.A., Amaya, D., Becker, E., Bograd, S.J., Brodie, S., *et al.* (2022). Global seasonal forecasts of marine heatwaves. *Nature*, 604, 486–490.

Jaquet, N. (2006). A simple photogrammetric technique to measure sperm whales at sea. *Mar. Mammal Sci.*, 22, 862–879.

Jaquet, N. & Gendron, D. (2002). Distribution and relative abundance of sperm whales in relation to key environmental features, squid landings and the distribution of other cetacean species in the Gulf of California, Mexico. *Mar. Biol.*, 141, 591–601.

Jaquet, N. & Gendron, D. (2009). The social organization of sperm whales in the gulf of California and comparisons with other populations. *J. Mar. Biol. Assoc. United Kingdom*, 89, 975–983.

Jaquet, N. & Whitehead, H. (1996). Scale-dependent correlation of sperm whale distribution with environmental features and productivity in the South Pacific. *Mar. Ecol. Prog. Ser.*, 135, 1–9.

Jensen, F.H., Johnson, M., Ladegaard, M., Wisniewska, D.M. & Madsen, P.T. (2018). Narrow Acoustic Field of View Drives Frequency Scaling in Toothed Whale Biosonar. *Curr. Biol.*, 1–8.

Jochens, a., Jochens, a., Biggs, D., Biggs, D., Benoit-Bird, K., Benoit-Bird, K., *et al.* (2008). Sperm whale seismic study in the Gulf of Mexico. Synthesis Report. *Mms*, 96, 3268.

Jones, J.M., Frasier, K.E., Westdal, K.H., Ootoowak, A.J., Wiggins, S.M. & Hildebrand, J.A. (2022). Beluga (Delphinapterus leucas) and narwhal (Monodon monoceros) echolocation click detection and differentiation from long-term Arctic acoustic recordings. *Polar Biol.*

Kahru, M. (2001). Windows image manager: image display and analysis program for Microsoft Windows with special features for satellite images.

Kasuya, T. & Miyashita, T. (1988). Distribution of sperm whale stocks in the North Pacific. *Sci. Reports Whales Res. Inst. Tokyo 3931-75. 1988.*, 39, 45.

Kato, H. (1984). Observations on tooth scars on the head of male sperm whale, as an indication of intra-sexual fightings. *Sci. Reports Whales Res. Inst.*, 35, 39–46.

Kattsov, V.M., Källén, E., Cattle, H.P., Christensen, J., Drange, H., Hanssen-Bauer, I., *et al.* (2005). Future climate change: modeling and scenarios for the Arctic. In: *Arctic Climate Impact Assessment*. Cambridge University Press, Cambridge, UK.

Kawakami, T. (1980). A review of sperm whale food. *Sci. Reports Whales Res. Inst.*, 32, 199–218.

Kobayashi, H., Whitehead, H. & Amano, M. (2020). Long-term associations among male sperm whales (Physeter macrocephalus). *PLoS One*, 15, 1–14.

Kooyman, G.L., Castellini, M.A. & Davis, R.W. (1981). Physiology of diving in marine mammals. *Annu. Rev. Physiol.*, 43, 343–356.

Koptenko, S. (2023). *Sound Speed in Sea Water*. *MATLAB Cent. File Exch.* Available at: https://www.mathworks.com/matlabcentral/fileexchange/4940-sound-speed-in-sea-water. Last accessed 7 March 2023.

Küsel, E.T., Mellinger, D.K., Thomas, L., Marques, T.A., Moretti, D. & Ward, J. (2011). Cetacean population density estimation from single fixed sensors using passive acoustics. *J. Acoust. Soc. Am.*, 129, 3610–3622.

Laidre, K.L., Stern, H., Kovacs, K.M., Lowry, L., Moore, S.E., Regehr, E. V., *et al.* (2015). Arctic marine mammal population status, sea ice habitat loss, and conservation recommendations for the 21st century. *Conserv. Biol.*, 29, 724–737.

Lee, D.S. & Wenzel, G.W. (2006). Narwhal hunting by Pond Inlet Inuit: An analysis of foraging mode in the floe-edge environment. *Études/Inuit/Studies*, 28, 133–157.

Lefort, K.J., Hussey, N.E., Jones, J.M., Johnson, K.F. & Ferguson, S.H. (2022). Satellite-tracked sperm whale migrates from the Canadian Arctic to the subtropical western North Atlantic. *Mar. Mammal Sci.*, 1–7.

Liang, K.Y. & Zeger, S.L. (1986). Longitudinal data analysis using generalized linear models. *Biometrika*, 73, 13–22.

Litzow, M.A., Ciannelli, L., Puerta, P., Wettstein, J.J., Rykaczewski, R.R. & Opiekun, M. (2018). Non-stationary climate-salmon relationships in the Gulf of Alaska. *Proc. R. Soc. B Biol. Sci.*, 285.

Lohrenz, S.E., Redalje, D.G., Verity, P.G., Flagg, C.N. & Matulewski, K. V. (2002). *Primary production on the continental shelf off Cape Hatteras, North Carolina*. *Deep. Res. Part II Top. Stud. Oceanogr.*

Di Lorenzo, E., Schneider, N., Cobb, K.M., Franks, P.J.S., Chhak, K., Miller, A.J., *et al.* (2008). North Pacific Gyre Oscillation links ocean climate and ecosystem change. *Geophys. Res. Lett.*, 35, 2–7.

Lüdecke, D., Ben-Shachar, M., Patil, I., Waggoner, P. & Makowski, D. (2021). performance: An R Package for Assessment, Comparison and Testing of Statistical Models. *J. Open Source Softw.*, 6, 3139.

Mackenzie, K. V. (1981). Nine-term equation for sound speed in the oceans. *J. Acoust. Soc. Am.*,

70, 807–812.

Madsen, P.T., Wahlberg, M. & Møhl, B. (2002). Male sperm whale (Physeter macrocephalus) acoustics in a high-latitude habitat: Implications for echolocation and communication. *Behav. Ecol. Sociobiol.*, 53, 31–41.

Mantua, N.J. (2023). *Pacific Decadal Oscillation (PDO).* Available at: https://www.ncei.noaa.gov/access/monitoring/pdo/. Last accessed 1 October 2023.

Mantua, N.J. & Hare, S.R. (2002). The Pacific Decadal Oscillation. *J. Oceanogr.*

Mantua, N.J., Hare, S.R., Zhang, Y., Wallace, J.M. & Francis, R.C. (1997). A Pacific Interdecadal Climate Oscillation with Impacts on Salmon Production. *Bull. Am. Meteorol. Soc.*, 78, 1069–1079.

Marques, T.A., Thomas, L., Ward, J., DiMarzio, N. & Tyack, P.L. (2009). Estimating cetacean population density using fixed passive acoustic sensors: An example with Blainville's beaked whales. *J. Acoust. Soc. Am.*, 125, 1982–1994.

Martins, A.M. & Pelegrí, J.L. (2006). CZCS chlorophyll patterns in the South Atlantic Bight during low vertical stratification conditions. *Cont. Shelf Res.*, 26, 429–457.

Masson-Delmotte, V., Zhai, P., Pirani, A., Connors, S.L., Péan, C., Berger, S., *et al.* (2020). *IPCC, 2021: Summary for Policymakers. Clim. Chang. 2021 Phys. Sci. Basis. Contrib. Work. Gr. I to Sixth Assess. Rep. Intergov. Panel Clim. Chang.*

Mate, B.R., Irvine, L.M. & Palacios, D.M. (2017). The development of an intermediate-duration tag to characterize the diving behavior of large whales. *Ecol. Evol.*, 7, 585–595.

Mathias, D., Thode, A.M., Straley, J. & Andrews, R.D. (2013). Acoustic tracking of sperm whales in the Gulf of Alaska using a two-element vertical array and tags. *J. Acoust. Soc. Am.*, 134, 2446–2461.

Maury, M.F. (1851). *"Whale Chart." Map. Washington, D.C. U.S. Navy, Natl. Obs. Norman B. Leventhal Map Educ. Cent.* Available at: https://collections.leventhalmap.org/search/commonwealth:x633f952x. Last accessed .

McClain, C.R., Balk, M.A., Benfield, M.C., Branch, T.A., Chen, C., Cosgrove, J., *et al.* (2015). Sizing ocean giants: Patterns of intraspecific size variation in marine megafauna. *PeerJ*, 2015.

Mellinger, K., Stafford, M. & Fox, G. (2004). Seasonal Occurence of Sperm Whale (Physeter Macrocephalus) Sounds in the Gulf of Alaska, 1999-2001. *Mar. Mammal Sci.*, 20, 48–62.

Merkens, K., Simonis, A. & Oleson, E. (2019). Geographic and temporal patterns in the acoustic detection of sperm whales Physeter macrocephalus in the central and western North Pacific Ocean. *Endanger. Species Res.*, 39, 115–133.

Merrick, R.L., Chumbley, M.K. & Byrd, G.V. (1997). Diet diversity of Steller sea lions (Eumetopias jubatus) and their population decline in Alaska: a potential relationship. *Can. J. Fish. Aquat. Sci.*, 54, 1342–1348.

Mesnick, S.L., Taylor, B.L., Archer, F.I., Martien, K.K., Treviño, S.E., Hancock-Hanser, B.L., *et al.* (2011). Sperm whale population structure in the eastern and central North Pacific inferred by the use of single-nucleotide polymorphisms, microsatellites and mitochondrial DNA. *Mol. Ecol. Resour.*, 11, 278–298.

Mizroch, S.A. & Rice, D.W. (2013). Ocean nomads: Distribution and movements of sperm whales in the North Pacific shown by whaling data and Discovery marks. *Mar. Mammal Sci.*, 29, 136–165.

Møhl, B., Wahlberg, M., Madsen, P.T., Heerfordt, A. & Lund, A. (2003). The monopulsed nature of sperm whale clicks. *J. Acoust. Soc. Am.*, 114, 1143–1154.

Møhl, B., Wahlberg, M., Madsen, P.T., Miller, L.A. & Surlykke, A. (2000). Sperm whale clicks: Directionality and source level revisited. *J. Acoust. Soc. Am.*, 107, 638–648.

Moore, J.E. & Barlow, J.P. (2014). Improved abundance and trend estimates for sperm whales in the eastern North Pacific from Bayesian hierarchical modeling. *Endanger. Species Res.*, 25, 141–150.

Moors-Murphy, H.B. (2014). Submarine canyons as important habitat for cetaceans, with special reference to the Gully: A review. *Deep. Res. Part II Top. Stud. Oceanogr.*, 104, 6–19.

Morato, T., Varkey, D.A., Damaso, C., Machete, M., Santos, M., Prieto, R., *et al.* (2008). Evidence of a seamount effect on aggregating visitors. *Mar. Ecol. Prog. Ser.*, 357, 23–32.

Mullin, K.D., Steiner, L., Dunn, C., Claridge, D., García, L.G., Gordon, J., *et al.* (2022). Long-Range Longitudinal Movements of Sperm Whales (Physeter macrocephalus) in the North Atlantic Ocean Revealed by Photo-Identification. *Aquat. Mamm.*, 48, 3–8.

Mullins, J., Whitehead, H. & Weilgart, L.S. (1988). Behaviour and vocalizations of two single sperm whales, Physeter macrocephalus, off Nova Scotia. *Can. J. Fish. Aquat. Sci.*, 45, 1736–1743.

NAFO. (2014). *NAFO/ICNAF - Environmental Surveys - NORWESTLANT 1-3, 1963: Fish eggs and larvae*. Available at: https://obis.org/dataset/cf78d68d-fc40-4f89-81ed-d64462660175. Last accessed 5 May 2021.

Nakamoto, S., Prasanna Kumar, S., Oberhuber, J.M., Ishizaka, J., Muneyama, K. & Frouin, R. (2001). Response of the equatorial Pacific to chlorophyll pigment in a mixed layer isopycnal ocean general circulation model. *Geophys. Res. Lett.*, 28, 2021–2024.

NASA/GSFC/OBPG. (2023). *Chlorophyll-a, Aqua MODIS, NPP, L3SMI, Global, 4km, Science Quality, 2003-present (1 Day Composite), Lon0360*. Available at: https://coastwatch.pfeg.noaa.gov/erddap/griddap/erdMH1chla1day_Lon0360.html. Last

accessed 1 August 2023.

Nash, R.D.M., Magnuson, J.J., Stanton, T.K. & Clay, C.S. (1989). Distribution of peaks of 70 kHz acoustic scattering in relation to depth and temperature during day and night at the edge of the Gulf Stream-EchoFront 83. *Deep Sea Res. Part A, Oceanogr. Res. Pap.*, 36, 587–596.

National Marine Fisheries Service. (2021). *State of the ecosystem: Mid-Atlantic. NOAA Fish.*

Naval Oceanographic Office. (2003). *Database Description for Bottom Sediment type (U).*

NEFSC & SEFSC. (2021). *Annual Report of a Comprehensive Assessment of Marine Mammal, Marine Turtle, and Seabird Abundance and Spatial Distribution in US waters of the Western North Atlantic Ocean – AMAPPS III. NOAA Tech. Rep. NMFS.*

Nishiwaki, M. (1966). Distribution and migration of the larger cetaceans in the North Pacific as shown by Japanese whaling results. *Whales, dolphins porpoises. Univ. Calif. Press. Berkeley*, 171–191.

Nishiwaki, M., Ohsumi, S. & Maeda, Y. (1963). Change of form in the sperm whale accompanied with growth. *Sci. Reports Whales Res. Inst.*, 17, 1–14.

NOAA Climate Prediction Center. (2023). *Oceanic Niño Index.* Available at: https://origin.cpc.ncep.noaa.gov/products/analysis_monitoring/ensostuff/ONI_v5.php. Last accessed .

NOAA NMFS SWFSC ERD. (2023). *SST, AQUA_MODIS, L3m.DAY.SST.sst.4km, Masked, SMI, NASA GSFC OBPG, R2019.0, Global, 0.04166°, Science Quality, 2003-2022 (Daily), Lon0360.* Available at: https://coastwatch.pfeg.noaa.gov/erddap/griddap/erdMH1sstd1dayR20190SQ_Lon0360.html. Last accessed 8 January 2023.

Norris, K.S. & Harvey, G.W. (1972). A Theory for the Function of the Spermaceti Organ of the Sperm Whale (Physeter catodon L.). *Anim. Obs. Navig.*, 397–417.

Nowak, R.M. (2003). *Walker's Marine Mammals of the World.* The Johns Hopkins University Press, Baltimore.

Ohsumi, S. (1965). Reproduction of the sperm whale in the north-west Pacific. *Sci. Reports Whales Res. Institute, Tokyo*, 19, 1–35.

Ohsumi, S. (1966). Sexual segregation of the sperm whale in the North Pacific. *Sci Rep Whales Res Inst*, 20, 1–16.

Okutani, T. & Nemoto, T. (1964). *Squids as the food of sperm whales in the Bering Sea and Alaska Gulf. Tokai Reg. Fish. Lab. Rep. No. 18.*

Olson, S., Jansen, M.F., Abbot, D.S., Halevy, I. & Goldblatt, C. (2022). The Effect of Ocean

Salinity on Climate and Its Implications for Earth's Habitability. *Geophys. Res. Lett.*, 49, 1–9.

Omura, H. (1950). On the Body. Weight of Sperm and Sei Whales located in the Adjacent Waters of Japan. *Sci. Reports Whales Res. Inst.*, 4, 27–113.

Ormseth, O.A. (2017). *Assessment of the squid stock complex in the Gulf of Alaska*. *Exec. Summ.*

Orr, D.C. & Bowering, W.R. (1997). A multivariate analysis of food and feeding trends among Greenland halibut (Reinhardtius hippoglossoides) sampled in Davis Strait, during 1986. *ICES J. Mar. Sci.*, 54, 819–829.

Palacios, D.M., Baumgartner, M.F., Laidre, K.L. & Gregr, E.J. (2013). Beyond correlation: Integrating environmentally and behaviourally mediated processes in models of marine mammal distributions. *Endanger. Species Res.*, 22, 191–203.

Palka, D. (2020). Cetacean Abundance in the US Northwestern Atlantic Ocean Summer 2016, 60.

Palka, D.L., Chavez-Rosales, S., Josephson, E., Cholewiak, D., Haas, H.L., Garrison, L., *et al.* (2017). *Atlantic Marine Assessment Program for Protected Species: 2010-2014*. Washington, DC.

Palka, Aichinger, Dias, Broughton, Chavez-Rosales, Cholewiak, *et al.* (2021). *Atlantic Marine Assessment Program for Protected Species: FY15 - FY19*.

Pan, W. (2001). Akaike's Informat ion Criterion in Generalized Estimating Equations. *Biometrics*, 57, 120–125.

Panigada, S., Zanardelli, M., MacKenzie, M., Donovan, C., Mélin, F. & Hammond, P.S. (2008). Modelling habitat preferences for fin whales and striped dolphins in the Pelagos Sanctuary (Western Mediterranean Sea) with physiographic and remote sensing variables. *Remote Sens. Environ.*, 112, 3400–3412.

Peterson, W.T., Robert, M. & Bond, N. (2016). The Blob is gone but has morphed into a strongly positive PDO/SST pattern. *PICES Press*, 21, 44–46.

Piatt, J.F. & Anderson, P. (1996). Response of Common Murres to the Exxon Valdez Oil Spill and Long-Term Changes in the Gulf of Alaska Marine Ecosystem. *Am. Fish. Soc. Symp.*, 18, 720–737.

Pierce, G.J., Santos, M.B., Smeenk, C., Saveliev, A. & Zuur, A.F. (2007). Historical trends in the incidence of strandings of sperm whales (Physeter macrocephalus) on North Sea coasts: An association with positive temperature anomalies. *Fish. Res.*, 87, 219–228.

Pike, G.C. (1965). Schooling and migration of sperm whales off British Columbia. *Unpubl. Manuscript, 18pp.*

Pirotta, E., Matthiopoulos, J., Mackenzie, M., Scott-hayward, L. & Rendell, L. (2011). Modelling sperm whale habitat preference : a novel approach combining transect and follow data. *Mar. Ecol. Prog. Ser.*, 436, 257–272.

Pisha, L.A., Snider, J., Jackson, K. & Jaffe, J.S. (2023). Introducing bellhopcxx/bellhopcuda: Modern, parallel BELLHOP(3D). *J. Acoust. Soc. Am.*, 153.

Polyak, L., Alley, R.B., Andrews, J.T., Brigham-Grette, J., Cronin, T.M., Darby, D.A., *et al.* (2010). History of sea ice in the Arctic. *Quat. Sci. Rev.*, 29, 1757–1778.

Popov, I. & Eichhorn, G. (2020). Occurrence of sperm whale (Physeter macrocephalus) in the Russian Arctic. *Polar Res.*, 39, 1–6.

Porter, M.B. & Bucker, H.P. (1987). Gaussian beam tracing for computing ocean acoustic fields. *J. Acoust. Soc. Am.*, 82, 1349–1359.

Potty, G.R., Miller, J.H. & Lynch, J.F. (2006). Sediment models for the East Coast based on a priori information, geological data, and sediment inversions. *J. Acoust. Soc. Am.*, 119, 3226.

Praca, E., Gannier, A., Das, K. & Laran, S. (2009). Modelling the habitat suitability of cetaceans: Example of the sperm whale in the northwestern Mediterranean Sea. *Deep. Res. Part I Oceanogr. Res. Pap.*, 56, 648–657.

R Core Team. (2022). R: A language and environment for statistical computing. *R Found. Stat. Comput.*

Redfern, J.V., Ferguson, M.C., Becker, E.A., Hyrenback, K.D., Good, C., Barlow, J., *et al.* (2006). Techniques for cetacean–habitat modeling. *Mar. Ecol. Prog. Ser.*, 310, 271–295.

Reid, J.L. (1973). The shallow salinity minima of the Pacific Ocean. *Deep. Res. Oceanogr. Abstr.*, 20, 51–68.

Rice, A., Širović, A., Trickey, J.S., Debich, A.J., Gottlieb, R.S., Wiggins, S.M., *et al.* (2021). Cetacean occurrence in the Gulf of Alaska from long - term passive acoustic monitoring. *Mar. Biol.*, 1–29.

Rice, D.W. (1974). CHAPTER 6. WHALES AND WHALE RESEARCH IN THE EASTERN NORTH PACIFIC Dale W. Rice. In: *The Whale Problem: A Status Report*. Harvard University Press, pp. 170–195.

Rice, D.W. (1989). Sperm whale Physter macrocephalus Linneaus. In: *Handbook of Marine Mammals* (eds. Ridgway, S.H. & Harrison, R.J.). Academic Press, London, U.K., pp. 177–233.

Rob J. Hyndman & Yeasmin Khandakar. (2008). Automatic Time Series Forecasting: The forecast Package for R. *J. Stat. Softw.*, 27, 22.

Roberts, J.J., Best, B.D., Mannocci, L., Fujioka, E., Halpin, P.N., Palka, D.L., *et al.* (2016).

Density Model for Sperm Whale (Physeter macrocephalus) for the U.S. East Coast: Supplementary Report Duke. *Sci. Rep.*, 6.

Roch, M.A., Soldevilla, M.S., Burtenshaw, J.C., Henderson, E.E. & Hildebrand, J.A. (2007). Gaussian mixture model classification of odontocetes in the Southern California Bight and the Gulf of California. *J. Acoust. Soc. Am.*, 121, 1737–1748.

Roch, M. a, Klinck, H., Baumann-Pickering, S., Mellinger, D.K., Qui, S., Soldevilla, M.S., *et al.* (2011). Classification of echolocation clicks from odontocetes in the Southern California Bight. *J. Acoust. Soc. Am.*, 129, 467–475.

Roden, G.I. (1991). *Subarctic-subtropical transition zone of the North Pacific: Large-scale aspects and mesoscale structure*. Biol. Oceanogr. Fish. North Pacific Transit. Zo. Subarct. Front. Zo. Pap. from North Pacific Transit. Zo. Work. Honolulu, Hawaii.

Rodhouse, P.G. & Hatfield, E.M.C. (1990). Age determination in squid using statolith growth increments.pdf. *Fish. Res.*, 8, 323–334.

Rohatgi, A. (2017). *WebPlotDigitizer*. Available at: https://automeris.io/WebPlotDigitizer. Last accessed 5 May 2021.

Rone, B.K., Zerbini, A.N., Douglas, A.B., Weller, D.W. & Clapham, P.J. (2017). Abundance and distribution of cetaceans in the Gulf of Alaska. *Mar. Biol.*, 164, 1–23.

Santos, M.B., Pierce, G.J., Boyle, P.R., Reid, R.J., Ross, H.M., Patterson, I.A.P., *et al.* (1999). Stomach contents of sperm whales Physeter macrocephalus stranded in the North Sea 1990-1996. *Mar. Ecol. Prog. Ser.*, 183, 281–294.

Schmidly, D.J. (1981). *Marine mammals of the southeastern United States coast and the Gulf of Mexico*. The Project.

Schreer, J.F. & Kovacs, K.M. (1997). Allometry diving capacity. *Can. J. Zool.*, 75, 339–358.

Seber, G.A.F. (1982). The estimation of animal abundance and related parameters.

Sen, P.K. (1968). Estimate of the regression coefficient based on Kendall's tau. *J. Am. Stat. Assoc.*, 63, 1379–1389.

Sigler, M.F., Lunsford, C.R., Straley, J.M. & Liddle, J.B. (2008). Sperm whale depredation of sablefish longline gear in the northeast Pacific Ocean. *Mar. Mammal Sci.*, 24, 16–27.

Smith, T.D. ed. (2021). *World Whaling Database: Individual Whale Catches, North Atlantic. M.G Barnard J.H Nicholls HMAP Data Pages*. Available at: www.hull.ac.uk/hmap. Last accessed 5 May 2021.

Smith, T.D., Reeves, R.R., Josephson, E.A. & Lund, J.N. (2012). Spatial and seasonal distribution of American whaling and whales in the age of sail. *PLoS One*, 7.

Soldevilla, M.S., Wiggins, S.M., Hildebrand, J.A., Oleson, E.M. & Ferguson, M.C. (2011). Risso's and Pacific white-sided dolphin habitat modeling from passive acoustic monitoring. *Mar. Ecol. Prog. Ser.*, 423, 247–260.

Solsona-Berga, A., Frasier, K.E., Baumann-Pickering, S. & Hildebrand, J.A. (2020). DetEdit, a Graphical User Interface for Annotating and Editing Events Detected in Acoustic Data. *PLOS Comput. Biol.*, 1–10.

Solsona-Berga, A., Posdaljian, N., Hildebrand, J.A. & Baumann-Pickering, S. (2022). Echolocation repetition rate as a proxy to monitor population structure and dynamics of sperm whales. *Remote Sens. Ecol. Conserv.*, 8, 827–840.

Solsona Berga, A. (2019). Advancement of methods for passive acoustic monitoring: a framework for the study of deep-diving cetacean. *TDX (Tesis Dr. en Xarxa)*. Unversitat Politecnica de Catalunya BarcelonaTech.

Sousa, A., Alves, F., Dinis, A., Bentz, J., Cruz, M.J. & Nunes, J.P. (2019). How vulnerable are cetaceans to climate change ? Developing and testing a new index. *Ecol. Indic.*, 98, 9–18.

Spreen, G., Kaleschke, L. & Heygster, G. (2008). Sea ice remote sensing using AMSR-E 89-GHz channels. *J. Geophys. Res. Ocean.*, 113, 1–14.

Stanistreet, J.E., Nowacek, D.P., Bell, J.T., Cholewiak, D.M., Hildebrand, J.A., Hodge, L.E.W., *et al.* (2018). Spatial and seasonal patterns in acoustic detections of sperm whales Physeter macrocephalus along the continental slope in the western North Atlantic Ocean. *Endanger. Species Res.*, 35.

Stevenson, M.G. (1996). Indigenous Knowledge in Environmental Assessment. *Arctic*, 49, 278–291.

Stewart, J.S., Hazen, E.L., Bograd, S.J., Byrnes, J.E.K., Foley, D.G., Gilly, W.F., *et al.* (2014). Combined climate- and prey-mediated range expansion of Humboldt squid (Dosidicus gigas), a large marine predator in the California Current System. *Glob. Chang. Biol.*, 20, 1832–1843.

Stimpert, A.K., DeRuiter, S.L., Falcone, E.A., Joseph, J., Douglas, A.B., Moretti, D.J., *et al.* (2015). Sound production and associated behavior of tagged fin whales (Balaenoptera physalus) in the Southern California Bight. *Anim. Biotelemetry*, 3, 1–12.

Storrie, L., Lydersen, C., Andersen, M., Wynn, R.B. & Kovacs, K.M. (2018). Determining the species assemblage and habitat use of cetaceans in the Svalbard Archipelago, based on observations from 2002 to 2014. *Polar Res.*, 37.

Straley, J.M., Schorr, G.S., Thode, A.M., Calambokidis, J., Lunsford, C.R., Chenoweth, E.M., *et al.* (2014). Depredating sperm whales in the Gulf of Alaska: Local habitat use and long distance movements across putative population boundaries. *Endanger. Species Res.*, 24, 125–135.

Teloni, V., Mark, J.P., Patrick, M.J.O. & Peter, M.T. (2008). Shallow food for deep divers: Dynamic foraging behavior of male sperm whales in a high latitude habitat. *J. Exp. Mar. Bio. Ecol.*, 354, 119–131.

Tjur, T. (2009). Coefficients of determination in logistic regression models - A new proposal: The coefficient of discrimination. *Am. Stat.*, 63, 366–372.

Tomlin, A.G. (1967). Mammals of the USSR and Adjacent Countries. Cetacea. Israel Program Sci. Transl. 9 (124): 717. *Natl. Tech. Inf. Serv. TT*, 65–50086.

Townsend, C.H. (1935). The distribution of certain whales as shown by logbook records of American whaleships.

Tracey, K.L. & Watts, D.R. (1986). On Gulf Stream meander characteristics near Cape Hatteras. *J. Geophys. Res.*, 91, 7587.

Tran, D., Huang, W., Bohn, A.C., Wang, D., Gong, Z., Makris, N.C., *et al.* (2014). Using a coherent hydrophone array for observing sperm whale range, classification, and shallow-water dive profiles. *Acoust. Soc. Am.*

Vachon, F., Hersh, T.A., Rendell, L., Gero, S. & Whitehead, H. (2022). Ocean nomads or island specialists? Culturally driven habitat partitioning contrasts in scale between geographically isolated sperm whale populations. *R. Soc. Open Sci.*, 9.

Walsh, J.E., Chapman, W.L., Fetterer, F. & Stewart, J.S. (2019). *Gridded Monthly Sea Ice Extent and Concentration, 1850 Onward, Version 2*. NSIDC Natl. Snow Ice Data Cent.

Walsh, J.E., Fetterer, F., Scott Stewart, J. & Chapman, W.L. (2017). A database for depicting Arctic sea ice variations back to 1850. *Geogr. Rev.*, 107, 89–107.

Wang, M. & Overland, J.E. (2009). A sea ice free summer Arctic within 30 years? *Geophys. Res. Lett.*, 36, 2–6.

Waring, G.T., Fairfield, C.P., Rhusam, C.M. & Sano, M. (1993). Sperm whales associated with Gulf Stream features off the north-eastern USA shelf. *Fish. Oceanogr.*, 2, 101–105.

Waring, G.T., Fairfield, C.P., Ruhsam, C.M. & Sano, M. (1992). *Cetaceans Associated with Gulf Stream Features off the Northeastern USA Shelf*. Int. Counc. Explor. Sea.

Waring, G.T., Hamazaki, T., Sheehan, D., Wood, G. & Baker, S. (2001). Characterization of beaked whale (Ziphiidae) and sperm whale (Physeter macrocephalus) summer habitat in shelf-edge and deeper waters off the northeast U.S. *Mar. Mammal Sci.*, 17, 703–717.

Watanabe, M. & Hibiya, T. (2002). Global estimates of the wind-induced energy flux to inertial motions in the surface mixed layer. *Geophys. Res. Lett.*, 29, 2–5.

Watkins, W.A. (1980). Acoustics and the behavior of sperm whales. In: *Animal Sonar Systems*. Springer, pp. 283–290.

Watkins, W.A., Daher, M.A., Dimarzio, N.A., Samuels, A., Wartzok, D., Fristrup, K.M., *et al.* (2002). Sperm whale dives tracked by radio tag telemetry. *Mar. Mammal Sci.*, 18, 55–68.

Watkins, W.A. & Schevill, W.E. (1977). Spatial distribution of Physeter catodon (sperm whales) underwater. *Deep. Res.*, 24, 693–699.

Watt, C.A. & Ferguson, S.H. (2015). Fatty acids and stable isotopes (δ13C and δ15N) reveal temporal changes in narwhal (Monodon monoceros) diet linked to migration patterns. *Mar. Mammal Sci.*, 31, 21–44.

Watwood, S.L., Miller, P.J.O., Johnson, M., Madsen, P.T. & Tyack, P.L. (2006). Deep-diving foraging behaviour of sperm whales (Physeter macrocephalus). *J. Anim. Ecol.*, 75, 814–825.

Weilgart, L. & Whitehead, H. (1988). Distinctive vocalizations from mature male sperm whales (Physeter macrocephalus). *Can. J. Zool.*, 66, 1931–1937.

Weir, C.R., Pollock, C., Cronin, C. & Taylor, S. (2001). Cetaceans of the Atlantic Frontier, north and west of Scotland. *Cont. Shelf Res.*, 21, 1047–1071.

Welch, P.D. (1967). The use of fast Fourier transform for the estimation of power spectra: A method based on time averaging over short, modified periodograms, 70–73.

Whalesightings Database. (2021). *Team Whale, Fisheries and Oceans Canada*. Darmouth, NS.

Whitehead, H. (1993). The behaviour of mature male sperm whales on the Galapagos Islands breeding grounds. *Can. J. Zool.*, 71, 689–699.

Whitehead, H. (2003). Society and culture in the deep and open ocean: The sperm whale and other cetaceans. In: *Animal social complexity: Intelligence, culture, and individualized societies*. Harvard University Press.

Whitehead, H., Antunes, R., Gero, S., Wong, S.N.P., Engelhaupt, D. & Rendell, L. (2012). Multilevel Societies of Female Sperm Whales (Physeter macrocephalus) in the Atlantic and Pacific: Why Are They So Different? *Int. J. Primatol.*, 33, 1142–1164.

Whitehead, H. & Arnbom, T. (1987). Social organization of sperm whales off the Galapagos Islands, February–April 1985. *Can. J. Zool.*, 65, 913–919.

Whitehead, H., Christal, J. & Dufault, S. (1997). Past and distant whaling and the rapid decline of sperm whales off the Galapagos Islands. *Conserv. Biol.*, 11, 1387–1396.

Whitehead, H. & Shin, M. (2022). Current global population size, post-whaling trend and historical trajectory of sperm whales. *Sci. Rep.*, 12, 1–12.

Whitehead, H., Waters, S. & Lyrholm, T. (1991). Social organization of female sperm whales and their offspring: constant companions and casual acquaintances. *Behav. Ecol. Sociobiol.*, 29, 385–389.

Whitehead, H. & Weilgart, L. (1991). Patterns of Visually Observable Behaviour and Vocalizations in Groups of Female Sperm Whales, 41, 256–279.

Whitney, F.A. & Freeland, H.J. (1999). Variability in upper-ocean water properties in the NE Pacific Ocean. *Deep. Res. Part II Top. Stud. Oceanogr.*, 46, 2351–2370.

Whitney, F.A. & Welch, D.W. (2002). Impact of the 1997-1998 El Niño and 1999 La Niña on nutrient supply in the Gulf of Alaska. *Prog. Oceanogr.*, 54, 405–421.

Wiggins, S.M. & Hildebrand, J.A. (2007). *High-frequency Acoustic Recording Package (HARP) for broad-band, long-term marine mammal monitoring. Symp. Underw. Technol. Work. Sci. Use Submar. Cables Relat. Technol.*

Wild, L.A., Mueter, F., Witteveen, B. & Straley, J.M. (2020). Exploring variability in the diet of depredating sperm whales in the Gulf of Alaska through stable isotope analysis. *R. Soc. Open Sci.*, 7.

Wilson, C. & Adamec, D. (2001). Correlations between surface chlorophyll and sea surface height in the tropical Pacific during the 1997-1999 El Niño - Southern Oscillation event. *J. Geophys. Res. Ocean.*, 106, 31175–31188.

Wong, S.N.P. & Whitehead, H. (2014). Seasonal occurrence of sperm whales (Physeter macrocephalus) around Kelvin Seamount in the Sargasso Sea in relation to oceanographic processes. *Deep. Res. Part I Oceanogr. Res. Pap.*

Wood, S.N. (2011). Fast stable restricted maximum likelihood and marginal likelihood estimation of semiparametric generalized linear models. *J. R. Stat. Soc. Ser. B Stat. Methodol.*, 73, 3–36.

Worden, E., Pearce, T., Gruben, M., Ross, D., Kowana, C. & Loseto, L. (2020). Social-ecological changes and implications for understanding the declining Beluga Whale (Delphinapterus leucas) harvest in Aklavik, northwest territories. *Arct. Sci.*, 6, 229–246.

Worthington, L.V. & Schevill, W.E. (1957). Underwater Sounds Heard from Sperm Whales. *Nature*, 291.

Yang, B., Emerson, S.R. & Angelica Penã, M. (2018). The effect of the 2013-2016 high temperature anomaly in the subarctic Northeast Pacific (the "blob") on net community production. *Biogeosciences*, 15, 6747–6759.

Yang, J. & Chen, K. (2021). The Role of Wind Stress in Driving the Along-Shelf Flow in the Northwest Atlantic Ocean. *J. Geophys. Res. Ocean.*, 126, 1–20.

Zador, S. (2011). *Appendix C Ecosystem considerations for 2012*.

Ziegenhorn, M.A., Hildebrand, J.A., Oleson, E.M., Baird, R.W., Wiggins, S.M. & Baumann-Pickering, S. (2023). Odontocete spatial patterns and temporal drivers of detection at sites in the Hawaiian islands. *Ecol. Evol.*, 13, 1–20.

Zuur, A.F. (2012). A beginner's guide to generalized additive models with R (pp. 1-206). *Mater. Sci. Eng. A*, 27, 1–14.